Pre-treatment of Ultramafic Nickel Ores for Improved Mineral Carbon Sequestration

by

Erin Rae Bobicki

A thesis submitted in partial fulfillment of the requirements for the degree of

Doctor of Philosophy

in

Chemical Engineering

Department of Chemical and Materials Engineering

University of Alberta

Abstract

Mineral carbon sequestration (MCS) is a type of carbon storage based on natural rock weathering processes where CO_2, dissolved in rainwater, reacts with alkaline minerals to form solid carbonates. Although MCS has advantages over other carbon storage techniques, an economic MCS process has not yet been developed. Two approaches were taken in this work to reduce the cost of MCS. The first approach was to use a waste material, serpentine waste from ultramafic nickel ore processing, as a feedstock. The second approach was to use pre-treatments to increase the carbon storage capacity of the waste material. Two pre-treatments were developed in this work. The first pre-treatment, microwave pre-treatment, was identified as a way not only to improve the carbon sequestration capacity of the waste, but also to improve the mineral processing of ultramafic nickel ores. Microwave pre-treatment was shown to successfully convert serpentine in ultramafic nickel ores to olivine, to improve the grindability of ultramafic nickel ores with consistent texture, to reduce the viscosity of ultramafic nickel ore slurries by an average of 80%, and to enhance the CO_2 storage capacity of ultramafic nickel ores by a factor of up to 5. The second pre-treatment developed was leaching with ligands at neutral to alkaline pH. Catechol, EDTA and tiron were shown to greatly improve the leaching rate and total magnesium leached from ultramafic nickel ores. While EDTA proved to be too strong of a ligand to allow the precipitation of $MgCO_3$ from solution, catechol and tiron promoted the formation of $MgCO_3$, particularly at pH 10. Overall, tiron was the most effective ligand for enhancing MCS and increased the CO_2 storage capacity of ultramafic

nickel ores by a factor of up to 3. Although the pre-treatment techniques developed required optimization, both microwave pre-treatment and leaching with ligands at neutral to alkaline pH show promise for ultimately reducing the cost of MCS.

Preface

This thesis is composed of a series of papers that have either been published or submitted for publication. The following is a statement of contributions made to the jointly authored papers contained in this thesis:

1. Bobicki, E.R., Liu, Q., Xu, Z., Zeng, H., 2012. Carbon capture and storage using alkaline industrial wastes. Progress in Energy and Combustion Science. 38, 302-320. Bobicki was responsible for conducting the literature review and writing the paper. Zeng was responsible for proofreading and constructing some of the figures. Liu and Xu provided proofreading. This paper forms chapter 2 of this thesis.

2. Bobicki, E.R., Liu, Q., Xu, Z., 2014. Microwave heating of ultramafic nickel ores and mineralogical effects. Minerals Engineering. 58, 22-25. Bobicki performed all experiments and data analysis, and wrote the paper. Liu and Xu provided proofreading. This paper forms chapter 3 of this thesis.

3. Bobicki, E.R., Liu, Q., Xu, Z., Manchak, N., Xu, M., 2013. Effect of microwave pre-treatment on grindability of ultramafic nickel ores. Proceedings of Materials Science and Technology (MS&T) 2013. 2013 October 27-31; Montreal, Quebec, Canada. Bobicki performed all experiments and data analysis, with the exception of the hardness experiments, which were conducted and interpreted by Manchak, and the mineral liberation analysis which was conducted by Andrew Lee at Vale Base Metals Technology Development Ltd. Bobicki wrote the entire paper. Liu, Z. Xu and M. Xu provided proofreading. This paper forms chapter 4 of this thesis.

4. Bobicki, E.R., Liu, Q., Xu, Z., 2014. Effect of microwave pre-treatment on ultramafic nickel ore slurry rheology. Minerals Engineering. 61, 97-104. Bobicki performed all experiments and data analysis, and wrote the paper. Liu and Xu provided proofreading. This paper forms chapter 5 of this thesis.

5. Bobicki, E.R., Liu, Q., Xu, Z., 2014. Ligand-promoted dissolution of serpentine in ultramafic nickel ores. *Accepted by Minerals Engineering.* Bobicki performed all experiments and data analysis, and wrote the paper. Liu and Xu provided proofreading. This paper forms chapter 6 of this thesis.

6. Bobicki, E.R., Liu, Q., Xu, Z., 2014. Mineral carbon storage in pre-treated ultramafic nickel ores. *Submitted to Minerals Engineering.* Bobicki performed all experiments and data analysis, and wrote the paper. Liu and Xu provided proofreading. This paper forms chapter 7 of this thesis.

Acknowledgements

I would like to express my sincere gratitude and appreciation to:

- My supervisors, Professor Qingxia Liu and Professor Zhenghe Xu, for their guidance and support.
- Mr. James Skwarok, Ms. Lisa Carreiro, Ms. Patricia Siferd, Ms. Jie Ru, Mr. Carl Corbett, Mr. Walter Boddez, Mr. Shiraz Merali, and Ms. Gayle Hatchard for administrative and technical assistance.
- Dr. Manqiu Xu and Dr. Ken Scholey from Vale Base Metals Technology Development Ltd. for encouraging me to pursue a PhD and for their support and feedback throughout the course of my studies.
- Professor Ken Cadien for his advice and guidance.
- Mr. Greg Nelson, Mr. Andrew Jo, Mr. Joshua Neumann, Mr. Elo Emessiri, Mr. Andy Tan and Ms. Erin Furnell, for laboratory assistance.
- Ms. Teresa Bisson, Dr. Meijiao Deng, Ms. Natalie Kuznicki, and Ms. Nicole Lee Robertson for continued moral support and friendship.
- Mr. Andreas Kusuma and Dr. Dingzheng Yang for thoughtful discussion.
- Ms. Nancy Manchak for collaboration on ore hardness measurements.
- Mr. Kevin Heidebrecht, Mr. Clark Bicknell, Mr. Herb Green and all members of the machine shop.
- All fellow members of the Oils Sands Research Group and C^5MPT.
- Vale Ltd. and Natural Sciences and Engineering Research Council of Canada (NSERC) for financial support.

Finally, my deepest gratitude goes to my family. To my mother and father, I thank you for instilling in me the value of hard work and education, and for your support during my studies. To my daughters Catherine and Adelaide, thank you for making me smile. Most of all, Dennis, my love, I thank you for your positivity and encouragement, and all the sacrifices you've made for me. It is to you that I dedicate this work.

Table of Contents

List of Tables

List of Figures

xviii

xxv

Chapter 1 Introduction

Carbon capture and storage (CCS) is a strategy for carbon dioxide (CO_2) emissions reduction and climate change mitigation. Mineral carbon sequestration (MCS) is a permanent form of carbon storage, can capture and store CO_2 in a single step, and can be used where geologic carbon storage is not feasible. MCS is based on rock weathering processes where atmospheric CO_2, dissolved in rainwater, reacts with alkaline minerals to produce solid carbonates. Despite the advantages over other carbon storage technologies, an economic process for MCS does not yet exist.

The primary objective of this research is to find ways to reduce the cost of MCS. Possible ways to achieve MCS cost reduction include identifying inexpensive and readily available mineral feedstocks, reducing the energy associated with grinding and activating the mineral feedstock, reducing the chemical reagent requirements of MCS processes, and integrating MCS beneficially into other processes. Recently, the concept of CCUS – carbon capture, utilization and storage – has become prominent. The idea is to capture and isolate CO_2 from the atmosphere in a way that is beneficial to another process, and to provide a financial incentive to do so. Examples include the use of captured CO_2 as chemical feedstock, in enhanced oil recovery (EOR) processes, to treat oil sands tailings, for wastewater treatment and for fuel production (Choi et al., 2003; Jiang et al., 2010; Metz et al., 2005; Park et al., 2011; Zhu et al., 2011). The cost of MCS may be further offset by producing saleable carbonation by-products, such as precipitated magnesium carbonate and silica, and by storing CO_2 directly from flue gas streams, thereby skipping the capture step.

1.1 Approach

The approaches taken in this work to attempt to reduce the cost of MCS include using a waste product as feedstock and developing pre-treatments to increase the CO_2 reactivity of the waste material. The waste product selected as feedstock was serpentine ($Mg_3Si_2O_5(OH)_4$) mineral processing wastes generated by ultramafic

nickel ore processing facilities. Two different pre-treatments were investigated for use on this waste material. The first, microwave pre-treatment, was tested as a way to enhance both mineral processing and MCS operations. While not true CCUS, the idea was to develop a pre-treatment that could not only enhance the storage of CO_2 but create value for another process. The hypothesis was that microwave pre-treatment would improve ultramafic nickel ore grindability and slurry rheology, thereby improving the mineral processing of these ores, as well as increase the carbon storage capacity of the flotation tailings. The effect of microwave pre-treatment on ore mineralogy, grindability, slurry rheology and carbon uptake was investigated in this work.

The second pre-treatment investigated was leaching with ligands at neutral to alkaline pH. The rate-limiting step in aqueous MCS is the dissolution of the mineral feedstock (Krevor and Lackner, 2011). Although a number of reagents have been used successfully to increase the mineral dissolution rate, most of these reagents have been applied at an acidic pH, after which an adjustment to alkaline pH has been required for carbonate precipitation. The leaching of minerals at acidic pH, and subsequent neutralization to alkaline pH for carbonate precipitation, has resulted in excessive reagent consumption and proven uneconomic (Teir et al., 2009). The leaching of ores with ligands at neutral to alkaline pH was tested in this work as a way to promote the dissolution of serpentine in the ores/tailings for the enhancement of MCS without the need for a secondary pH adjustment. The effect of different ligands on the leaching rate, the total magnesium leached, and the carbon uptake of ultramafic nickel ores was studied in this work.

It should be noted that while the overriding objective of this work was to reduce the cost of MCS, the pre-treatments developed were investigated from a fundamental perspective and were not optimized.

2

1.2 Thesis Structure

This thesis has been structured as a compilation of papers. Chapters 2-7 are published or submitted works in scientific journals or conference proceedings. Chapter 2 is a review paper, while Chapters 3 to 7 are research papers.

Chapter 1: This chapter provides the overall introduction to the thesis, which includes some background information and describes the objectives and approach of the thesis.

Chapter 2: This chapter is a comprehensive literature review on mineral carbon sequestration and the use of waste products as feedstock. A version of this chapter has been published in:

Bobicki, E.R., Liu, Q., Xu, Z., Zeng, H., 2012. Carbon capture and storage using alkaline industrial wastes. Progress in Energy and Combustion Science. 38, 302-320.

Chapter 3: This chapter describes the microwave heating of ultramafic nickel ores and the changes in mineralogy that occur as a result. A version of this paper has been published in:

Bobicki, E.R., Liu, Q., Xu, Z., 2014. Microwave heating of ultramafic nickel ores and mineralogical effects. Minerals Engineering. 58, 22-25.

Chapter 4: This chapter describes the effects of microwave pre-treatment on the grindability, pentlandite liberation and specific surface area of ultramafic nickel ores. Energy usage in microwave-assisted grinding is also discussed. A version of this chapter has been published in conference proceedings:

Bobicki, E.R., Liu, Q., Xu, Z., Manchak, N., Xu, M., 2013. Effect of microwave pre-treatment on grindability of ultramafic nickel ores. Proceedings of Materials Science and Technology (MS&T) 2013. 2013 October 27-31; Montreal, Quebec, Canada.

Chapter 5: This chapter examines the effects of microwave pre-treatment on ultramafic ore slurry rheology. Impacts on flow rheology and yield stress are discussed. A version of this chapter has been published in:

Bobicki, E.R., Liu, Q., Xu, Z., 2014. Effect of microwave pre-treatment on ultramafic nickel ore slurry rheology. Minerals Engineering. 61, 97-104.

Chapter 6: This chapter investigates the effect of five different ligands on the leaching of serpentine in ultramafic nickel ores. Attention is paid to both the total magnesium leached and the leaching rate. A version of this chapter has been accepted for publication:

Bobicki, E.R., Liu, Q., Xu, Z., 2014. Ligand-promoted dissolution of serpentine in ultramafic nickel ores. *Accepted by Minerals Engineering*.

Chapter 7: This chapter discusses the carbonation of ores pre-treated with microwaves and leached with ligands. A version of this chapter has been submitted for publication:

Bobicki, E.R., Liu, Q., Xu, Z., 2014. Mineral carbon storage in pre-treated ultramafic nickel ores. *Submitted to Minerals Engineering.*

Chapter 8: This chapter summarizes the overall conclusions and major contributions, and provides direction for future work.

Appendices A-F at the end of the thesis contain additional data from solution modeling work completed to support Chapters 6 and 7.

1.3 References

Choi, S.K., Ko, K.S., Chin, H.D., Kim, J.G., 2003. Utilization of carbon dioxide for neutralization of alkaline wastewater. In: Gale J and Kaya Y, editors. Greenhouse Gas Control Technologies, Volume II: Proceedings of the 6th International Conference on Greenhouse Gas Control Technologies; 2002 Oct 1–4; Kyoto, Japan. Amsterdam: Elsevier; p. 1871-1874.

Jiang, Z., Xiao, T., Kuznetsov, V.L., Edwards, P.P., 2010. Turning carbon dioxide into fuel. Philosophical Transactions of the Royal Society A. 368, 3343-3364.

Krevor, S.C.M., Lackner, K.S., 2011. Enhancing serpentine dissolution kinetics for mineral carbon dioxide sequestration. International Journal of Greenhouse Gas Control. 5, 1073-1080.

Metz, B., Davidson, O., de Coninck, H.C., Loos, M., Meyer, L.A., editors, 2005. IPCC Special Report on Carbon Dioxide Capture and Storage. Prepared by Working Group III of the Intergovernmental Panel on Climate Change. Cambridge, UK and New York, NY: Cambridge University Press.

Park, J.B.K., Craggs, R.J., Shilton, A.N., 2011. Wastewater treatment high rate algal ponds for biofuel production. Bioresource Technology. 102, 35-42.

Teir, S., Eloneva, S., Fogelholm, C.-J., Zevenhoven, R., 2009. Fixation of carbon dioxide by producing hydromagnesite from serpentinite. Applied Energy. 86, 214-218.

Zhu, R., Liu, Q., Xu, Z., Masliyah, J.H., Khan, A., 2011. Role of dissolving carbon dioxide in densification of oil sands tailings. Energy and Fuels. 25, 2049-2057.

Chapter 2 Carbon Capture and Storage Using Alkaline Industrial Wastes[1]

2.1 Introduction

It is postulated that the current warming of the global climate is a result of an increase in anthropogenic greenhouse gas (GHG) emissions, particularly CO_2, since pre-industrial times (Field and Raupach, 2004). Global average atmospheric CO_2 has increased from 280 ppm in the 1750s to 397 ppm in 2013 (Bernstein et al., 2007; Tans, 2012; Canadell et al., 2007). The increase in atmospheric CO_2 over the last two and a half centuries has been attributed to two major anthropogenic forcing fluxes: (i) emissions from fossil fuel combustion and industrial processes and (ii) land use change (Canadell et al., 2007; Solomon et al., 2007; Raupach et al., 2007). Since the use and supply of global energy is projected to continue to grow, especially as developing countries pursue industrialization, fossil fuels are expected to maintain their dominance in the global energy mix to 2030 and beyond. If no proactive mitigative action is taken, energy-related CO_2 emissions are likely to be 40-110% higher in 2030 than they were in 2000 (23.5 Gt CO_2 per annum) (Metz et al., 2007; IEA, 2012). The latest figures indicate world CO_2 emissions from fuel combustion were 30.3 Gt in 2010 (IEA, 2012). By 2100, atmospheric CO_2 concentrations could reach 540 to 970 ppm (Houghton et al., 2001), resulting in a global mean temperature increase of 1.8 to 4°C (Solomon et al., 2007). It is recognized that a temperature increase of this magnitude would have wide-ranging and drastic implications for water and food availability, human health, ecosystems, coastlines and biodiversity (Bernstein et al., 2007).

In response to the hypothesis that global climate change is linked to the emission of anthropogenic GHGs, governments around the world have made commitments

---

[1] A version of this chapter has been published. Bobicki, E.R., Liu, Q., Xu, Z., Zeng, H., 2012. Carbon capture and storage using alkaline industrial wastes. Progress in Energy and Combustion Science. 38, 302-320.

to reduce their greenhouse gas emissions. To meet their targets, governments are enacting legislation and introducing incentives for capping GHG emissions, particularly CO_2, within their borders. In some areas of the world these types of regulations are already being implemented in the form of carbon or CO_2 taxes (Sweden, Norway, the Netherlands, Denmark, Finland, Italy (Baranzini et al., 2000), the UK (Metcalf et al., 2009) and Ireland (IDF, 2010)) and emissions trading schemes (New Zealand (NZME, 2007) and the European Union (Skjærseth et al., 2010)). Governments, individuals, and industry, in particular, will have to adopt specific CO_2 abatement strategies to achieve compliance and stay in business. Technical strategies commonly identified to reduce CO_2 emissions and combat climate change include reducing energy consumption, increasing energy utilization efficiency, reducing the carbon intensity of energy sources, broadening energy portfolios by increasing the use of renewable energy sources, enhancing biological CO_2 absorption, and implementing carbon capture and storage (CCS) (Yamasaki, 2003; Metz et al., 2005).

CCS is a three step process consisting of (i) the separation of CO_2 from gaseous waste streams, (ii) the transport of CO_2 to storage locations, and (iii) the long-term isolation of CO_2 from the atmosphere (carbon storage or sequestration) (Metz et al., 2005). CCS is attracting growing interest around the world, particularly in countries where electricity generation and export income are heavily dependent on fossil fuels, such as China, Western Europe, Australia, Canada and the US (van Alphen et al., 2010). CCS is viewed as an important bridging technology that will allow CO_2 emissions to be managed during fossil fuel dependence while society steadily increases the use of renewable energy sources (van Alphen et al., 2010a; Stephens, 2006; Praetorius and Schumacher, 2009). In fact, it has been surmised that CCS may contribute up to 15-55% of the cumulative global climate change mitigation effort by 2100 and that the inclusion of CCS in a mitigation portfolio could reduce the costs of stabilizing atmospheric CO_2 concentrations by 30% or more (Metz et al., 2005).

CCS is not a new concept. The technologies and practices associated with carbon capture and transport, and some types of carbon sequestration, geologic storage for example, have been in commercial operation within various industries for 10-50 years (Praetorius and Schumacher, 2009). CO_2 capture systems are present in coal and natural gas fired power generation, coal gasification facilities and various industrial facilities. In the US alone, there are more than 6200 kilometers of dedicated CO_2 pipelines and the oil industry has been injecting CO_2 into oil formations to enhance oil recovery (EOR) since the 1970s (Praetorius and Schumacher, 2009; Dooley et al., 2009). Currently four complete, end-to-end commercial CCS facilities are utilizing geologic storage. They are Sleipner West and Snøhvit in Norway, Weyburn in Saskatchewan, and In Salah in Algeria. All are tied to natural gas and syngas operations (Dooley et al., 2009). In addition, numerous research and demonstration projects are underway around the world (Van Alphen et al., 2010b; Jürgen-Friedrich et al., 2009; van Alphen et al., 2009). Despite the attention CCS has received over the past several years, with only several large, complete commercial facilities in operation, none including large power plants fully integrated with CCS, carbon capture and storage is still in its infancy (van Alphen et al., 2010a; Hansson and Bryngelsson, 2009).

A number of technologies exist for each phase of CCS. CO_2 may be captured post-combustion, pre-combustion, from oxy-fuel combustion or from industrial process streams (Metz et al., 2005; Gibbins and Chalmers, 2008). Technologies used in these systems include the separation of CO_2 with sorbents, membranes, cryogenic distillation and chemical-looping (Metz et al., 2005; Olajire, 2010; Grasa and Abanades, 2006), with chemical absorption being the most commonly used method (Elwell and Grant, 2006). CO_2 transport can be carried out using pipelines or marine, rail and road tankers (Dooley et al., 2009; Kornneef et al., 2010; Gale and Davison, 2004; Svensson et al., 2004), with transport by pipeline being considered the preferred option for large scale CCS projects (Metz et al., 2005; Praetorius and Schumacher, 2009). CO_2 storage, or sequestration, can be accomplished through geologic storage, ocean storage, industrial use and mineral

sequestration. The advantages, disadvantages, and costs associated with these storage options are given in Table 2-1.

Table 2-1: Summary of methodologies for CO_2 storage.

CO_2 Storage Method	Advantages	Disadvantages	Cost[a] (US$/t CO_2 stored)
Geologic Sequestration	• Feasible on a large scale • Substantial storage capacity known • Extensive experience • Low cost	• Monitoring necessary • Leakage possible	0.5 – 8.0 (storage) 0.1 – 0.3 (monitoring)
Ocean Carbon Sequestration	• Large storage capacity	• Temporary storage • Potential harmful effects on aquatic microbes and biota	6 – 31 (pipeline) 12 – 16 (tanker)
Industrial use	• CO_2 incorporated into valuable products	• Limited storage capacity • Storage time short	-
Mineral Carbon Sequestration	• Only known form of permanent storage • Minerals required available in quantities capable of binding all fossil-fuel bound carbon • Carbonation products environmentally benign	• Energy intensive • High cost	50 – 100

[a]Does not include capture costs (Metz et al., 2005).

2.2 Mineral Carbon Sequestration

Mineral carbon sequestration technology is based on the process of natural rock weathering where carbonic acid, generated through the dissolution of CO_2 in rain water, is neutralized with mineral alkalinity to form carbonate minerals (Huijgen and Comans, 2003; Lackner, 2002). The products of mineral carbonation remain

naturally in the solid state and, thus, there is no possibility of CO_2 release after sequestration. In fact, substantial energy is required to regenerate CO_2 from carbonates (Lackner et al., 1995). Mineral carbon sequestration can be accomplished either *in situ* (underground in geologic formations) or *ex situ* (above ground in a chemical processing plant) (Gerdemann et al., 2004). A schematic of *ex situ* mineral carbon sequestration showing the material fluxes is given in Figure 2-1.
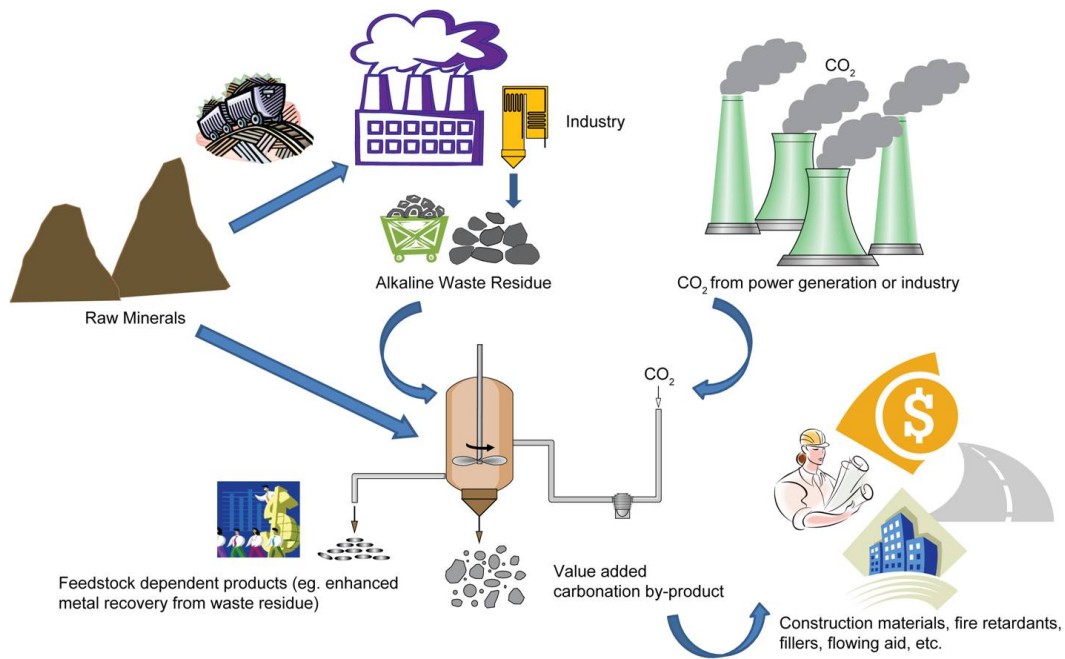
Figure 2-1: Material fluxes associated with mineral carbonation of silicate rocks and industrial residues.

Mineral carbon sequestration has a number of advantages over other carbon storage techniques. Not only is mineral carbon sequestration a permanent method of CO_2 disposal (Lackner et al., 1995; Goff and Lackner, 1998), but the products are environmentally benign and could potentially be sold for profit (Maroto-Valer et al., 2005). In addition, mineral carbon sequestration can be used in areas where other storage techniques, such as geologic carbon sequestration, are either not available or are infeasible (Zevenhoven and Fagerlund, 2010). More importantly, using mineral carbonation, CCS may be accomplished in a single step.

Mineral carbonation reactions are exothermic and occur spontaneously in nature, although on geologic time scales (Metz et al., 2005; Huijgen and Comans, 2003). Carbonate and silicate rocks undergo weathering by carbonic acid. Carbonate weathering generates bicarbonates, while silicate weathering generates carbonates or bicarbonates. It is easier to transform carbonates into bicarbonates than it is to generate carbonates from silicates. However, the generation of carbonates from silicates is usually targeted in *ex situ* CO_2 sequestration schemes. This is because carbonates are almost insoluble in water and, thus, provide controlled storage, while bicarbonates are quite soluble and must be diluted into the environment (Lackner, 2002).

Both alkali and alkaline earth metals may be carbonated, but alkali carbonates are too soluble to be stored above ground (Huijgen and Comans, 2003). Calcium and magnesium are the most abundant alkaline earth metals and, therefore, are generally selected for *ex situ* mineral CO_2 sequestration purposes ((Huijgen and Comans, 2003). Calcium and magnesium oxides are the ideal feedstocks for mineral carbonation, as the reactions of these minerals with CO_2 generate the most heat (reactions 2.1 and 2.2). However, these minerals are rarely found in nature because of their relatively high reactivity (Metz et al., 2005). Nonetheless, many common minerals are a variation of these oxides in a silicate matrix. The incorporation of these minerals into the matrix reduces the energy released in the carbonation reaction, but does not change the exothermic nature of the reaction. Natural silicate minerals commonly selected for mineral carbonation include wollastonite, olivine and serpentine (reactions 2.3, 2.4 and 2.5) (Huijgen and Comans, 2003; Lackner et al., 1995). One disadvantage of mineral carbon sequestration is that vast quantities of silicate ores are required to sequester a significant fraction of emitted CO_2 (Huijgen et al., 2005). While the aforementioned minerals exist, collectively, in quantities capable of binding all fossil fuel-bound carbon (Zevenhoven et al., 2002), the environmental impact and costs associated with the utilization of these minerals on the kind of scale necessary for CCS would be substantial. The cost of mining and preparing

silicate ore for mineral carbonation has been estimated at 10 US$/t CO_2 stored with 2% additional CO_2 emissions (Metz et al., 2005).

$$CaO + CO_2 \rightarrow CaCO_3 \qquad\qquad \Delta H_{rxn} = \text{-179 kJ/mol} \quad (2.1)$$

$$MgO + CO_2 \rightarrow MgCO_3 \qquad\qquad \Delta H_{rxn} = \text{-118 kJ/mol} \quad (2.2)$$

$$CaSiO_3 + CO_2 \rightarrow CaCO_3 + SiO_2 \qquad\qquad \Delta H_{rxn} = \text{-90 kJ/mol} \quad (2.3)$$

$$Mg_2SiO_4 + 2CO_2 \rightarrow 2MgCO_3 + SiO_2 \qquad\qquad \Delta H_{rxn} = \text{-89 kJ/mol} \quad (2.4)$$

$$Mg_3Si_2O_5(OH)_4 + 3CO_2 \rightarrow 3MgCO_3 + 2SiO_2 + 2H_2O \ \Delta H_{rxn} = \text{-64 kJ/mol} \quad (2.5)$$
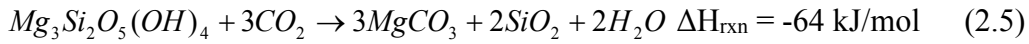
The challenge of mineral carbon sequestration is to accelerate the carbonation process and exploit the heat of reaction with minimal energy and material losses. Unfortunately, with current CCS schemes using mineral carbonation there is always a net demand for energy. Energy is utilized in the preparation of solid reactants, processing, and purification or disposal of the resultant carbonates and by-products. Natural minerals require varying degrees of pre-treatments, from mining and fine grinding, to heat treatment and chemical activation, to make them sufficiently reactive. The energy intensity required to achieve sufficient reaction rates (estimated at 30-50% of power plant output) and the consequent high cost of mineral carbon sequestration have prevented the technology from being implemented at an industrial scale thus far (Metz et al., 2005; Goldberg et al., 2001).

Alkaline industrial waste residues represent alternative sources of readily available and reactive materials suitable for mineral carbonation. Although their total amounts are considered to be too small to substantially reduce CO_2 emissions, they could help establish mineral carbon sequestration technology and their use may be a stepping-stone towards the development of economic CCS processes utilizing natural minerals. Waste products that have been considered for mineral carbonation include steelmaking slags, concrete wastes, mining and

mineral processing wastes, combustion waste ashes and alkaline paper mill wastes (Metz et al., 2005; Huijgen and Comans, 2003; Gerdemann et al., 2007).

The carbonation of industrial wastes is accomplished *ex situ.* A number of processes have been developed to achieve *ex situ* mineral carbon sequestration with acceptable kinetics (summarized in Table 2-2). In general, *ex situ* mineral carbonation can be divided into two categories: (i) direct carbonation and (ii) indirect carbonation (Figure 2-2). Direct carbonation can be accomplished via gas-solid reactions or mineralization in aqueous solutions. Indirect carbonation routes include hydrochloric (HCl) acid extraction, the molten salt process, other acid extraction, bioleaching, ammonia extraction and caustic extraction followed by carbonation reactions. These technologies can be applied to both natural minerals and alkaline waste residues and will be briefly reviewed prior to a detailed discussion on the types of wastes that can be utilized for mineral carbon sequestration (Table 2-3, found at end of chapter).
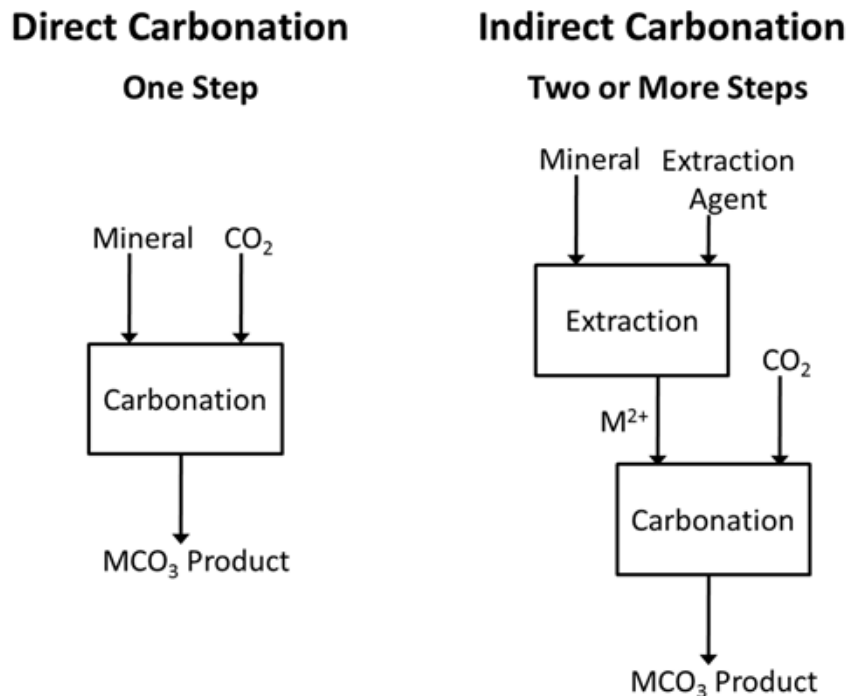
Figure 2-2: Direct mineral carbonation is accomplished in one step, while indirect mineral carbonation is conducted in two or more steps. Note M refers to either calcium (Ca) or magnesium (Mg).

Table 2-2: Summary of mineral carbon sequestration process routes.

Mineral Carbon Sequestration Methods		Characteristic
Direct Carbonation	Gas-Solid	• CO_2 reacted with mineral in a gas-solid reaction • Simplest method of mineral carbonation • Not feasible for silicate minerals
	Aqueous	• CO_2 reacted with mineral in aqueous suspension • Pre-treatment required • Most promising technique
Indirect Carbonation	HCl Extraction	• Metal ion extracted from mineral using HCl • Metal ion precipitated as a hydroxide for carbonation • HCl recovered • Very energy intensive
	Molten Salt	• Molten magnesium chloride salt used to extract metal ion from silicate minerals • Metal ion precipitated as a hydroxide for carbonation • Molten salt highly corrosive • Make-up chemical cost is prohibitive
	Acid Extraction	• Acids used to extract metal ion from minerals • Extracted metal carbonated aqueously • Various acids used • High carbonate conversions achieved • Multiple process steps allow contaminants to be separated, resulting in a pure carbonation product • Chemically intensive • Energy intensive if acid recovered
	Bioleaching	• Chemolithotrophic bacteria combined with acid generating substances and silicate minerals to extract metal ions for aqueous carbonation • Passive and inexpensive
	Ammonia Extraction	• Ammonia salts used to extract metal ion from silicate rock for carbonation • Selective leaching of alkaline earth metals • Reagent recovery possible • Reasonable carbonate conversions achieved
	Caustic Extraction	• Caustic solid used to extract metal ion from silicate rock for carbonation • Not a promising technique

2.2.1 Direct Carbonation

Direct mineral carbonation is accomplished through the reaction of a solid alkaline mineral with CO_2 either in the gaseous or aqueous phase. It may involve mineral pre-treatment, but does not include the extraction of reactive components

(eg. calcium or magnesium ions) from the mineral prior to carbonation. Advantages of direct mineral carbonation are the simplicity of the process and the minimal use of chemical reagents.

2.2.1.1 Gas-Solid Carbonation

The reaction of gaseous CO_2 with particulate metal oxides at suitable temperatures and pressures (reactions 2.1-2.5) is the most basic form of direct mineral carbonation (Metz et al., 2005). This process has the potential to produce high temperature steam that can be used to generate electricity while fixing CO_2 (Sipilä et al., 2008). Fine grinding of the mineral prior to carbonation is required (Goldberg et al., 2001). To improve the reaction kinetics, temperatures and pressures must be elevated during the process. Due to the high entropy of gaseous CO_2, however, the equilibrium shifts towards free CO_2 with increasing temperature, resulting in an upper limit at which carbonation can occur. For common natural silicate minerals, this temperature limit ranges from 170ºC to 410ºC (Lackner et al., 1997). Unfortunately, even under "ideal" conditions, direct gas-solid reactions are too slow to be practical for calcium and magnesium silicates. Carbonation of calcium-and-magnesium-containing oxides or hydroxides, however, has been proven to be feasible (Metz et al., 2005; Lackner et al., 1997). While these minerals are rare in nature, they can be found in industrial waste residues or extracted from silicate minerals. If the process is applied to extracted calcium or magnesium oxides or hydroxides derived from silicates, it becomes the second stage of an indirect carbonation process. Research on the direct solid-gas carbonation process has mainly focused on the use of CaO and MgO for CO_2 capture, rather than storage, in cyclic carbonation/calcinations schemes, known as chemical looping (Grasa and Abanades, 2006; Gupta and Fan, 2002; Le et al., 2008), and on utilizing industrial waste streams of high CaO or MgO content as the source materials (Baciocchi et al., 2009b; Lim et al., 2010; Prigiobbe et al., 2009a; Larachi et al., 2010).

2.2.1.2 Aqueous Carbonation

Direct aqueous mineral carbonation involves the reaction of CO_2 with alkaline minerals in an aqueous suspension in a single stage (Sipilä et al., 2008). CO_2 reacts with water to form bicarbonate and a proton, the proton liberates the metal ion from the mineral, and the metal ion reacts with bicarbonate to produce a carbonate precipitate (O'Connor et al., 2000a). The direct aqueous carbonation of olivine, Mg_2SiO_4, is shown in reactions 2.6-2.8 and a schematic of the process with serpentine, $Mg_3Si_2O_5(OH)_4$, and olivine is depicted in Figure 2-3.

$$CO_2 + H_2O \rightarrow H_2CO_3 \rightarrow H^+ + HCO_3^-$$
(2.6)

$$Mg_2SiO_4 + 4H^+ \rightarrow 2Mg^{2+} + SiO_2 + 2H_2O$$
(2.7)

$$Mg^{2+} + HCO_3^- \rightarrow MgCO_3 + H^+$$
(2.8)
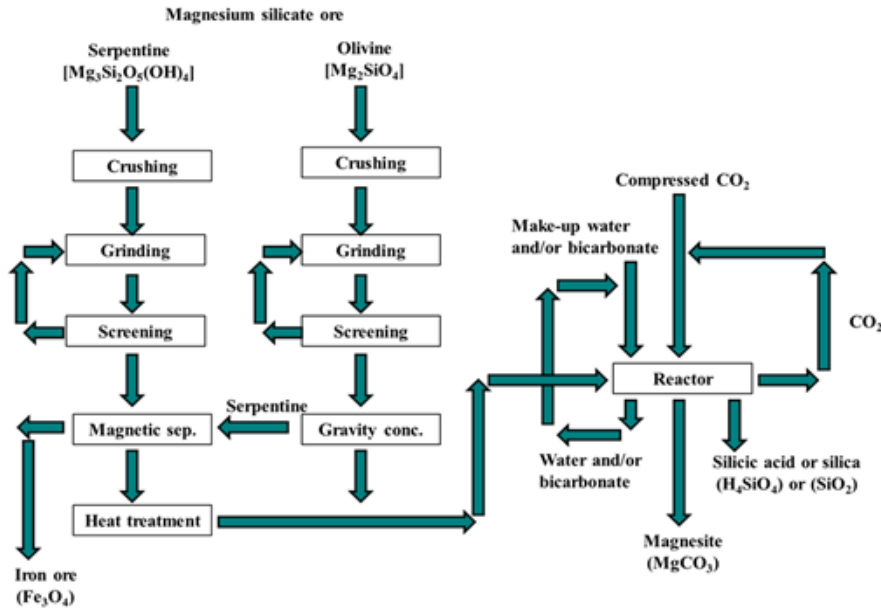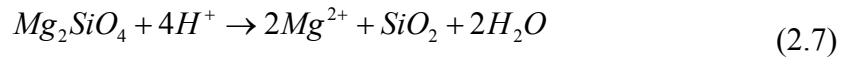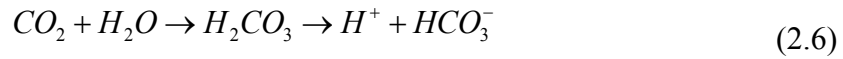
Figure 2-3: Process flow diagram for the direct mineral carbonation of serpentine and olivine in the aqueous phase from O'Connor et al. (2000a). Reprinted with permission from CSIRO Publishing (www.publish.csiro.au).

16

Elevated pressure and temperature enhance direct aqueous mineral carbonation. Increased pressure facilitates the dissolution of CO_2, thereby driving the reaction forward. Increases in temperature decrease the solubility constant of both $CaCO_3$ and $MgCO_3$ and increase the dissociation of aqueous CO_2 to bicarbonate, and then to carbonate. Increasing temperature, however, decreases the solubility of CO_2, placing an upper limit on the degree to which increased temperature can enhance the reaction. For olivine and heat-treated serpentine, optimum temperatures for direct aqueous carbonation at 150 bar have been reported as 185ºC and 155ºC respectively (Gerdemann et al., 2003; Chen et al., 2006). The carbonation reaction rate can be further accelerated by utilizing a bicarbonate/salt ($NaHCO_3$/$NaCl$) mixture as the slurry supernatant (Metz et al., 2005; Huijgen and Comans, 2003; Maroto-Valer et al., 2005; Sipilä et al., 2008; O'Connor et al., 2000a), adding acids or other chemical activators (Maroto-Valer et al., 2004), and employing various pre-treatment techniques, such as comminution to small particle sizes (typically < 75 μm) (O'Connor et al., 2000a; Gerdemann et al., 2003; Alexander et al., 2007), magnetic separation to remove any magnetite liberated during mineral comminution (iron compounds form a passivating layer on silicate particles and inhibit carbonation) (Alexander et al., 2007), and heat treatment to remove hydration water in the case of serpentine (Gerdemann et al., 2007; Gerdemann et al., 2003; O'Connor et al., 2000b).

High carbonate conversions and acceptable reaction rates have been achieved using the direct aqueous method by optimizing the reaction conditions, modifying the solution chemistry, and using pre-treatments (Huijgen and Comans, 2003; Maroto-Valer et al., 2005; Goldberg et al., 2001). Unfortunately, the pre-treatments tend to be very energy intensive. As a result the direct aqueous carbonation process is still too expensive to be applied on a large scale (Sipilä et al., 2008). Research has been focused on understanding the reaction mechanisms and kinetics (Prigiobbe et al., 2009b; Prigiobbe et al., 2009c; Dufaud et al., 2009), improving the kinetics by varying the process conditions and contents of the aqueous phase (Krevor and Lackner, 2009; Zhao et al., 2010), developing improved pre-treatment techniques (Haug et al., 2010; Jang et al., 2010) and

studying the applicability of different kinds of waste products as source materials (Uibu et al., 2010; Baciocchi et al., 2009a; Wang et al., 2010). Despite the fact that no direct aqueous mineral carbonation scheme has yet been proven economical, it is thought by many to be the most promising CO_2 mineralization technique to date (Huijgen and Comans, 2003; Sipilä et al., 2008; Lackner, 2003).

2.2.2 Indirect Carbonation

Indirect mineral carbonation refers to any mineral carbonation process that takes place in more than one stage. Typically indirect carbonation involves the extraction of reactive components (Mg^{2+}, Ca^{2+}) from the minerals, using acids or other solvents, followed by the reaction of the extracted components with CO_2 in either the gaseous or aqueous phase. An advantage of indirect carbonation is that it allows pure carbonates to be produced because impurities, such as silica and iron, can be removed prior to carbonate precipitation (Eloneva et al., 2008a). A number of technologies are available for extracting the reactive components from the minerals including HCl extraction, the molten salt process, other acid extraction, bioleaching, ammonia extraction and caustic extraction.

2.2.2.1 HCl Extraction

The hydrochloric acid (HCl) extraction process was developed in the 1940's and 1950's for the extraction of magnesium from serpentine (Goff and Lackner, 1998). It consists of three extraction steps followed by a carbonation step, shown by reactions 2.9-2.12 (Huijgen and Comans, 2003; Goff and Lackner, 1998; Ziock et al., 1998). While the process is effective, it has a number of shortcomings. It is very energy intensive (Ziock et al., 1998), does not work well when there is greater than 1% alkali metals in the feedstock, and can result in extraction and precipitation of iron, which becomes an undesirable contaminant during the carbonation process (Huijgen and Comans, 2003). For these reasons, the HCl extraction process has not generated much interest since the late 1990s, although it has formed the basis for the development of several other extraction procedures, including the molten salt process and other acid extraction techniques.

$$Mg_3Si_2O_5(OH)_{4(s)} + 6HCl_{(aq)} + H_2O \xrightarrow{100^oC} 3MgCl_2 \cdot 6H_2O_{(aq)} + 2SiO_{2(s)} \quad (2.9)$$

$$MgCl_2 \cdot 6H_2O_{(aq)} \xrightarrow{250^oC} MgCl(OH)_{(aq)} + HCl_{(aq)} + 5H_2O \quad (2.10)$$

$$2MgCl(OH)_{(aq)} \xrightarrow{Cooling} Mg(OH)_{2(s)} + MgCl_{2(aq/s)} \quad (2.11)$$

$$Mg(OH)_{2(s)} + CO_{2(g)} \rightarrow MgCO_{3(s)} + H_2O \quad (2.12)$$
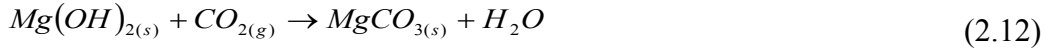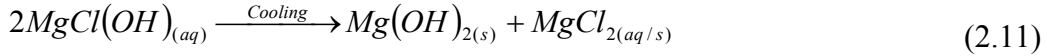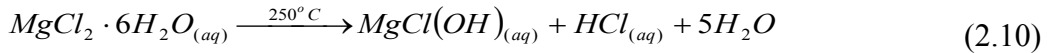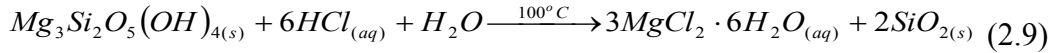
2.2.2.2 Molten Salt Process

The molten salt process was developed in an effort to lower the energy requirements of the HCl extraction process. It is very similar, except the molten salt, $MgCl_2 \cdot 3.5H_2O$, instead of HCl, is used as the extraction agent (Huijgen and Comans, 2003). There are two variations of the process. The first occurs in multiple stages (reactions 2.13-2.16) while the second is really a direct carbonation process where the carbonation takes place directly in molten $MgCl_2 \cdot 3.5H_2O$ at 300°C under 30 bar CO_2 pressure (Huijgen and Comans, 2003; Ziock et al., 1998).

$$Mg_3Si_2O_5(OH)_{4(s)} + 3MgCl_2 \cdot 3.5H_2O_{(aq)} \xrightarrow{200^oC} 6Mg(OH)Cl_{(aq)} + 2SiO_{2(s)} + 9.5H_2O$$
$$(2.13)$$

$$Mg(OH)Cl_{(aq)} + nH_2O \xrightarrow{150^oC} MgCl_2 \cdot nH_2O_{(aq)} + Mg(OH)_{2(s)} \quad (2.14)$$

$$MgCl_2 \cdot nH_2O_{(aq)} \xrightarrow{100-250^oC} MgCl_2 \cdot 3.5H_2O_{(aq)} + (n-3.5)H_2O_{(l)} \quad (2.15)$$

$$Mg(OH)_{2(s)} + CO_{2(g)} \rightarrow MgCO_{3(s)} + H_2O \quad (2.16)$$
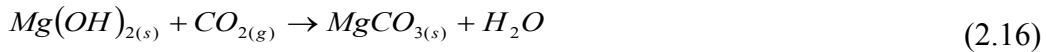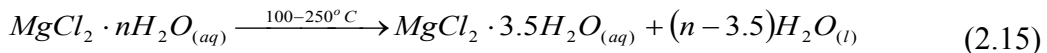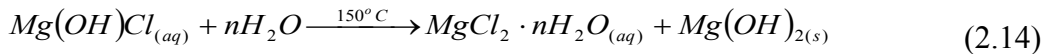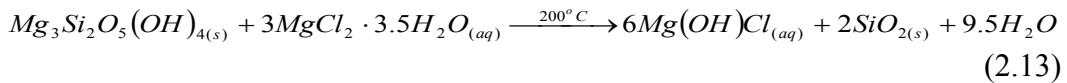
While the molten salt process is less energy intensive than the HCl extraction process, the solvent is extremely corrosive and difficult to work with. In addition, despite the fact the solvent is recycled, make-up $MgCl_2 \cdot 3.5H_2O$ is inevitably required. It has been estimated that even if a commercial supply of $MgCl_2$ could be attained, it would be unaffordable (Huijgen and Comans, 2003). Additional issues with the process include continuous dilution of the solvent by water released from the minerals (if serpentine is used), and the potential for the formation of sorel cements (Ziock et al., 1998). Because of these issues, the

molten salt process for mineral carbon sequestration has not received much interest over the last 10 years.

2.2.2.3 Other Acid Extraction

Aside from HCl, a number of other acids have been investigated as extraction agents in indirect mineral carbonation processes. Teir et al., (2007a) found that acetic acid (CH_3COOH), sulphuric acid (H_2SO_4), nitric acid (HNO_3) and formic acid (HCOOH), as well as HCl, all leached a significant amount of magnesium from serpentine. Krevor and Lackner (2009) established that the sodium salts of citrate, oxalate, and ethylenediaminetetraacetic acid (EDTA) significantly enhanced the dissolution of serpentine under weakly acidic conditions. Succinic acid was found by Baldyga et al. (2010) to be an efficient leaching agent for calcium from wollastonite. Park et al. (2003) demonstrated that a mixture of 1 vol.% orthophosphoric acid, 0.9 wt.% oxalic acid and 0.1 wt.% EDTA greatly enhanced the leaching of magnesium from serpentine. The use of internal agitation with grinding media during acid digestion has been reported by Park and Fan (2004) and Van Essendelft and Schobert (2009) to greatly improve the extraction of magnesium from serpentine.

Indirect mineral carbon sequestration utilizing acid extraction can be accomplished in several ways. The simplest method involves mixing the mineral and acid, usually in a stirred reactor at a specified temperature and pressure to extract the reactive components, followed by carbonation of the extract. Shortcomings of this approach include poor dissolution of CO_2 under acidic conditions and the requirement of high pH for effective carbonate precipitation (Park and Fan , 2004; Teir et al., 2007b). To address these issues, Park and Fan (2004) developed a pH swing process in which after the acid extraction, the pH is raised to 9.5 for the carbonation phase. In this process, impurities, such as iron, can be removed at an intermediate pH prior to carbonate precipitation, producing high purity carbonates as a value-added, marketable product (Park and Fan, 2004).

It is generally recognized that mineral carbon sequestration processes using acid extraction cannot be economically feasible without chemical recycle (Teir et al., 2007a). Several contemporary acid extraction processes have been developed in an attempt to efficiently recover and re-use the reagents (Teir et al., 2007b; Kakizawa et al., 2001). A process developed by Teir et al. (2007b) is similar in some ways to both the HCl extraction and pH swing processes and uses either 4 M HCl or HNO_3 as the extraction agent. Magnesium is extracted from serpentine at 70°C over 1-2 hours with acid, after which the acid is recovered (70-80%) by distillation. The solids are then dried to remove as much acid as possible before being recombined with water at pH 7 to precipitate iron. Lastly, the pH is increased to 9.5 with NaOH for the carbonation step. This process results in high magnesium to carbonate conversions and yields relatively pure carbonate, but the exorbitant reagent costs ($600-1600/t CO_2 for NaOH and make-up acid) are prohibitively high and render the process impractical for mineral carbon sequestration (Teir et al., 2007b). Kakizawa et al. (2001) developed a process for mineral carbon sequestration using calcium silicates as the source material and acetic acid as the extraction agent. In this process, the mineral is first treated with acetic acid to extract the calcium and precipitate the silica. The resultant solution is then reacted with CO_2 to carbonate the calcium and regenerate the acetic acid (Figure 2-4). The Gibbs free energy of these two steps is negative and the reactions should proceed spontaneously. Depending on the CO_2 pressure, however, the Gibbs free energy of the second step may not always be sufficiently large to obtain high carbonate conversions (Kakizawa et al., 2001). The acetic acid extraction process, estimated to cost US$27/ton CO_2 (Kakizawa et al., 2001), could potentially be competitive with geologic carbon sequestration processes, although the assumptions used to determine the process economics were based on a limited set of experimental data (Metz et al., 2005). Even though effective, indirect mineral carbon sequestration with acid extraction is generally still too expensive to be competitive with other CO_2 storage techniques.

21
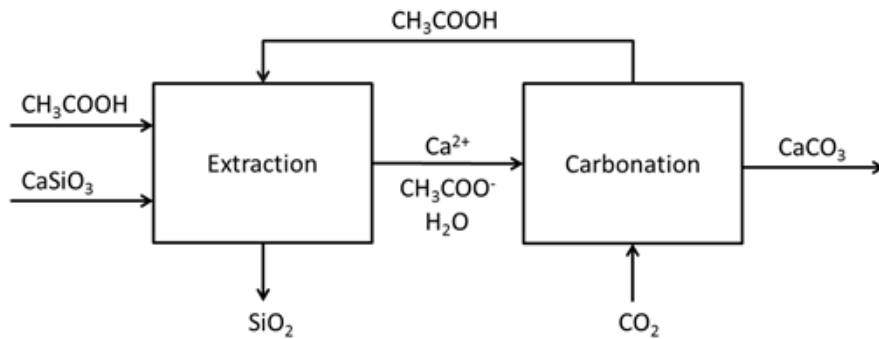
Figure 2-4: Schematic of an acetic acid extraction process for mineral carbon sequestration.

2.2.2.4 Bioleaching

Bioleaching, the process of utilizing bacteria to extract metals from minerals (Bosecker, 1997), can be applied for the extraction of calcium and magnesium from silicates for the purpose of mineral carbon sequestration. In natural environments, the weathering of silicate rocks is enhanced by the biological production of inorganic and organic acids in soils that overlay bedrock (Schwartzman and Volk, 1989). The process can be artificially augmented by combining acid generating substances (AGS), such as sulphides and elemental sulphur, with silicate minerals and chemolithotrophic bacteria, such as *Acidithiobacillus (A.) ferrooxidans* and *A. thiooxidans* (Power et al., 2010). *A. ferrooxidans* oxidizes both ferrous ions and reduced sulphur compounds while *A. thiooxidans* oxidizes only reduced sulphur compounds: both generate sulphuric acid as a by-product of metabolism (Bosecker, 1997). Thus, the AGS provides the food for the bacteria, the bacteria in turn generate sulphuric acid, and the sulphuric acid leaches metal ions from the silicate minerals. The leached metal ions can then be carbonated for the purpose of CO_2 sequestration. In addition, *A.* species use CO_2 from the atmosphere, rather than organic carbon, for the synthesis of new cell material (Bosecker, 1997; Power et al., 2010). As a result, carbon is also fixed biologically during the process. A tailings impoundment

designed to facilitate passive mineral carbon sequestration by bioleaching is depicted in Figure 2-5.
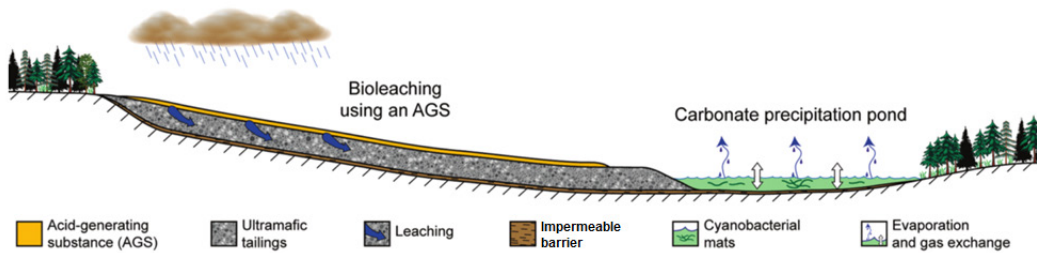
Figure 2-5: Schematic of a geoengineered tailings facility for mineral carbon sequestration using bioleaching. Reprinted with permission from Power et al. (2010). Copyright 2010 American Chemical Society.

The bioleaching process for mineral carbon sequestration has not been optimized to achieve high leaching rates and, in fact, Power et al. (2010) limited the addition of AGS to avoid the generation of acidic leachate. While the process currently cannot compete with other indirect mineral carbon sequestration techniques in terms of reaction kinetics, bioleaching represents an innovative, low cost, passive process geared towards using waste products for both the metal ion and acid source while accelerating mineral dissolution by bacteria for carbon sequestration. It has all the hallmarks of a sustainable process, and with further development, could be used by facilities that generate and store alkaline waste residues as well as acid generating substances, such as sulphide mining operations, to mitigate their CO_2 emissions.

2.2.2.5 Ammonia Extraction

Various ammonium salts have been tested for extracting metals from silicate rocks for the purpose of mineral carbon sequestration. The original process, designed for the production of silica, iron oxide and magnesium carbonate from serpentine, CO_2 and ammonium bisulphate, was described by Pundsack (1967) in a US patent. The pertinent reactions are:

$$Mg_3Si_2O_5(OH)_4\left(Fe^{2+},Fe^{3+}\right)_{(s)} + 6NH_4HSO_{4(aq)} \xrightarrow{heat} 3MgSO_4\left(Fe^{2+},Fe^{3+}\right)_{(aq)}$$
$$+ 2SiO_{2(s)} + 3(NH_4)_2SO_{4(aq)} + 5H_2O$$

$$(2.17)$$

$$3MgSO_4\left(Fe^{2+},Fe^{3+}\right)_{(aq)} + 8NH_4OH_{(aq)} \xrightarrow{pH\ to\ 8.5} \frac{Fe_2O_3}{FeO}_{(s)} + 3MgSO_4 + 8NH_4^+$$
$$+ 4H_2O$$

$$(2.18)$$

$$6MgSO_4 + 6(NH_4)_2SO_{4(aq)} + \frac{24}{5}CO_{2(g)} + 12NH_4OH_{(aq)} \rightarrow$$
$$\frac{6}{5}(4MgCO_3 \cdot Mg(OH)_2 \cdot 5H_2O)_{(s)} + 12(NH_4)_2SO_{4(s)}$$

$$(2.19)$$

$$(NH_4)_2SO_{4(s)} \xrightarrow{320^o C} NH_4HSO_{4(aq)} + NH_{3(g)} \qquad (2.20)$$
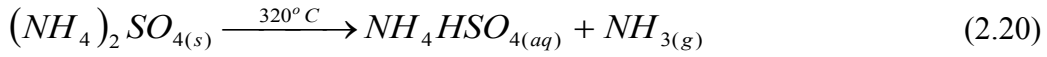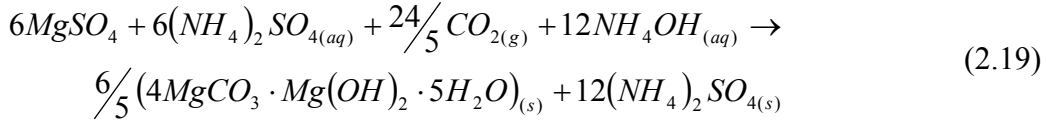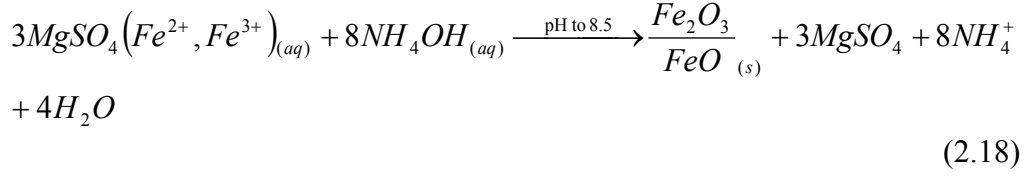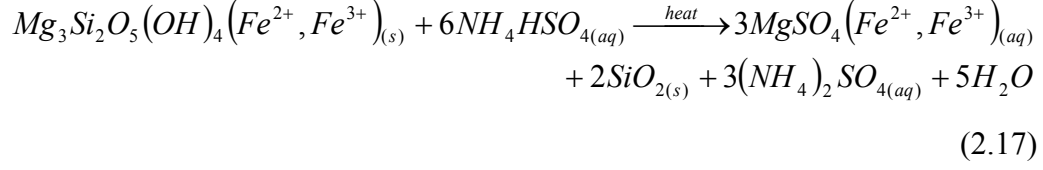
While the process developed by Pundsack (1967) was not intended for carbon sequestration, it can be used for this purpose. In fact, the first three steps are essentially analogous to the pH swing process developed by Park and Fan (2004). A variation of the two processes using NH_4Cl as the extraction agent, which is regenerated during carbonation, was developed by Kodama et al (reactions 2.21 and 2.22) (Kodama et al., 2008). A caustic agent is not required to raise the pH for carbonate precipitation in this process as the generation of ammonia as the reaction proceeds renders the solution more alkaline. The selectivity of calcium extraction by this technique has been reported to be as high as 99% (Kodama et al., 2008).

$$4NH_4Cl_{(aq)} + 2CaO \cdot SiO_{2(s)} \rightarrow 2CaCl_{2(aq)} + 2SiO_{2(s)} + 4NH_{3(aq)} + 2H_2O \qquad (2.21)$$

$$4NH_{3(aq)} + 2CO_{2(g)} + 2CaCl_{2(aq)} + 4H_2O \rightarrow 2CaCO_{3(s)} + 4NH_4Cl_{(aq)} \qquad (2.22)$$
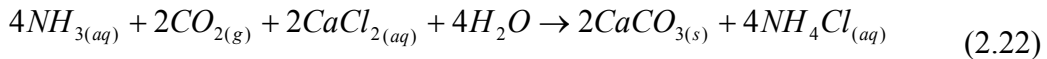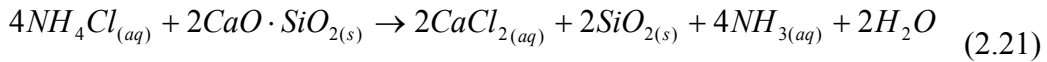
Although not ready for commercialization, the ammonia extraction process appears to be a promising technique as part of a mineral carbon sequestration scheme given the potential for reagent recovery and the selectivity of the leaching agents.

2.2.2.6 Caustic Extraction

The use of caustic soda for the extraction of Ca and Mg from silicate minerals for the purpose of mineral carbonation was first proposed by Blencoe et al. (2004). The process using wollastonite as a feedstock is given in reactions 2.23-2.25. Other minerals such as anorthite, labradorite, Ca-rich fly ash, olivine and serpentine, were also proposed as source minerals for Ca and Mg extraction by caustics, but no experimental results are currently available (Blencoe et al., 2004).

$$CaSiO_{3(s)} + NaOH_{(aq)} \xrightarrow{200^o C} NaCaSiO_3(OH)_{(s)} \tag{2.23}$$

$$2NaOH_{(aq)} + CO_{2(aq)} \xrightarrow{200^o C} Na_2CO_{3(aq)} + H_2O \tag{2.24}$$

$$Na_2CO_{3(aq)} + NaCaSiO_3(OH)_{(s)} + H_2O \xrightarrow{200^o C} 4NaOH_{(aq)} + CaCO_{3(s)} + NaCa_2Si_3O_8(OH)_{(s)} \tag{2.25}$$
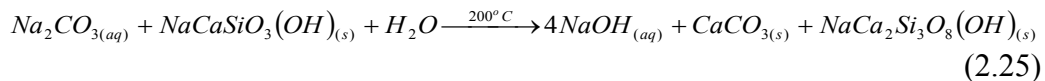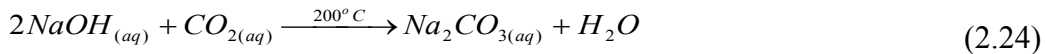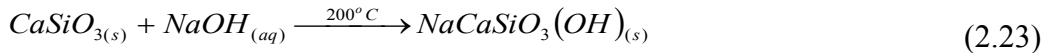
Teir et al. (2007a) tested the use of caustic soda for extraction of Mg from serpentine; however, the results were not promising. Based on the lack of interest in caustic extraction and the inherent limitations of the process, caustic extraction does not appear to be a promising technique for indirect mineral carbonation.

2.3 Waste Products for Mineral Carbonation

Alkaline waste residues have some distinct advantages over natural mineral feedstocks for carbon capture and storage by mineral carbonation. When waste residues are used in mineral carbonation, mining is not required and the consumption of raw materials is avoided (Huijgen and Comans, 2005), as are the costs and environmental impacts associated with these operations. In many cases, comminution may also be avoided as the wastes are already of a particle size suitable for mineral carbonation (Gerdemann et al., 2007). In general, the wastes tend to be of little value, are available cheaply (Huijgen and Comans, 2003), and are generated in industrial areas near point sources of CO_2 emissions, greatly reducing the cost of transporting either CO_2 or mineral carbonation feedstock. Alkaline waste residues are, in general, highly reactive and do not require pre-treatment to achieve high carbonate conversions (Huijgen and Comans, 2003). In

addition, the carbonation of alkaline waste residues can improve their environmental qualities (Huijgen and Comans, 2003) and allow them to be stored more safely, reused, or sold as value-added by-products. Although the quantity of alkaline wastes available is small compared to known resources of natural silicate minerals, they could fix a meaningful amount of CO_2 in some industries, especially where alkaline wastes and CO_2 are produced by the same facility. In addition, because of the cost advantages and general ease with which they can be carbonated, alkaline waste residues could help introduce the technology into the marketplace at an industrial scale (Metz et al., 2005; Huijgen and Comans, 2005).

Criteria similar to that applied to the selection of natural minerals for mineral carbon sequestration is used in the selection of alkaline waste residues. Residues containing a substantial amount of the alkaline earth metals calcium and magnesium and a high degree of alkalinity are desirable. Wastes that do not require comminution or are generated in close proximity to the CO_2 source are also preferable. A variety of alkaline waste residues have been tested for mineral carbonation purposes, including steelmaking slags, cement wastes, mining and mineral processing wastes, waste ashes, and alkaline paper mill wastes. The carbon sequestration capacity of these wastes varies and largely depends on the content of calcium and/or magnesium and their accessibility in the mineral phases present. For example, a waste containing a high percentage of free calcium in oxide form carbonates more readily than a waste with the same calcium content, but with the calcium present in silicates. It is difficult, however, to compare the desirability and efficiency of various alkaline wastes for mineral carbon sequestration. First of all, mineral carbonation research results presented in the literature are in a variety of forms that are not easily translated from one to another. Results may be presented in mass of CO_2 sequestered per mass of waste residue, percent of the alkaline earth metal converted to carbonate, or as percent carbonates in the final product. Secondly, the wastes possess different and contrasting attributes. One waste may have a low carbon sequestration capacity but be generated in large quantities, while another may have a high carbon sequestration capacity but be generated in very limited quantities. Thirdly, the

type and extent of information available, such as data on the process economics, scalability and life cycle analysis, varies from one waste to another. Thus, instead of comparing the wastes directly, the pros and cons of each waste will be weighed, the different mechanisms by which they can be carbonated discussed, and carbonation results presented. A survey of the literature and available information on mineral carbonation sequestration using alkaline waste residues is presented below.

2.3.1 Steelmaking Slags

Steelmaking operations produce significant quantities of CO_2 (6-7% of total CO_2 emissions worldwide (Doucet, 2010); 0.28-1 ton of CO_2/ton of steel produced (Bonenfant et al., 2008a)) and slags (315-420 Mt/yr globally (Eloneva et al., 2008b)) that can be used as feedstock for mineral carbonation (Gerdemann et al., 2007). Slags are produced at various stages of the steelmaking process through the reaction of process impurities (primarily silica) with lime (Eloneva et al., 2010; Teir et al., 2007c). There are four main types of steelmaking slags, including blast furnace (BF), basic oxygen furnace (BOF), electric arc furnace (EAF), and ladle furnace (LF) slag, named for the processes from which they are produced. The slags are a consolidated mix of many compounds, primarily calcium, iron, silicon, aluminum, magnesium, and manganese oxides that are present in different phases (Bonenfant et al., 2008a). The composition of these slags tends to be highly variable, even within the same plant (Teir et al., 2007). The slags are highly alkaline (~pH 12), and this, combined with their high calcium content (32-52% CaO) (Eloneva et al., 2008a), makes them a candidate for mineral carbon sequestration. It is estimated that, worldwide, steelmaking slags could store up to 171 Mt of CO_2 every year (Eloneva et al., 2008a), about 0.6% of global CO_2 emissions from fuel combustion (IEA, 2012). Generally speaking, steelmaking slags have to undergo comminution to be suitable for mineral carbon sequestration. However, the cost of mining and, in many cases, the cost of transporting the minerals to CO_2 emissions sites can be avoided. Steelmaking slag can be used to produce precipitated calcium carbonate (PCC),

which is used as a filler and coating pigment in plastics, rubbers, paints, and papers (Eloneva et al., 2008b). In addition, the carbonation of steel slag can improve its mechanical characteristics and make it more desirable for use as construction material (Baciocchi et al., 2009c). Research on the carbonation of steel making slags for the purpose of CO_2 sequestration has largely been focused on direct and indirect aqueous phase carbonation.

The direct aqueous carbonation of steelmaking slags has been studied by Huijgen et al. (2005), Bonenfant et al. (2008a), and Lekakh et al. (2008). Carbonation has been accomplished successfully both at ambient conditions (24.7 g CO_2/100 g slag (Bonenfant et al., 2008a)) and at elevated temperatures and pressures (74% carbonate conversion at 100°C and 19 bar (Huijgen et al., 2005)), generally with water as the medium. Although the extent of carbonation achieved appears to depend primarily on the elemental and mineral composition of the slag, the carbonation kinetics are significantly faster at increased temperatures and pressures. Slags with higher Ca content are more reactive, especially if the Ca is present primarily as free CaO or $Ca(OH)_2$ as opposed to calcium silicate (Bonenfant et al., 2008a). Particle size is also an important variable, with smaller particles (38-106 μm) carbonating significantly better than larger ones (Huijgen et al., 2005; Bonenfant et al., 2008a; Lekakh et al., 2008). The carbonation of steelmaking slags utilizing the direct aqueous method has been found to take place in two steps: dissolution and precipitation. After rapid carbonation of any $Ca(OH)_2$ present , calcium from Ca-silicates diffuses to the surface of the particles and is leached. The leached Ca is then carbonated and precipitated on the surface of the slag particles. The leaching of Ca results in a Ca-depleted SiO_2 zone around a Ca silicate core (Figure 2-6). The layer of precipitated calcium carbonation impedes the diffusion of Ca from the particle interior and reduces the reaction rate (Huijgen et al., 2005; Lekakh et al., 2008). Given that positive results have been achieved under a variety of process conditions, direct aqueous mineral carbon sequestration utilizing steelmaking slags appears promising, although the economics of such processes have not been established.
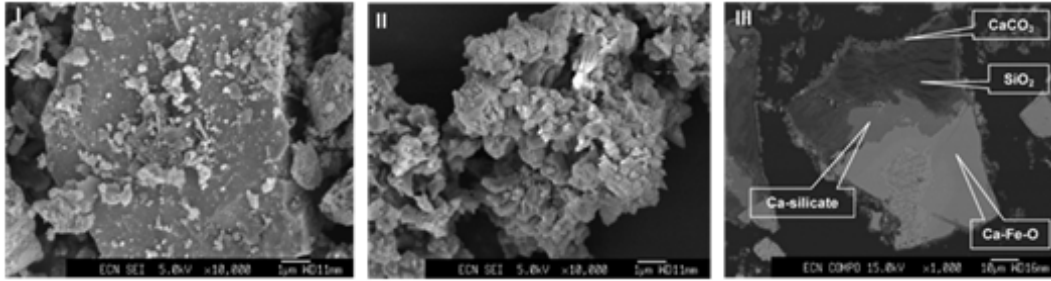
Figure 2-6: SEM micrographs of (I) fresh slag, (II) carbonated slag and (III) a polished section of carbonated slag embedded in resin. Reprinted with permission from Huijgen et al. (2005). Copyright 2005 American Chemical Society.

Various extraction agents have been investigated for indirect aqueous mineral carbonation of steelmaking slag, including nitric acid (HNO_3), sulphuric acid (H_2SO_4), sodium hydroxide ($NaOH$) (Doucet (2010)), ammonium chloride (NH_4Cl) (Kodama et al., 2008)), and acetic acid (CH_3COOH) (Eloneva et al., 2008b; Bao et al., 2010). The work by Doucet (2008) focused mainly on the extraction phase of the indirect carbonation process at room temperature. HNO_3 and H_2SO_4 were found to be effective leaching agents, whereas $NaOH$ was not. Over one hour, HNO_3 and H_2SO_4 extracted 71-89% and > 95% Ca respectively. Since much of the leached Ca in the H_2SO_4 experiment reacted with sulphate ions and precipitated as gypsum, it was less available for reaction with CO_2. Thus, HNO_3 was concluded to be a better extraction agent than H_2SO_4. The effective sequestration capacity of the slags tested using nitric acid as the extraction agent was determined to be 0.26 to 0.38 kg CO_2/kg slag (Doucet, 2010).

The indirect aqueous mineral carbonation of steelmaking slag utilizing NH_4Cl as the extraction agent has been studied by Kodama et al. (2008). They found that the extent of leaching increased with decreasing particle size and increasing reaction temperature, while the carbonate conversion increased with decreasing particle size and temperature. At 80°C and atmospheric pressure, 60% of Ca was extracted from the mineral with 99% selectivity. Conversion of the extracted Ca to carbonate was 70% and the calcium carbonate produced was quite pure (98%).

Based on the data provided in this study, the carbon sequestration capacity of the slag was calculated to be 0.16 kg CO_2/kg slag. Although costs for the process were not given, the energy consumption was estimated to be 300 kWh/t-CO_2 (Kodama et al., 2008).

In the studies using acetic acid as an extraction agent by Eloneva et al. (2008b) and Bao et al. (2010), the primary goal, aside from fixing CO_2, was to produce pure PCC. Both groups of researchers encountered difficulties with poor selectivity during the leaching stage. Other elements, such as aluminum, silica and iron, were also extracted into the aqueous phase with calcium. These elements co-precipitate with calcium carbonate in the carbonation step and contaminate the product. Using a weak acid solution improved the selectivity, but it reduced net Ca extraction (Eloneva et al., 2008b; Bao et al., 2010). Increased temperatures and longer reaction times were found to favour the selective extraction of Ca (Bao et al., 2010). Another challenge encountered was that the precipitation of $CaCO_3$ was not favoured at the low pH conditions generated by the acetic acid. This was resolved by the addition of NaOH (Eloneva et al., 2008b). Using the acetic acid extraction technique, the conversion of extracted Ca to carbonate has been reported as 31-86% while producing PCC of 99.5-99.8% purity (Eloneva et al., 2008b). Based on the results reported by Eloneva et al. (2008b), the carbon sequestration capacity of the slag processed in this manner was estimated to be 0.09 kg CO_2/kg slag at a cost of € 1167/t CO_2. On this basis, the acetic acid extraction process is too expensive to be economically feasible. At this time, the direct aqueous approach appears to be the superior technique for the mineral carbonation of steelingmaking slags.

2.3.2 Cement Wastes

Traditional Portland cement, the main binder used in the production of concrete, is composed primarily of lime (usually from limestone), silica (from sand or fly ash), alumina (from clay, shale or fly ash), and iron oxide (from iron ore). These materials are combined and calcined in a kiln, where temperatures can exceed 1400°C, to produce clinker. The clinker is cooled and, just prior to packaging,

combined with gypsum to produce Portland cement (Huntzinger and Eatmon, 2009). Annually, world output of cement is 2.8 Gt, and this is expected to increase to 4.0 Gt (Schneider et al., 2011). The cement industry is one of the world's largest CO_2 emitters, generating 5% of global CO_2 emissions (Huntzinger and Eatmon, 2009; Huntzinger et al., 2009). Roughly half the CO_2 is generated during calcining (where limestone, mostly calcite, is converted to lime), while the other half is from the combustion of fossil fuels (Huntzinger et al., 2009). In addition to CO_2, the cement industry also produces millions of tonnes of cement kiln dust (CKD). For every 100 t of cement produced, 15-20 t of CKD is generated (van Oss and Padovani, 2003). CKD, composed of fine particulates of unburned and partially burned raw materials, is collected from the combustion gases within pre-heater and kiln systems. This waste material is usually landfilled or stockpiled. Due to its caustic nature and potential as a skin, eye and respiratory irritant, CKD is a potentially hazardous waste (Huntzinger and Eatmon, 2009).

A waste product similar to CKD is waste cement. Waste cement is generated as a by-product of aggregate recycling processes where waste concrete, primarily from demolished buildings, is pulverized and classified to separate the aggregate from the waste cement. Waste cement can be used as a roadbed material, but it most often disposed of (Katsuyama et al., 2005). All concrete that goes into building materials will eventually become a waste product as the average lifetime of a building is 50-100 years (Rodrigues and Joekes, 2011). Considering world concrete production is estimated at 10 Gt (Rodrigues and Joekes, 2011), and the quantity of waste cement generated in aggregate recycling processes can be as high as 1/3 the mass of the waste concrete (Katsuyama et al., 2005), waste cement represents a potentially huge source of mineral carbon sequestration feedstock. Examples of current annual waste concrete production values include 663 Mt in the European Union (78% of 850 Mt construction and demolition waste) (Fischer and Werge, 2011), an estimated 239 Mt in China (Li, 2008), and 200 Mt in the United States (US EPA, 2011).

CKD and waste cement have the potential to be used for mineral carbon sequestration. Both have a high mass fraction of CaO (20-60%), are available in large quantities, and are highly reactive due to their small particle sizes, although waste cement must be ground if it does not come from an aggregate recovery process. The carbonation product, $CaCO_3$, is less hazardous than the feedstock and can be re-used in cement manufacturing (preventing the release of CO_2 from virgin limestone) or in other industrial processes. Thus, the carbonation of cement wastes not only sequesters carbon and recycles cement, but also mitigates the potential health hazards associated with CKD disposal (Huntzinger et al., 2009; Iizuka et al., 2004).

While the potential of cement wastes for carbon sequestration has been widely recognized (Metz et al., 2005; Huijgen and Comans, 2003; Stolaroff et al., 2005; Fernández Bertos et al., 2004a), few experimental results on the carbonation of cement wastes are available in open literature (in comparison to the literature on the carbonation of steelmaking slags). Huntzinger et al. (2009) and Gunning et al. (2010) studied the direct carbonation of CKD. Because CKD is separated during preheating of the feed to the cement kiln, where the temperature is not sufficient for total calcination, significant carbonates can be present in the dust, reducing the carbon sequestration capacity of the waste despite high Ca content. Thus, the CO_2 uptake by mass achieved in these studies was only 11.5% (at ambient temperature and pressure over 3 days (Huntzinger et al., 2009)) and 9% (at ambient temperature and 2 bar over 72 hours (Gunning et al., 2010)). Gunning et al. (2010) also investigated the mineral carbonation of cement bypass dust (CBD). Because CBD is removed from the cement manufacturing process after kiln firing, the carbonate content in the source material is much lower than CKD and, thus, the extent of carbonation achieved was improved at 26% by weight (Gunning et al., 2010). Assuming a CO_2 uptake of 10% by mass, and taking the mass of CKD generated on a global basis each year to be 15% of 2.8 Gt (Schneider et al., 2011; van Oss and Padovani, 2003), CKD has the potential to store 42 Mt of CO_2 annually, about 0.1% of global CO_2 emissions from fuel combustion (IEA, 2012).

Teramura et al. (2000) and Katsuyama et al. (2005) examined the direct carbonation of waste concrete. Teramura et al. (2000) developed a building material from recycled waste concrete using a CO_2-activated hardening process. In this process, waste cement powder was mixed with water to a moisture content of 50% before being cast in a mold and pressed to form bricks. The bricks were cured with CO_2 under pressure and then dried in an oven. A carbonate conversion of 100%, or 16.5% CO_2 by mass, was achieved at 4 bar in 0.8 hours (Teramura et al., 2000). Katsuyama et al. (2005) evaluated the feasibility of producing $CaCO_3$ through the direct aqueous carbonation of waste concrete (Figure 2-7). The process used 200μm waste cement containing approximately 24.3% Ca and was assumed to occur in water at 323 K and 30 bar CO_2, followed by a lower pressure stage at 1 bar, with a total retention time of 6 minutes. The researchers concluded that it is be possible to produce $CaCO_3$ with a purity of 98% for US$136/tonne, a figure highly competitive with the market price of $CaCO_3$ of about US$400/tonne (Katsuyama et al.. 2005). Assuming a CO_2 uptake of 16.5%, and taking the waste concrete produced in the European Union, China, the United States to be approximately one third waste cement, these countries could collectively sequester nearly 61 Mt of CO_2 on an annual basis using cement waste alone, accounting for 0.2% of global CO_2 emissions from fuel combustion (IEA, 2012). Mineral carbon sequestration using cement wastes appears to be attractive due to the large quantity of waste available, the ease with which the wastes are carbonated, and the potential for the wastes to be converted to reusable products.
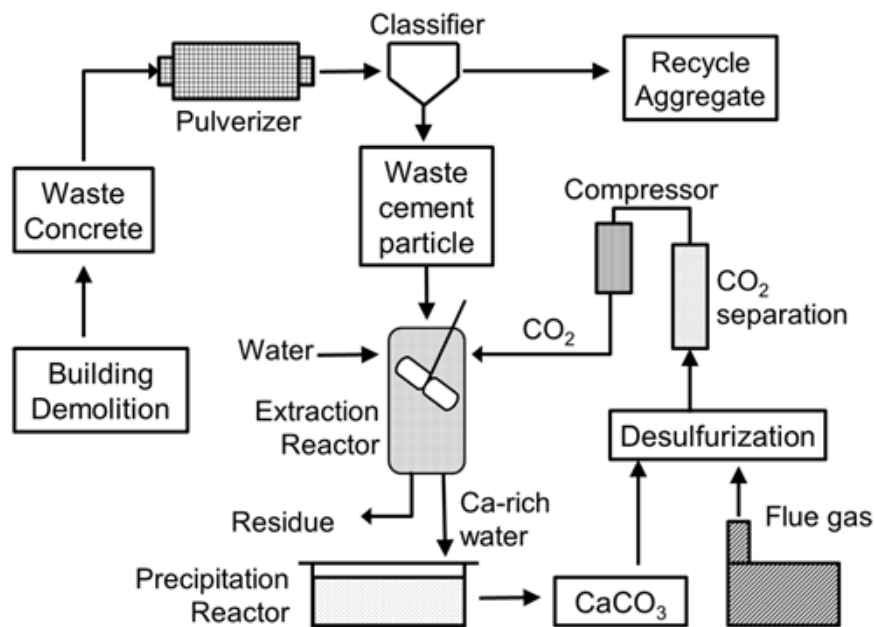
Figure 2-7: Process flow diagram for production of CaCO₃ from CO₂ and cement waste. The CaCO₃ produced could be sold as a high purity reagent or used as a desulfurization agent. Reprinted with permission from Katsuyama et al. (2005). Copyright 2008 Wiley InterScience.

2.3.3 Mining and Mineral Processing Wastes

Alkaline mining and mineral processing wastes are desirable as mineral carbonation feedstock as they have already been mined and ground to fine particle sizes for metal extraction (Larachi et al., 2010; Power et al., 2010; Wilson et al., 2009a). A number of deposit types, most hosted in ultramafic rock, produce tailings suitable for mineral carbonation. These include asbestos deposits and copper-nickel-PGE (platinum group elements) deposits hosted by dunite, serpentinite, and gabbronorite, as well as diamondiferous kimberlite pipes and podiform chromite deposits (Power et al., 2010; Wilson et al., 2009a). Another type of mineral processing waste suitable for mineral carbon sequestration is bauxite residue, or red mud, from alumina processing (Sahu et al., 2010; Yadav et al., 2010; Bonenfant et al., 2008b). The carbonation of these residues, particularly

asbestos tailings and red mud, not only sequesters CO_2, but also improves the properties of the wastes so they can be more safely stored or used for secondary purposes. In addition, the carbonation of alkaline wastes generated at mining and mineral processing sites could provide a practical solution for lowering carbon emissions (Hitch et al., 2010), which will be more tightly regulated in this industry in the near future (Marcuson et al., 2009). The carbon sequestration capacity of the waste generated at these sites often exceeds the greenhouse gas production of the operation (Wilson et al., 2009b), and, thus, represents an opportunity for the sequestration of external CO_2 streams. Under a carbon cap-and-trade scheme, or other incentive plan to reduce carbon emissions, the use of mineral wastes for carbon sequestration could translate into another revenue stream for mining and milling operations (Hindle and Hitch, 2010).

2.3.3.1 Asbestos Tailings

Chrysotile is the principal type of asbestos used for insulation and construction materials (Goff and Lackner, 1998). It is also the most reactive mineral in the serpentine group (Metz et al., 2005). World production of asbestos is about 4 Mt, and for each tonne of asbestos produced, 20 tonnes of tailings are generated (Habashi, 2001). The tailings from chrysotile mining and processing typically contain residual asbestos and are often classified as hazardous. These tailings could be ideal for mineral carbonation, not only because of their high MgO content (about 40% (Habashi, 2001)) and the fact that mining and size reduction have already taken place, but because the asbestiform nature of the mineral is destroyed when chrysotile is carbonated. Thus, carbonation of these tailings could result in both the remediation of a hazardous waste and the sequestration of CO_2 (Gerdemann et al., 2007). Although asbestos mining has been reduced or eliminated in many parts of the world, active asbestos mining still occurs in Russia, Kazakhstan, Brazil and Zimbabwe (O'Dell and Claassen, 2009). Asbestos tailings are also available from historical mining operations in the United States (5-8 Mt (Gerdemann et al., 2007)), Canada (> 165 Mt (Gerdemann

et al., 2007)), Australia, Swaziland, Italy, France, Serbia and Greece (O'Dell and Claassen, 2009).

Although the idea of using asbestos tailings for mineral carbon sequestration has been around for some time (Goff and Lackner, 1998), little work has been done to actively carbonate this waste, perhaps due to the hazardous nature of working with asbestos. Several research groups have investigated the passive carbonation of old asbestos tailings. Wilson et al. (2009a) examined the passive carbonation (accelerated natural weathering) of chrysotile tailings at Clinton Creek, Yukon Territory, and Cassiar, British Columbia. The tailings at both mines were stored subaerially in piles and, at the time of the study, both mines had been closed for more than 10 years. The researchers estimated the chrysotile in the tailings piles had carbonated at approximately 0.3% per year and attributed the accelerated weathering rate to the increase in surface area incurred during the milling process. It was suggested that steps could be taken to enhance the carbon sequestration of the tailings, for example optimizing the surface area/particle size of the tailings or seeding the tailings with microorganisms such as cyanobacteria (Wilson et al., 2009a). Power et al. (2010) also examined the carbonation of tailings from Clinton Creek, but focused on the use of bioleaching to accelerate the process. By combining acid generating materials and *Acidithiobacillus spp*. with the chrysotile tailings, the researchers were able to leach 14.3% of the Mg in the tailings over a period of one year (Power et al., 2010). In contrast to the passive techniques, Larachi et al. (2010) investigated the active carbonation, by the direct gas-solid method, of chrysotile from Thetford Mines, Quebec, one of the last active asbestos mines in the world. The experiments were conducted over a range of temperatures and low CO_2 pressures. The highest carbonate conversion observed was 0.5% after 5 hours at 375°C and 0.1 MPa. They concluded the slow carbonation rate was at least partially due to low CO_2 pressure, and that the low reaction extent was the result of the accumulation of a hydromagnesite passivation layer on the chrysotile particles (Larachi et al., 2010).

In the studies mentioned above, very low carbonate conversions were observed. At a CO_2 uptake of 0.5%, the carbonation of asbestos tailings would have an almost negligible effect on the global carbon balance. However, given an MgO content of 40%, a CO_2 uptake of up to 44% by mass, or 0.1% of global CO_2 emissions from fuel combustion (IEA, 2012), is theoretically possible using newly generated tailings without considering historical tailings. It appears the direct, or indirect, aqueous carbonation of asbestos tailings, perhaps at elevated temperatures and pressures, would be more successful in utilizing this waste mineral resource to its full potential for CO_2 sequestration. Some type of pre-treatment, such as that used for raw serpentine, would also likely render the material more reactive. However, an analysis of the environmental, health, and safety implications of implementing these types of processes would need to be conducted as disturbing and handling material from old asbestos piles inherently carries with it some risks.

2.3.3.2 Nickel Tailings

Economically mineable nickel is found in sulphide and lateritic deposits. Even though most of the known resource is contained within laterites, global nickel production has historically been sulphide-derived (Mudd, 2010; Xu et al., 2010). At present, existing high grade sulphide deposits are being depleted, and new ones have become scarce. Consequently, nickel production from laterites has been steadily increasing and, in 2007, laterites overtook sulphides as the leading nickel source (856.5 vs. 817 kt Ni, respectively (Mudd, 2010)). Laterites, though, require more complex processing than sulphide ores to produce nickel (Mudd, 2010). In addition, the pressure acid leaching systems developed for the processing of lateritic deposits have led to unexpected challenges with regard to capital and operating costs (Xu et al., 2010). As such, the nickel industry has become increasingly interested in low-grade sulphide resources, which are often hosted in ultramafic rocks (Xu et al., 2010).

Producing nickel from low-grade ultramafic deposits is not without challenges. Serpentine minerals, which are frequently present in ultramafic ores, are difficult

to disperse and reject efficiently and these ores are associated with low recoveries. For example, at Mt Keith, Australia, nickel recovery from ores containing 0.58% Ni and 40% MgO was only 60% during the first 5 years of operation (Senior and Thomas, 2005), and researchers working with Vale Thompson low-grade ultramafic nickel ore (Figure 2-8) have found the presence of 15% MgO can reduce nickel recovery from 90% to 20% (Xu et al., 2010). Operations processing ultramafic ores generally have to run high tonnages in order to be profitable, inevitably generating vast quantities of tailings that must be managed. These tailings, however, are high in MgO and have the potential to be utilized for mineral carbon sequestration. Turning ultramafic tailings into a valuable feedstock could make some marginal nickel projects economically feasible (Hitch et al., 2010). In addition, some ultramafic nickel deposits contain chrysotile asbestos and the carbonation of these tailings can reduce the environmental impact of the waste (Gerdemann et al., 2007; Xu et al., 2010).
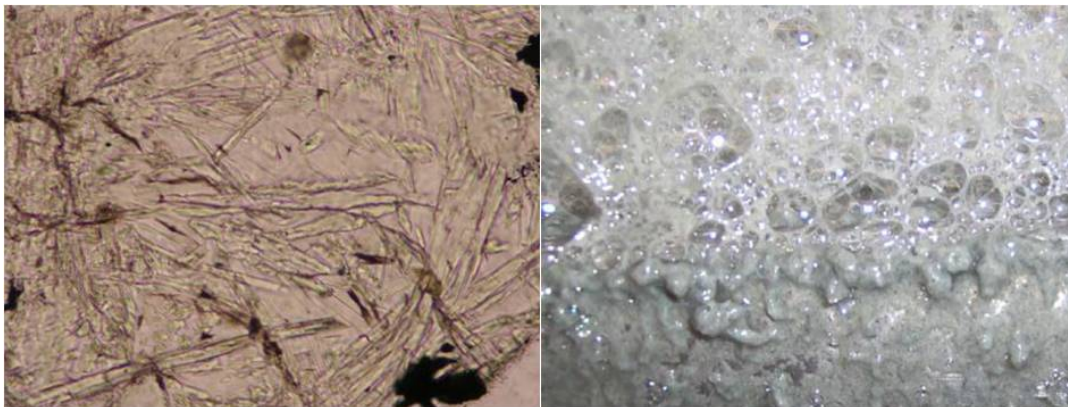
Figure 2-8: Photomicrograph of a thin section of Vale Thompson low-grade ultramafic nickel ore showing the occurance of chysotile (left), and the flotation froth of the same ore which is viscous and pasty (right). Reprinted with permission from Xu et al. (2010).

Work on the carbonation of ultramafic nickel tailings to date has been limited. Tier et al. (2007a, 2007b, 2009) examined the indirect aqueous mineral carbonation of serpentine from the stockpile of the Hitura nickel mine in central Finland (74-125 μm and ~40% MgO). Different extraction agents, including

various acids, bases and ammonium salt solutions, were investigated, for leaching magnesium from the tailings. The extracted magnesium was carbonated in a multistage process which produced separate precipitates of silica, iron oxide and hydromagnesite. H_2SO_4, HCl, and HNO_3 were found to be the most effective dissolution agents, extracting 100% of the magnesium at 70°C. The extracted magnesium was carbonated aqueously at ambient pressure, 30°C and pH 9. Carbonate conversions as high as 94% were achieved, producing hydromagnesite of 93 to 99% purity (Teir et al., 2007b). Unfortunately the chemical costs of this process ((US$600-1600/t CO_2) were deemed too high for it to be economically feasible (Teir et al., 2009).

The financial feasibility of integrating carbon sequestration by mineral carbonation into a proposed nickel mining operation at Turnagain in Northern British Columbia was assessed by Hindle and Hitch (2010). Capital and operating costs were evaluated in the presence of a cap-and-trade system, which created a revenue stream through the sale of carbon credits generated by the operation through carbon sequestration. The cost of carbon was assumed to be $200/t CO_2. Operating costs, including mining, processing, transportation, CO_2 capture, sequestration, disposal and monitoring, were estimated at $74/t CO_2. The costs of mining and monitoring were considered negligible. Based on a sequestration plant capacity of 680,885 t CO_2/yr, a figure derived from the proposed mine output of MgO and assuming 80% sequestration efficiency, capital costs were estimated to be $66 million. With a project life of 29 years, the net present value (NPV) of the project was estimated (using discounted cash flow analysis) to be $68.4 million with a payback period of 4 years. The positive NPV suggests that the project, combining mining, milling and CO_2 sequestration, at Turnagain may be feasible under a carbon cap-and-trade scheme (Hindle and Hitch, 2010).

The studies show that carbonation of nickel tailings is achievable. Assuming a 94% conversion of magnesium ions to carbonate, an ore containing 40% MgO would have a CO_2 uptake capacity of 41% by mass. Given this CO_2 sequestration capacity, an operation such as Mt. Keith, which processes 11 Mt of ore per annum

(Senior and Thomas, 2005), could store approximately 4.5 Mt of CO_2 in its tailings each year. While the amount of CO_2 stored is small in global terms, it is almost 13 times the annual CO_2-equivalent emissions (0.35 Mt) of the mine (Wilson et al., 2009a). Although CO_2 sequestration in nickel tailings is expensive, with further technological development to reduce the price of sequestration, and given a carbon regulatory framework including a cap-and-trade scheme and sufficiently high carbon price, integrating nickel mining operations with carbon sequestration is a possibility.

2.3.3.3 Red Mud

The Bayer process is the primary method used to produce alumina from bauxite. The process involves the digestion of bauxite ore in a caustic liquor of sodium and calcium hydroxides, resulting in two process streams: alumina liquor for further processing and a waste slurry product referred to as red mud (Johnston et al., 2010). Red mud is highly alkaline (pH > 13) and consists of Fe_2O_3 (30-60%), Al_2O_3 (10-20%), SiO_2 (3-50%), Na_2O (2-10%), CaO (2-8%) and TiO_2 (trace – 10%) (Sahu et al., 2010). Annually, 70 million tonnes of red mud is generated (Dilmore et al., 2008), 1.0 to 1.5 t for each tonne of alumina produced (Yadav et al., 2010). Storage of red mud is a serious environmental problem for alumina producers as its caustic nature is a risk to living organisms (Bonenfant et al., 2008b), and any leakage into the groundwater can mobilize iron, aluminum and hydroxyl ions (Dilmore et al., 2008). CO_2, however, can be used to neutralize red mud slurry. Red mud carbonation reduces its toxicity, diminishes the long-term liability associated with storing highly alkaline material, and sequesters CO_2, although the sequestration capacity is limited (Dilmore et al., 2008). In addition, carbonated red mud can be used as a soil amendment, to remove nitrogen and phosphorous from sewage effluent, as a fertilizer additive, in brick and tile manufacture, as a filler in plastics, and in cement production (Bonenfant et al., 2008b).

Red mud is normally carbonated via the direct aqueous process route at relatively low pressures and ambient temperature, and the reaction time is typically less than

one hour. Yadav et al. (2010), Sahu et al. (2010) and Bonenfant et al. (2008b) all studied this process. A typical value for the sequestration capacity of red mud is 0.05 kg CO_2/kg red mud. Alcoa has built a red mud treatment plant with this technology at Kwinana in Western Australia that annually sequesters 70,000 t of CO_2/year from a nearby ammonia plant (ICMM, 2008). The primary source of alkalinity in red mud is present in the liquid phase (NaOH from the Bayer process), although other sources of alkalinity can be found within the solid phase, such as tricalcium aluminate (Dilmore et al., 2008). Although some calcium carbonates are formed during carbonation, because the primary source of alkalinity is NaOH, the main products of carbonation are Na_2CO_3 and $NaHCO_3$ (Sahu et al., 2010). These compounds are soluble and, thus, provide a less permanent and less stable form of CO_2 storage than solid carbonates. Based on a CO_2 uptake of 5%, red mud is capable of storing 3.5 Mt of CO_2 annually, or 0.01% of global CO_2 emissions from fuel combustion (IEA, 2012).

Johnston et al. (2010) and Dilmore et al. (2008) studied a variation of red mud carbonation where red mud is mixed with a brine solution prior to carbonation (Figure 2-9). Johnston et al. (2010) used a synthetic brine solution of hydrated calcium and magnesium chlorides, whereas Dilmore et al. (2008) employed oil and gas waste brine consisting of sodium, calcium, strontium, potassium and magnesium chlorides. In these studies, red mud was successfully neutralized and the carbonation products were primarily precipitated carbonate compounds (Johnston et al., 2010; Dilmore et al., 2008). The carbon sequestration capacity was not found to be higher than the plain CO_2 neutralization process (Johnston et al., 2010). Although both methods of red mud carbonation (with and without brine) successfully neutralize the waste residue and sequester carbon, the method utilizing brine provides a more permanent CO_2 storage solution.
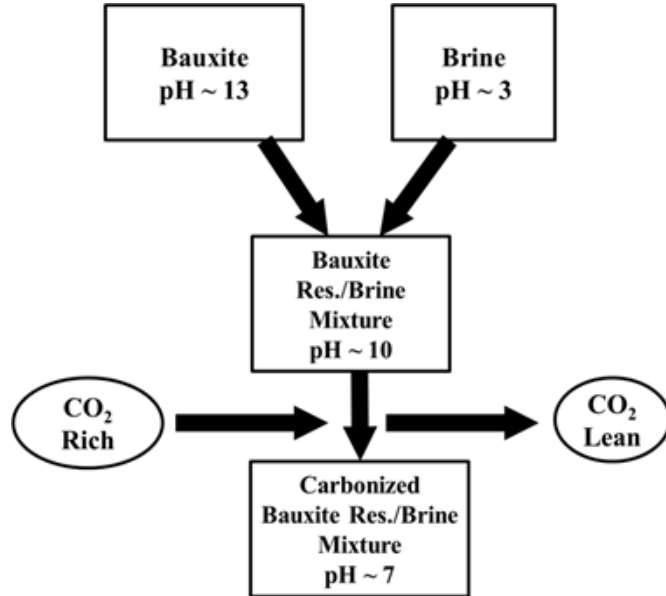
Figure 2-9: CO₂ sequestration concept by bauxite residue and brine mixture. Reprinted with permission from Dilmore et al. (2008). Copyright 2008 American Chemical Society.

2.3.4 Waste Ash

Industrial combustion processes result in the generation of several waste ash residues, including municipal solid waste ash, coal fly ash and oil shale ash. These ashes all contain CaO in varying quantities. Although the carbon sequestration capacity of many waste ashes is somewhat low compared to other alkaline waste residues, they are of small particle size and do not require comminution, and are produced in huge volumes in close proximity to point sources of CO_2 emissions. Oil shale ash appears to have a higher CO_2 sequestration capacity than coal fly ash and municipal solid waste ash. The carbon sequestration capacity of these ashes is directly related to the CaO content, and the mineral phase in which it occurs. Direct gas-solid and aqueous processes are typically selected for the carbonation of these residues.

2.3.4.1 Municipal Solid Waste Incinerator Ash

The increasing amount of municipal solid waste (MSW) produced is a global environmental problem. Incineration is a popular management option, especially where recycling or reuse are not possible. It reduces the mass and volume of waste by 65-70% and 90% respectively, and offers disinfection, the reduction of organic matter and the possibility of energy recovery (Wang et al., 2010; Fernández Bertos et al., 2004b; Li et al., 2007). However, MSW incineration also generates solid residues and gaseous effluent containing approximately 12% vol./vol. CO_2 (Rendek et al., 2006). The solid residues consist of two waste streams: bottom ash (80%) and air pollution control (APC) residues (20%). Both are rich in calcium oxide (Fernández Bertos et al., 2004b). Bottom ash is a mixture of slag, metals, ceramics, glass, other non-combustibles and unburned organics (Li et al., 2007). It is typically considered a non-hazardous waste (Fernández Bertos et al., 2004b). APC residues are a particulate mixture of fly ash, lime and carbon. Fly ash is considered a hazardous waste due to its high concentration of lime, heavy metals, soluble salts and chlorinated compounds (Fernández Bertos et al., 2004b; Li et al., 2007). While these residues can be used for other purposes, they first require treatment. For example, municipal solid waste incinerator (MSWI) bottom ash, after several weeks of natural weathering, can be used as a secondary building material or in road sub-bases, the construction of embankments, and in wind and noise barriers (Rendek et al., 2006). Alternatively, accelerated mineral carbonation can be used to stabilize MSWI ash prior to re-use or landfilling. Carbonation of the residues neutralizes the alkalinity of the ash, reduces the mobility of heavy metals and can sequester CO_2 generated by the incineration process. The high CaO content and small particle size, in addition to the proximity in which the residue and CO_2 are generated, make MSWI ash a good candidate for mineral carbon sequestration (Fernández Bertos et al., 2004b).

Research on the mineral carbonation of MSWI ash has been focused on the direct gas-solid process route. The carbon sequestration capacity of these residues is

low; however, the theoretical capacity is easily achieved at ambient temperature and reasonable pressures. Rendek et al. (2006) found the carbon sequestration capacity of MSWI bottom ash to be 24 L CO_2/kg ash at ambient temperature and CO_2 pressures as low as 1 bar. Li et al. (2007) observed MSWI fly ash to combine with 7-10% w/w CO_2 at ambient temperature and 3 bar. Fernández Bertos et al. (2004b) detected a mass increase of 3.19% and 7.31% for MSWI bottom ash and APC respectively after carbonation at ambient temperature and 3 bar pressure. Ash moisture content has been noted as an important variable for carbonation. While water is necessary to promote the reaction with CO_2, too much water limits the reaction by blocking the pores in the solid (Li et al., 2007). The optimum value for the liquid-to-solid ratio has been reported as 0.3 (Fernández Bertos et al., 2004b; Li et al., 2007). Carbonating MSWI ash, aside from fixing CO_2, has an effect on leachate characteristics. Carbonation not only reduces the pH of leachate from the ash (which is initially extremely alkaline), but can also reduce the leaching of heavy metals and other compounds (Fernández Bertos et al., 2004b; Li et al., 2007; Rendek et al., 2006). Rendek et al. (2006) estimated a potential of 0.5 to 1.0% reduction in CO_2 emissions from incinerator facilities by CO_2 sequestration using MSWI bottom ash. Thus, the primary benefit achieved by carbonating MSWI ash is toxicity reduction.

2.3.4.2 Coal Fly Ash

Coal-fired power plants currently provide approximately 40% of world's electricity (Montes-Hernandez et al., 2009), generating 12,000 million metric tonnes of CO_2 (US DOE, 2006) and 600 million metric tonnes of fly ash annually (Montes-Hernandez et al., 2009). Only about 16% of coal fly ash is utilized (in cement and concrete manufacture), with the rest disposed of, primarily in landfills. The amount of coal burned and the quantity of coal fly ash generated have increased along with global energy demands, and the disposal of the residue has become a serious problem. Coal fly ash is potentially toxic due to the presence of concentrated contaminants from flue gas, and it is believed the re-utilization of this material is preferable to its direct disposal (Ahmaruzzaman,

2010). Since fly ash contains free lime and is generated near CO_2 emission sources in power generating plants, it could be used for mineral carbon sequestration.

The carbon sequestration potential of coal fly ash is similar to that of MSWI ash, and, thus, is low compared to some other alkaline solid residues. Research on the mineral carbonation of coal fly ash has been focused mainly on the direct aqueous route under mild process conditions with either water or brine as the reaction medium. Montes-Hernandez et al. (2009) achieved a carbonate conversion of 82% and a carbon sequestration capacity of 26 kg CO_2/t ash at 30°C and 10 bar initial CO_2 pressure over 18 hours in water. Uliasz-Bochenczyk et al. (2009) found a maximum carbon sequestration capacity of 7.85 g CO_2/100 g ash at ambient temperature and 10 bar CO_2 initial pressure over 24 hours in water, but noted that the CO_2 sequestration capacity greatly depended on the characteristics of the ash used. Soong et al. (2006) evaluated the carbonation of coal fly ash in oil and gas waste brine. At 20°C and 1.36 MPa CO_2 over 2 hours, the carbonate content of ash was increased from 1% to 53% and it was noted that Ca from both waste streams contributed to the formation of $CaCO_3$ (Soong et al., 2006). Assuming an average carbon sequestration capacity of 5%, coal fly ash could be used to sequester 0.25% of CO_2 emissions from coal fired power plants (Montes-Hernandez et al., 2009; US DOE, 2006). Hence, coal fly ash alone cannot be used to significantly reduce CO_2 emissions from coal fired power plants.

2.3.4.3 Oil Shale Ash

Oil shale is a fine-grained sedimentary rock and low-grade carbonaceous fossil fuel (Uibu et al., 2010; Külaots et al., 2010). Worldwide deposits of oil in oil shales are estimated at 2.8 trillion barrels, with the largest deposits being found in Australia, China and the United States. At present, however, only Israel, Russia, Germany, Brazil, Estonia and China are exploiting their reserves (Külaots et al., 2010). The combustion of oil shale leads to high specific carbon emissions (29.1 t carbon/TJ versus 25.8 and 15.2 for coal and natural gas (Uibu et al., 2010)) and the generation of large quantities of ash (45-48% of oil shale is left over as ash

45

after combustion (Mõtlep et al., 2010)). Most oil shale ash, which can contain 10 to 25% free lime depending on the combustion technology used (Uibu et al., 2010), is deposited in landfills where it poses a threat to the groundwater. The ash is highly alkaline in nature and unburned polycyclic-aromatic hydrocarbons, heavy metals and phenols can be leached from it (Külaots et al., 2010). Oil shale ash, similar to MSWI and coal fly ash, has a small particle size and is generated at sites where it can be well used to mitigate CO_2 emissions. However, compared to the other waste ashes reviewed, oil shale ash has a much higher free lime content, giving it a superior CO_2 sequestration capacity. Although there are few published results on the carbonation of oil shale ash, those available are positive. Uibu et al. (2010) studied the direct aqueous carbonation of oil shale ash at ambient temperature and pressure in a continuous flow reactor. The carbonated product was found to contain 17-20% bound CO_2 and the researchers concluded oil shale ash from the SC Narva Power Plants in Estonia could be used to bind 1-1.2 million tonnes of CO_2 annually (Uibu et al., 2010), 5-6% of Estonia's total CO_2 emissions (20.5 million tonnes (UNSD, 2010)).

2.3.5 Alkaline Paper Mill Waste

Kraft pulping is the principal process for the production of chemical pulp. It involves the cooking of woodchips with sodium sulphide (Na_2S) in a caustic solution for 2-4 hours at 170ºC to dissolve the lignin and separate the cellulose fibres (Gierer, 1980; Pérez-López et al., 2008). After cooking, the fibres are recovered by sieving and the residual liquids are regenerated for re-use in a boiler followed by alkalization with lime. The regeneration of the cooking liquor results in the formation of several types of portlandite-rich wastes, collectively referred to as alkaline paper mill wastes (APMW) (Figure 2-10) (Pérez-López et al., 2008). These wastes can be sold for use in cement manufacture or as a soil amendment, but are most often landfilled (Pöykiö et al., 2006). The alkaline nature of these wastes and their high concentration of CaO make them a suitable candidate for mineral carbonation (Pérez-López et al., 2008). CO_2 is generated at pulp mills in both the recovery boiler and lime kiln (Nurmesniemi et al., 2008).

This CO_2 could be used to carbonate the APMW to produce $CaCO_3$, either for use in the pulp and paper industry or for sale as a value-added by-product (Pérez-López et al., 2008). Despite these attributes, research on the carbonation of this waste is very limited. Pérez-López et al. (2008) investigated the direct aqueous carbonation of APMW, specifically calcium mud from ENCE-Huelva in Spain, containing 83.2% CaO. Calcium mud was selected as it had the highest CaO content of the APMW; however, other APMW, such as green liquor dregs, are produced in much greater quantities (Pérez-López et al., 2011). A carbon sequestration capacity of 218 kg CO_2/t calcium mud was attained at 30°C and 10 bar in 2 hours. It was calculated a total of 1000 t of CO_2 could be stored in the 4500 t of calcium mud generated annually by the mill (Pérez-López et al., 2010). These researchers concluded that APMW is an ideal material for mineral carbonation because the reaction occurs quickly, independent of temperature and pressure, and the carbon sequestration capacity is high (Pérez-López et al., 2008). They also found the calcite powder produced by the carbonation of APMW is suitable for the neutralization of acid mine drainage (Pérez-López et al., 2010). Unfortunately, the 1000 t of CO_2 that could be captured by the calcium mud accounts for only 0.3% of the 0.35 Mt of CO_2 that was emitted by the ENCE-Huelva operation in 2009 (ENCE, 2009).
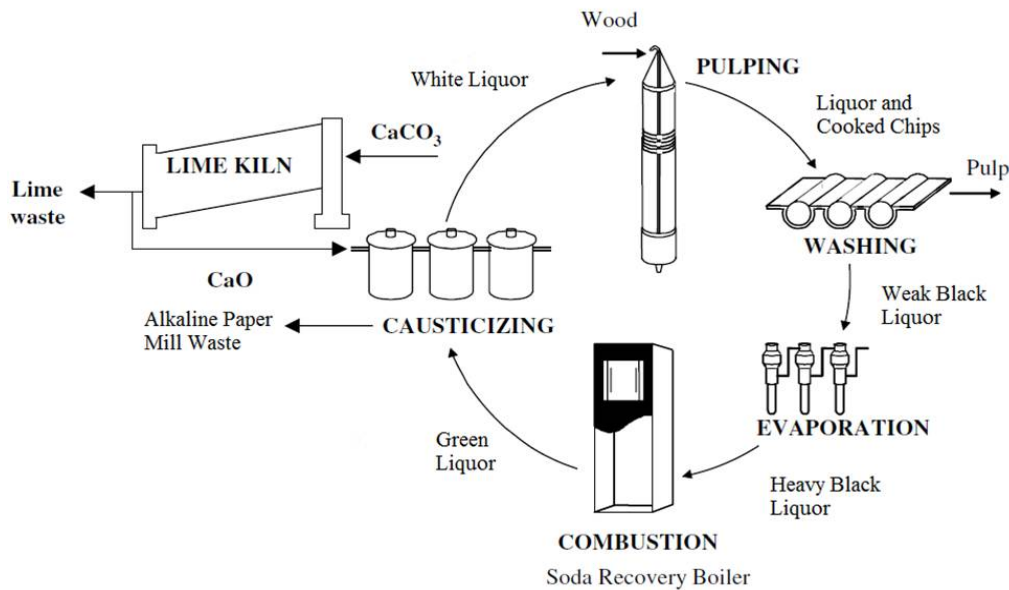
Figure 2-10: Kraft pulp mill chemical recovery circuit and generation of alkaline paper mill waste. Reprinted from Chemosphere, Vol 65, Issue 11, Pöykiö et al., The use of a sequential leaching procedure for assessing the heavy metal leachability in lime waste from the lime kiln at a causticizing process of a pulp mill, Pages 2122-2129, Copyright 2006, with permission from Elsevier.

2.4 Conclusions

The global climate system is warming and it has been proposed that the increase in anthropogenic GHG emissions since pre-industrial times, particularly CO_2 from the combustion of fossil fuels, is largely responsible. Carbon capture and storage is gaining in popularity as a means to combat climate change as it allows carbon emissions to be managed during fossil fuel dependence while sustainable infrastructure is established. Mineral carbon sequestration is the only known form of permanent carbon storage and offers the possibility of carbon capture and storage in a single step. A number of methods can be used to achieve the carbonation including direct and indirect process routes. The direct aqueous carbonation process appears the most promising, although indirect aqueous carbonation processes, such as those involving extraction of the alkaline earth

48

metal by acids or ammonium salts, also show potential. Calcium and magnesium silicate minerals are often used for mineral carbonation, but require expensive, energy intensive pre-treatments to achieve reasonable carbonate conversions and acceptable kinetics. Certain waste residues provide an alternative source of mineral alkalinity for use in mineral carbon sequestration. Besides fixing CO_2, carbonating alkaline waste residues can improve their environmental stability or result in the production of value-added by-products, such as precipitated calcium carbonate (PCC).

It is difficult to directly compare different wastes for mineral CO_2 sequestration. Carbon sequestration capacity results have been published in a variety of forms, which are not readily converted from one to another, and each waste has its own unique set of advantages and disadvantages. Steelmaking slags have high carbon sequestration capacities and are generated in close proximity to point sources of CO_2; however, they must undergo size reduction to be used for mineral carbonation. Cement wastes are available in large quantities and contain a large fraction of CaO, although the carbon sequestration capacity may be limited if carbonates are predominant in the waste. Mining and mineral processing wastes, such as asbestos tailings, nickel tailings, and red mud, can be remediated by carbonation. In addition, the use of tailings, such as those from low grade nickel operations, for mineral carbon sequestration could make some economically marginal projects feasible. Municipal solid waste incinerator ash and coal fly ash are generated in vast quantities but have low carbon sequestration capacities. The benefit of carbonating these wastes is primarily toxicity reduction. In contrast, oil shale ash has a fairly high carbon sequestration capacity and could be used to fix a noteworthy amount of CO_2 from the combustion of this fuel. Alkaline paper mill wastes, despite limited availability, appear to carbonate easily and have a high carbon sequestration capacity. While available in small quantities compared to resources of natural silicate minerals, alkaline industrial waste residues could be used to sequester meaningful quantities of CO_2, especially if the waste residues are generated near a large point source of CO_2, and could help introduce mineral sequestration technology on an industrial scale.

Table 2-3: Summary of waste products for mineral carbonation.

Waste	Carbonation Route	Waste Composition (%)		CO₂ Storage Capacity^b (kg CO₂/kg waste)	Results^c	Reference	Advantages	Disadvantages
Steelmaking Slags	Direct Aqueous – 100°C, 19bar, 30 min, <38μm	CaO MgO	31.7 6.0	0.31	0.19kg CO₂/kg slag	Huijgen et al. (2005)	• **High CO₂ sequestration capacity** • **Generated in large quantities** • **Generated near CO₂ source** • **Carbonation improves mech. char. of slag**	• **Must undergo comminution**
	Direct Aqueous – amb. T&P, 40 hrs, 38-106μm	CaO MgO	58.1 6.2	0.52	24.7g CO₂/100g slag	Bonenfant et al. (2008a)		
	Direct Aqueous - amb. T&P, 20min, 45-75μm	CaO MgO	32.1 9.4	0.35	6% carbonation	Lekakh et al. (2008)		
	Indirect Aqueous w/ acetic acid - 30°C, amb P, 2hrs, 125-250μm	CaO MgO	45.9 3.7	0.40	0.09kg CO₂/kg slag	Eloneva et al. (2008b)		
	Indirect Aqueous w/ NH₄Cl – 80°C, amb P, 2 hrs, <63μm	CaO MgO	44.5 7.6	0.43	0.16kg CO₂/kg slag	Kodama et al. (2008)		
Cement Kiln Dust	Direct – 38% moisture, amb. T&P, 3.3 days	CaO MgO	34.5 2.08	0.29	11.5% carbonation	Huntzinger et al. (2009)	• **Large quantities** • **Generated near CO₂ source (CKD)** • **Carbonated product can be reused in cement manufacture** • **CKD has a fine particle size** • **Carbonation reduces health hazard**	• **Waste cement must be ground if it doesn't come from an aggregate recovery process** • **Some wastes may already be partially carbonated, reducing their CO₂ storage capacity**
	Direct – paste, amb T, 2 bar, 72 hrs	CaO MgO	46.2 1.5	0.38	26% carbonation	Gunning et al. (2010)		
Waste Cement	Direct – 50% moisture, amb T, 4 bar, 0.8 hrs, P₈₀ = 80μm	CaO MgO	25.2 0.3	0.20	100% conversion of Ca to carbonate	Teramura et al. (2000)		

50

Waste	Carbonation Route	Waste Composition (%)	CO$_2$ Storage Capacity[b] (kg CO$_2$/kg waste)	Results[c]	Reference	Advantages	Disadvantages
Asbestos Tailings	Passive (tailings piles) – amb T&P	-	-	0.3% carbonation per year	Wilson et al. (2009a)	**Carbonation destroys the asbestiform nature of the mineral** • **Comminution not required**	**New asbestos tailings are not being generated in large quantities** • **Low carbon sequestration capacities achieved**
	Direct gas-solid – 375°C, 0.1MPa, 5 hrs, 37-75µm	CaO 0.16 MgO 39.4	0.43	0.5% carbonation	Larachi et al. (2010)		
Nickel Tailings	Indirect aqueous w/ H$_2$SO$_4$, HCl, and HNO$_3$ – 30°C, amb P, 40 min	Ca 3.4 Mg 21.8	0.43	94% conversion of Mg to carbonate	Tier et al (2007a, 2007b, 2009)	**Large quantities of tailings generated in localized areas** • **Comminution not required** • **Destroy chrysotile (asbestos) in tailings if present**	**Currently expensive to achieve high carbonate conversion**
Red Mud	Direct aqueous – amb T, 3.5 bar, 12 hrs, 30µm	CaO 2.99 Na$_2$O 6.0	0.07	5.3g CO$_2$/100g red mud	Yadav et al. (2010)	**Carbonation stabilizes red mud for disposal or re-use**	**Low carbon sequestration capacity** • **Bicarbonates generated primarily, rather than carbonates**
	Direct aqueous – amb T&P, 72 hrs, <160µm	CaO 0.23 MgO 0.18 Na$_2$O 5.79	0.09	26.33% CO$_2$ in product	Sahu et al. (2010)		
	Direct aqueous – 20°C, amb P, 24 hrs, <1000µm	CaO 7.77 MgO 0.86 Na$_2$O 8.08	0.19	4.15g CO$_2$/100g red mud	Bonenfant et al. (2008b)		
	Direct aqueous w/ brine - amb T&P, 30 min mixing, overnight settling	-	-	17g CO$_2$/kg red mud	Johnston et al. (2010)		

Waste	Carbonation Route	Waste Composition (%)		Max CO_2 Storage Capacity[b] (kg CO_2/kg waste)	Results[c]	Reference	Advantages	Disadvantages
MSWI Bottom Ash	Direct gas-solid – amb T, 17 bar, 3.5 hrs, 20% moisture, <4mm	CaO 16.3 MgO 2.6		0.16	24 L CO_2/kg ash	Rendek et al. (2006)	• **Large quantity of ash generated** • **Generated near CO_2 source** • **Carbonation reduces toxicity and pH of ash for disposal or re-use** • **Comminution not required**	• **Low carbon sequestration capacity**
	Direct gas-solid – amb T, 3 bar, 2.5 hrs	-		-	3.19% weight gain	Fernández Bertos et al. (2004b)		
MSWI Fly Ash/APC	Direct gas-solid – 21ºC, 3 bar, 3 hrs	CaO 36.268		0.28	7-10% CO_2 in product	Li et al. (2007)		
	Direct gas-solid – amb T, 3 bar, 2.5 hrs	-		-	7.31% weight gain	Fernández Bertos et al. (2004b)		
Coal Fly Ash	Direct aqueous – 30ºC, 10 bar, 18 hrs, 40μm	CaO 5		0.04	26kg CO_2/t ash	Montes-Hernandez et al. (2009)	• **Large quantity of ash generated** • **Generated near CO_2 source** • **Comminution not required**	• **Low carbon sequestration capacity**
	Direct aqueous – amb T, 10 bar, 24 hrs	CaO 15.72 MgO 1.91		0.14	7.85g CO_2/100g ash	Uliasz-Bochenczyk et al. (2009)		
	Direct aqueous w/ brine – 20ºC, 13.6 bar, 2 hrs	CaO 25 MgO 1		0.21	Carbonate content increased by 52%	Soong et al. (2006)		

Waste	Carbonation Route	Waste Composition (%)		Ma x CO_2 Storage Capacity[b] (kg CO_2/kg waste)	Results[c]	Reference	Advantages	Disadvantages
Oil Shale Ash	Direct aqueous – amb T&P, continuous flow reactor	CaO MgO	49.69 6.49	0.46	Final product contained 17-20% bound CO_2	Uibu et al. (2010)	• **High carbon sequestration capacity** • **Generated near CO_2 source** • **Comminution not required**	• **Waste available in few areas**
Alkaline Paper Mill Waste	Direct aqueous – 30ºC, 10 bar, 2 hours, 15μm	CaO MgO	83.2 0.35	0.66	218kg CO_2/t APMW	Pérez-López et al. (2008)	• **High carbon sequestration capacity** • **Generated near CO_2 source** • **Comminution not required**	• **Generated in small quantities**

[b] Calculated based on complete stoichiometric conversion of compounds listed in waste composition column.

[c] Results listed with units as reported in the literature.

2.5 References

Ahmaruzzaman, M., 2010. A review on the utilization of fly ash. Progress in Energy and Combustion Science. 36, 327-363.

Alexander, G., Maroto-Valer, M.M., Gafarova-Aksoy, P.G., 2007. Evaluation of reaction variables in the dissolution of serpentine for mineral carbonation. Fuel. 86, 273-281.

Baciocchi. R., Costa, G., Bartolomeo, E.D., Polettini, A., Pomi, R., 2009a. The effects of accelerated carbonation on CO_2 uptake and metal release from incineration APC residues. Waste Management. 29, 2994-3003.

Baciocchi, R., Costa, G., Polettini, A., Pomi, R., Prigiobbe, V., 2009b. Comparison of different reaction routes for carbonation of APC residues. Energy Procedia. 1, 4851-4858.

Baciocchi, R., Costa, G., Polettini, A., Pomi, R., 2009c. Influence of particle size on the carbonation of stainless steel slag for CO_2 storage. Energy Procedia. 1, 4859-4866.

Baldyga, J., Henczka, M., Sokolnicka, K., 2010. Utilization of carbon dioxide by chemically accelerated mineral carbonation. Materials Letters. 64, 702-704.

Bao, W., Li, H., Zhang, Y., 2010. Selective leaching of steelmaking slag for indirect CO_2 mineral sequestration. Industrial and Engineering Chemistry Research. 49, 2055-2063.

Baranzini, A., Goldemberg, J., Speck, S., 2000. A future for carbon taxes. Ecological Economics. 32, 395-412.

Bernstein, L., Bosch, P., Canziani, O., Chen, Z., Christ, R., Davidson, O., et al., 2007. Climate Change 2007: Synthesis Report. Contribution of Working Groups I, II and III to the Forth Assessment Report of the Intergovernmental Panel on Climate Change. Cambridge, UK and New York, NY, USA: Cambridge University Press.

Blencoe, J.G., Palmer, D.A., Anovitz, L.M., Beard, J.S., 2004. Carbonation of metal silicates for long-term CO_2 sequestration. Patent application. WO 2004/094043.

Bonenfant, D., Kharoune, L., Sauvé, S., Hausler, R., Niquette, P., Mimeault, M., Kharoune, M., 2008a. CO_2 sequestration potential of steel slags at ambient pressure and temperature. Industrial and Engineering Chemistry Research. 47, 7610-7616.

Bonenfant, D., Kharoune, L., Sauve, S., Hausler, R., Niquette, P., Mimeault, M., Kharoune, M., 2008b. CO_2 sequestration by aqueous red mud carbonation at ambient pressure and temperature. Industrial and Engineering Chemistry Research. 47, 7617-7622.

Bosecker, K., 1997. Bioleaching:metal solubilization by microorganisms. FEMA Microbiology Reviews. 20, 591-604.

Canadell, J.G., Le Quéré, C., Raupach, M.R., Field, C.B., Buitenhuis, E.T., Ciais, P., et al., 2007. Contributions to accelerating atmospheric CO_2 growth from economic activity, carbon intensity, and efficiency of natural sinks. PNAS. 104(47), 18866-18870.

Chen, Z.-Y., O'Connor, W.K., Gerdemann, S.J., 2006. Chemistry of aqueous mienral carbonation for carbon sequestration and explanation of experimental results. Environmental Progress. 25(2),161-166.

Dilmore, R., Lu, P., Allen, D., Soong, Y., Hedges, S., Fu, J.K., et al., 2008. Sequestration of CO_2 in mixtures of bauxite residue and saline wastewater. Energy and Fuels. 22, 343-353.

Dooley, J.J., Davidson, C.L., Dahowski, R.T., 2009. An Assessment of the Commercial Availability of Carbon Dioxide Capture and Storage Technologies as of June 2009. Richland, WA: Pacific Northwest National Laboratory, US Department of Energy; 2009 June. Contract No.: DE-AC05-76RL01830.

Doucet, F.J., 2010. Effective CO_2-specific sequestration capacity of steel slags and variability in their leaching behaviour in view of industrial mineral carbonation. Minerals Engineering. 23, 262-269.

Dufaud, F., Martinez, I., Shilobreeva, S., 2009. Experimental study of Mg-rich silicates carbonation at 400 and 500°C and 1 kbar. Chemical Geology. 265, 79-87.

Eloneva, S., Puheloinen, E.-M., Kanerva, J., Ekroos, A., Zevenhoven, R., Fogelholm, C.-J., 2010. Co-utilization of CO_2 and steelmaking slags for production of pure $CaCO_3$ - legislative issues. Journal of Cleaner Production. 18(18), 1833-1839.

Eloneva, S., Teir, S., Salminen, J., Fogelholm, C.-J., Zevenhoven, R., 2008a. Fixation of CO_2 by carbonating calcium derived from blast furnace slag. Energy. 33, 1461-1467.

Eloneva, S., Teir, S., Salminen, J., Fogelholm, C.-J., Zevenhoven, R., 2008b. Steel converter slag as a raw material for precipitation of pure calcium carbonate. Industrial and Engineering Chemistry Research. 47, 7104-7111.

Elwell, L.C., Grant, W.S., 2006. Technology options for capturing CO_2. Power Magazine. 150(8), 60.

ENCE, 2009. Declaración Ambiental 2009 [Internet]. [cited 2011 Jun 28]. Available from: http://www.ence.es/en/descargas/DA_EnceHuelva09.pdf

Fernández Bertos, M., Simons, S.J.R., Hills, C.D., Carey, P.J., 2004a. A review of accelerated carbonation technology in the treatment of cement-based materials and sequestration of CO_2. Journal of Hazardous Materials. B112, 193-205.

Fernández Bertos, M., Li, X., Simons, S.J.R., Hills, C.D., Carey, P.J., 2004b. Investigation of accelerated carbonation for the stabilisation of MSW incinerator ashes and the sequestration of CO_2. Green Chemistry. 6, 428-436.

Field, C.B., Raupach, M.R., editors., 2004. The global carbon cycle: Integrating humans, climate and the natural world. Washington, DC: Island Press.

Fischer, C., Werge, M., 2009. EU as a Recycling Society. ETC/SCP Working Paper 2 [Internet]. 2009 [Cited 2011 Jun 27]. Available from: http://scp.eionet.europa.eu/publications/wp2009_2/wp/wp2009_2

Gale, J., Davison, J., 2004. Transmission of CO_2 – safety and economic considerations. Energy. 29, 1319-1328.

Gerdemann, S.J., Dahlin, D.C., O'Connor, W.K., Penner, L.R., Rush, G.E., 2004. Ex-situ and in-situ mineral carbonation as a means to sequester carbon dioxide. Proceedings of Twenty-First Annual International Pittsburgh Coal Conference; 2004 Sep 13-17; Osaka, Japan. Pittsburgh, PA: Pittsburgh Coal Conference (PCC).

Gerdemann, S.J., Dahlin, D.C., O'Connor, W.K., Penner, L.R., 2003. Carbon dioxide sequestration by aqueous mineral carbonation of magnesium silicate minerals. Albany, OR: Albany Research Center.

Gerdemann, S.J., O'Connor, W.K., Dahlin, D.C., Penner, L.R., Rush, H., 2007. Ex situ aqueous mineral carbonation. Environmental Science and Technology. 41, 2587-2593.

Gibbins, J., Chalmers, H., 2008. Carbon capture and storage. Energy Policy. 36, 4317-4722.

Gierer, J., 1980. Chemical aspects of kraft pulping. Wood Science and Technology. 14, 241-266.

Goff, F., Lackner, K.S., 1998. Carbon dioxide sequestering using ultramafic rocks. Environmental Geosciences. 5(3), 89-101.

Goldberg, P., Chen, Z.-Y., O'Connor, W., Walters, R., Ziock, H., 2001. CO_2 mineral sequestration studies in US. Proceedings of the First National Conference on Carbon Sequestration. 2001 May 14-17; Washington, DC.

Grasa, G.S., Abanades, J.C., 2006. CO_2 capture capacity of CaO in long series of carbonation/calcination cycles. Industrial and Engineering Chemistry Research. 45(26), 8846-8851.

Gunning, P.J., Hills, C.D., Carey, P.J., 2010. Accelerated carbonation treatment of industrial wastes. Waste Management. 30, 1081-1090.

Gupta, H., Fan, L.-S., 2002. Carbonation-calcination cycle using high reactivity calcium oxide for carbon dioixde separation from flue gas. Industrial and Engineering Chemistry Research. 41(16), 4035-4042.

Habashi, F., 2001. Asbestos. In: Buschow KHJ, Cahn R, Flemings M, Ilschner B, Kramer E, Mahajan S, Veyssiere, editors. Encyclopedia of Materials: Science and Technology. Waltham, MA: Elsevier. pp. 1-5.

Hansson, A., Bryngelsson, M., 2009. Expert opinions on carbon dioxide capture and storage – A framing of uncertainties and possibilities. Energy Policy. 37, 2273-2282.

Haug, T.A., Kleiv, R.A., Munz, I.A., 2010. Investigating dissolution of mechanically activated olivine for carbonation purposes. Applied Geochemistry. 25(10), 1547-1563.

Hindle, S., Hitch, M., 2010. Financial feasibility of integrating mineral carbonation into proposed mining operations at the Turnagain Nickel Site, Northern BC. Proceedings of the CIM Conference and Exhibition 2010; 2010 May 10-12; Vancouver, BC.

Hitch, M., Ballantyne, S.M., Hindle, S.R., 2010. Revaluing mine waste rock for carbon capture and storage. International Journal of Mining, Reclamation and Environment. 24, 64-79.

Houghton, J.T., Ding, Y., Griggs, D.J., Noguer, M., van der Linden, P.J., Dai, X., et al., editors, 2001. Climate Change 2001: The Scientific Basis. Contribution of Working Group I to the Third Assessment Report of the Intergovernmental Panel on Climate Change. Cambridge, UK and New York, NY, USA: Cambridge University Press.

Huijgen, W.J.J., Comans, R.N.J., 2003. Carbon dioxide sequestration by mineral carbonation. Petten, NL: Energy Research Centre of the Netherlands.

Huijgen, W.J.J., Witkamp, G.-J., Comans, R.N.J., 2005. Mineral CO_2 sequestration by steel slag carbonation. Environmental Science and Technology. 39, 9676-9682.

Huntzinger, D.N., Eatmon, T.D., 2009. A life-cycle assessment of Portland cement manufacturing: comparing the traditional process with alternative technologies. Journal of Cleaner Production. 17, 668-675.

Huntzinger, D.N., Gierke, J.S., Sutter, L.L., Kawatra, S.K., Eisele, T.C., 2009. Mineral carbonation for carbon sequestration in cement kiln dust from waste piles. Journal of Mazardous Materials. 168, 31-37.

ICMM, 2008. Case Study: Alcoa develops carbon capture process. International Council on Mining and Metals [Internet]. 2008 [cited 2011 Mar 2]. Available from: http://www.icmm.com/page/2420/alcoa-develops-carbon-capture-process

Iizuka, A., Fujii, M., Yamasaki, A., Yanagisawa, Y., 2004. Development of a new CO_2 sequestration process utilizing the carbonation of waste cement. Industrial and Engineering Chemistry Research. 43, 7880-7887.

International Energy Agency, 2012. CO_2 Emissions from Fuel Combustion [Internet]. Paris (France): OECD/IEA; [cited 2014 Jan 29]. Available from: http://www.iea.org/co2highlights/CO2highlights.pdf

Irish Department of Finance, 2010. Finance Bill 2010: List of Items. Dublin, Ireland.

Jang, N.-H., Park, S.-K., Shim, H.-M., Kim, H.-T., 2010. Comparison of pretreatment method for the enhancement of CO_2 mineralogied sequestration using by serpentine. Journal of the Korean Industrial and Engineering Chemistry. 21, 24-28.

Johnston, M., Clark, M.W., McMahon, P., Ward, N., 2010. Alkalinity conversion of bauxite refinery residues by neutralization. Journal of Hazardous Materials. 182, 710-715.

Jürgen-Friedrich, H., Hubert, H., Olga, S., Jochen, S., 2009. CCS for Germany: Policy, R&D and demonstration activities. Energy Procedia. 1(1), 3917-3925.

59

Kakizawa, M., Yamasaki, A., Yanagisawa, Y., 2001. A new CO_2 disposal process via artifical weathering of calcium silicate accelerated by acetic acid. Energy. 26, 341-354.

Katsuyama, Y., Yamasaki, A., Iizuka, A., Fuhii, M., Kumagai, K., Yanagisawa, Y., 2005. Development of a process for producing high-purity calcium carbonate ($CaCO_3$) from waste cement using pressurized CO_2. Environmental Progress. 24, 162-170.

Kodama, S., Nishimoto, T., Yamamoto, N., Yogo, K., Yamada, K., 2008. Development of a new pH-swing CO_2 mineralization process with a recyclable reaction solution. Energy. 33, 776-784.

Koornneef, J., Spruijt, M., Molag, M., Ramírez, A., Turkenburg, W., Faaij, A., 2010. Quantitative risk assessment of CO_2 transport by pipelines – A review of uncertainties and their impacts. Journal of Hazardous Materials. 177, 12-27.

Krevor, S.C., Lackner, K.S., 2009. Enhancing process kinetics for mineral carbon sequestration. Energy Procedia. 1, 4867-4871.

Külaots, I., Goldfarb, J.L., Suuberg, E.M., 2010. Characterization of Chinese, American and Estonian oil shale semicokes and their sorptive potential. Fuel. 89, 3300-3306.

Lackner, K.S., Butt, D.P., Wendt, C.H., 1997. Progress on binding CO_2 in mineral substrates. Energy Conversion and Management. 38, S259-S264.

Lackner, K.S., Wendt, C.H., Butt, D.P., Joyce, E.L., Sharp, D.H., 1995. Carbon dioxide disposal in carbonate minerals. Energy. 20(11), 1153-1170.

Lackner, K.S., 2002. Carbonate chemistry for sequestering fossil carbon. Annual Reviews of Energy and the Environment. 27, 193-232.

Lackner, K.S., 2003. Climate change: A guide to CO_2 sequestration. Science. 300, 1677-1678.

Larachi, F., Daldoul, I., Beaudoin, G., 2010. Fixation of CO_2 by chrysotile in low-pressure dry and moist carbonation: Ex-situ and in-situ characterizations. Geochimica et Cosmochimica Acta. 74, 3051-3075.

Lee, S.C., Chae, H.J., Lee, S.J., Choi, B.Y., Yi, C.K., Lee, J.B., et al., 2008. Development of regenerable MgO-based sorbent promoted with K_2CO_3 for CO_2 capture at low temperature. Environmental Science and Technology. 42(8), 2736-2741.

Lekakh, S.N., Rawlins, C.H., Robertson, D.G.C., Richards, V.L., Peaslee, K.D., 2008. Kinetics of aqueous leaching and carbonization of steelmaking slag. Metallurgical and Materials Transactions B. 39B, 125-134.

Li. X., Fernández Bertos. M., Hills, C.D., Carey, P.J., Simon, S., 2007. Accelerated carbonation of municipal solid waste incineration fly ashes. Waste Management. 27, 1200-1206.

Li, X., 2008. Recycling and reuse of waste concrete in China. Part I. Material behaviour of recycled aggregate concrete. Resources, Conservation and Recycling. 53, 36-44.

Lim, M., Han, G.-C., Ahn, J.-W., You, K.-S., 2010. Environmental remediation and conversion of carbon dioxide (CO_2) into useful green products by accelerated carbonation technology. International Journal of Environmental Research and Public Health. 7, 203-228.

Marcuson, S.W., Hooper, J., Osborne, R.C., Chow, K, Burchell, J., 2009. Sustainability in Nickel Projects: 50 Years of Experience at Vale Inco. Engineering and Mining Journal [Internet], [cited 2011 Mar 2]. Available from: http://www.e-mj.com/index.php/features/117-sustainability-in-nickel-projects-50-years-of-experience-at-vale-inco.html

Maroto-Valer, M.M., Kuchta, M.E., Zhang, Y., Andrésen, J.M., Fauth, D.J., 2005. Activation of magnesium rich minerals as carbonation feedstock materials for CO_2 sequestration. Fuel Processing Technology. 86, 1627-1645.

Maroto-Valer, M.M., Kuchta, M.E., Zhang, Y., Andrésen, J.M., Fauth, D.J., 2004. Comparison of physical and chemical activation of serpentine for enhanced CO_2 sequestration. Prepr. Pap.-Am. Chem. Soc., Div. Fuel Chem. 49(1), 373-375.

Metcalf, G.E., Weisback, D., 2009. The design of a carbon tax. Harvard Environmental Law Review. 33(2), 499-556.

Metz, B., Davidson, O., de Coninck, H.C., Loos, M., Meyer, L.A., editors, 2005. IPCC Special Report on Carbon Dioxide Capture and Storage. Prepared by Working Group III of the Intergovernmental Panel on Climate Change. Cambridge, UK and New York, NY: Cambridge University Press.

Metz, B., Davidson, O.R., Bosch, P.R., Dave, R., Meyer, L.A., editors, 2007. Climate Change 2007: Mitigation. Contribution of Working Group III to the Fourth Assessment Report of the Intergovernmental Panel on Climate Change. Cambridge, UK and New York, NY, USA: Cambridge University Press.

Montes-Hernandez, G., Pérez-López, R., Renard, F., Nieto, J.M., Charlet, L., 2009. Mineral sequestration of CO_2 by aqueous carbonation of coal combustion fly-ash. Journal of Hazardous Materials. 161, 1347-1354.

Mõtlep, R., Sild, T., Puura, E., Kirsimäe, K., 2010. Composition, diagenetic transformation and alkalinity potential of oil shale ash sediments. Journal of Hazardous Materials. 184(1-3), 567-573.

Mudd, G.M., 2010. Global trends and environmental issues in nickel mining: Sulfides versus laterites. Ore Geology Reviews. 38(1-2). 9-26.

New Zealand Ministry for the Environment, 2007. The Framework for a New Zealand Emissions Trading Scheme: Executive Summary. Wellington, NZ: New Zealand Ministry for the Environment and The Treasury.

Nurmesniemi, H., Pöykiö, R., Perämäki, P., Kuokkanen, T., 2008. Extractability of trace elements in precipitated calcium carbonate (PCC) waste from an integrated pulp and paper mill complex. Chemsphere. 70, 1161-1167.

O'Dell, R.E., Claassen, V.P., 2009. Serpentine revegetation: A Review. Northeastern Naturalist. 16(Special Issue 5), 253-271.

O'Connor, W.K., Dahlin, D.C., Nilsen, D.N., Rush, G.E., Walters, R.P., Turner, P.C., 2000a. CO_2 storage in solid form: A study of direct mineral carbonation.

Greenhouse Gas Control Technologies: Proceedings of the 5th International Conference on Greenhouse Gas Technologies; 2000 Aug 14-18; Cairns, AU.

O'Connor, W.K., Dahlin, D.C., Nilsen, D.N., Rush, G.E., Walters, R.P., Turner, P.C., 2000b. Carbon dioxide sequestration by direct mineral carbonation with carbonic acid. Proceedings of the 25th International Technical Conf. on Coal Utilization & Fuel Systems, Coal Technology Assoc; 2000 Mar 6-9; Clear Water, FL, USA.

Olajire, A.A., 2010. CO_2 capture and separation technologies for end-of-pipe applications – A review. Energy. 35, 2610-2628.

Park, A.-H., Fan, L.-S., 2004. CO_2 mineral sequestration: physically activated dissolution of serpentine and pH swing process. Chemical Engineering Science. 59, 5241-5247.

Park, A.-H., Jadhav, R., Fan, L.-S., 2003. CO_2 mineral sequestration: chemically enhanced aqueous carbonation of serpentine. Canadian Journal of Chemical Engineering. 81, 885-890.

Pérez-López, R., Castillo, J., Quispe, D., Nieto, J.M., 2010. Neutralization of acid mine drainage using the final product from CO_2 emissions capture with alkaline paper mill waste. Journal of Hazardous Materials. 177, 762-772.

Pérez-López, R., Montes-Hernandez, G., Nieto, J.M., Renard, F., Charlet., L., 2008. Carbonation of alkaline paper mill waste to reduce CO_2 greenhouse gas emissions into the atmosphere. Applied Geochemistry. 23, 2292-2300.

Pérez-López, R., Quispe, D., Castillo, J., Nieto, J.M., 2011. Acid neutralization by dissolution of alkaline paper mill wastes and implications for treatment of sulfide-mine drainage. American Mineralogist. 96, 781-791.

Power, I.M., Dipple, G.M., Southam, G., 2010. Bioleaching of ultramafic tailings by *Acidithiobacillus spp.* for CO_2 sequestration. Environmental Science and Technology. 44, 456-462.

Pöykiö, R., Nurmesniemi, H., Kuokkanen, T., Perämäki, P., 2006. The use of a sequential leaching procedure for assessing the heavy metal leachability in lime

waste from the lime kiln at a cautizicing process of a pulp mill. Chemosphere. 65, 2122-2129.

Praetorius, B., Schumacher, K., 2009. Greenhouse gas mitigation in a carbon constrained world: The role of carbon capture and storage. Energy Policy. 37, 5081-5093.

Prigiobbe, V., Polettini, A., Baciocchi, R., 2009a. Gas-solid carbonation kinetics of Air Pollution Control residues for CO_2 storage. Chemical Engineering Journal. 148, 270-278.

Prigiobbe, V., Hänchen, M., Werner, M., Baciocchi, R., Mazzotti, M., 2009b. Mineral carbonation process for CO_2 sequestration. Energy Procedia. 1, 4885-4890.

Prigiobbe, V., Hänchen, M., Werner, M., Baciocchi, R., Mazzotti, M., 2009c. Analysis of the effect of temperature, pH, CO_2 pressure and salinity on the olivine dissolution kinetics. Energy Procedia. 1, 4881-4884.

Pundsack, F.L., 1967. Recovery of silica, iron oxide, and magnesium carboante from the treatment of serpentine with ammonium bisulphate. United States patent 3,338,667. 1967 Aug 29.

Raupach, M.R., Marland, G., Ciais, P., Le Quéré, C., Canadell, J.G., Klepper, G., Field, C.B., 2007. Global and regional drivers of accelerating CO_2 emissions. PNAS. 104(24), 10288-10293.

Rendek, E., Ducom, G., Germain, P., 2006. Carbon dioxide sequestration in municipal solid waste incinerator (MSWI) bottom ash. Journal of Hazardous Materials. B128, 73-79.

Rodrigues, F.A., Joekes, I., 2011. Cement industry: sustainability, challenges and perspectives. Environmental Chemistry Letters. 9:151-166.

Sahu, R.C., Patel, R.K., Ray, B.C., 2010. Neutralization of red mud using CO_2 sequestration cycle. Journal of Hazardous Materials. 179, 28-34.

Schneider, M., Romer, M., Tschudin, M., Bolio, H., 2011. Sustainable cement production – present and future. Cement and concrete research. 41, 642-650.

Schwartzman, D.W., Volk, T., 1989. Biotic enhancement of weathering and the habitability of the Earth. Nature. 340, 457-460.

Senior, G.D., Thomas, S.A., 2005. Development and implementation of a new flowsheet for the flotation of a low grade nickel ore. International Journal of Mineral Processing. 78, 49-61.

Sipilä, J., Teir, S., Zevenhoven, R. 2008. Carbon dioxide sequestration by mineral carbonation: Literature review update 2005-2007. Turku, Finland: Abo Akademi University, Faculty of Technology, Heat Engineering Laboratory.

Skjærseth, J.B., Wettestad, J., 2010. Making the EU Emissions Trading System: The European Commission as an entrepreneurial epistemic leader. Global Environmental Change. 20, 314-321.

Solomon, S., Qin, D., Manning, M., Chen, Z., Marquis, M., Averyt, K.B., et al., editors, 2007. Climate Change 2007: The Physical Science Basis. Contribution of Working Group 1 to the Forth Assessment Report of the Intergovernmental Panel on Climate Change. Cambridge, UK and New York, NY, USA: Cambridge University Press.

Soong, Y., Fauth, D.L., Howard, B.H., Jones, J.R., Harrison, D.K., Goodman, A.L., et al., 2006. CO_2 sequestration with brine and fly ashes. Energy Conversion and Management. 47, 1676-1685.

Stephens, J.C., 2006. Growing interest in carbon capture and storage (CCS) for climate change mitigation. Sustainability: Science, Practice and Policy. 2(2), 4-13.

Stolaroff, J.K., Lowry, G.V., Keith, D.W., 2005. Using CaO- and MgO-rich industrial waste streams for carbon sequestration. Energy Conversion and Management. 46, 687-699.

Svensson, R., Odenberger, M., Johnsson, F., Strömberg, L., 2004. Transportation systems for CO_2 – application to carbon capture and storage. Energy Conversion and Management. 45, 2343-2353.

Tans, P., 2014. Trends in Atmospheric Carbon Dioxide [Internet]. NOAA/ESRL; 2014 [cited 2014 Jan 29]. Available from: www.esrl.noaa.gov/gmd/ccgg/trends/

Teir, S., Revitzer, H., Eloneva, S., Fogelholm, C.-J., Zevenhoven, R., 2007a. Dissolution of natural serpentine in mineral and organic acids. International Journal of Mineral Processing. 83, 36-46.

Teir, S., Kuusik, R., Fogelholm, C.-J., Zevenhoven, R., 2007b. Production of magnesium carbonates from serpentine fro long-term storage of CO_2. International Journal of Mineral Processing. 85, 1-15.

Teir, S., Eloneva, S., Fogelholm, C.-J., Zevenhoven, R., 2007c. Dissolution of steelmaking slags in acetic acid for precipitated calcium carbonate production. Energy. 32, 528-539.

Teir, S., Eloneva, S., Fogelholm, C.-J., Zevenhoven, R., 2009. Fixation of carbon dioxide by producing hydromagnesite from serpentinite. Applied Energy. 86, 214-218.

Teramura, S., Isu, N., Inagaki, K., 2000. New building material from waste concrete by carbonation. Journal of Materials in Civil Engineering. 12, 288-293.

Uibu, M., Velts, O., Kuusik, R., 2010. Developments in CO_2 mineral carbonation of oil shale ash. Journal of Hazardous Materials. 174, 209-214.

Uliasz-Bocheńczyk, A., Mokrzycki, E., Piotrowski, Z., Pomykała, R., 2009. Estimation of CO_2 sequestration potential via mineral carbonation in fly ash from lignite combustion in Poland. Energy Procedia. 1, 4873-4879.

UNSD, 2010. Carbon dioxide emissions (CO_2), thousand metric tons of CO_2 (CDIAC) [Internet]. United Nations Statistics Division. [cited 2011 Mar 2]. Available from: http://mdgs.un.org/unsd/mdg/SeriesDetail.aspx?srid=749&crid=

US DOE, 2006. World Carbon Dioxide Emissions from the Consumption of Coal [Internet]. Washington, DC: Energy Information Administration, International Energy Annual, Department of Energy; [cited 2011 Jan 23]. Available from: http://www.eia.doe.gov/iea/coal.html

US EPA, 2011. Solid Waste Management and Greenhouse Gases: Documentation for Greenhouse Gas Emission and Energy Factors Used in the Waste Reduction Model (WARM). Concrete [Internet]. [cited 2011 Jun 27]. Available from:

http://www.epa.gov/climatechange/wycd/waste/downloads/concrete-chapter10-28-10.pdf

van Alphen, K., Hekkert, M.P., Turkenburg, W.C., 2010a. Accelerating the deployment of carbon capture and storage technologies by strengthening the innovation system. International Journal of Greenhouse Gas Control. 4(2), 396-409.

van Alphen, K., Noothout, P.M., Hekkert, M.P., Turkenburg, W.C., 2010b. Evaluating the development of carbon capture and storage technologies in the United States. Renewable and Sustainable Energy Reviews. 14, 971-986.

van Alphen, K., Hekkert, M.P., Turkenburg, W.C., 2009. Comparing the development and deployment of carbon capture and storage technologies in Norway, the Netherlands, Australia, Canada and the United States – An innovation system perspective. Energy Procedia. 1(1), 4591-4599.

Van Essendelft, D.T., Schobert, H.H., 2009. Kinetics of the acid digestion of serpentine with concurrent grinding. 1. Initial investigations. Industrial and Engineering Chemistry Research. 48, 2556-2565.

van Oss, H.G., Padovani, A.C., 2003. Cement manufacture and the environment, part II: environmental challenges and opportunities. Journal of Industrial Ecology. 7(1), 93–127.

Wang, L., Jin, Y., Nie, Y., 2010. Investigation of accelerated and natural carbonation of MSWI fly ash with a high content of Ca. Journal of Hazardous Materials. 174, 334-343.

EIONET, 2009. What is waste? [Internet]. European Topic Centre on Sustainable Consumption and Production. [cited 2011 Jun 27]. Available from: http://scp.eionet.europa.eu/themes/waste/#4

Wilson, S.A., Dipple, G.M., Power, I.M., Thom, J.M., Anderson, R.G., Raudsepp, M., et al., 2009a. Carbon dioxide fixation within mine wastes of ultramafic-hosted ore deposits: Examples from the Clinton Creek and Cassiar crysotile deposits, Canada. Economic Geology. 104, 95-112.

Wilson, S.A., Raudsepp, M., Dipple, G.M., 2009b. Quantifying carbon fixation in trace minerals from processed kimberlite: A comparative study of quantitative methods using X-ray powder diffraction data with applications to the Diavik Diamond Mine, Northwest Territories, Canada. Applied Geochemistry. 24, 2312-2331.

Xu, M., Dai, Z., Dong, J., Ford, F., Lee, A., 2010. Fibrous minerals in ultramafic nickel sulphide ores. Proceedings of Conference of Metallurgists; 2010 Oct 3-6; Vancouver, BC.

Yadav, V.S., Prasad, M., Khan, J., Amritphale, S.S., Singh, M., Raju, C.B., 2010. Sequestration of carbon dioxide (CO_2) using red mud. Journal of Hazardous Materials. 176, 1044-1050.

Yamasaki, A., 2003. An overview of CO_2 mitigation options for global warming – emphasizing CO_2 sequestration options. Journal of Chemical Engineering of Japan. 36(4), 361-375.

Zevenhoven, R., Fagerlund, J., 2010. Fixation of carbon dioxide into inorganic carbonates: the natural and artificial "weathering of silicates". In: Aresta M, editor. Carbon Dioxide as Chemical Feedstock. Weinheim, Germany: Wiley-VCH; p. 353-379.

Zevenhoven, R., Kohlmann, J., Mukherjee, A.B., 2002. Direct dry mineral carbonation for CO_2 emissions reduction in Finland. Proceedings: 27th International Technical Conference on Coal Utilization & Fuel Systems; 2002 Mar 4-7. Clearwater, FL, USA.

Zhao, L., Sang, L., Chen, J., Ji, J., Teng, H.H., 2010. Aqueous carbonation of natural brucite: Relevance to CO_2 sequestration. Environmental Science and Technology. 44, 406-411.

Ziock, H.-J., Butt, D.P., Lackner, K.S., Wendt, C.H., 1998. The need and options available for permanent CO_2 disposal. 1998 Topical Conference on Pollution Prevention and Environmental Risk Reduction; 1998 Nov 15-20; Miami Beach, FL, USA.

Chapter 3 Microwave Heating of Ultramafic Nickel Ores and Mineralogical Effects[2]

3.1 Introduction

Mineral carbon sequestration (MCS) is a permanent form of carbon storage modeled on rock weathering processes where CO_2, dissolved in rain water, reacts with alkaline minerals to form carbonates (Lackner et al., 1995). Benefits of MCS include that it has the potential to capture and store CO_2 in a single step, it can be used where geologic carbon storage is not feasible, there is the potential for valuable by-products to be produced, and the products are environmentally benign (Bobicki et al., 2012).

The ideal feedstocks for MCS are pure calcium and magnesium oxides. The reactions of these minerals with CO_2 are the most exothermic; however, because of their reactivity, they are rarely found in nature. Thus, the naturally abundant and alkaline silicate minerals olivine (Mg_2SiO_4) and serpentine ($Mg_3Si_2O_5(OH)_4$) are commonly chosen as source materials for MCS (Figure 3-1). Olivine is a mineral consisting of a hexagonal close-packed array of oxygen atoms in which one-half of the octahedra voids are occupied by magnesium (or iron) atoms, and one-eighth of the available tetrahedral voids are occupied by silicon atoms (Birle et al., 1968). Essentially, olivine is composed of isolated SiO_4 tetrahedra linked by octahedrally coordinated magnesium ions (Alexander et al., 2007). Serpentine, in contrast, is a phyllosilicate mineral comprised of 1:1 stacked sheets of SiO_4 tetrahedra and $MgO_2(OH)_4$ octahedra held together by weak van der Waals forces (Alvarez-Silva et al., 2010). Three primary polymorphs of serpentine exist: lizardite, antigorite and chrysotile. Lizardite has a platy structure, antigorite has a modulated or corrugated structure, and chrysotile (also known as white asbestos) has a coiled, fibrous structure (McKelvy et al., 2004). In their naturally occurring

---

states, olivine is more reactive than serpentine as bonds between the isolated silicate tetrahedra and magnesium octahedra in olivine are not as strong as those between the linked silica tetrahedra in serpentine (Alexander et al., 2007).
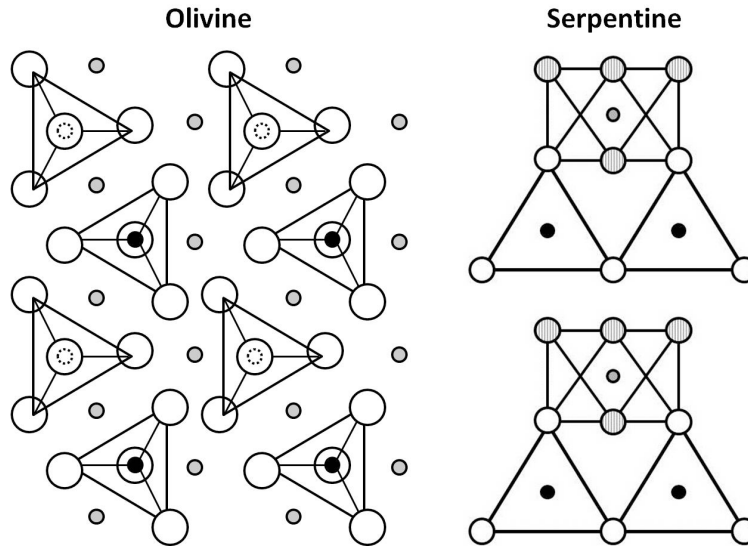
Figure 3-1: Olivine and serpentine mineral structures. White circles indicate oxygen atoms, black circles indicate silicon atoms, grey circles indicate magnesium atoms, and stripped circles indicate a hydroxyl group.

MCS may be achieved by reacting alkaline minerals with CO_2 directly in either the gaseous or aqueous phase, or indirectly by first extracting Mg^{2+} (or Ca^{2+}) from minerals in solution, separating the leached ions from the remaining solid phase, and then precipitating the ions as carbonates (Bobicki et al., 2012). In some indirect MCS processes, the divalent cations ions are precipitated as hydroxides before reaction with CO_2 (Nduagu et al., 2013). At present, an economic process for MCS has not yet been developed and all known process schemes require a net input of energy. Energy is utilized to prepare solid reactants, to drive the carbonation reaction at an acceptable rate, and to purify or dispose of the products (Metz et al., 2005). In general, the most successful MCS schemes have employed aqueous processes. Direct aqueous MCS processes have involved fine grinding of the mineral feedstock, which has accounted for up to 75% of the process costs (O'Connor et al., 2000; Gerdemann et al., 2003). In cases where serpentine is

used as the feedstock in direct aqueous processes, heat treatment to dehydroxylate serpentine and convert it to olivine, in addition to fine grinding, is required to render the mineral sufficiently reactive (Gerdemann et al., 2007; Maroto-Valer et al., 2005). Even with fine grinding and heat treatment, these processes require severe processing conditions (15 MPa, 155-185°C) (Gerdemann et al., 2007; O'Connor et al., 2000). The indirect processes, while demonstrated to more successfully convert magnesium to $MgCO_3$, especially when using serpentine as feedstock, are associated with exorbitant chemical reagent costs (Krevor and Lackner, 2011; Teir et al., 2009). The cost of MCS has been estimated at $50-100 US per tonne of CO_2 stored (excluding capture costs), an order of magnitude greater than the cost of geologic storage (Bobicki et al., 2012).

Two ways to reduce MCS process costs include using alkaline industrial wastes as feedstock, and combining MCS with other processes so the expenses (and benefits) may be shared. Alkaline industrial wastes are available cheaply, tend to be of a particle size appropriate for MCS, and are often produced close to point sources of CO_2 (Bobicki et al., 2012). One such material is serpentine waste generated by the processing of ultramafic nickel ores. Ultramafic nickel ores tend to be low-grade and are difficult to process. Because of the low-grade, operations processing ultramafic nickel ores have to run high tonnages in order to be profitable and, thus, generate large quantities of tailings. These tailings are a liability as a waste product, but, as MCS feedstock, they have the potential to store sizable quantities of CO_2. A serpentine waste containing 40% MgO could theoretically store 0.44 kg of CO_2 per kg of waste. A mining operation producing 50,000 tonnes per day of serpentine waste could store 22,000 tonnes per day of CO_2, or up to 8 million tonnes of CO_2 per year. This is equivalent to the CO_2 emissions from a 1GW coal-fired power plant (Kelly et al., 2011). Given a regulatory framework with a monetary incentive to capture and store CO_2 emissions, the use of serpentine wastes as MCS feedstock could generate revenue for mining and mineral processing operations (Bobicki et al., 2012).

In addition to carbonating the tailings for CO_2 storage, there is the potential to pre-treat ultramafic nickel ores in a way that could enhance both mineral processing and MCS operations. As mentioned, ultramafic nickel ores are difficult to process, and the difficulty is largely due to the presence of serpentine. The processing of ultramafic nickel ores involves upgrading by froth flotation, on which serpentine minerals have a particularly negative effect. The surface charge of serpentine minerals is opposite that of the valuable nickel-bearing mineral, pentlandite, at the pH of flotation (pH 9-10) (Edwards et al., 1980; Bremmel et al., 2005; Feng et al., 2012). Hence, serpentine tends to slime-coat pentlandite during flotation and render it unrecoverable. Fibrous serpentine can also form fibre-bubble aggregates that report to the froth, resulting in a diluted concentrate and creating problems downstream during smelting operations (Xu et al., 2010). In addition, serpentine also greatly increases the viscosity of ore slurries due to its morphology and anisotropic nature (Ndlovu et al., 2011), inhibiting the separation of minerals and necessitating that grinding and flotation be conducted at low solids content, which is inefficient and energy intensive (Xu et al., 2010; Senior and Thomas, 2005). Thus, the destruction of serpentine minerals in ultramafic nickel ores by dehydroxylation would likely be beneficial for mineral processing, as well as MCS.

A new process is proposed where ultramafic nickel ore is treated with microwave radiation prior to grinding as part of mineral processing operations. Microwave radiation is electromagnetic radiation with frequencies of 0.3-300 GHz and wavelengths of 0.001-1 m. The internationally recognized frequency bands used for industrial and domestic applications are 915 and 2450 MHz (Pickles, 2009a) respectively, and electrical energy is converted to microwave energy with efficiencies of 85% and 50% for these frequencies (Haque, 1999). Microwaves can be transmitted, reflected, or absorbed, and can efficiently and instantaneously generate heat in microwave-absorbing materials (Haque, 1999; Pickles, 2009a). Microwave heating is unique in that heating is from the inside-out. During microwave heating, microwave radiation penetrates a material where it is transformed to heat, which is then conducted through the material back to the

surface. During conventional heating, by contrast, the surface of the object is heated first, and heat then flows to the inside by conduction (Pickles, 2009a). Advantages of microwave heating include that it is non-contact, rapid, material selective (although this is restricted by heat conduction) and start-up and shut-down are relatively swift (Haque, 1999). Microwaves have been applied to a number of metallurgical applications including drying, grinding, leaching, calcination, sintering, reduction, roasting/smelting, and spent carbon regeneration, and have been used for the processing of oxide ores, slags, electric arc furnace dust, gaseous effluents and gold-bearing materials (Pickles, 2009b; Haque, 1999).

It is hypothesized that the microwave pre-treatment of ultramafic nickel ores should result in heating, serpentine dehydroxylation and the formation of olivine (reaction 3.1).

$$2Mg_3Si_2O_5(OH)_4 \rightarrow 3Mg_2SiO_4 + SiO_2 + 4H_2O \qquad (3.1)$$
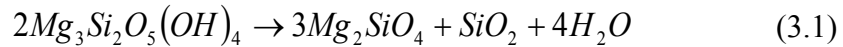
Olivine is not fibrous or anisotropic, and has an isoelectric point close to that of pentlandite (Fuerstenau and Pradip, 2005). Thus, the negative effects of serpentine on grinding and flotation, including slime-coating, froth dilution by fibre-bubble aggregates, and high viscosity, should be reduced or eliminated by microwave pre-treatment. In addition, the flotation tailings should be more reactive to CO_2.

Microwave treatment has been used by others to dehydroxylate serpentine. Corradi et al. (2003) and Leonelli et al. (2006) both report that microwave radiation has been used to convert chrysotile asbestos waste to olivine with no hazardous or fibrous content. Microwaves have also been investigated in a limited way as a means of improving mineral CO_2 sequestration. White et al. (2004) investigated (1) the reactivity of CO_2 with serpentine at 1 bar and 375-650°C in a gas-solid reaction in a microwave furnace, (2) the dehydroxylation of serpentine in a microwave furnace, and (3) the reaction of serpentine with bicarbonates in a microwave hydrothermal apparatus at 15 bar and 200°C. In the first and third sets of experiments, little reaction was observed. However, in the

73

second set of experiments, 0.5 g serpentine was dehydroxylated in a 2000 W, 2.45 GHz commercial microwave furnace after 30 minutes of exposure to microwave irradiation. The fact that serpentine was dehydroxylated in a microwave furnace is promising. The poor carbonation results were due to unsuitable reaction conditions. Both gas-solid and direct aqueous carbonation processes are known to yield poor results at low pressures (Bobicki et al., 2012; Gerdemann et al., 2007).

Although microwave treatment has been tested on pure serpentine and numerous other ores, including other nickel ores (Henda et al., 2005; Samouhos et al., 2012), it has not previously been tested on ultramafic nickel ores. In addition to the primary gangue mineral, serpentine, and the valuable nickel mineral, pentlandite, various other minerals are present in these ores including magnetite, pyrrhotite, and quartz. While serpentine and quartz are low- and non-microwave responsive minerals, magnetite, pyrrhotite and pentlandite are highly responsive to microwave radiation (Liu et al., 1990; Haque, 1999). In theory, the presence of microwave responsive minerals amidst the low- and non-microwave responsive minerals should improve the heating of ultramafic nickel ores compared to pure serpentine. This, however, needs to be confirmed. In addition, while the conversion of serpentine to olivine is expected and desired, there will likely be other mineralogical changes that occur in ultramafic ores as a result of exposure to microwave radiation. Thus, the objective of this paper is to determine the microwave heating characteristics of ultramafic nickel ores, and to characterize the resultant changes in mineralogy. Particular attention is paid to changes in magnesium silicate and nickel mineralogy, with a view to predict whether or not microwave pre-treatment can improve the processing of ultramafic nickel ores and carbonation of the tailings.

3.2 Materials and Methods

3.2.1 Mineral Feedstock

Two low-grade ultramafic nickel ores were used in this study. The first, referred to as the "OK ore", was obtained from the Okanogan nickel deposit in

Washington State, USA. The second ore, referred to as the "Pipe ore", was sourced from the Vale-owned Pipe deposit located in the Thomson Nickel Belt. The OK ore was received as cobbles of 9-20 cm. It was crushed to < 2.5 mm using a jaw crusher (BB 200, Retsch, Burlington, ON, Canada), and then reduced to < 1.0 mm with a disc mill (DM 200, Retsch, Burlington, ON, Canada). The < 1.0 mm material was sieved using standard techniques to isolate the 0.425-1 mm size fraction. The Pipe ore was received pre-crushed to < 2 mm. It was sieved to isolate the 0.425-1 mm size fraction. The 0.425-1 mm size fractions of both the OK and Pipe ore were split into 100 g samples for microwave test work using a Jones riffle sample splitter. Elemental composition of the OK and Pipe ores is shown in Table 3-1.

Table 3-1: Elemental composition of OK and Pipe ores.

	MgO	CaO	SiO_2	Al_2O_3	Fe	Ni	S
Method	XRF	XRF	XRF	XRF	ICP	ICP	CHNS
OK Ore (wt.%)	45.8	0.8	40.7	1.1	4.6	0.26	0.66
Pipe Ore (wt.%)	39.5	1.1	34.8	1.8	6.0	0.23	2.18

3.2.2 Microwave Heating

A 1000 W, 2.45 GHz household microwave oven manufactured by Panasonic (NN-SF550M Flat and Wide) was used for the microwave treatment. The microwave oven was modified to allow purge gas to flow through a reactor stationed inside the oven. Microwave leakage was tested after modification of the microwave oven and found to be well below legal limits. The microwave reactor was fabricated of quartz and was insulated with ceramic wool. 100 g samples of ore (0.425-1 mm size fraction) were placed in a 100 mL quartz crucible, which was then placed in the microwave reactor. During microwave treatment, the reactor was purged continuously with 1 L/min of nitrogen gas. To establish microwave heating curves, ore samples were exposed to microwave radiation for various lengths of time. Immediately following treatment, the samples were removed from the reactor and the temperature of the samples was determined by

inserting the tip of a Type K thermocouple into the center of the sample. In all other tests, samples were allowed to cool for a minimum of two hours in the microwave reactor under a nitrogen atmosphere.

3.2.3 Materials Characterization

X-ray fluorescence (XRF) spectroscopy (Orbis PC Micro-EDXRF Elemental Analyzer, EDAX, Mahwah, NJ, USA) was used to determine the elemental composition of the ores for elements heavier than sodium. Prior to analysis, powdered samples were pressed into 1 inch diameter pellets. The XRF microprobe was operated at 40 kV and 250 µA and the X-ray source was monochromatic Rh Kα radiation.

Inductively coupled plasma mass spectrometry (ICP-MS) (Perkin Elmer Elan 6000, Waltham, Massachusetts, USA) was used to determine the elemental composition of the ores. A mixture of 0.2 g of powered sample, 5 mL HNO_3 and 5 mL HF was heated on a hot plate for 48 hours. The sample was then dried and mixed with 5 mL HNO_3 and 5 mL HCl and heated for a further 24 hours on a hot plate. After the second heating, the sample was dried again, then combined with 8 N HNO_3 and analyzed.

Sulphur analysis was conducted using a combustion technique (Vario MICRO Cube, Elementar, Hanau, Germany).

Quantitative XRD analysis was performed on several samples using the Rietveld refinement technique by PMET Inc. of New Brighton, Pennsylvania, USA.

Fourier transform infrared spectroscopy (FTIR) was used to identify changes in the molecular structure of ore samples. Infrared spectra were collected across the mid-infrared range (4000-400 cm^{-1}) using a Bio-Rad FTS 6000 Fourier Transform Infrared Spectrophotometer (Bio-Rad Laboratories, Hercules, CA, USA). Samples were diluted in powdered potassium bromide (KBr) at concentration of 5% prior to the analysis. The collected spectra were interpreted by comparison to spectra reported in the literature.

Scanning electron microscopy (SEM) was used to study pre-treated and untreated ore. Prior to the analysis, ore samples were set in resin, polished to reveal particle cross sections, and coated with carbon (to minimize charging effects). A Hitachi S-2700 Scanning Electron Microscope equipped with a Princeton Gamma-Tech IMIX digital imaging system was used to obtain the micrographs. A PGT PRISM Intrinsic Germanium detector was used for EDX (Energy Dispersive X-Ray) analysis and BSE (Backscattered Electron) analysis was performed using a GW Electronics 47 four quadrant solid state backscattered electron detector. The probe was operated with an accelerating voltage of 20 kV and a current of 0.5 nA. The working distance was 17 mm.

3.3 Results and Discussion

3.3.1 Microwave Heating

The temperature of the OK and Pipe ores versus microwave heating time is depicted in Figure 3-2, while the heating rates versus temperature are shown in Figure 3-3. Both ores heated well in response to microwave treatment, but demonstrated somewhat different heating characteristics. The heating behavior of the two ores can be explained by differences in mineralogical composition and microwave theory. The heating rate of a material as a result of exposure to microwave radiation (Equation 3.1) is directly proportional to power dissipation $(P(z))$, and inversely proportional to the material density (ρ) and specific heat capacity (C_p) (Pickles, 2009a). The power dissipation of microwave energy for nonmagnetic dielectric materials $(P_E(z))$ is a function of microwave frequency (f), the dielectric loss factor (ε_r''), the permittivity of free space (ε_o), and the electric field intensity (E) (Equation 3.2) (Pickles, 2009a). Non-metallic, magnetic materials may also heat due to magnetic losses, in which case there is additional power dissipation $(P_H(z))$ given by Equation 3.2, where μ_o is the permeability of free space, μ_r'' is the magnetic loss factor, and H is the magnetic field intensity (Hill, 2000; Peng, 2012). Total power dissipation in a non-metallic, magnetic, dielectric material can be found by summing Equations 3.2 and 3.3 (Peng, 2012).

$$\frac{dT}{dt} = \frac{P(z)}{\rho C_p}$$

(3.1)

$$P_E(z) = 2\pi f \varepsilon_o \varepsilon_r{}'' E^2$$

(3.2)

$$P_H(z) = 2\pi f \mu_o \mu_r{}'' H^2$$

(3.3)
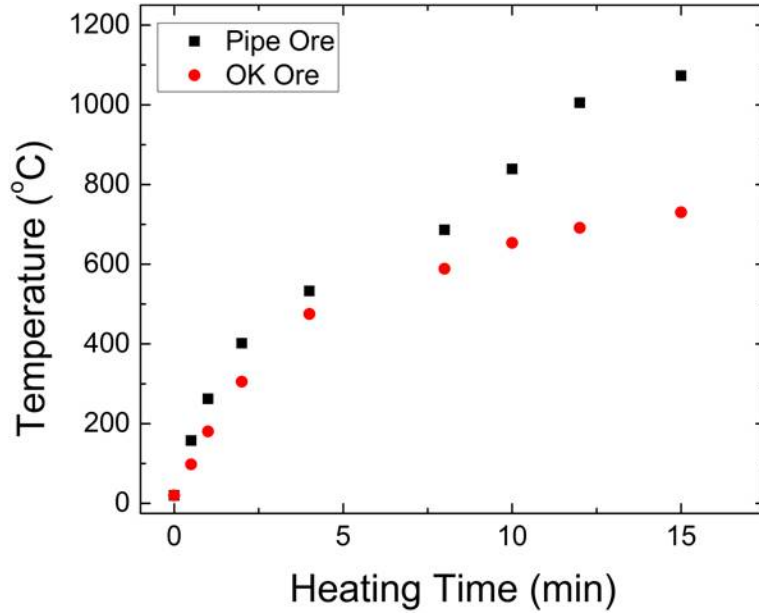
Figure 3-2: Temperature versus microwave exposure time for OK and Pipe ores.
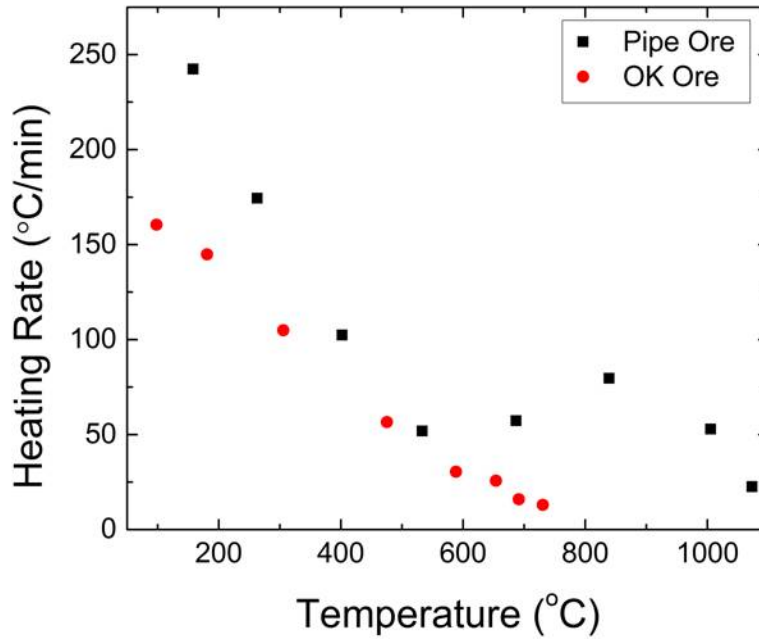
Figure 3-3: Heating rate as a result of exposure to microwave radiation versus temperature for OK and Pipe ores.

The OK ore heating curve was logarithmic in shape, with a high initial heating rate that declined with increasing microwave exposure time. The OK ore heating rate decreased with increasing temperature and appears to have been governed largely by the properties of serpentine (a plot of serpentine loss factor over heat capacity generates a curve nearly the same shape as the OK ore heating rate curve) (Figures 3-4 and 3-5). It should be noted that the heat capacity and dielectric data presented in Figures 3-4 and 3-5 is from the literature and that the values given likely differ somewhat from those for the minerals in the ores studied due to natural variations in mineral composition. The OK ore attained a maximum bulk temperature of 730°C after 15 minutes heating time.
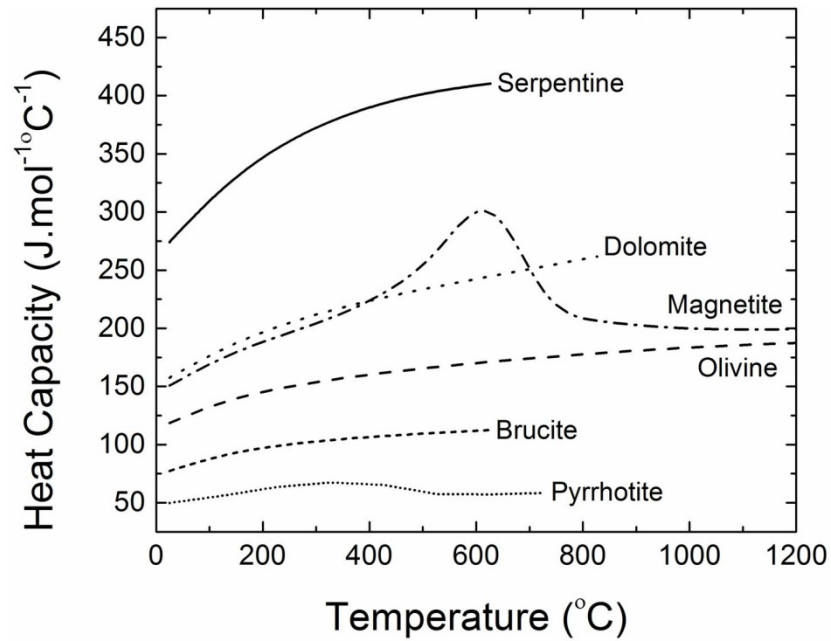
Figure 3-4: Heat capacities for serpentine, dolomite, magnetite, olivine, brucite and pyrrhotite (Robie and Hemingway, 1995).
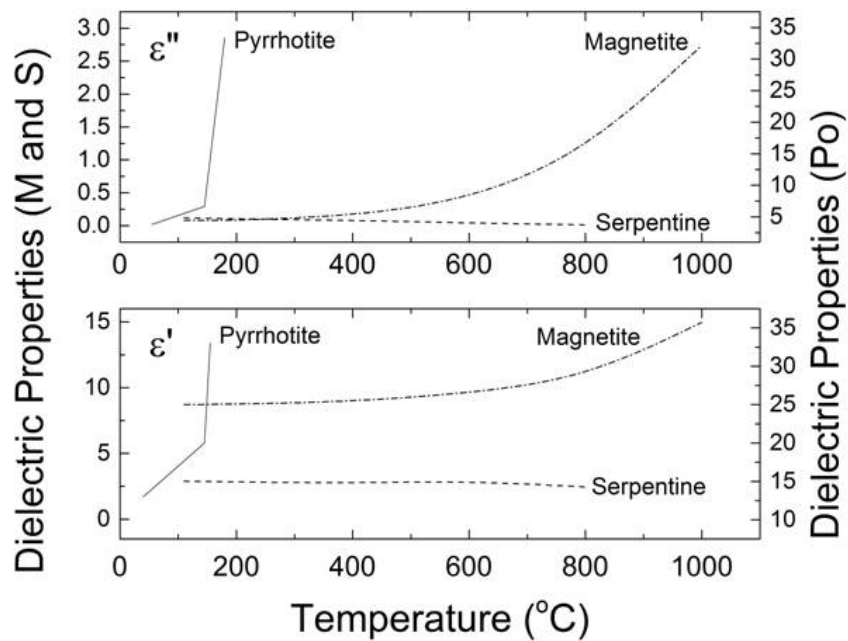
Figure 3-5: Dielectric constant (ε') and dielectric loss factor (ε") data for pyrrhotite, magnetite and serpentine from literature (AECL and Voss Associates, 1990).

The Pipe ore heating and heating rate curves were somewhat different from those for the OK ore. Up until 8 minutes microwave heating time, the Pipe ore also demonstrated a high initial heating rate that declined with increasing microwave exposure time. After 8 minutes of microwave heating time, however, an increase in heating rate was observed. The increase in heating rate was accompanied by the appearance of a molten state in the centre of the Pipe ore sample which fused upon cooling. During the initial stage of heating (up to approximately 600°C), the Pipe ore heating rate appears to have been dominated by serpentine (similar to the OK ore, the shape of the Pipe heating rate curve was similar in shape to a plot of serpentine loss factor over heat capacity in this region). Above 600°C, the Pipe ore heating rate seems to have been heavily influenced by magnetite (second most abundant mineral in Pipe ore, nearly double that in the OK ore). At 600°C, the heat capacity of magnetite decreases while the loss factor increases exponentially with increasing temperature (Figures 3-4 and 3-5). Although magnetite is a magnetic material, and magnetic losses have been shown to dominate the heating of magnetite at low temperatures, magnetic absorption of microwave energy has been shown to be very small above the Curie point (585°C) (Hotta et al., 2011; Peng, 2012). Thus, it is probable that the combination of decreasing magnetite heat capacity and increasing magnetite dielectric loss factor at 600°C led to the jump in the Pipe ore heating rate at this temperature. Overall, the Pipe ore attained a maximum bulk temperature of 1073°C after 15 minutes heating time.

Microwave heating curves for comparable ores have not been found in the literature; however there is data on the microwave heating response of the individual minerals (Haque, 1999; Hua and Lin, 1996; AECL and Voss, 1990). In general, iron oxides and sulphides, such as magnetite, pyrrhotite and pentlandite, are reported to heat well in response to microwave radiation, while silicates, including serpentine, olivine and quartz, are reported to heat little or not at all (Haque, 1999). For example, AECL and Voss Associates (1990) report that exposing 35 g of serpentine to microwave radiation in a 1.4 kW oven for 20 minutes only raised the temperature of the mineral to 288°C, while treating 35 g of magnetite in the same oven for 2 minutes resulted in a final temperature of

730ºC. Similarly, Haque (1999) reports that 25 g of pyrrhotite exposed to microwave radiation for 1.75 minutes reached a temperature of 886ºC. The fact that both the OK and Pipe ores heated better in response to microwave radiation than the pure serpentine reported by AECL and Voss Associates (1990) suggests the iron oxide and sulphide minerals present in these ores played a role in their heating response. The greater concentration of magnetite and pyrrhotite in the Pipe ore likely lead to its greater heating rate at low and high temperatures, and higher ultimate temperature achieved compared to the OK ore. The enhanced microwave heating response of ultramafic nickel ores means less applied energy is required to dehydroxylate serpentine contained in these ores compared to pure serpentine.

3.3.2 Mineralogy

3.3.2.1 XRD

The results of quantitative XRD analysis of untreated and microwave pre-treated OK and Pipe ore are shown in Table 3-2. The serpentine and olivine content in the ores is shown graphically in Figure 3-6. Prior to microwave pre-treatment, both ores were primarily composed of serpentine. The XRD results indicate that microwave heating times up to 4 minutes had little effect on the serpentine content. However, after 8 minutes microwave treatment time, serpentine began to breakdown markedly and form olivine. For the OK ore, a microwave pre-treatment time of 15 minutes decreased the serpentine content from 84.0 wt.% to 15.8 wt.% and increased the olivine content from 0 wt.% to 80.2 wt.%. For the Pipe ore, a microwave pre-treatment time of 8 minutes reduced the serpentine content from 63.7 wt.% to 23.7 wt.% and increased the olivine content from 7.7 wt. % to 51.1 wt.%. The substantial conversion of serpentine to olivine in the OK and Pipe ores should be beneficial for both carbon storage and mineral processing. A potentially negative impact (for flotation) of microwave pre-treatment of ultramafic nickel ores is that pentlandite was demonstrated to break down into another nickel phase that was not detected by XRD.

Table 3-2: Mineral composition of untreated and microwave treated OK and Pipe ores as determined by quantitative XRD analysis.

Composition of OK Ore (wt.%)		Microwave Treatment Time (min)				
		0	2	4	8	15
Serpentine	$Mg_3Si_2O_5(OH)_4$	84.0	85.0	86.6	54.5	15.8
Olivine	Mg_2SiO_4	0.0	1.3	2.4	34.7	80.2
Brucite	$Mg(OH)_2$	5.1	4.0	0.8	0.0	0.0
Magnetite	Fe_3O_4	6.7	5.9	6.5	6.7	4.0
Pyrrhotite	$Fe_{1-x}S$	0.0	0.0	0.0	1.8	0.0
Pentlandite	$(Fe,Ni)_9S_8$	4.3	3.9	3.8	2.3	0.0
Composition of Pipe Ore (wt/%)		Microwave Treatment Time (min)				
		0	1	2	4	8
Serpentine	$Mg_3Si_2O_5(OH)_4$	63.7	66.4	65.0	62.1	23.7
Olivine	Mg_2SiO_4	7.7	5.5	5.3	9.6	51.1
Cordierite	$Mg_2Al_4Si_5O_{18}$	1.0	1.0	1.4	1.9	1.0
Vermiculite	$Mg_2Si_4O_{10}(OH)_2$	0.7	0.0	0.0	0.0	0.0
Dolomite	$CaMg(CO_3)_2$	5.5	5.3	5.6	3.5	1.4
Magnetite	Fe_3O_4	12.3	12.1	12.5	12.7	14.1
Pyrrhotite	$Fe_{1-x}S$	4.7	5.0	5.1	5.5	5.6
Pentlandite	$(Fe,Ni)_9S_8$	2.8	2.6	2.7	1.9	0.8
Quartz	SiO_2	1.6	2.1	2.4	2.8	2.3
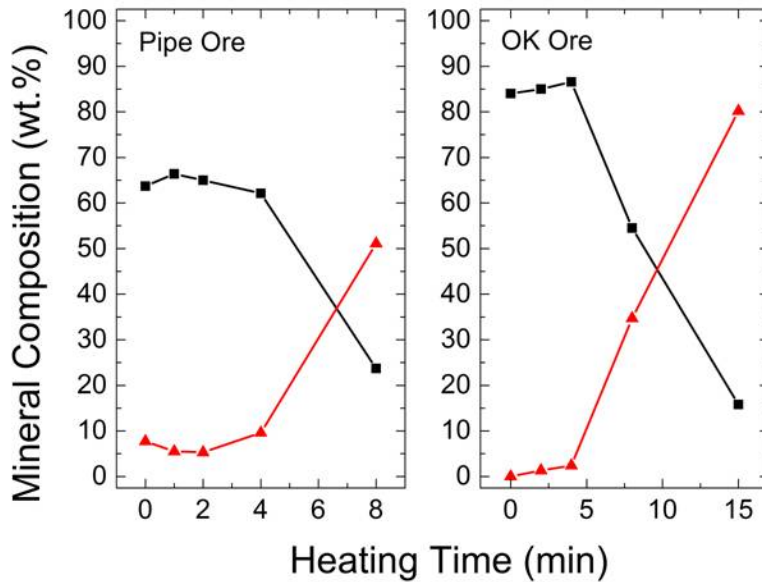
Figure 3-6: Serpentine (■) and olivine (▲) content of Pipe and OK ores as a function of microwave heating time.

3.3.2.2 SEM

To better understand the fate of nickel in the OK and Pipe ores after microwave pre-treatment, which will have implications for the effect of microwave pre-treatment on the flotation of these ores, samples of untreated and pre-treated OK and Pipe ore were analyzed by SEM-EDX. Figures 3-7a and 3-7c depict SEM-BSE images of untreated OK and Pipe ore respectively. Figure 3-7b shows an SEM-BSE image of OK ore microwave pre-treated for 15 minutes and Figure 3-7d displays Pipe ore microwave pre-treated for 8 minutes. The continuous dark grey material of various shades in the OK and Pipe ore SEM-BSE images was composed of magnesium, silicon and oxygen. This material is the serpentine and olivine detected by XRD. The light grey material observed clearly in the SEM-BSE image shown of the untreated OK ore (Figure 3-7a) was similar in composition to the dark grey, although it also contained iron. This material was most probably serpentine with iron substituted for magnesium in the octahedral layer. The bright white material in the SEM-BSE images of the OK and Pipe ore was composed of iron, nickel and sulphur in various ratios. Magnetite also appeared bright white in the SEM-BSE images, however, the texture was finer than the Fe-Ni-S material.
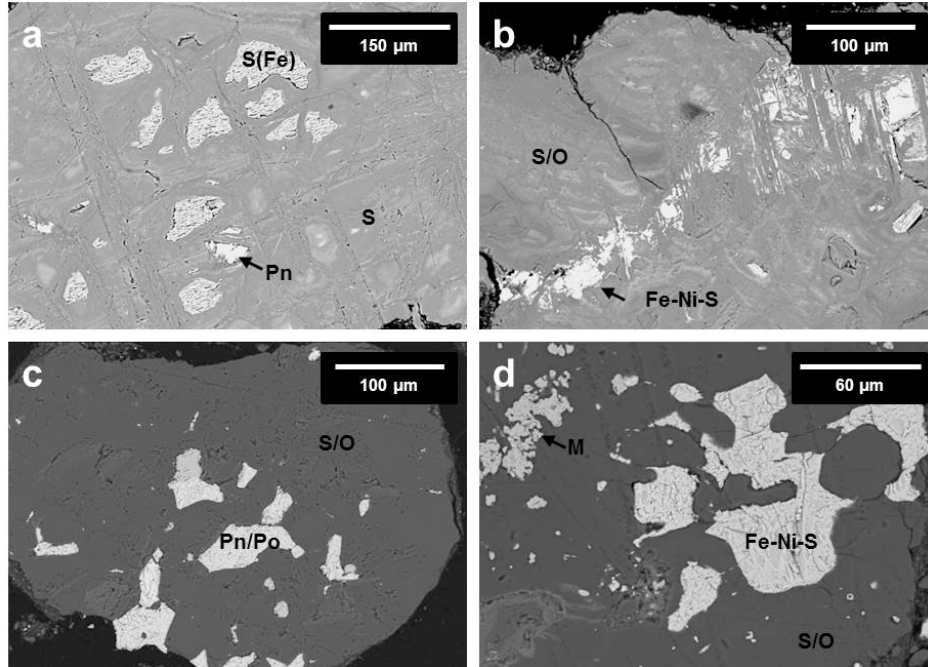
Figure 3-7: SEM-BSE images of (a) untreated OK ore, (b) OK ore microwave pre-treated for 15 minutes, (c) untreated Pipe ore, and (d) Pipe ore microwave pre-treated for 8 minutes. The phases are designated as follows: serpentine (S), iron-substituted serpentine (S(Fe)), olivine (F), pentlandite (Pn), pyrrhotite (Po), iron-nickel sulphide (Fe-Ni-S), and magnetite (M).

As is evident from the SEM-BSE images, nickel remained in a Fe-Ni-S phase in the Pipe and OK ores after microwave pre-treatment. The Fe-Ni-S minerals observed in the microwave pre-treated ores had metal-to-sulphur (M:S) ratios representative of pyrrhotite (high-sulphur) and pentlandite (low sulphur); however, the high-sulphur material was mostly nickel-rich (up to 23 at.%) while the nickel content of the low-sulphur material was variable, ranging from 1-36 at.%. Upon heating, pentlandite is reported to degrade to a monosulphide solid-solution (mss) of the formula $(Fe,Ni)_{1-x}S$ at temperatures above 610°C (Etschmann et al., 2004; Wang, 2006). Some researchers assert the mss coexists with a $Ni_{3\pm x}S$ phase (Kullerud, 1963; Raghavan, 2004), while others believe a high-temperature pentlandite solid-solution (hpn) appears with mss at temperatures below 870°C (above which hpn breaks down into mss and liquid) (Sugaki and Kitakaze, 1998; Kitakaze et al., 2011). Upon quenching and cooling

to room temperature, pentlandite re-forms from the high-temperature phases (Kullerud, 1963; Etschmann et al., 2004). Under natural conditions (slow cooling, sulphur-rich composition, and presence of impurities), however, pentlandite is reported to exsolve over a period of 3,000 to 30,000 years (Etschmann et al., 2004). Thus, it appears Ni remained in high-temperature phases after slow cooling in the microwave pre-treated OK and Pipe ores. The transition of pentlandite to other nickel phases may have implications for mineral processing and the upgrading of ultramafic nickel ores by froth flotation.

3.2.2.3 FTIR

FTIR analysis was done to better understand the conversion of serpentine to olivine by microwave treatment. FTIR spectra collected for untreated and microwave pre-treated OK and Pipe ore are shown in Figures 3-8 and 3-9. The spectra collected for all samples were similar, but with important differences (Tables 3-3 and 3-4). Three main adsorption bands were observed in the IR spectrum: the first in the 3700-3300 cm^{-1} region, the second in the 1100-800 cm^{-1}, and the third in the 800-500 cm^{-1} region. The peaks in the first region correspond to the stretching vibrations of the hydroxyl groups bonded to octahedrally coordinated cations in the serpentine brucite layer (Fuchs et al, 1998; Foresti et al., 2009; Mellini et al., 2002; Anbalagan et al., 2010; Liu et al., 2010). The main peak at 3687-3690 cm^{-1} in the OK and Pipe ore can be attributed to hydroxyl groups bonded to magnesium ions. The weaker peaks are the result of substitution by aluminum, nickel, and ferrous ions for magnesium (3668 cm^{-1}, 3650 cm^{-1} and 3575 cm^{-1}) (Fialips et al., 2000; Fuchs et al, 1998; Scholtzová et al., 2003). The shoulder (tail towards lower wavenumbers) adjacent to the hydroxyl peaks indicates variations in M-OH bond strengths (Mellini et al., 2002).
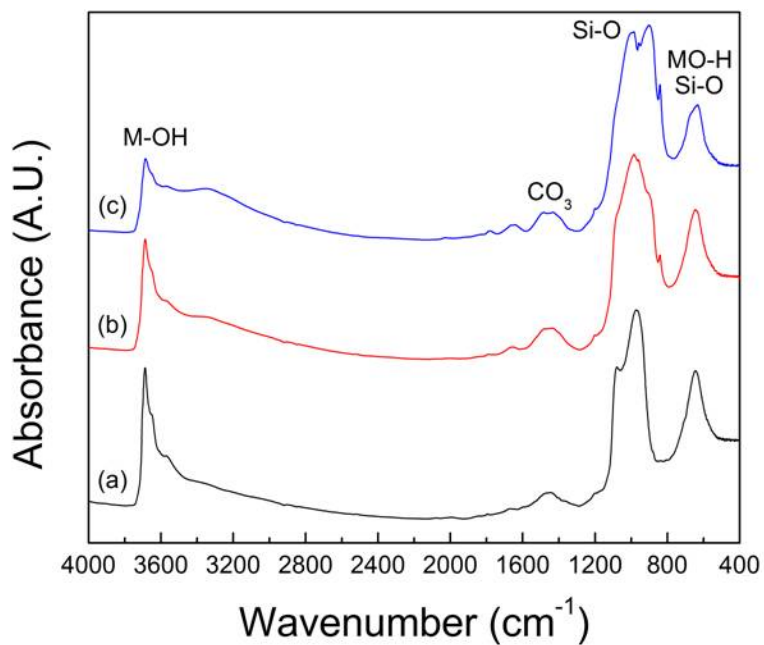
Figure 3-8: FTIR spectra obtained for untreated OK ore (a) and OK ore microwave pre-treated for 8 (b) and 15 (c) minutes.
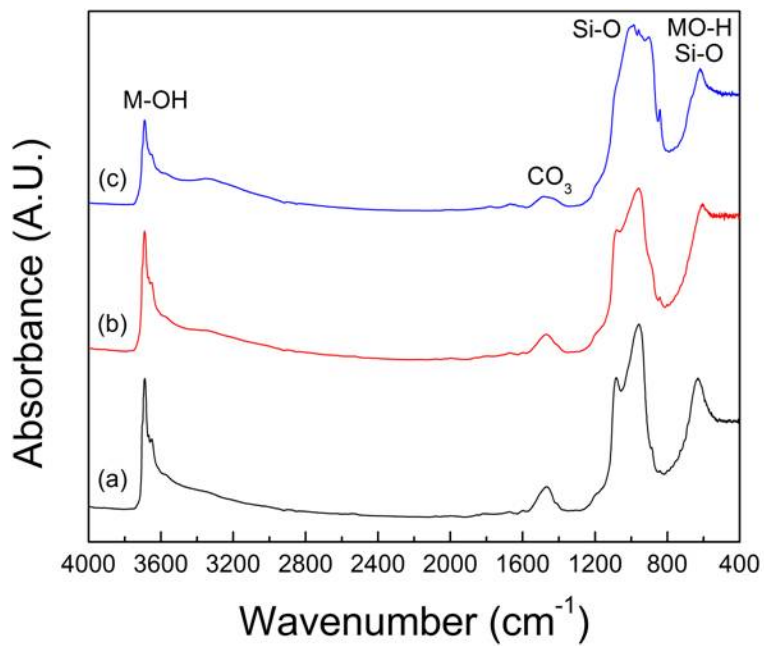
Figure 3-9: FTIR spectra obtained for untreated Pipe ore (a) and Pipe ore microwave pre-treated for 4 (b) and 8 (c) minutes.

Table 3-3: Major FTIR absorbance peaks for spectra collected from untreated OK ore (OK UT) and OK ore microwave pre-treated for 2, 4, 8 and 15 minutes (OK 2, OK 4, OK 8, and OK 15 respectively).

Sample	Region 1			Region 2					Region 3
OK UT	3688	3575	-	1079	-	971	-	-	648
OK 2	3688	3575	-	1079	-	971	-	-	648
OK 4	3687	3576	-	1074	-	970	-	842	648
OK 8	3687	3576	3357	-	985	960	-	841	646
OK 15	3686	3574	3352	-	985	957	901	841	629

Table 3-4: Major FTIR absorbance peaks for spectra collected from untreated Pipe ore (Pipe UT) and Pipe ore microwave pre-treated for 1, 2, 4, and 8 minutes (Pipe 1, Pipe 2, Pipe 4 and Pipe 8 respectively).

Sample	Region 1				Region 2						Region 3
Pipe UT	3690	3668	3651	-	1083	-	958	-	886	842	629
Pipe 1	3690	3668	3650	-	1082	-	959	-	886	842	628
Pipe 2	3690	3668	3651	-	1081	-	960	-	886	842	615
Pipe 4	3691	3669	3652	-	1079	-	960	-	-	842	610
Pipe 8	3690	-	3653	3355	-	985	960	903	-	842	609

The peaks in the second region are related to the vibrations of Si-O bonds. Some of the peaks are associated with the serpentine siloxane layer, including the 1074-1083 cm^{-1} bands (stretching of the apical Si-O bond perpendicular to the basal plane) and the 960-971 cm^{-1} bands (arising from the stretching of the basal Si-O-Si bonds that bridge pairs of corner-sharing Si tetrahedra) (Anbalagan et al, 2010; Fuchs et al, 1998; Mellini et al, 2002). Other peaks, including those at 841-842 cm^{-1}, 886 cm^{-1}, 901-903 cm^{-1}, 957-960 cm^{-1} and 985 cm^{-1} are due to stretching vibrations of Si-O bonds in the isolated silica tetrahedra of olivine (Franco et al., 2006; Russell et al., 2010; Makreski et al., 2005).

The origin of absorption in the 800-500 cm^{-1} range is more difficult to precisely define as many peaks overlap. In the case of serpentine, it appears absorption in this range may be attributed to the deformation of hydroxyl groups: bands in the range of 605-625 cm^{-1} can be attributed to the bending vibrations of MgO-H bonds on the inside of the brucite layer, whereas bands in the range of 640-650

cm^{-1} represent the vibrations of external MgO-H bonds (Foresti et al., 2009; Franco et al, 2006; Mellini et al, 2002). In the case of olivine, bands near 600 cm^{-1} are reported to be the result of SiO$_4$ bending modes (Makreski et al., 2005; Frost et al., 2007). The minor peak at 1450 cm^{-1} can be attributed to the asymmetric stretching of carbonate groups (Alstadt et al., 2012; Farmer, 1974).

Some differences between the OK and Pipe ore infrared spectra include the presence of olivine peaks in untreated Pipe ore and the position of weak hydroxyl peaks in region 1. The position of the weak hydroxyl peaks indicates that the substitution of Fe^{2+} for Mg^{2+} is dominant in the OK ore, whereas Al^{3+} and Ni^{2+} are substituted for Mg^{2+} more frequently in the Pipe ore. This correlates with the observation of Fe-substituted serpentine during SEM-EDX analysis.

Microwave pre-treatment resulted in some interesting changes in the FTIR spectra. In both the OK and Pipe ore, the area under the hydroxyl peaks in Region 1 was diminished with increasing microwave pre-treatment time, indicating that serpentine was progressively dehydroxylated. However, the area under the hydroxyl peaks did not diminish significantly until after 8 minutes microwave pre-treatment for both the OK and Pipe ores. This is in agreement with the XRD data which indicated that the serpentine content of the ores did not decrease markedly, and the olivine content did not increase significantly, until after 8 minutes of microwave pre-treatment. In addition to the diminishment of the hydroxyl peaks in Region 1, the hydroxyl shoulder became more pronounced, indicating that remaining hydroxyl bonds were weakened. Also, an additional peak appeared in the OK and Pipe ores at 3352-3357 cm^{-1}. This peak can be attributed to Fe^{3+} substitution for Mg^{2+} in olivine (Berry et al., 2005). In Region 2, the peaks shifted from peaks associated with serpentine to peaks associated with olivine. In addition, the olivine peak at 886 cm^{-1} in the Pipe ore disappeared, apparently overshadowed by the more intense olivine peak at 901 cm^{-1}. In Region 3, the area under the peaks in both OK and Pipe ores was diminished, and the peaks shifted to lower wavenumbers, indicating MgO-H bonds were broken and those that remained were weakened. It is also possible that the peaks remaining in

this region after longer microwave pre-treatments were actually the result of olivine SiO_4 bending modes. Interestingly, the serpentine Si-O peaks did not diminish in intensity until after the diminishment of the Mg-OH and MgO-H peaks. Apparently the octahedral brucite layer is disrupted during the microwave pre-treatment of serpentine prior to the breaking apart of the tetrahedral siloxane layer. Trittschack and Groberty (2012) observed a similar phenomenon during the conventional heat treatment of serpentine. Upon the collapse of the siloxane layer, olivine forms from the newly isolated silica tetrahedra surrounded by dehydroxylated octahedral magnesium, as evidenced by the subsequent increase in intensity of the Si-O peaks associated with olivine.

3.4 Conclusions

Ultramafic nickel ores were found to respond well to microwave radiation, and the heating rate of these ores, as well as the temperature achieved, was found to be dependent on the mineralogy. Ores that contain higher concentrations of highly microwave responsive minerals, such as magnetite, heated better in response to microwave radiation than ores with lower concentrations of these minerals. The enhanced microwave heating response of ultramafic nickel ores likely means the serpentine contained in these ores can be dehydroxylated at lower cost compared to pure serpentine. The temperatures achieved during the microwave pre-treatment of ultramafic nickel ores were sufficient to dehydroxylate serpentine; however, complete serpentine dehydroxylation was not achieved (serpentine content reduced from 84.0 wt.% to 15.8 wt.% for the OK ore and from 63.7 wt.% to 23.7 wt.% for the Pipe ore). FTIR analysis revealed that during serpentine dehydroxylation by microwave pre-treatment, the serpentine brucite layer broke down prior to the siloxane layer. In addition to the dehydroxylation of serpentine, several other mineralogical changes occurred as a result of microwave pre-treatment. Most notably, pentlandite was found to break down into pyrrhotite and another nickel phase that was not detectable by XRD. SEM-EDX analysis of microwave pre-treated ore revealed that the nickel remained in Fe-Ni-S compounds after microwave pre-treatment. The Fe-Ni-S compounds observed in

microwave pre-treated ore had metal-to-sulphur ratios resembling pyrrhotite (high-sulphur), but with high nickel content, and pentlandite (low-sulphur), but with variable nickel content. It was concluded that the nickel remained in high-temperature phases after microwave pre-treatment due to the slow kinetics of pentlandite/pyrrhotite exsolution under natural cooling conditions. The transition of pentlandite to other nickel phases as a result of microwave pre-treatment may have implications for the upgrading of ultramafic nickel ores by flotation.

3.5 References

Alexander, G., Maroto-Valer, M.M., Gafarova-Aksoy, P., 2007. Evaluation of reaction variables in the dissolution of serpentine for mineral carbonation. Fuel. 86, 273-281.

Alstadt, K.N., Katti, D.R., Katti, K.S., 2012. An in situ FTIR step-scan photoacoustic investigation of kerogen and minerals in oil shale. Spectrochimica Acta Part A: Molecular and Biomolecular Spectroscopy. 89, 105-113.

Alvarez-Silva, M., Uribe-Salas, A., Mirnezami, M., Finch, J.A., 2010. The point of zero charge of phyllosilicate minerals using the Mular-Roberts titration technique. Minerals Engineering. 23, 383-389.

Anbalagan, G., Sivakumar, G., Prabakaran, A.R., Gunasekaran, S., 2010. Spectroscopic characterization of natural chrysotile. Vibrational Spectroscopy. 52, 122-127.

Atomic Energy of Canada Limited Research Company (AECL) and Voss Associates Engineering Ltd, 1990. Microwaves and Minerals. Industrial Mineral Background Paper #14. Ontario Ministry of Northern Development and Mines. 77p.

Berry, A.J., Hermann, J., O'Neill, H.S.C., Foran, G.J., 2005. Fingerprinting the water site in mantle olivine. Geology. 33(11), 869-872.

Birle, J.D., Gibbs, G.V., Moore, P.B., Smith, J.V., 1968. Crystal structures of natural olivines. American Mineralogist. 53, 807-824.

Bobicki, E.R., Liu, Q., Xu, Z., Zeng, H., 2012. Carbon capture and storage using alkaline industrial wastes. Progress in Energy and Combustion Science. 38, 302-320.

Bremmel, K.E., Fornasiero, D., Ralston, J., 2005. Pentlandite-lizardite interactions and implications for their separation by flotation. Colloids and Surfaces A: Physiochemical and Engineering Aspects. 252, 207-212.

Corradi, A., Siligardi, C., Veronesi, P., Marucci, G., Annibali, M., Ragazzo, G., 2003. Microwave irradiation of asbestos containing materials. Proceedings of the 3rd World Congress on Microwave and Radio Frequency Applications. 2002 September; Sydney, Australia. Westerville: American Ceramic Society.

Edwards, C.R., Kipkie, W.B., Agar, G.E., 1980. The effect of slime coatings of the serpentine minerals, chrysotile and lizardite, on pentlandite flotation. International Journal of Mineral Processing. 7, 33-42.

Etschmann, B., Pring, A., Putnis, A., Grguric, B.A., Studer, A., 2004. A kinetic study of the exsolution of pentlandite $(Ni,Fe)_9S_8$ from the monosulfide solid solution (Fe,Ni)S. American Mineralogist. 89, 39-50.

Farmer, V.C., 1974. The infrared spectra of minerals. London, England: Mineralogical Society. 539pp.

Feng, B., Feng, Q., Lu, Y., 2012. A novel method to limit the detrimental effect of serpentine on the flotation of pentlandite. International Journal of Mineral Processing. 114-117, 11-13.

Fialips, C., Petit, S., Decarreau, A., Beaufort, D., 2000. Influence of synthesis pH on kaolinite "crystallinity" and surface properties. Clays and Clay Minerals. 48(2), 173-184.

Foresti, E., Fornero, E., Lesci, I.G., Rinaudo, C., Zuccheri, T., Roveri, N., 2009. Asbestos health hazrd: A spectroscopic study of synthetic geoinspried F-doped chrysotile. Journal of Hazardous Materials. 167, 1070-1079.

Franco, F., Pérez-Maqueda, L.A., Ramírez-Valle, V., Pérez-Rodríguez, J.L., 2006. Spectroscopic study of the dehydroxylation process of a sonicated antigorite. European Journal of Mineralogy. 18, 257-264.

Frost, R.L., Palmer, S.J., Reddy, B.J., 2007. Near-infrared and mid-IR spectroscopy of selected humite minerals. Vibrational Spectroscopy. 44, 154-161.

Fuchs, Y., Linares, J., Mellini, M., 1998. Mössbauer and infrared spectrometry of lizardite-1T from Monte Fico, Elba. Physical Chemistry of Minerals. 26, 111-115.

Fuerstenau, D.W., Pradip., 2005. Zeta potentials in the flotation of oxide and silicate minerals. Advances in Colloid and Interface Science. 114-116, 9-26.

Gerdemann, S.J., Dahlin, D.C., O'Connor, W.K., Penner, L.R., 2003. Carbon dioxide sequestration by aqueous mineral carbonation of magnesium silicate minerals. Albany, OR: Albany Research Center.

Gerdemann, S.J., O'Connor, W.K., Dahlin, D.C., Penner, L.R., Rush, H., 2007. Ex situ aqueous mineral carbonation. Environmental Science and Technology. 41, 2587-2593.

Haque, K.E., 1999. Microwave energy for mineral treatment processes – a review. International Journal of Mineral Processing. 57, 1-24.

Henda, R., Hermas, A., Gedye, R., Islam, M.R., 2005. Microwave enhanced recovery of nickel-copper ore: Comminution and flotatbility aspects. International Microwave Power Institute. 40(1), 7-16.

Hill, M.J., 2000. The microwave palaeointensity technique and its application to lava. Doctoral dissertation, University of Liverpool.

Hotta, M., Hayashi, M., Nagata, K., 2011. High temperature measurement of complex permittivity and permeability of Fe_3O_4 powders in the frequency range of 0.2 to 13.5 GHz. ISIJ International. 51(3), 491-497.

Hua, Y., Lin, C., 1996. Heating rate of minerals and compounds in microwave field. Transactions of NFsoc. 6(1), 35-40.

Kelly, K.E., Silcox, G.D., Sarofim, A.F., Pershing, D.W., 2011. An evaluation of ex situ, industrial-scale, aqueous CO_2 mineralization. International Journal of Greenhouse Gas Control. 5, 1587-1595.

Kitakaze, A., Sugaki, A., Itoh, H., Komatsu, R., 2011. A revision of phase relations in the system Fe-Ni-S from 650ºC to 450ºC. The Canadian Mineralogist. 49, 1687-1710.

Krevor, S.C.M., Lackner, K.S., 2011. Enhancing serpentine dissolution kinetics for mineral carbon dioxide sequestration. International Journal of Greenhouse Gas Control. 5, 1073-1080.

Kullerud G., 1963. Thermal stability of pentlandite. The Canadian Mineralogist. 7(3), 353-366.

Lackner, K.S., Wendt, C.H., Butt, D.P., Joyce, E.L., Sharp, D.H., 1995. Carbon dioxide disposal in carbonate minerals. Energy. 20(11), 1153-1170.

Leonelli, C., Veronesi, P., Boccaccini, D.N., Rivasi, M.R., Barbieri, L., Andreola, F., Lancellotti, I., Rabitti, D., Pellacani, G.C., 2006. Microwave thermal inertisation of asbestos containing waste and its recycling in traditional ceramics. Journal of Hazardous Materials. B135, 149-155.

Liu, C., Xu, Y., Hua, Y., 1990. Application of microwave radiation to extractive metallurgy. Chinese Journal of Metallurgical Science and Technology. 6, 121-124.

Liu, K., Chen, Q., Hu, H., Yin, Z., 2010. Characterization of lizardite in Yuanjiang laterite ore. Applied Clay Science. 47, 311-316.

Makreski, P., Jovanovski, G., Stojančeska, S., 2005. Minerals from Macedonia XIII: Vibration spectra of some commonly appearing nesosilicate minerals. Journal of Molecular Structure. 744-547, 79-92.

Maroto-Valer, M.M., Kuchta, M.E., Zhang, Y., Andrésen, J.M., Fauth, D.J., 2005. Activation of magnesium rich minerals as carbonation feedstock materials for CO_2 sequestration. Fuel Processing Technology. 86, 1627-1645.

McKelvy, M.J., Chizmeshya, A.V.G., Diefenbacher, J., Béarat, H., Wolf, G., 2004. Exploration of the role of heat activation in enhancing serpentine carbon sequestration. Environmental Science and Technology. 38, 6897-6903.

Mellini, M., Fuchs, Y., Viti, C., Lemaire, C., Linarés, J., 2002. Insights into the antigorite structure from Mössbauer and FTIR spectroscopy. European Journal of Mineralogy. 14, 97-104.

Metz, B., Davidson, O., de Coninck, H.C., Loos, M., Meyer, L.A., editors, 2005. IPCC Special Report on Carbon Dioxide Capture and Storage. Prepared by Working Group III of the Intergovernmental Panel on Climate Change. Cambridge, UK and New York, NY: Cambridge University Press. 443p.

Ndlovu, B.N., Forbes, E., Becker, M., Deglon, D.A., Franzidis, J.P., Laskowski, J.S., 2011. The effects of chrysotile mineralogical properties on the rheology of chrysotile suspensions. Minerals Engineering, 24, 1004-1009.

Nduagu, E., Romão, I., Fagerlund, J., Zevenhoven, R., 2013. Performance assessment of producing $Mg(OH)_2$ for CO_2 sequestration. Applied Energy. 106, 116-126.

O'Connor, W.K., Dahlin, D.C., Nilsen, D.N., Rush, G.E., Walters, R.P., Turner, P.C., 2000. CO_2 storage in solid form: A study of direct mineral carbonation. Greenhouse Gas Control Technologies: Proceedings of the 5th International Conference on Greenhouse Gas Technologies; 2000 Aug 14-18; Cairns, AU.

Peng, Z., 2012. Heat transfer in microwave heating. Doctoral dissertation, Michigan Technological University, 263p.

Pickles, C.A., 2009a. Microwaves in extractive metallurgy: Part 1 – Review of Fundamentals. Minerals Engineering. 22, 1102-1111.

Pickles, C.A., 2009b. Microwaves in extractive metallurgy: Part 2 – A review of applications. Minerals Engineering. 22, 1112-1118.

Raghavan, V., 2004. Fe-Ni-S (Iron-Nickel-Sulfur). Journal of Phase Equilibria and Diffusion. 25(4), 373-381.

Robie, R.A., Hemingway, B.S., 1995. Thermodynamic properties of minerals and related substances at 298.15K and 1 bar pressure and at higher temperatures. US Geological Survey Bulletin 2131. 470p.

Russell, S.D.J., Longstaffe, F.J., King, P.L., Larson, T.E., 2010. The oxygen-isotope composition of chondrules and isolated forsterite and olivine grains from the Tagish Lake carbonaceous chondrite. Geochemical et Cosmochimica Acta. 74, 2484-2499.

Samouhos, M., Taxiarchou, M., Hutcheon, R., Devlin, E., 2012. Microwave reduction of a nickeliferous laterite ore. Minerals Engineering. 34, 19-29.

Scholtzová, E., Tunega, D., Nagy, L.T., 2003. Theoretical study of cation substitution in trioctahedral sheet of phyllosilicates. An effect on inner OH group. Journal of Molecular Structure (Theochem). 620, 1-8.

Senior, G.D., Thomas, S.A., 2005. Development and implementation of a new flowsheet for the flotation of a low grade nickel ore. International Journal of Mineral Processing. 78, 49-61.

Sugaki, A., Kitakaze, A., 1998. High form pentlandite and its thermal stability. American Mineralogist. 83, 133-140.

Teir, S., Eloneva, S., Fogelholm, C.-J., Zevenhoven, R., 2009. Fixation of carbon dioxide by producing hydromagnesite from serpentinite. Applied Energy. 86, 214-218.

Trittschack, R., Grobety, B., 2012. Dehydroxylation kinetics of lizardite. European Journal of Mineralogy. 24, 47-57.

Wang, H., 2006. Isothermal kinetics of the pentlandite exsolution from mss/pyrrhotite using model-free method. Tsinghua Science and Technology. 11(3), 368-373.

White, B., Silsbee, M.R., Kearns, B.J., 2004. Reaction mechanisms of magnesium silicates with carbon dioxide in microwave fields. Final Report to the U.S. Department of Energy, National Energy Laboratory. February 18, 2004. Award No. DE –FG26-02NT41545.

Xu, M., Dai, Z., Dong, J., Ford, F., Lee, A., 2010. Fibrous minerals in ultramafic nickel sulphide ores. Proceedings of the 49th Conference of Metallurgists. 2010 October 3-6; Vancouver, Canada. Westmount: CIM; p. 223-36.

Chapter 4 Effect of Microwave Pre-treatment on Grindability of Ultramafic Nickel Ores[3]

4.1 Introduction

The energy efficiency of comminution is very low (< 1%) (Radziszewski, 2013). In fact, comminution has been reported to consume 75% of the energy used by mining operations (Tromans, 2008) and 2% of the total electric power generated worldwide (Herbst et al., 2003). Similarly, fine grinding in mineral carbon sequestration processes has been responsible for up to 75% of the process energy costs (O'Connor et al., 2000; Gerdemann et al., 2003). As such, great efforts have been made to reduce the energy intensity of grinding processes. Microwave pre-treatment has been identified as one way to improve the energy efficiency of grinding (Walkiewicz et al., 1991). Conventional size reduction involves the application of mechanical energy to break a particle into finer units. The greater the number of imperfections in a particle, the more easily it will break under mechanical stress. Since minerals have varying microwave absorption characteristics, different minerals within the same particle heat differentially upon exposure to microwave radiation. The differential heating of constituent minerals generates thermal stresses within particles and can lead to fracture. The fracturing often occurs along mineral grain boundaries, leading to improved mineral liberation and grinding efficiency (Amankwah and Ofori-Sarpong, 2011; Kingman et al., 2004).

A number of researchers have investigated microwave-assisted comminution and reported that microwave pre-treatment has improved the grindability of treated ore. Walkiewicz et al. (1991) demonstrated that microwave pre-treatment (3 kW, 2.45 GHz) for 3.5 minutes reduced the Bond work index of an iron ore by 10 to 24%. Henda et al. (2005) found that the exposure of a nickel sulphide ore to

---

[3] A version of this chapter has been published. Bobicki, E.R., Liu, Q., Xu, Z., Manchak, N., Xu, M., 2013. Effect of microwave pre-treatment on grindability of ultramafic nickel ores. Proceedings of Materials Science and Technology 2013. 27-31 Oct 2013, 1926-1933.

microwave radiation for 10 seconds (1.4 kW, 2.45 GHz) improved the grindability of the ore and produced a relative work index of 23%. Amankwah and Ofori-Sarpong (2011) found that microwave pre-treatment (800 W, 2.45 GHz) of a free-milling gold ore containing quartz, silicates and iron oxides enhanced the grindability of the ore and reduced the crushing strength by 31.2%. In most cases, despite improved grindability, the energy expended during microwave pre-treatment has been reported to be greater than the energy saved during comminution (Walkiewicz et al., 1991; Kingman et al., 2000). There are cases, however, where net energy savings have been realized. For example, Kingman et al. (2004) demonstrated that microwave treatment (15 kW for 0.2 s) reduced the total comminution energy by over 30% and improved the liberation of copper sulphide minerals in a copper carbonate ore with energy inputs of less than 1 kWh/t.

In general, microwave-assisted comminution appears to be most effective for ores composed of minerals that are good absorbers of microwave radiation in a transparent gangue matrix (Kingman et al., 2000). Ultramafic nickel ores seem to fit this description, containing mostly serpentine, which is not a good absorber of microwave energy (AECL and Voss Associates, 1990), and lesser concentrations of highly microwave responsive minerals, including magnetite, pentlandite and pyrrhotite (Liu et al., 1990). The objective of this paper is to explore the effects of microwave pre-treatment on ultramafic nickel ores in terms of ore grindability, specific surface area and pentlandite liberation. The results are discussed with respect to mineral processing, mineral carbon sequestration, and energy usage in comminution.

4.2 Materials and Methods

4.2.1 Feedstock

The feedstock material used for this study consisted of two low-grade ultramafic nickel ores: the "OK ore" from the Okanogan nickel deposit in Washington State, USA, and the "Pipe ore" from the Vale-owned Pipe deposit located in the

Thompson Nickel Belt. The OK ore consisted of 84.0 wt.% serpentine [$Mg_3Si_2O_5(OH)_4$], 6.6 wt.% magnetite [Fe_3O_4], 5.1 wt.% brucite [$Mg(OH)_2$] and 4.3 wt.% pentlandite [$(Fe,Ni)_9S_8$]. The Pipe ore contained 63.7 wt.% serpentine, 12.3 wt.% magnetite, 7.7 wt.% olivine [Mg_2SiO_4], 5.5 wt.% dolomite [$CaMg(CO_3)_2$], 4.7 wt.% pyrrhotite [$Fe_{1-x}S$], 2.8 wt.% pentlandite and trace quartz, cordierite and vermiculite. The ores were crushed and sieved to isolate the 0.425-1 mm and 1-2 mm size fractions, and split into 100 g samples.

4.2.2 Microwave Pre-Treatment

100 g ore samples were pre-treated in a quartz reactor placed inside a 1000 W, 2.45 GHz microwave oven (NN-SF550M Flat and Wide, Panasonic Corporation, Kadoma, Japan). During microwave pre-treatment, the reactor was purged continuously with 1 L/min of N_2 gas. The temperature achieved was determined by inserting a Type K thermocouple into the centre of the sample after heating. Samples used for temperature measurement were discarded. Samples pre-treated for grinding tests and micro-hardness measurements were cooled for 2 hours under nitrogen.

4.2.3 Grinding

100 g samples of 0.425-1 mm ore were ground aqueously at 30 wt.% solids in a stirred attrition mill (01-HD Laboratory Attritor, Union Process, Akron, OH) with alumina media (Union Process, Akron, Ohio, USA). The standard grinding time was 15 minutes. The relative work index (RWI) method described by Berry and Bruce (1966), as given by Equation 4.1, was used to assess the effect of microwave pre-treatment on the grindability of the ores, where P and F are the 80% passing size in μm of the product and feed materials respectively, r refers to the reference sample (untreated) and t refers to the test sample (microwave pre-treated). A RWI of 100% indicates no change in grindability, while a RWI of less than 100% indicates improved grindability and smaller product size, and a RWI greater than 100% indicates worsened grindability and a larger product size.

$$RWI = \left[\left(\frac{10}{\sqrt{P_r}} - \frac{10}{\sqrt{F_r}} \right) \middle/ \left(\frac{10}{\sqrt{P_t}} - \frac{10}{\sqrt{F_t}} \right) \right] \times 100\% \tag{4.1}$$

4.2.4 Materials Characterization

The particle size distribution of ground samples was determined using sieving techniques (Fisherbrand Sieves, Tyler Rotap) for particles > 250 µm and a light scattering technique (Mastersizer 2000, Malvern Instruments Ltd., Malvern, Worchestershire, UK) for particles < 250 µm. Light scattering, along with the use of sonication and a dispersant, was required to assess the particle size distribution of < 250 µm particles due to the severe aggregation of particles in this size class. Microhardness measurement (Tukon 1102 Knoop/Vickers Hardness Tester, Buehler, Lake Bluff, Illinois, USA) was performed on 1-2 mm ore particles set in resin and polished using the Vickers microhardness testing standard outlined in ASTM E384-11 (ASTM, 2012). The degree of cracking present in ore samples was determined by measuring the crack length per unit area (Image Pro Plus 7.0 software, Media Cybernetics, Rockville, MD) visible in SEM images (Hitachi S-2700, Tokyo, Japan) of polished cross-sections of randomly selected 0.425-1 mm unground particles. The mineral composition of the ores was determined by qualitative X-ray diffraction (XRD) (Rigaku XRD System, Rigaku, ON, Canada). Quantitative XRD analysis was performed on several samples by PMET Inc. of New Brighton, PA using the Rietveld refinement technique. The surface area of samples after grinding was determined by the multi-point Brunauer-Emmett-Teller (BET) method using an automated Autosorb-1 gas sorption analyzer (Quantachrome Instruments, Boynton Beach, FL, USA). Mineral liberation analysis (MLA, FEI Company, Brisbane, Australia) was conducted on ore samples after grinding by Vale Base Metals Technology Development (Mississauga, ON, Canada).

4.3 Results and Discussion

4.3.1 Ore Grindability

The product size (P_{80}) and RWI resulting from the attrition milling of microwave pre-treated Pipe and OK ores are depicted in Figures 4-1 and 4-2. Microwave pre-treatment of the OK ore drastically reduced the product size after milling and improved the grindability of the ore. The product size decreased with increasing pre-treatment time from a P_{80} of 606 μm with no pre-treatment to 19 μm after 15 minutes microwave pre-treatment (RWI = 3.6%). Similar improvements in ore grindability as a result of microwave pre-treatment have been observed by others (Amankwah and Ofori-Sarpong, 2011; Henda et al., 2005; Kingman et al., 2000; Walkiewicz et al., 1991). In contrast, microwave pre-treatment increased the product size of the Pipe ore and decreased the grindability. Without microwave pre-treatment, the Pipe ore ground as well as the OK ore pre-treated with microwaves for 15 minutes (P_{80} = 19 μm). With increasing microwave pre-treatment time, the P_{80} and RWI of the Pipe ore increased with increasing microwave heating time up to a microwave exposure time of 4 minutes (P_{80} = 148 μm). After 8 minutes of microwave pre-treatment, the P_{80} returned to a value near that of the untreated Pipe ore (P_{80} = 27 μm). Almost no instances of microwave pre-treatment worsening the grindability of ore have been reported in the literature, with the exception of Kaya (2010) who found the microwave pre-treatment of a porphyry copper ore increased the bond work index by 7%. The researchers attributed the decrease in grindability to the fusion of chalcopyrite particles (Kaya, 2010).
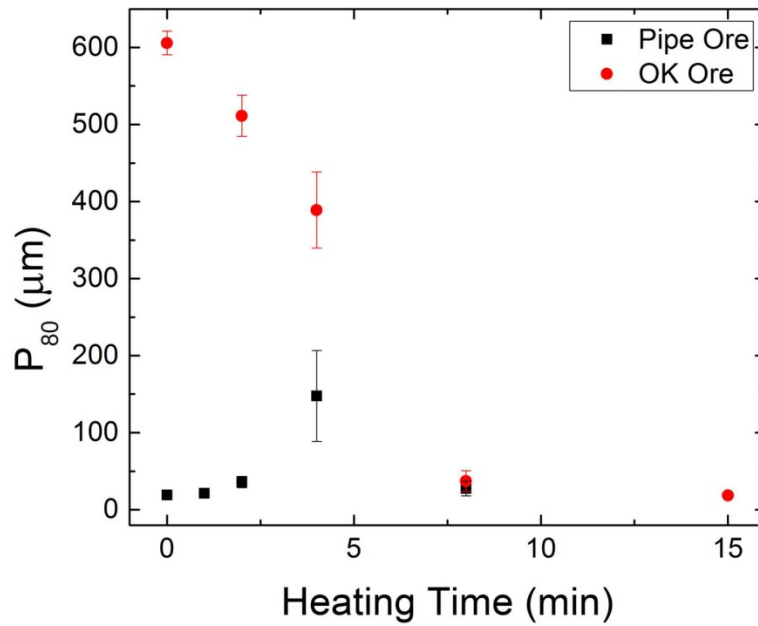
Figure 4-1: Product size (P$_{80}$) versus microwave heating time for Pipe and OK ores after grinding.
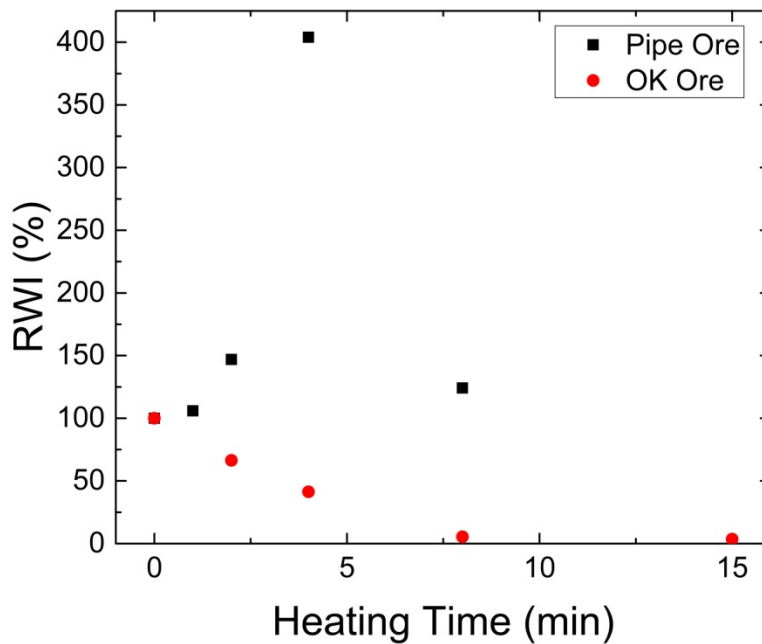
Figure 4-2: Relative work index (RWI) of Pipe and OK ores versus microwave heating time.

A breakdown of the particle size distributions into three broad size categories (> 425 μm, 106-425 μm, and < 106 μm) revealed that while particles in the OK ore

were normally distributed regardless of microwave treatment time, particles in the Pipe ore were concentrated in the > 425 μm and < 106 μm size fractions (bimodal distribution). With increasing microwave pre-treatment time up to 4 minutes, the percentage of particles in the large size fraction increased (mass of > 425 μm fraction increased by 11%). The increase in large, unground particles in the Pipe ore suggests that some particles underwent a mineralogical change that made them harder and reduced their grindability. After 8 minutes microwave pre-treatment, the percentage of particles in the large size fraction returned to a value similar to that for the untreated Pipe ore.

4.3.2 Mineralogy

To determine if a harder mineral phase was forming in the Pipe ore during microwave pre-treatment and concentrating in the large size fraction, and to compare the texture of the OK and Pipe ores, untreated and microwave treated OK and Pipe ore was sieved into three size fractions after grinding (> 425 μm, 106-425 μm, and < 106 μm) and analyzed by XRD. For the untreated OK ore, the three size fractions had the same mineral composition. For OK ore microwave treated for 8 and 15 minutes (temperatures of 588°C and 730°C achieved respectively), the three size fractions were very similar with the exception that the larger size fraction exhibited fewer olivine peaks than the two smaller size fractions. In contrast, XRD analysis of the Pipe ore revealed that the mineral composition of the different size fractions in the untreated and microwave treated ore was varied. Analysis of the untreated and microwave pre-treated Pipe ore indicated magnetite, pyrrhotite and pentlandite were concentrated in the smaller size fractions. In the Pipe ore treated with microwaves for 4 minutes (temperature of 533°C achieved), olivine was also concentrated in the two smaller size fractions while serpentine, quartz and cordierite were concentrated in the large size fraction (Figure 4-3). After 8 minutes of microwave treatment (temperature of 686°C achieved), the different size fractions of the Pipe ore produced more similar XRD patterns, although olivine, magnetite, pentlandite and pyrrhotite were still

concentrated in the two smaller size fractions, and serpentine was concentrated in the > 425 μm size fraction.
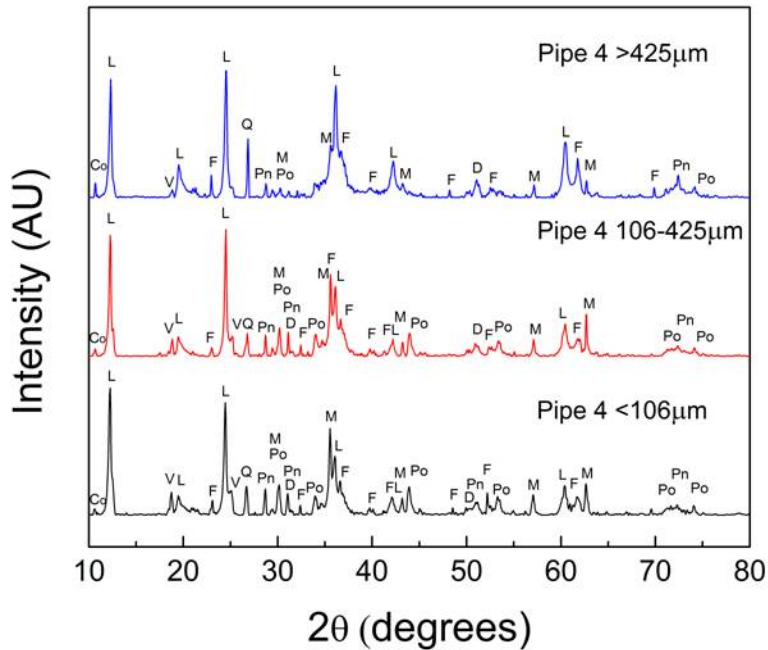
Figure 4-3: XRD patterns for Pipe ore microwave pre-treated for 4 minutes, attrition milled for 15 minutes, and sieved into < 106 μm, 106-425 μm, and > 425 μm size fractions. Mineral phases identified include: cordierite (Co), dolomite (D), forsterite (F), lizardite (L), magnetite (M), pentlandite (Pn) pyrrhotite (Po), quartz (Q) and vermiculite (V).

The size-by-size XRD analysis of the OK and Pipe ores suggests that while minerals within the OK ore were evenly distributed and the ore texture was quite consistent, the opposite was true for the Pipe ore. In the OK ore, different particles heated relatively evenly, and differences in particle heating were due primarily to the location of particles within the microwave reactor (particles near the centre of the microwave reactor heat better than samples near the reactor wall). The concentration of olivine in the smaller size fractions in the microwave treated OK ore indicates that particles which reached a higher temperature were more likely to break than other particles during grinding. In the Pipe ore, since the texture was inconsistent, some particles heated better in response to microwave radiation than others. Similar to the OK ore, particles that heated

better also ground better in the Pipe ore, since olivine was concentrated in the smaller size fractions in the microwave treated Pipe ore. The fact that highly microwave responsive minerals, such as magnetite, pyrrhotite, and pentlandite, were also concentrated in the smaller size fractions suggests that particles that contained these minerals were heated preferentially and, therefore, ground preferentially. The textural differences between the OK and Pipe ore explains why the OK ore responded better to microwave assisted grinding than the Pipe ore, but does not explain why the grindability of the Pipe ore decreased with microwave pre-treatment.

4.3.3 Hardness Measurements

Hardness measurement results for untreated and microwave treated OK and Pipe ores are shown in Figure 4-4. The results indicate that the hardness of both ores increased with increasing microwave pre-treatment. Since the primary reaction that occurs during microwave pre-treatment is the conversion of serpentine to olivine, and olivine is reported to be harder than serpentine (Mohs hardness of 7 versus 2.5 (RUFF, 2012)), this result is not surprising. While the increase in ore hardness with microwave pre-treatment partially explains the decrease in grindability of the Pipe ore up to 4 minutes microwave pre-treatment time, it does not explain the relative improvement in grindability after 8 minutes microwave pre-treatment, and does not correlate with the improved grindability of the OK ore. Thus, another mechanism is largely responsible for the trends in grindability observed for the OK and Pipe ores with increasing microwave pre-treatment.

106
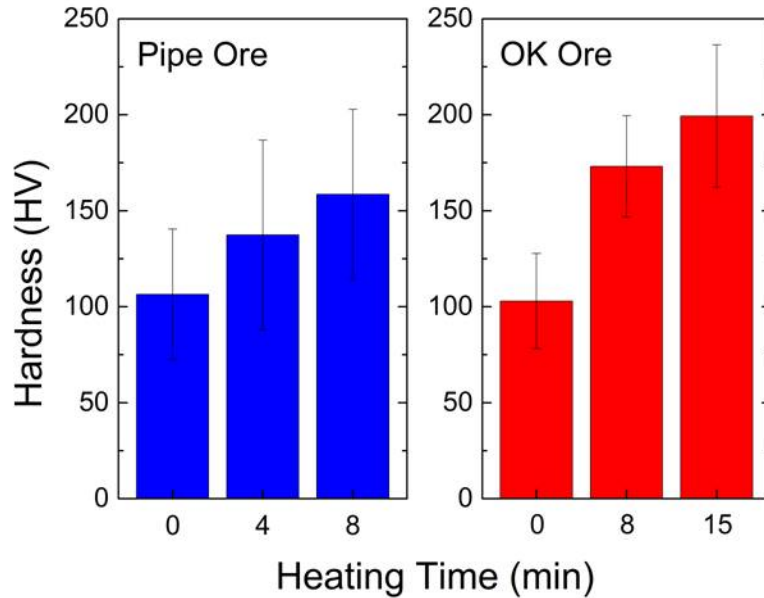
Figure 4-4: Micro-hardness results for untreated and microwave pre-treated Pipe and OK ores. Data collected by Nancy Manchak and used with permission.

4.3.4 Crack Analysis

During the examination of unground OK and Pipe ore particles by SEM, it was noticed that significant cracking was present in microwave pre-treated particles compared to the untreated particles. The cracking occurred microscopically, both along mineral grain boundaries, as well as in the bulk magnesium silicate (Figure 4-5). It is believed cracks formed along mineral grain boundaries due to thermal stresses generated by the differential heating of different minerals upon exposure to microwaves, and that the cracks formed in the bulk magnesium silicate due to the evolution of water vapor during serpentine dehydroxylation.
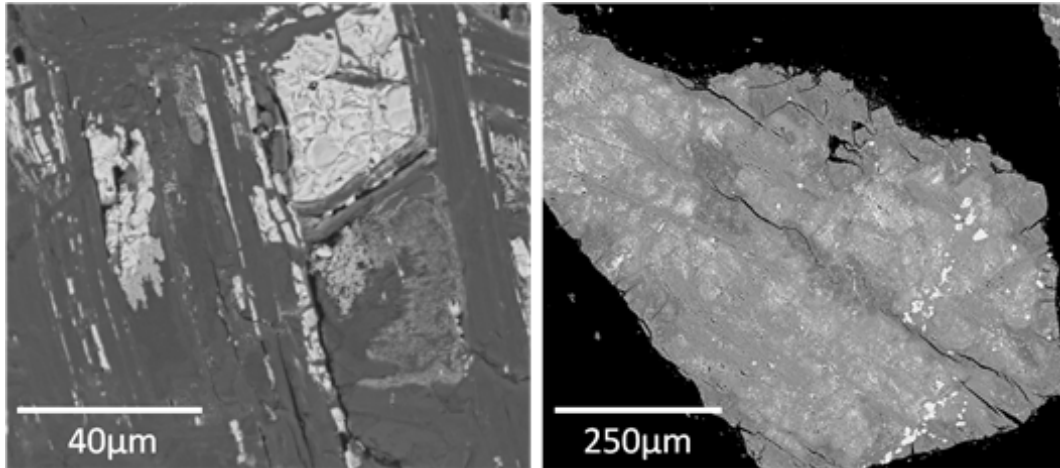
Figure 4-5: SEM-BSE images of particle cross-sections of crushed, unground (0.425-1 mm) OK ore microwave pre-treated for 15 minutes. The image on the left depicts cracking along mineral grain boundaries, while the image on the right shows cracking in the bulk magnesium silicate.

The extent of cracking in untreated and microwave pre-treated OK and Pipe ore was quantified and the results are shown in Figure 4-6. The degree of cracking increased with increasing microwave pre-treatment for both the OK and Pipe ores. For the OK ore, there was a substantial increase in crack length per unit area with each increment of microwave pre-treatment. For the Pipe ore, there was a small average increase in crack length per unit area after 4 minutes microwave pre-treatment; however, a substantial increase in cracking was not observed until after 8 minutes microwave pre-treatment.
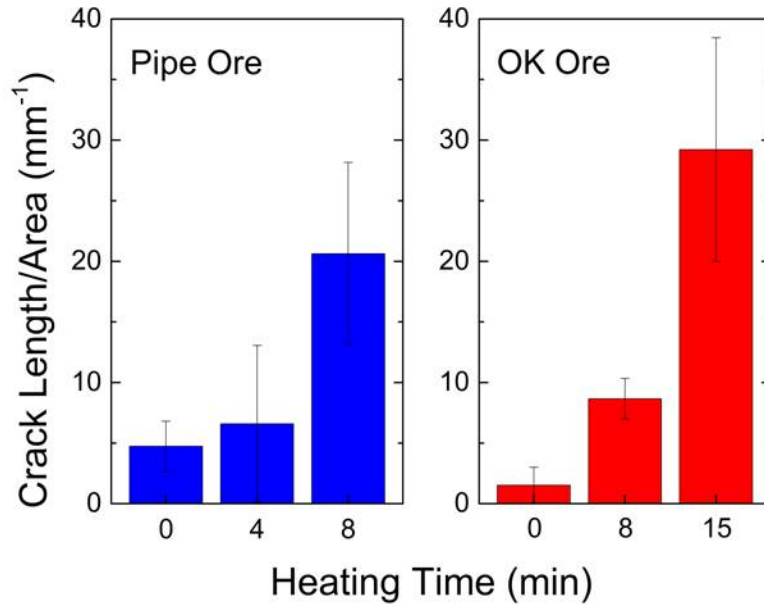
Figure 4-6: Crack length per unit area in untreated and microwave pre-treated ores.

It appears that the OK ore grindability improved with increasing microwave pre-treatment, despite increasing ore hardness, due to the cracking that occurred, both by the differential heating of different minerals and by the escape of water vapour due to serpentine dehydroxylation. Since highly microwave responsive minerals (such as iron oxides and sulphides) were well distributed within the OK ore, and since the OK ore had high serpentine content (84 wt.%), cracking was systemic, and a great improvement in grindability was observed. For the Pipe ore, since highly microwave responsive minerals were not as well dispersed throughout the ore, cracking due to thermal stress was not as widespread. In addition, the Pipe ore contained less serpentine (63.7 wt.%) than the OK ore and cracking due to the escape of water vapour during serpentine dehydroxylation was also less significant. Thus, as the Pipe ore became harder with increasing microwave treatment, the grindability of the ore decreased until sufficient cracking occurred to overcome the increase in hardness.

4.3.5 Pentlandite Liberation

Pentlandite liberation for the Pipe and OK ores was found to increase with increasing microwave pre-treatment time (Figure 4-7). The combination of microwave treatment and grinding was ultimately found to achieve greater pentlandite liberation at larger pentlandite P_{80} compared to samples that were ground for longer periods of time (Figure 4-8). Improved mineral liberation by microwave pre-treatment has been reported by others. It is commonly understood that the mechanism of improved liberation as a result of microwave pre-treatment is the differential heating of minerals within individual particles, leading to thermal stress and cracking along mineral grain boundaries (Kingman et al., 2004; Jones et al., 2005). Pentlandite liberation in the Pipe ore improved with increasing microwave treatment despite decreased grindability because cracking and particle breakage were concentrated in those particles that contained pentlandite.
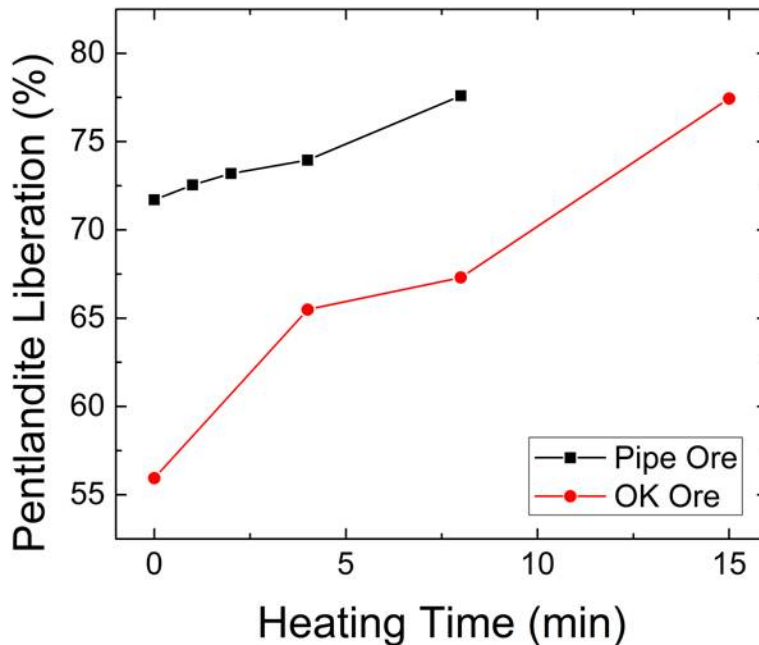
Figure 4-7: Pentlandite liberation versus microwave heating time after 15 minutes grinding for the Pipe and OK ores.
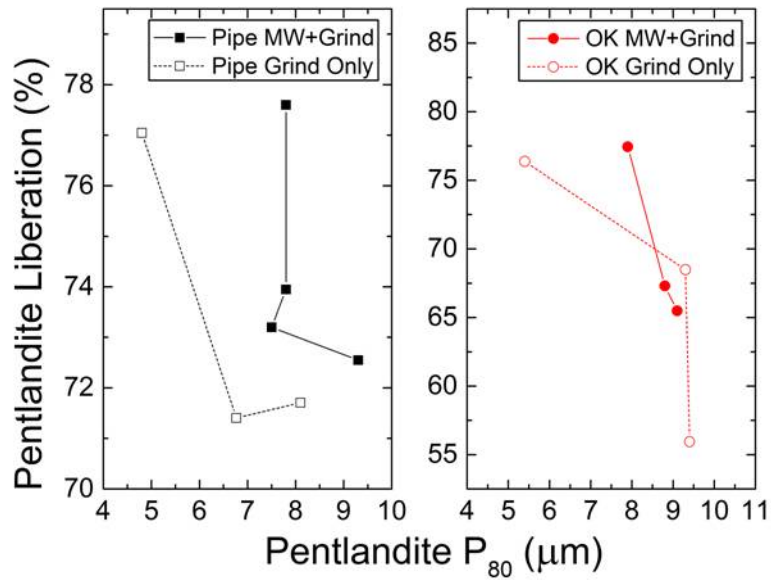
Figure 4-8: Pentlandite liberation versus pentlandite P_{80} for ore microwave treated for various times and ground for 15 minutes (MW+grind), or ground for 15-60 minutes (Grind Only).

4.3.6 Specific Surface Area

The effect of microwave pre-treatment on the specific surface area (SSA) of OK and Pipe ores is depicted in Figure 4-9. Up to 4 minutes heating time, the SSA of both ores was not affected. However, after 8 minutes microwave pre-treatment, the SSA of both the Pipe and OK ore was greatly improved. At the maximum microwave pre-treatment time (15 minutes for OK ore, 8 minutes for Pipe ore) the SSA of the OK and Pipe ores increased by an average of 3.2 and 1.7 times, respectively, for a given grinding time (15, 30 or 60 minutes). Similarly, the combination of maximum microwave pre-treatment and grinding resulted in higher SSA for a given particle size compared to grinding alone (Figure 4-10).
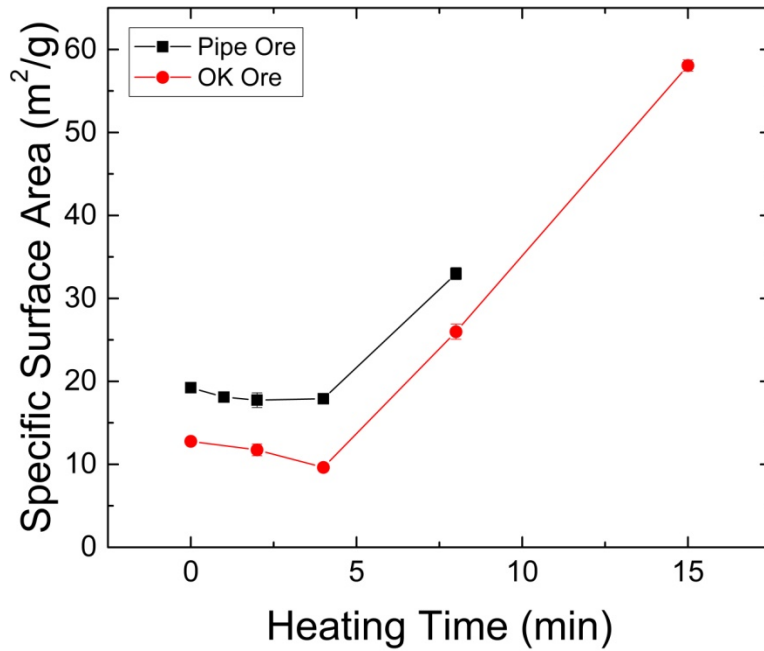
Figure 4-9: Specific surface area versus microwave heating time for Pipe and OK ores ground for 15 minutes.
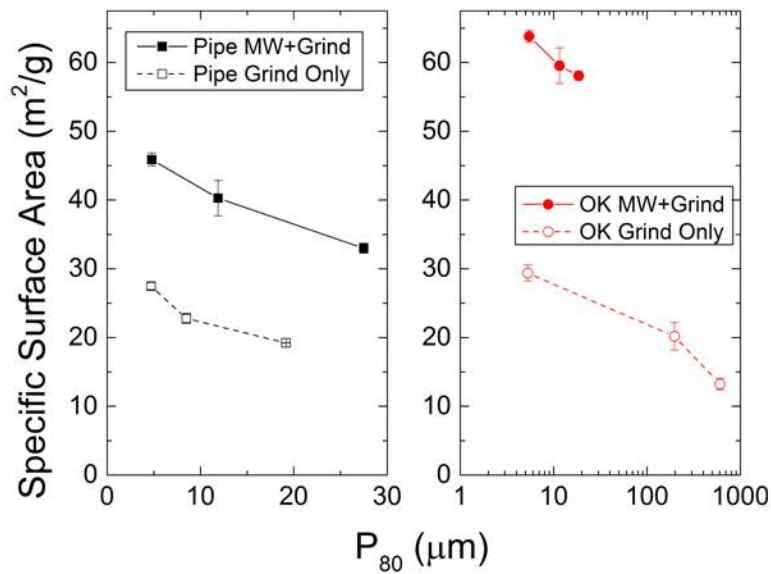
Figure 4-10: Specific surface area versus P$_{80}$ for Pipe and OK ores microwave pre-treated (15 minutes for OK ore, 8 minutes for Pipe ore) and ground for various lengths of time (15, 30 and 60 minutes), and untreated ore ground for various lengths of time (15, 30 and 60 minutes).

The conversion of serpentine to olivine and resultant cracking is believed to be primarily responsible for the SSA trend with increasing microwave pre-treatment for the Pipe and OK ores, as well as particle size. A plot of serpentine and olivine in the ores versus microwave heating time (Figure 3-6) reflects the trends observed in the SSA versus microwave heating time curves (Figure 4-9), and a plot of ore olivine content divided by particle size (specific surface area and particle size are inversely related) is linear (Figure 4-11). At microwave heating times of 4 minutes or less, cracking was due primarily to thermal stress between mineral grains of different composition. These cracks were small and contributed minimal surface area compared to the cracks generated by the release of water vapour during serpentine dehydroxylation at extended microwave heating times (8 minutes or more).
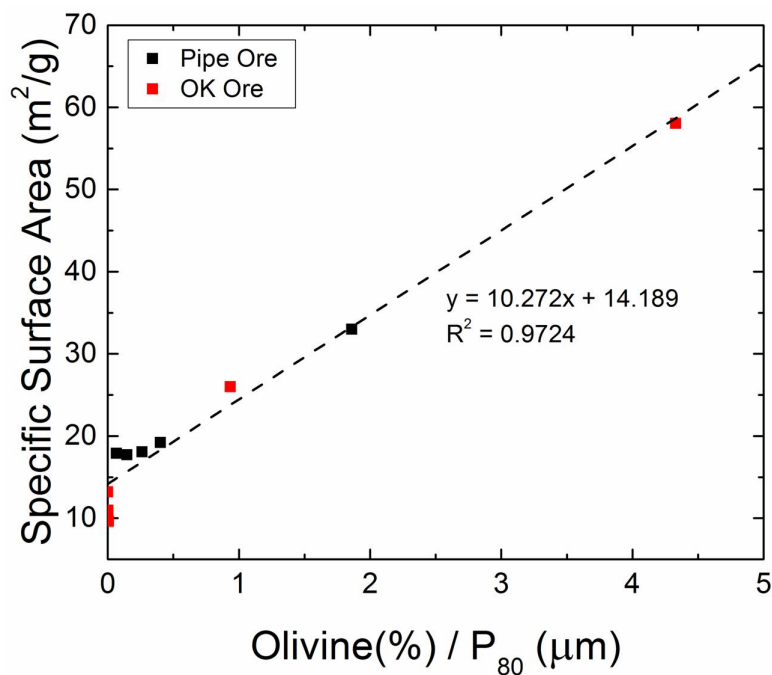
Figure 4-11: A plot of specific surface area versus the olivine content divided by the particle size is linear for the Pipe and OK ores.

4.3.7 Energy Considerations

To determine if microwave pre-treatment enhanced the efficiency of comminution for the two ultramafic nickel ores studied, the energy used in microwave treatment

and grinding to achieve a certain product size, degree of pentlandite liberation and specific surface area was compared to that achieved with the energy used in grinding alone (Figures 4-12, 4-13 and 4-14). It should be noted that the energy consumption of both microwave pre-treatment (167 kWh/t per minute) and grinding (41 kWh/t per minute) was very high and efforts were not made to optimize energy usage at the lab scale. Overall, microwave pre-treatment did not improve the energy used in grinding for the OK ore and increased the energy used in grinding for the Pipe ore. Although the energy used in grinding was not reduced, pentlandite liberation was greater for microwave treated Pipe ore compared to ore only attrition milled across the energy input range. The trend was opposite for the OK ore, however, although ultimately microwave pre-treatment resulted in slightly greater pentlandite liberation compared to grinding alone. In terms of specific surface area, at high energy inputs, the combination of microwave pre-treatment and grinding resulted in higher surface area than could be achieved by attrition milling alone. Increased specific surface area of the ores as a result of microwave pre-treatment should be beneficial for both flotation and mineral carbon sequestration processes.
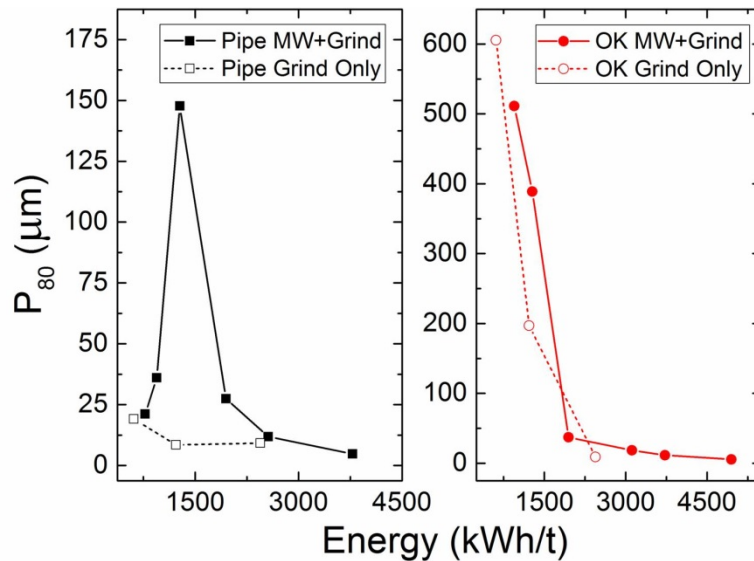
Figure 4-12: Sample P_{80} versus energy expended for Pipe and OK ore microwave pre-treated and ground for various times (MW+Grind), or ground only for various lengths of time (Grind Only).

114
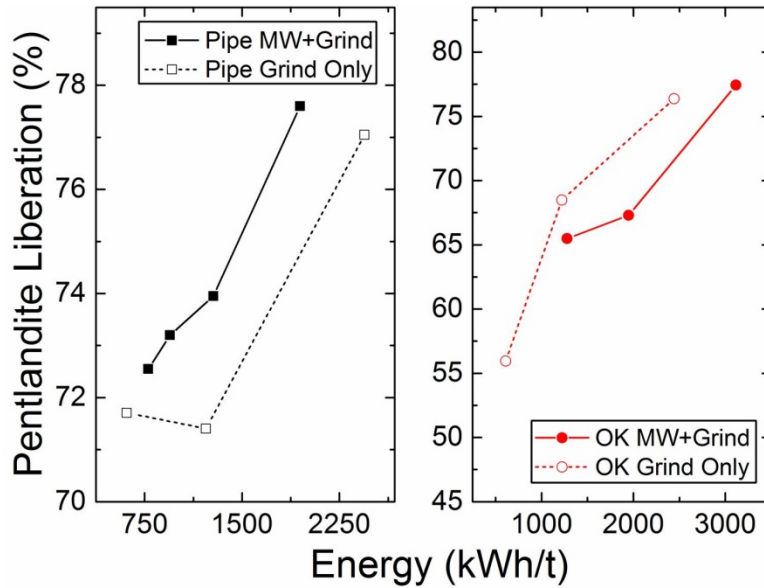
Figure 4-13: Pentlandite liberation versus energy expended during particle size reduction for Pipe and OK ore either microwave pre-treated for various times and ground for 15 minutes (MW+Grind), or ground for various lengths of time (15-60 minutes) (Grind Only).
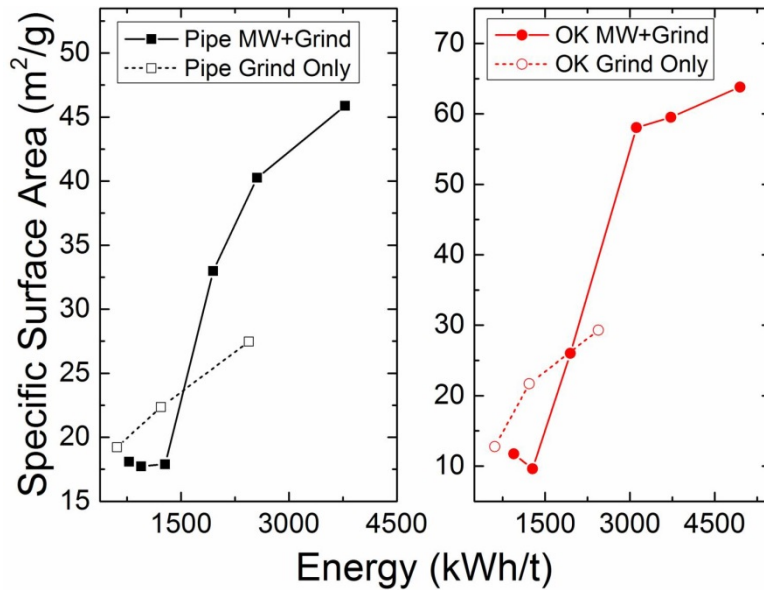
Figure 4-14: Specific surface area versus energy expended for Pipe and OK ore microwave pre-treated and ground for various times (MW+Grind), or ground only for various lengths of time (Grind Only).

4.4 Conclusions

The grindability of the OK ore improved with increasing microwave pre-treatment. In contrast, the grindability of the Pipe ore decreased with moderate microwave pre-treatment, and resembled that of the untreated ore after extended treatment. Increasing microwave pre-treatment improved pentlandite liberation in both ores, and microwave pre-treatment of 8 minutes or longer greatly improved the specific surface area of ground ores.

It is believed that the grindability of the OK ore improved with increasing microwave pre-treatment, despite increasing ore hardness, due to cracking generated in ore particles by the differential heating of different minerals and the release of water vapour due to serpentine dehydroxylation. Since microwave responsive minerals were well dispersed throughout the OK ore, particles heated relatively evenly in response to microwave radiation and cracking was widespread, leading to a great improvement in grindability. For the Pipe ore, since microwave responsive minerals were not well dispersed throughout the ore, some particles heated better than others and cracking was not as extensive as in the OK ore. Therefore, as the Pipe ore became harder with increasing microwave pre-treatment, the grindability of the ore decreased until sufficient cracking occurred to overcome the increase in hardness. Pentlandite liberation improved for both ores with increasing microwave pre-treatment because cracking was concentrated in particles that contained microwave responsive minerals, such as pentlandite. The improvement in specific surface area of the ores at longer microwave pre-treatment times was linked to the conversion of olivine to serpentine: cracks due to the release of water from serpentine dehydroxylation were much larger, and contributed more surface area, than cracks that occurred due to thermal stress at lesser microwave pre-treatment.

Ultimately, microwave pre-treatment was not found to decrease the energy required for comminution of ultramafic ores. However, the combination of microwave pre-treatment and grinding resulted in greater specific surface area at high energy inputs for the Pipe and OK ores, and improved pentlandite liberation

116

at all energy inputs compared to grinding alone for the Pipe ore. Microwave pre-treatment did not reduce the energy required for pentlandite liberation in the OK ore; however, microwave pre-treatment ultimately resulted in the highest pentlandite liberation observed.

4.5 References

Amankwah, R.K., Ofori-Sarpong, G., 2011. Microwave heating of gold ores for enhanced grindability and cyanide amenability. Minerals Engineering. 24, 541-544.

ASTM Standard E384-11, 2012, "Standard Test Method for Knoop and Vickers Hardness of Materials," ASTM International, West Conshohocken, PA, 2012, DOI 10.1520/E0384-11E01, www.astm.org.

Atomic Energy of Canada Limited Research Company (AECL) and Voss Associates Engineering Ltd, 1990. Microwaves and Minerals. Industrial Mineral Background Paper #14. Ontario Ministry of Northern Development and Mines. 77p.

Berry, T.F., Bruce, R.W., 1966. A simple method of determining the grindability or ores. Canadian Mining Journal. 7, 63-65.

Gerdemann, S.J., Dahlin, D.C., O'Connor, W.K., Penner, L.R., 2003. Carbon dioxide sequestration by aqueous mineral carbonation of magnesium silicate minerals. Albany, OR: Albany Research Center.

Henda, R., Hermas, A., Gedye, R., Islam, M.R., 2005. Microwave enhanced recovery of nickel-copper ore: Comminution and flotatbility aspects. International Microwave Power Institute. 40(1), 7-16.

Herbst, J.A., Lo, Y.C., Flintoff, B., 2003. Size reduction and liberation. In: Principles of mineral processing, ed. M.C. Fuerstenau and K.N. Han, Englewood, CO: Society for Mining Metallurgy and Exploration, pp 61-118.

Jones, D.A., Kingman, S.W., Whittles, D.N., Lowndes, I.S., 2005. Understanding microwave assisted breakage. Minerals Engineering. 18, 659-669.

Kaya, E., 2010. Comminution behaviour of microwave heated two sulphide copper ores. Indian Journal of Chemical Technology. 17, 455-61.

Kingman, S.W., Jackson, K., Cumbane, A., Bradshaw, S.M., Rowson, N.A., Greenwood, R., 2004. Recent developments in microwave-assisted comminution. International Journal of Mineral Processing. 74, 71-83.

Kingman, S.W., Vorster, W., Rowson, N.A., 2000. The influence of mineralogy on microwave assisted grinding. Minerals Engineering. 13(3), 313-327.

Liu, C., Xu, Y., Hua, Y., 1990. Application of microwave radiation to extractive metallurgy. Chinese Journal of Metallurgical Science and Technology. 6, 121-124.

O'Connor, W.K., Dahlin, D.C., Nilsen, D.N., Rush, G.E., Walters, R.P., Turner, P.C., 2000. CO_2 storage in solid form: A study of direct mineral carbonation. Greenhouse Gas Control Technologies: Proceedings of the 5th International Conference on Greenhouse Gas Technologies; 2000 Aug 14-18; Cairns, AU.

Radziszewski, P., 2013. Energy recovery potential in comminution processes. Minerals Engineering. 46-47, 83-88.

RRUFF, 2012. Handbook of Mineralogy (PDF). http://rruff.geo.arizona.edu/doclib/hom/ *Last accessed Nov 27, 2012.*

Tromans, D., 2008. Mineral comminution: Energy efficiency considerations. Minerals Engineering, 21, 613-620.

Walkiewicz, J.W., Clark, A.E., McGill, S.L., 1991. Microwave-assisted grinding. IEEE Transactions on Industry Applications. 27(2), 239-243.

Chapter 5 Modification of Ultramafic Nickel Ore Slurry Rheology by Microwave Pre-treatment[4]

5.1 Introduction

Interest in low-grade ultramafic nickel ores has increased in recent years as traditional high-grade nickel sulphide deposits are being depleted and laterite ores have proven technically difficult and costly to process (Xu et al., 2010). While ultramafic ores represent a large potential resource of both nickel and mineral carbon sequestration feedstock, they are challenging to process due to their high serpentine content (Senior and Thomas, 2005; Uddin et al., 2012). Serpentine is a phyllosilicate mineral comprised of 1:1 stacked sheets of silica tetrahedra and magnesium hydroxide octahedra, with adjacent sheets held together by weak van der Waals forces (Alexander et al., 2007; Alvarez-Silva et al., 2010). There are three primary polymorphs of serpentine: lizardite (platy), antigorite (corrugated) and chrysotile (coiled, fibrous) (McKelvy et al., 2004).

Serpentine minerals are anisotropic and have three different surfaces that can be exposed in solution (Figure 5-1), each with a different surface chemistry. The basal planes of both the tetrahedral and octahedral sheets are electrically neutral upon crystal cleavage; however, pH-independent charging can develop through lattice defects (vacancies or substitutions) (Alvarez-Silva et al., 2010). The edge surfaces, in contrast, are highly polar due to the breakage of bonds, and pH-dependent charging occurs in solution through hydrolysis (Alvarez-Silva et al., 2010; Yan et al., 2013). The anisotropic nature of serpentine leads to complex rheology, which is compounded by the non-spherical shape of serpentine particles (Ndlovu et al., 2013). Suspensions of serpentine minerals, especially those of the fibrous chrysotile, are known to exhibit high viscosity and yield stress (Ndlovu et al., 2011).

---

[4] A version of this chapter has been published. Bobicki, E.R., Liu, Q., Xu, Z., 2014. Effect of microwave pre-treatment on ultramafic nickel ore slurry rheology. Minerals Engineering. 61, 97-104.
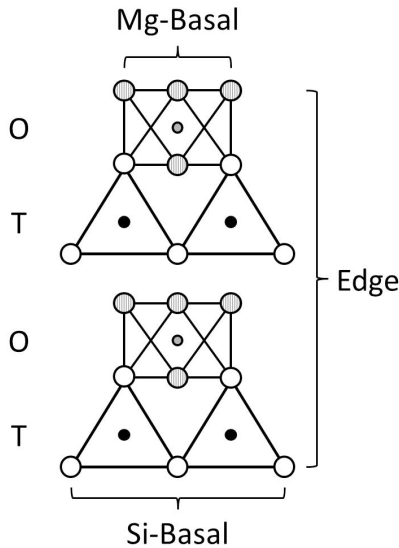
Figure 5-1: Diagram showing serpentine structure and surfaces. T indicates a tetrahedral layer, O indicates an octahedral layer, a white circle indicates an oxygen atom, a black circle indicates a silicon atom, a grey circle indicates a magnesium atom, and a stripped circle indicates a hydroxyl group.

In mineral processing, high pulp viscosity and yield stress can be detrimental to comminution and flotation. By extension, these properties are likely also inimical to mineral carbon sequestration due to similarities between the fundamental processes used in mineral processing and aqueous mineral carbonation. The presence of serpentine minerals in ores has been shown to reduce grinding efficiency, necessitating that grinding be conducted at lower densities (Ndlovu et al., 2014; Patra et al., 2010; Xu et al., 2010). With regard to flotation, high slurry viscosity results in reduced gas dispersion and mixing efficiency, cavern formation, increased turbulence damping, bubble coalescence and high gangue recovery (Becker et al., 2013; Cruz et al., 2013; Ndlovu et al., 2013; Todd, 2004; Shabalala et al., 2011). The flotation performance of ultramafic nickel ores is poor without some kind of serpentine neutralization or removal strategy (Senior and Thomas, 2005; Xu et al., 2010). Methods employed to improve the flotation of ultramafic nickel ores include desliming by cyclones (Senior and Thomas, 2005; Xu et al., 2011), the addition of chemicals such as carboxymethylcellulose

or salts (Senior and Thomas, 2005; Peng and Seaman, 2011), and acid treatment of the flotation pulp (Uddin et al., 2012). Each of these strategies is focused on removing or deactivating serpentine.

A new method of reducing the viscosity and yield stress of ultramafic nickel ore slurries is proposed: microwave pre-treatment. Microwave radiation is electromagnetic radiation with frequencies of 0.3-300 GHz and wavelengths of 0.001-1 m (Haque, 1999). Microwaves have been used in a number of extractive metallurgical applications (Haque, 1999; Pickles, 2009), but never before for the modification of pulp rheology. Upon exposure to microwave radiation, ultramafic nickel ores are heated, resulting in the dehydroxylation of serpentine and the formation of olivine (Bobicki et al., 2014).

Olivine is a mineral composed of isolated SiO_4 tetrahedra linked by octahedrally coordinated magnesium ions (Alexander et al., 2007). Olivine is isotropic, non-fibrous, and is not reported to have complex rheology or cause problems in ultramafic nickel ore processing. The objectives of this work are (1) to study the rheology of two ultramafic nickel ores, one containing chrysotile and one containing only lizardite serpentine, (2) to determine if microwave pre-treatment can be used to improve the rheology of ultramafic nickel ores, and (3) to explain the mechanisms behind any rheological changes that occur in ultramafic nickel ores as a result of microwave pre-treatment.

5.2 Materials and Methods

5.2.1 Mineral Feedstock

Two different ultramafic nickel ores were studied. The first ore was from the Okanogan nickel deposit in Washington State, USA (referred to as "OK ore"). The second was from the Vale-owned Pipe deposit located in the Thomson Nickel Belt (referred to as "Pipe ore"). The ores were crushed and sieved to isolate the 0.425-1 mm size fraction for microwave pre-treatment. The mineral composition of the OK and Pipe ores before and after microwave pre-treatment is shown in Table 5-1 (Bobicki et al., 2014). The serpentine present in the OK ore is of the

lizardite form, while the serpentine in the Pipe ore is primarily lizardite with approximately 1 wt.% chrysotile.

Table 5-1: Mineral composition of OK and Pipe ores before (OK UT and Pipe UT) and after (OK MW and Pipe MW) microwave pre-treatment from quantitative XRD analysis (Bobicki et al, 2014).

Mineral	Formula	OK UT	OK MW	Pipe UT	Pipe MW
Serpentine (wt.%)	$Mg_3Si_2O_5(OH)_4$	84.0	15.8	63.7	23.7
Olivine (wt.%)	Mg_2SiO_4	-	80.2	7.7	51.1
Cordierite (wt.%)	$Mg_2Al_4Si_5O_{18}$	-	-	1.0	1.0
Vermiculite (wt.%)	$Mg_2Si_4O_{10}(OH)_2$	-	-	0.7	-
Brucite (wt.%)	$Mg(OH)_2$	5.1	-	-	-
Dolomite (wt.%)	$CaMg(CO_3)_2$	-	-	5.5	1.4
Magnetite (wt.%)	Fe_3O_4	6.6	4.0	12.3	14.1
Pyrrhotite (wt.%)	$Fe_{1-x}S$	-	-	4.7	5.6
Pentlandite (wt.%)	$(Fe,Ni)_9S_8$	4.3	-	2.8	0.8
Quartz (wt.%)	SiO_2	-	-	1.6	2.3

5.2.2 Microwave Treatment

A 1000 W, 2.45 GHz household microwave oven (Panasonic NN-SF550M Flat and Wide) was used to conduct microwave treatment. 100 g ore samples were placed in 100 mL quartz crucibles, which were then placed in the microwave reactor for treatment. The OK ore was exposed to microwave radiation for 15 minutes, during which time the ore reached a temperature of 730^oC. The Pipe ore was exposed to microwave radiation for 8 minutes, during which time a temperature of 686^oC was achieved. The Pipe ore was only exposed to microwave radiation for 8 minutes because any further treatment caused the Pipe ore to melt. The microwave reactor was purged continuously with 1 L/min of nitrogen gas both during microwave treatment and cooling of the samples. A detailed explanation of the heating characteristics of the ores and the mineralogical changes that occur as a result of microwave pre-treatment are given in Bobicki et al. (2014).

5.2.3 Grinding

100 g samples of untreated and microwave pre-treated OK and Pipe ore (0.425-1 mm size fraction) were ground aqueously in a stirred attrition mill (01-HD Laboratory Attritor with 1400 cc tank, Union Process, Akron, Ohio, USA). Grinding was conducted at 1000 rpm using 1300 g (560 mL) of 99.5% 3/16" alumina balls (Union Process, Akron, Ohio, USA) and 250 mL of 10^{-2} M KCl. Each sample was ground to a P_{90} of 8.5±0.2 μm.

5.2.4 Slurry Preparation

After grinding, the solids content of the slurry samples was adjusted by adding or removing 10^{-2} M KCl (Crystalline/Certified ACS, Fisher Chemical) solution. KCl solution was removed by pipette after allowing the samples to settle. The pH of the slurry samples was adjusted using either 50 wt.% KOH (Fisher Chemical) or 37 wt.% HCl (Acros Organics). After pH adjustment, the slurry solids content was adjusted again if necessary in the same manner described.

5.2.5 Rheology

5.2.5.1 Flow Rheology

Rheogram data was collected at 20°C using a rotational rheometer (TA Instruments ARES-2G) with the concentric cylinder attachment. Flow rheology tests were conducted at 10, 20 and 30 wt.% solids, all at pH 10. pH 10 is approximately the pH at which ultramafic nickel ores are processed (Patra et al., 2012; Uddin et al., 2012; Yang et al., 2013). 10^{-2} M KCl was used as the background electrolyte in all tests. Shear stress and viscosity were observed over the shear range of 1-200 s^{-1}.

5.2.5.2 Direct Yield Stress Measurement

Direct yield stress measurements were collected using a rotational rheometer (TA Instruments ARES-2G) with the vane concentric cylinder attachment. Yield stress measurements were collected at varying pH values (pH 4-11) with constant slurry solids content (10 wt.%), and with constant pH (pH 10) at varying slurry

solids content (10-30 wt.%). 10^{-2} M KCl was used as the background electrolyte in all tests. The Vane Method described by Dzuy and Boger (1985) was employed to determine the yield stress of the slurry samples. A constant shear rate of 0.1 s^{-1} was used.

5.3 Results and Discussion

5.3.1 Flow Rheology

Shear stress and shear viscosity versus shear rate for microwave pre-treated and untreated OK and Pipe ores at pH 10 and 10, 20 and 30 wt.% solids are shown in Figure 5-2. All suspensions exhibited non-Newtonian, shear thinning behaviour with a yield stress regardless of ore type and slurry solids content. The rheogram data for all slurries were successfully fitted with the modified Cross model (Equation 5.1). In the modified Cross model, the shear viscosity (η) is expressed as a function of the shear rate (γ), yield stress (τ_o), plateau viscosity (η_p), and infinite viscosity (η_∞), as well as a time constant (α_c) and a dimensionless exponent (m). The modified Cross model differs from the conventional Cross model in that it possesses a yield stress term (Rao, 2007; Rayment et al., 1998). The fitted parameters for the modified Cross model are given in Table 5-2.
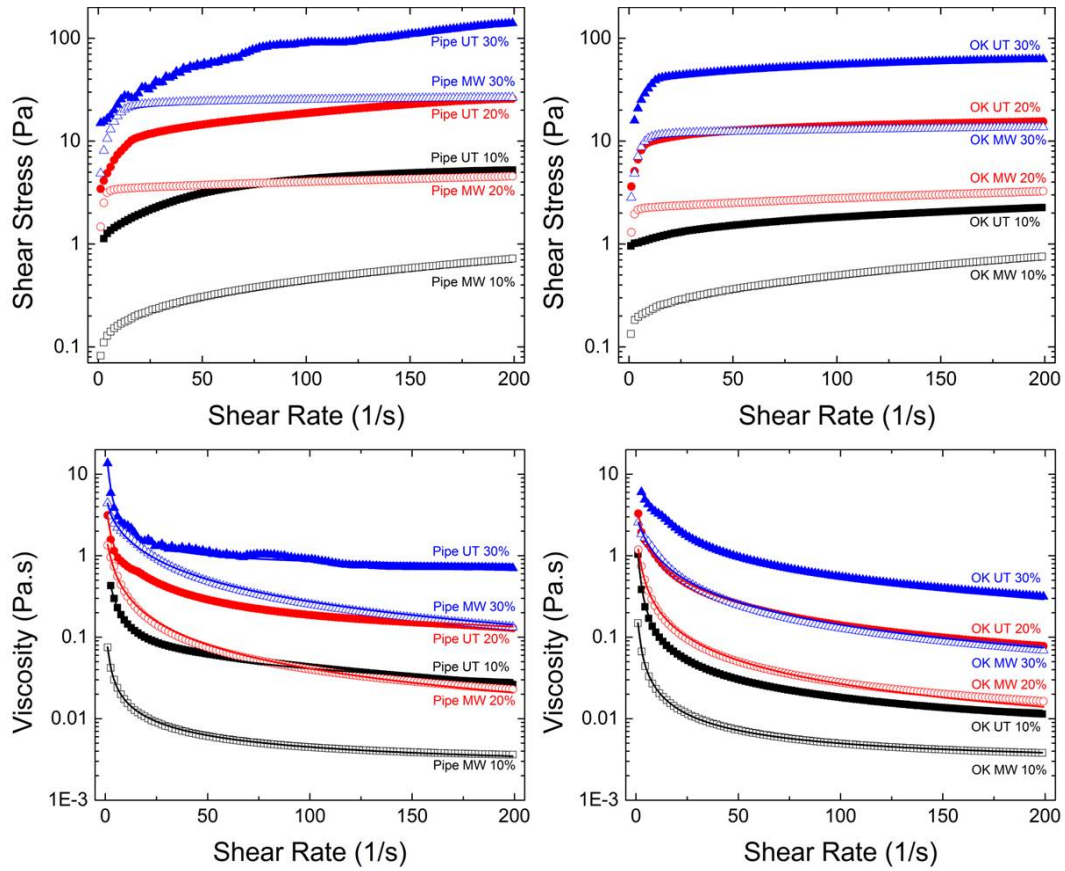
Figure 5-2: Shear stress (top) and shear viscosity (bottom) versus shear rate for untreated Pipe ore (Pipe UT) and microwave pre-treated Pipe ore (Pipe MW) (left), and untreated OK ore (OK UT) and microwave pre-treated OK ore (OK MW) (right), all at 10, 20 and 30 wt.% solids and pH 10. Fitted curves shown as solid lines.

$$\eta = \frac{\tau_0}{\gamma} + \eta_\infty + \frac{\eta_p - \eta_\infty}{1 + (\alpha_c \gamma)^m} \qquad (5.1)$$

Table 5-2: Modified Cross model fitted parameters for untreated and microwave pre-treated OK and Pipe ore slurries at 10, 20 and 30 wt.% solids, where η_p and η_∞ are the plateau and infinite-shear viscosities (Pa.s), respectively, τ_o is yield stress (Pa), α_c is a time constant (s), and m is a dimensionless exponent (Rao, 2007; Raymett et al., 1998).

Sample	% Solids	η_p	η_{inf}	τ_o	m	α_c	R^2
	10%	1.13	0.01	0.63	1.00	2.37	0.9994
OK UT	20%	3.51	0.01	0.92	0.89	0.37	0.9967
	30%	6.44	0.01	2.94	1.00	0.12	0.9976
	10%	0.49	0.00	0.00	0.95	2.73	0.9999
OK 15	20%	2.14	0.00	0.00	1.00	0.92	0.9985
	30%	3.16	0.00	0.00	1.00	0.22	0.9953
	10%	1.68	0.01	0.64	0.55	18.86	0.9973
Pipe UT	20%	9.86	0.02	1.13	0.60	8.59	0.9930
	30%	13.26	0.71	10.40	0.99	2.56	0.9939
	10%	0.83	0.00	0.00	0.77	18.85	0.9996
Pipe 8	20%	2.41	0.00	0.00	1.00	0.51	0.9969
	30%	3.56	0.00	1.38	1.00	0.13	0.9965

For both the Pipe and OK ores, the shear stress and viscosity values observed at a given shear rate, as well as the modeled plateau (zero-shear) viscosities (η_p), increased with increasing slurry solids content. The modeled infinite-shear viscosity (η_∞) remained approximately the same regardless of slurry solids content for the OK ore and increased with increasing slurry solids content for the untreated Pipe ore. In general, the Pipe ore exhibited higher shear stress and viscosity for a given shear rate than the OK ore. Correspondingly, modeled plateau and infinite viscosities (when non-zero, for untreated ore) were generally larger for Pipe ore slurries than OK ore slurries. Based purely on the serpentine content, it would be expected that the OK ore would be more viscous than the Pipe ore, since the untreated OK ore contains more serpentine. The greater viscosity of the Pipe ore is attributed to the presence of chrysotile. Although the Pipe ore contains only 1 wt.% chrysotile, even small amounts of this fibrous

mineral have been shown to greatly increase the viscosity and yield stress of mineral ore slurries (Patra et al. 2012). Indeed, modeled yield stress (τ_o) values for the untreated Pipe ore also tended to be larger than those for the untreated OK ore (Table 5-2).

The shear stress and viscosity values observed at a given shear rate for the microwave pre-treated OK and Pipe ores were significantly reduced compared to those observed for untreated ores. Modeled plateau viscosities (η_p) were also diminished, and the infinite-shear viscosities (η_∞) went to zero for microwave pre-treated Pipe and OK ore at all slurry solids concentrations. In fact, slurries of microwave pre-treated ore exhibited similar shear stress and viscosity values at high shear as untreated slurries that contained 10 wt.% fewer solids (shear viscosity at 200 s^{-1} versus slurry solids content shown in Figure 5-3). For example, microwave pre-treated Pipe ore at 30 wt.% solids had similar shear stress and viscosity values at 200 s^{-1} as untreated Pipe ore at 20 wt.% solids. At Vale, ultramafic nickel ore slurries have had to be diluted to 20 wt.% solids to achieve satisfactory flotation results (Patra et al., 2010). If the flotation pulp density could be increased from 20 to 30 wt.% solids by microwave pre-treatment, the volume of the pulp could be reduced by 40%, likely resulting in significant savings in infrastructure and materials handling costs. On average, microwave pre-treatment decreased the viscosity of OK and Pipe ore slurries by 80% at a shear rate of 200 s^{-1}. In addition, the modeled yield stress term (τ_o) went to a value of zero for all the microwave pre-treated ore slurries, with the exception of the Pipe ore at 30 wt.% solids. For the Pipe ore at 30 wt.% solids, microwave pre-treatment reduced τ_o by an order of magnitude. The reduction in slurry viscosity and modeled yield stress as a result of microwave pre-treatment is attributed to the conversion of serpentine minerals to olivine. Microwave pre-treatment of the OK and Pipe ores reduced the serpentine content from 84.0 wt% to 15.8 wt.% and from 63.7 to 23.7 wt.%, respectively (Bobicki et al., 2014).
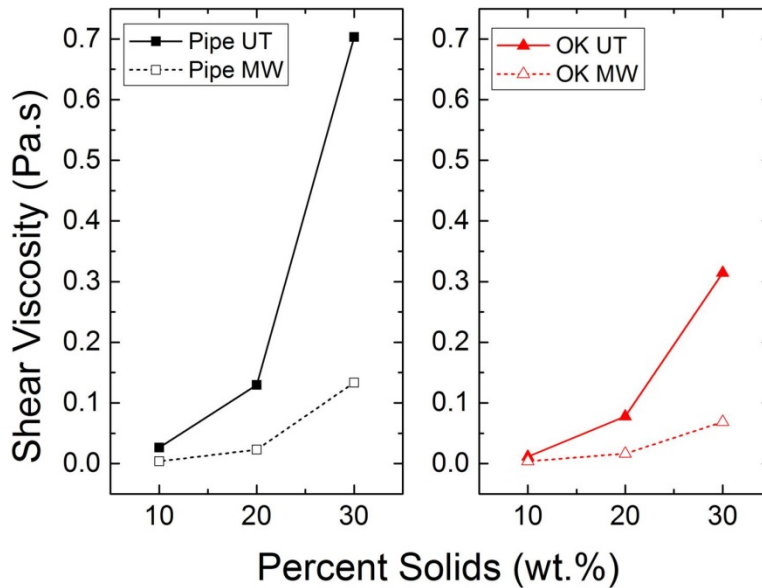
Figure 5-3: Shear viscosity observed at a shear rate of 200 s^{-1} versus slurry solids content (wt.%) for untreated Pipe ore (Pipe UT) and microwave pre-treated Pipe ore (Pipe MW) (left), and untreated OK ore (OK UT) and microwave pre-treated OK ore (OK MW) (right), all at pH 10.

5.3.2 Direct Yield Stress Measurements

Direct yield stress measurements were conducted to further explore the rheology of ultramafic nickel ore slurries and the effect of microwave pre-treatment on slurry rheology. Yield stress as a function of slurry solids content for untreated and microwave pre-treated OK and Pipe ores is shown in Figure 5-4. Slurry yield stress increased exponentially with increasing slurry solids content for the Pipe and OK ores, both for the untreated and microwave pre-treated material. Microwave pre-treatment was shown to reduce the direct yield stress (by an average of 87% at slurry solids contents of 10-30 wt.%), and to reduce the rate with which yield stress increased with increasing slurry solids content. The yield stress of Pipe ore slurries was higher at all slurry solids contents than for the OK ore. The higher yield stress of the Pipe ore compared to the OK ore is believed to be due to the presence of chrysotile in the Pipe ore. Patra et al. (2012) showed that the addition of 1 wt.% chrysotile to a copper ore slurry at 25 wt.% solids increased the yield stress of the slurry from 5 Pa to 25 Pa.
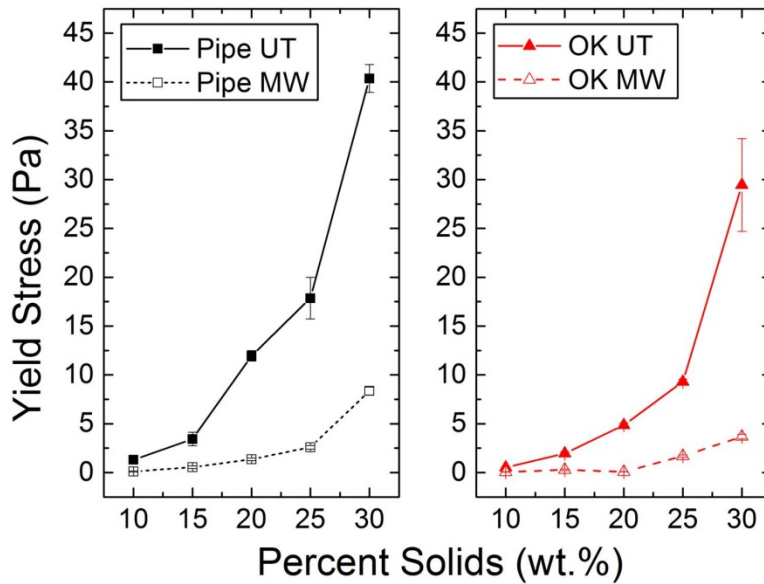
Figure 5-4: Direct yield stress versus slurry weight percent solids for untreated Pipe ore (Pipe UT) and microwave pre-treated Pipe ore (Pipe MW) (left), and untreated OK ore (OK UT) and microwave pre-treated OK ore (OK MW) (right), all at pH 10.

Yield stress as a function of pH for untreated and microwave pre-treated OK and Pipe ore slurries are shown in Figure 5-5. The yield stress for the untreated Pipe ore was high across the pH range, while the yield stress for the OK ore exhibited two peaks, one at pH 10 and one at pH 4.5. The yield stress for the untreated Pipe ore at all pH values was higher than for the untreated OK ore. In fact, the magnitude of the elongated peak, or plateau, yield stress for the Pipe ore was twice the highest peak yield stress for the OK ore. The yield stress versus pH curves seen here are unique. Maximum yield stress in mineral suspensions occurs when there is maximum particle coagulation. In pure isotropic mineral systems, peak yield stress occurs at the isoelectric point, when the surface charge is zero and attractive van der Waals forces dominate. In mixed mineral systems, or mineral systems involving anisotropic minerals, peak yield stress occurs when there is maximum aggregation due to the electrostatic attraction between oppositely charged particles or particle planes. For isotropic mineral systems, it is valuable to compare yield stress with zeta potential versus pH curves. For

systems involving anisotropic minerals such as serpentine, however, zeta potential measurements (as well as potentiometric titration curves) can be misleading as they provide average electric potential values and do not reveal the charge of individual surfaces (Ndlovu et al., 2011; Yan et al., 2013). Ideally, the surface charge of all faces within the mineral system would be known. In the absence of this data, it is valuable to consider the yield stress versus pH curves for individual minerals, zeta potential measurements for isotropic minerals, and to hypothesize as to the probable value of the surface charges of the anisotropic minerals found within the Pipe and OK ore systems.
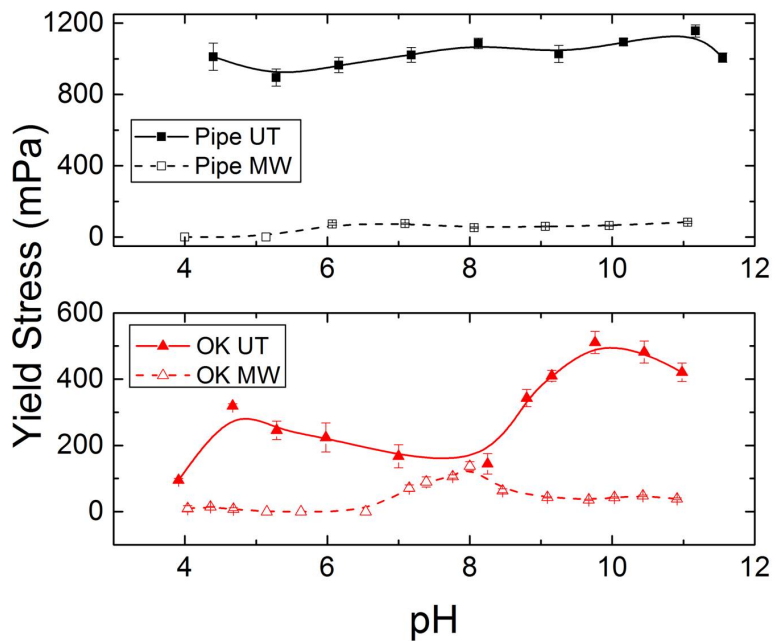
Figure 5-5: Direct yield stress versus pH for untreated Pipe ore (Pipe UT) and microwave pre-treated Pipe ore (Pipe MW) (top), and untreated OK ore (OK UT) and microwave pre-treated OK ore (OK MW) (bottom), all at pH 10.

The yield stress versus pH curves for chrysotile and lizardite are shown in Figures 5-6 and 5-7, respectively. The plateau yield stress observed for the untreated Pipe ore is also apparent in the yield stress versus pH curve for chrysotile (from Ndlovu et al. (2011)). Similarly, the two peaks at pH 4.5 and pH 10 in the yield stress versus pH curve for the OK ore appear in the yield stress versus pH curve

for lizardite. The similarities between the yield stress versus pH curves for the ultramafic ores and those for serpentine minerals confirm that chrysotile dominated the rheology of the Pipe ore, and lizardite dominated the rheology of the OK ore. The difference in shape of the chrysotile and lizardite yield stress versus pH curves and, thus, the difference between the Pipe and OK ore curves, can be explained by considering the probable surface charges on the different faces of the serpentine minerals and the morphology.
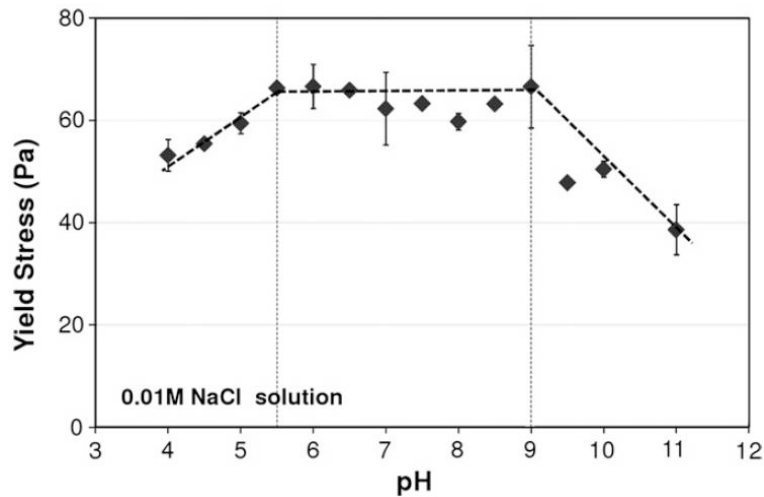
Figure 5-6: Yield stress of 2 vol.% chrysotile suspensions as a function of pH in 0.01 M NaCl from Ndlovu et al. (2011).
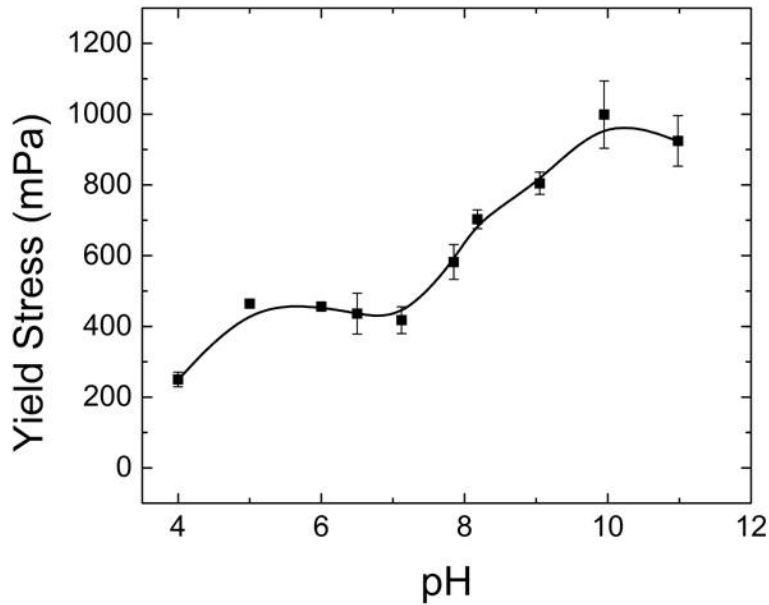
Figure 5-7: Yield stress of lizardite suspensions at 10 wt.% solids in 10^{-2} M KCl as a function of pH.

Serpentine minerals have three different faces: a magnesium hydroxide basal plane, a silica basal plane and an edge, consisting of both magnesium and silica groups (Figure 5-1). As noted previously, charging on the basal plane surfaces occurs independently of pH, while pH dependent charging occurs on the edge. Although the charges present on the different serpentine mineral faces have not been measured, the surface charges present on the different faces of talc ($Mg_3Si_4O_{10}(OH)_2$), a phyllosilicate mineral similar to serpentine, have been determined by Yan et al., (2013). While serpentine is composed of 1:1 stacked sheets of silica (tetrahedral) and magnesium hydroxide (octahedral) layers, talc is composed of an octahedral magnesium hydroxide layer sandwiched between two tetrahedral silica layers (Yan et al., 2013). Talc, therefore, has two faces: a silica basal plane and an edge, consisting of both silica and magnesium groups. Similar to serpentine, charging on the talc basal plane is pH independent, while charging on the edge is pH dependent. Yan et al. (2013) found the surface charge of the talc silica basal plane to be negatively charged across the pH range studied (pH 3-9) while the edge surface was found to have a point-of-zero charge (pzc) of pH 8. Below pH 8 the talc edge charge was positive and above pH 8 the talc edge

132

charge was negative (Yan et al., 2013). Since the talc and serpentine silica basal planes have the same composition and structure, it is likely the serpentine basal plane is also negatively charged across the pH range. Additionally, since the talc edge surface is similar in composition to the serpentine edge surface, it is likely the serpentine edge surface has a pzc, and that the pzc is close to that determined for the talc edge surface. As for the serpentine magnesium hydroxide basal plane, although measurements on similar surfaces have not been conducted, it can be surmised that it is positively charged because: (1) Mg^{2+} ions in the octahedral layer are often substituted by the trivalent ions Al^{3+} and Fe^{3+} (Alvarez-Silva et al., 2010; Mellini, 1982) and (2) zeta potential measurements, which represent the average potential values of all surfaces in solution, are positive at all pH values for serpentine minerals (Figure 5-8) (Kusuma et al., 2013).
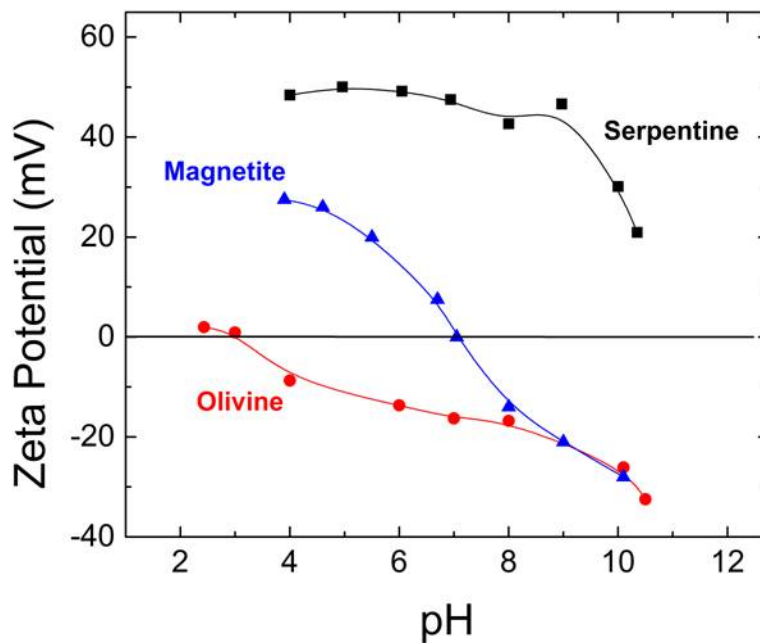
Figure 5-8: Zeta potential versus pH for minerals relevant to the Pipe and OK ore systems. Data for lizardite serpentine and olivine from Kusuma et al. (2013), and magnetite from Potapova et al. (2011). All tests conducted in 10^{-2}M KCl or NaCl.

Figure 5-9 summarizes the proposed surface charges for the different faces of serpentine. It is important to note that no attempt has been made to measure the

133

surface charges on the basal planes or edges of serpentine. According to the proposed model, aggregation of serpentine particles would occur across the pH range due to electrostatic attraction between the two basal planes. Also, there would be additional aggregation at low pH due to the attraction of the silica basal plane and the edge, and at high pH due to the attraction of the brucite basal plane and the edge. Given a platy morphology, where each type of surface is exposed, there would be two peak yield stress values, as observed for lizardite and for the untreated OK ore sample. Given a fibrous morphology, however, the situation would be different. In the case of chrysotile, the particles are tubular with the sheets coiled so as to expose the magnesium hydroxide basal plane on the outside. The magnesium hydroxide-silica edge surface is exposed at the edge of the tube, as well as along the length (Genc et al., 2012). Since only the magnesium hydroxide basal plane and edge surfaces are exposed on chrysotile particles, it would be expected that peak yield stress for chrysotile would occur near pH 10. Since chrysotile yield stress remains high across a wide range of pH values, it appears particle morphology may be more important than the surface charge. Chrysotile fibres in solution have been shown to orientate themselves in several directions, resulting in entanglement within individual and adjacent fibres (Ndlovu et al., 2011). Further to the point, Patra et al. (2012) found that increases in slurry viscosity and yield stress due to fibre entanglement occurred independent of mineral surface chemistry. Hence, the plateau yield stress observed for untreated Pipe ore and chrysotile was likely primarily due to the fibrous nature of the mineral. The extended plateau observed for the Pipe ore (the yield stress for pure chrysotile was observed by Ndlovu et al. (2011) to drop off below pH 5.5 and about pH) was likely due to the interaction of chrysotile fibres and other oppositely charged minerals present in the Pipe ore (see Figure 5-8 for zeta potential data of primary minerals).
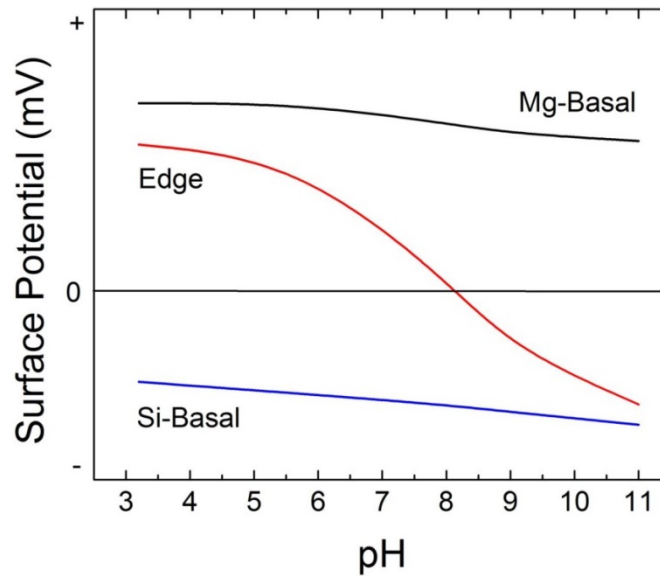
Figure 5-9: Proposed surface charge versus pH for the magnesium hydroxide basal plane (Mg-Basal), silica basal plane (Si-Basal) and edge surfaces of serpentine minerals.

The direct yield stress values measured across the pH range for the microwave pre-treated OK and Pipe ores were greatly reduced compared to that observed for untreated ores. For the Pipe ore, microwave pre-treatment significantly reduced the yield stress of ore slurries across the pH range. The microwave pre-treated Pipe ore plateau yield stress was 93% lower than for the untreated material. Even with the reduction in yield stress, the microwave pre-treated Pipe ore yield stress versus pH curve was reflective of the chrysotile yield stress versus pH curve, indicating that even at very low concentrations, chrysotile still dominates slurry rheology. Microwave pre-treatment also reduced the yield stress of OK ore slurries at low and high pH (92% reduction at pH 10). At pH 8, where peak yield stress was observed for microwave pre-treated OK ore, yield stress values observed for untreated and microwave pre-treated material were of similar magnitudes. The peak yield stress of the microwave pre-treated OK ore at pH 8 appears to be due to the aggregation of olivine, which is negatively charged (Figure 5-8), and the positively charged surfaces of lizardite (likely the magnesium hydroxide basal plane) remaining in the ore. Since it has been proven

135

that the rheology of the OK and Pipe ore slurries is dominated by serpentine minerals, and since the primary reaction that occurs as a result of microwave pre-treatment is the dehydroxylation of serpentine, it can be stated that the destruction of serpentine minerals in the OK and Pipe ores by microwave pre-treatment was responsible for the reduction in pulp yield stress and viscosity.

5.4 Conclusions

The rheology of two ultramafic ores, both primarily composed of serpentine, before and after microwave pre-treatment was studied. The serpentine present in the OK ore was of the lizardite form. The serpentine present in the Pipe ore was also mostly lizardite, although it also contained 1 wt.% chrysotile. Slurries of both ores exhibited shear thinning behaviour with a yield stress, and the rheology of both ores was shown to be dominated by serpentine minerals. The untreated OK ore slurry yield stress versus pH curve was reflective of the same curve for lizardite, while the yield stress versus pH curve for the Pipe ore was reflective of the same curve for chrysotile. The shape of the yield stress versus pH curve for lizardite (double peak) is hypothesized to be due to interactions between the differently charged faces of the mineral, while the shape of the yield stress versus pH curve for chrysotile (plateau) is believed to be due to its fibrous morphology. A model for the charges present on different serpentine mineral surfaces was proposed: this model needs to be validated experimentally. The Pipe ore exhibited higher shear stress, shear viscosity, and yield stress compared to the OK ore due to its chrysotile content. Microwave pre-treatment was shown to reduce the shear stress and shear viscosity (average 80% reduction at 200 s^1) observed at a given shear rate, as well as the direct yield stress (peak yield stress reduced by 92-93%), for both the OK and Pipe ores. The minimal chrysotile remaining in the Pipe ore after microwave pre-treatment still dominated the slurry rheology (plateau shaped yield stress versus pH curve), while interactions between olivine and the remaining serpentine are believed to have resulted in a single peak yield stress for the microwave pre-treated OK ore. The reduction in slurry viscosity

and yield stress observed as a result of microwave pre-treatment for the OK and Pipe ores is believed to be due to the destruction of serpentine minerals.

5.5 References

Alexander, G., Maroto-Valer, M.M., Gafarova-Aksoy, P., 2007. Evaluation of reaction variables in the dissolution of serpentine for mineral carbonation. Fuel. 86, 273-281.

Alvarez-Silva, M., Uribe-Salas, A., Mirnezami, M., Finch, J.A., 2010. The point of zero charge of phyllosilicate minerals using the Mular-Roberts titration technique. Minerals Engineering. 23, 383-389.

Becker, M., Yorath, G., Ndlovu, B., Harris, M., Deglon, D., Franzidis, J.-P., 2013. A rheological investigation of the behaviour of two Southern African platinum ores. Minerals Engineering. 49, 92-97.

Bobicki, E.R., Liu, Q., Xu, Z., 2014. Microwave heating of ultramafic nickel ores and mineralogical effects. Minerals Engineering. 58, 22-25.

Cruz, N., Peng, Y., Farrokhpay, S., Bradshaw, D., 2013. Interactions of clay minerals in copper-gold flotation: Part 1 – Rheological properties of clay mineral suspensions in the presence of flotation reagents. Minerals Engineering. 50-51, 30-37.

Dzuy, N.Q., Boger, D.V., 1985. Direct yield stress measurement with the vane method. Journal of Rheology. 29(3), 335-347.

Genc, A.M., Kilickaplan, I., Laskowski, J.S., 2012. Effect of pulp rheology on flotation of nickel sulphide ore with fibrous gangue particles. Canadian Metallurgical Quarterly. 51(4), 368-375.

Haque, K.E., 1999. Microwave energy for mineral treatment processes – a review. International Journal of Mineral Processing. 57, 1-24.

Kusuma, A.M., Zeng, H., Liu, Q., 2013. Understanding mineral interaction mechanisms by zeta potential and surface force measurements. Proceedings of the 10th International Mineral Processing Conference. 2013 October 15-18; Santiago, Chile.

McKelvy, M.J., Chizmeshya, A.V.G., Diefenbacher, J., Béarat, H., Wolf, G., 2004. Exploration of the role of heat activation in enhancing serpentine carbon sequestration. Environmental Science and Technology. 38, 6897-6903.

Mellini, M., 1982. The crystal structure of lizardite 1T: hydrogen bonds and polytypism. American Mineralogist. 67, 587-598.

Ndlovu, B., Farrokhpay, S., Bradshaw, D., 2013. The effect of phyllosilicate minerals on mineral processing industry, International Journal of Mineral Processing. 125(10), 149-156.

Ndlovu, B., Forbes, E., Farrokhpay, S., Becker, M., Bradshaw, D., Deglon, D., 2014. A preliminary rheological classification of phyllosilicate group minerals. Minerals Engineering. 55, 190-200.

Ndlovu, B.N., Forbes, E., Becker, M., Deglon, D.A., Franzidis, J.P., Laskowski, J.S., 2011. The effects of chrysotile mineralogical properties on the rheology of chrysotile suspensions. Minerals Engineering. 24, 1004-1009.

Patra, P., Bhambhani, T., Nagaraj, D.R., Somasundaran, P., 2010. Effect of morphology of altered silicate minerals on metallurgical performance: Transport of Mg silicates to the froth phase. Proceedings of the 49th Conference of Metallurgists. 2010 October 3-6; Vancouver, Canada. Westmount: CIM. p. 31-42.

Patra, P., Bhambhani, T., Nagaraj, D.R., Somasundaran, P., 2012. Impact of pulp rheological behavior on selective separation of Ni minerals from fibrous serpentine ores. Colloids and Surfaces A: Physicochemical and Engineering Aspects. 411, 24-26.

Peng, Y., Seaman, D., 2011. The flotation of slime-fine fractions of Mt. Keith pentlandite ore in de-ionised and saline water. 24, 479-481.

Pickles, C.A., 2009. Microwaves in extractive metallurgy: Part 2 – A review of applications. Minerals Engineering. 22, 1112-1118.

Potapova, E., Yang, X., Grahn, M., Holmgren, A., Forsmo, S.P.E., Fredriksson, A., Hedlund, J., 2011. The effect of calcium ions, sodium silicate and surfactant on charge and wettability of magnetite. Colloids and Surfaces A: Physicochemical and Engineering Aspects. 386, 79-86.

Rao, M.A., 2007. Rheology of Fluid and Semisolid Foods: Principles and Applications, second ed., Springer, New York.

Rayment, P., Ross-Murphy, S.B., Ellis, P.R., 1998. Rheological properties of guar galactomannan and rice starch mixtures. II. Creep measurements. Carbohydrate Polymers. 35, 55-63.

Senior, G.D., Thomas, S.A., 2005. Development and implementation of a new flowsheet for the flotation of a low grade nickel ore. International Journal of Mineral Processing. 78, 49-61.

Shabalala, N.Z.P., Harris, M., Leal Filho, L.S., Deglon, D.A., 2011. Effect of slurry rheology on gas dispersion in a pilot-scale mechanical flotation cell. Minerals Engineering. 24, 1448-1453.

Todd, D.B., 2004. Mixing of highly viscous fluids, polymers and pastes. In: Handbook of Industrial Mixing: Science and Practice. Eds: Paul, E.L., Atiemo-Obeng, V.A., Kresta, S.M. Hoboken: John Wiley & Sons. 987-1025.

Uddin, S., Rao, S.R., Mirnezami, M, Finch, J.A., 2012. Processing an ultramafic ore using fibre disintegration by acid attack. International Journal of Mineral Processing. 102-103, 38-44.

Xu, M., Dai, Z., Dong, J., Ford, F., Lee, A., 2010. Fibrous minerals in ultramafic nickel sulphide ores. Proceedings of the 49th Conference of Metallurgists. 2010 October 3-6; Vancouver, Canada. Westmount: CIM; p. 223-36.

Xu, M., Scholey, K., Marcuson, S., 2011. Vale-Cytec-University Research Consortium on Processing Low Grade Ultramafic Nickel Ore. Proceedings of the 50th Conference of Metallurgists. 2011 October 2-5; Montreal, Canada. Westmount: CIM.

Yan, L., Masliyah, J.H., Xu, Z., 2013. Understanding suspension rheology of anisotropically-charged platy minerals from direct interaction force measurement using AFM. Current Opinion in Colloid and Interface Science. 18, 149-156.

Yang, S., Pelton, R., Abarca, C., Dai, Z., Montgomery, M., Xu, M., Bos, J.-A., 2013. Towards nanoparticle flotation collectors for pentlandite separation. International Journal of Mineral Processing. 123, 137-144.

Chapter 6 Ligand-Promoted Dissolution of Serpentine in Ultramafic Nickel Ores[5]

6.1 Introduction

The rate limiting step during aqueous mineral carbon sequestration (MCS) is the dissolution of the silicate mineral (Krevor and Lackner, 2011). To overcome the slow dissolution kinetics, a number of extraction agents have been investigated for use in indirect aqueous MCS schemes, including acids and ammonium salts (Baldyga et al., 2010; Kakizawa et al., 2001; Kodama et al., 2008; Park and Fan, 2004; Pundsack, 1967; Tier et al., 2007). Indirect aqueous MCS involves the extraction of reactive components (Mg^{2+}, Ca^{2+}) from silicate minerals, followed by the reaction of the extracted components with CO_2 in the aqueous phase (Bobicki et al., 2012). In both acid and ammonia extraction, a proton is used to liberate the alkaline earth metal ion from the silicate matrix. It is believed that lone pairs of electrons present on oxygen atoms in the silicate structure undergo protonation as the proton concentration increases. The protonation of oxygen atoms polarizes and weakens Mg-O-Si bonds, enabling the release of magnesium ions into solution, as shown by reaction 6-1 (Alexander et al., 2007; Oelkers, 2001; Stumm, 1992).

$$Mg_3Si_2O_5(OH)_4 + 6H^+ \rightarrow 3Mg^{2+} + 2SiO_2 + 5H_2O \qquad (6.1)$$
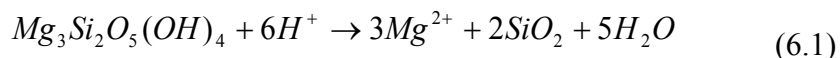
Although indirect aqueous MCS processes utilizing proton-promoted dissolution can achieve high carbonate conversions under relatively mild processing conditions, the chemical reagent requirements can be prohibitively high as chemicals must be added both for extraction of the reactive component, and to adjust the pH after leaching for carbonate precipitation (Teir et al., 2009).

Recently, interest in developing a chemically-enhanced direct aqueous MCS process has arisen (Krevor and Lackner, 2011; Bonfils et al., 2012). In the proposed process, ligands are used to aid in the dissolution of the silicate mineral and there is no separation of the extracted magnesium and the remaining solids prior to carbonation. In fact, the ligands continue to aid mineral dissolution during carbonation. Ligand-enhanced dissolution of silicate minerals for MCS is particularly interesting because the chelating effects can occur at neutral to alkaline pH. As a result, the consumption of large quantities of acids and bases is not required, as it would be in the classic pH swing process (Krevor and Lackner, 2011; Prigiobbe and Mazzotti, 2011; Park et al., 2003; Wogelius and Walther, 1991). If the dissolution of silicate minerals could be promoted at a pH value conducive to carbonate precipitation, the chemical cost of aqueous MCS processes could be reduced. Additional benefits of using ligands to enhance direct MCS processes include the potential for the recycling of the leach solution after carbonation, and that ligands could prevent the re-precipitation of iron during leaching, which would otherwise inhibit dissolution of silicate minerals (Park et al., 2003).

Ligands, or chelating agents, aid in mineral dissolution by specifically adsorbing on mineral surfaces and forming highly soluble complexes with metal ions (e.g. magnesium in serpentine). The formation of ligand-metal complexes at the mineral surface shifts the electron density towards the metal ion, which destabilizes the Me-O lattice bonds and facilitates the detachment of metal ions into solution (Stumm, 1992). Ligands also enhance the dissolution of minerals by forming complexes with leached ions in solution, thus, lowering the apparent solubilization of the mineral (Prigiobbe and Mazzotti, 2011). The ligand (oxalate shown) promoted dissolution of alumina is shown in Figure 6-1.

$+ C_2O_4^{2+} + H^+ \longrightarrow \quad +2H_2O$

$+2H^+ \longrightarrow \quad + Al^+$
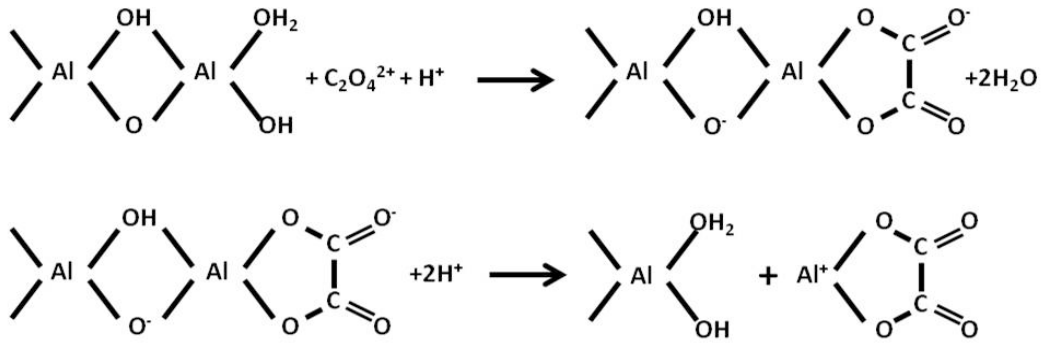
Figure 6-1: Illustration of ligand-promoted dissolution.

A number of ligands have been shown to improve the dissolution of silicates in nature, including oxalate, citrate, diphenols, and hydroxycarboxylic acids (Stumm, 1992). In the laboratory, acetate, ascorbate, citrate, EDTA, potassium hydrogen phthalate, oxalate and tannate have been shown to enhance the dissolution of olivine (Grandstaff, 1986; Hänchen et al., 2006; Olsen and Rimstidt et al., 2008; Prigiobbe and Mazzotti, 2011; Wogelius and Walther, 1991). Similarly, it has been demonstrated that catechol, citrate, EDTA and oxalate improve the dissolution of serpentine (Bales and Morgan, 1985; Krevor and Lackner, 2011; Park and Fan, 2004). To date, ligands have primarily been investigated for the dissolution of silicate minerals at acidic to neutral pH. However, carbonation under the same conditions has not resulted in the complete conversion of the leached magnesium to magnesium carbonate (Krevor and Lackner, 2011; Park and Fan, 2004). To preferentially precipitate the leached magnesium as magnesium carbonate, an adjustment of leachate to pH 9 or 10 has been required, just as when acid extraction is used in indirect aqueous MCS schemes (Park and Fan, 2004). Thus, the effectiveness of ligands to improve the leaching of magnesium from silicate minerals at neutral to alkaline pH is of particular interest for MCS.

The objective of this paper is to investigate the effectiveness of five different ligands for improving the leaching of magnesium from serpentine in ultramafic nickel ores at neutral to alkaline pH and room temperature. Solution modeling was used to determine the capacity of the ligands to enhance the solubility of Mg

across the pH range. The ability of the ligands to enhance the dissolution of Mg from ultramafic ores was examined experimentally at pH 7 and 10. The effect of ligand concentration on total Mg leached was also examined. Subsequently, the effect of the ligands on Mg leaching rates was investigated at several ligand concentrations, again at pH 7 and pH 10. The ligands tested include catechol ($C_6H_4O_2^{2-}$), citrate ($C_6H_5O_7^{3-}$), ethylenediaminetetraacetic acid (EDTA, $C_{10}H_{12}O_8N_2^{4-}$), oxalate ($C_2O_4^{2-}$) and tiron ($C_6H_2O_8S_2^{4-}$) (Figure 6-2). The ligands were selected based on the strength of their stability constants and their affinity for magnesium (Table 6-1). Ultramafic nickel ores were selected as feedstock in this work as the waste material produced by nickel extraction is primarily serpentine, a common MCS feedstock material. The use of waste materials for MCS feedstock is highly desirable as (1) mining for raw materials is not required, (2) the waste is available cheaply, and (3) the waste is already ground to a particle size suitable for carbonation (Bobicki et al., 2012).

Table 6-1: Stability constants for Mg-ligand complexes (Smith and Martell, 1975). [a] 20°C [b] 18°C, [c] 30°C.

Leaching Agent	Product	Reactions	pK (Temperature, Ionic Strength)	
			25°C, 0.1	25°C, 1.0
EDTA	$MgEDTA^{2-}$	$Mg^{2+} + EDTA^{4-} = MgEDTA^{2-}$	-8.83	-
$C_{10}H_{12}O_8N_2^{4-}$	$MgHEDTA^-$	$H^+ + MgEDTA^{2-} = MgHEDTA^-$	-3.85[a]	-
Oxalate	$MgOx$	$Mg^{2+} + Ox^{2-} = MgOx$	-2.76	-3.43[b]
$C_2O_4^{2-}$	$Mg(Ox)_2^{2-}$	$Mg^{2+} + 2Ox^{2-} = Mg(Ox)_2^{2-}$	-4.24	-
Catechol $C_6H_4O_2^{2-}$	$MgCat$	$Mg^{2+} + Cat^{2-} = MgCat$	-5.7[c]	-
Citrate	$MgCit^-$	$Mg^{2+} + Cit^{3-} = MgCit^-$	-3.37	-3.25
$C_6H_5O_7^{3-}$	$MgHCit$	$Mg^{2+} + HCit^{2-} = MgHCit$	-1.92	-1.6
	MgH_2Cit^+	$Mg^{2+} + H2Cit^- = MgH_2Cit^+$	-	-0.84
Tiron	$MgTiron^{2-}$	$Mg^{2+} + Tiron^{4-} = MgTiron^{2-}$	-6.86	-
$C_6H_2O_8S_2^{4-}$	$MgHTiron^-$	$Mg^{2+} + HTiron^{3-} = MgHTiron^-$	-1.98	-
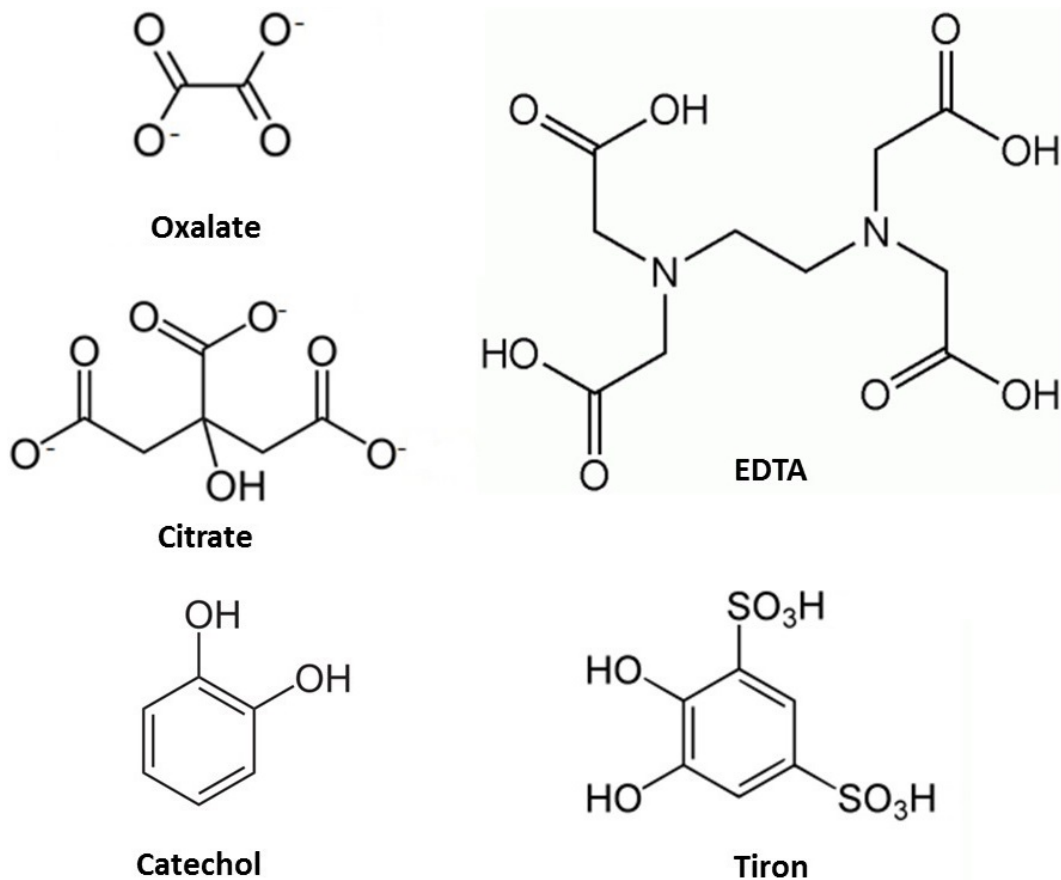
Figure 6-2: Ligands investigated for enhancing the leaching of magnesium from ultramafic nickel ores.

6.2 Methods and Materials

6.2.1 Modeling

The percent speciation for magnesium and ligands in water was calculated iteratively across the pH range from 0 to 14 in Microsoft Excel using the equilibrium constants tabulated in Appendix A. The species considered in the calculations included those found in the magnesium hydroxide-in-water system (Mg^{2+}. $MgOH^+$, $Mg(OH)_{2(aq)}$ and $Mg(OH)_{2(s)}$), as well as the respective ligands, including the protonated and metal-complexed forms. All equilibrium constant data found relevant to the system was used in the modeling. The magnesium hydroxide-in-water system was chosen for the modeling work due to its simplicity. A magnesium concentration of 0.1 M was selected as this is

representative of the total Mg present in 1 g of the ores dissolved in 100 mL of solution (conditions used in experimental work). Ligand concentrations of 0.1 M were used for the speciation versus pH calculations as this was the most concentrated solution of ligand used in the experimental work. The effect of ligand concentration (0 to 2 M) on the concentration of soluble Mg species in solution was also modeled at pH 7 and 10. All calculations were conducted for systems at 25°C.

6.2.2 Mineral Feedstock

Two ultramafic nickel ores were used in this study, the OK ore from Washington State, USA, and the Pipe ore from Manitoba, Canada. Both ores were high in MgO (45.8 wt.% for OK ore, 39.5 wt.% for Pipe ore) and SiO_2 (40.7 wt.% for OK ore, 34.8 wt.% for Pipe ore) with lesser amounts of iron, alumina, sulphur and nickel (0.26 wt.% for OK ore, 0.23 wt.% for Pipe ore). The mineral composition of the ores is shown in Table 6-2. Although the waste produced from the processing of these ores is the target feedstock, whole ores were used in this study because (1) neither of the ores are currently being mined for nickel production and tailings are not being generated, and (2) the tailings produced by the processing of these low-grade ores will be similar in composition to the whole ores. The ores were crushed using a BB 200 Jaw Crusher (Retsch, Burlington, ON, Canada), milled using a DM 200 Disc Mill (Retsch, Burlington, ON, Canada) and sieved to isolate the < 45 μm size fraction. The particle size distributions, as determined by a light scattering technique (Mastersizer 2000, Malvern Instruments Ltd., Malvern, Worchestershire, UK), for the < 45 μm OK and Pipe ore material is shown in Figure 6-3. The < 45 μm material was split into 1 g samples using a spatula technique.

Table 6-2: Mineral composition of OK and Pipe ores from quantitative XRD analysis.

Mineral	Formula	OK Ore	Pipe Ore
Serpentine (wt.%)	$Mg_3Si_2O_5(OH)_4$	84.0	63.7
Olivine (wt.%)	Mg_2SiO_4	-	7.7
Cordierite (wt.%)	$Mg_2Al_4Si_5O_{18}$	-	1.0
Vermiculite (wt.%)	$Mg_2Si_4O_{10}(OH)_2$	-	0.7
Brucite (wt.%)	$Mg(OH)_2$	5.1	-
Dolomite (wt.%)	$CaMg(CO_3)_2$	-	5.5
Magnetite (wt.%)	Fe_3O_4	6.6	12.3
Pyrrhotite (wt.%)	$Fe_{1-x}S$	-	4.7
Pentlandite (wt.%)	$(Fe,Ni)_9S_8$	4.3	2.8
Quartz (wt.%)	SiO_2	-	1.6
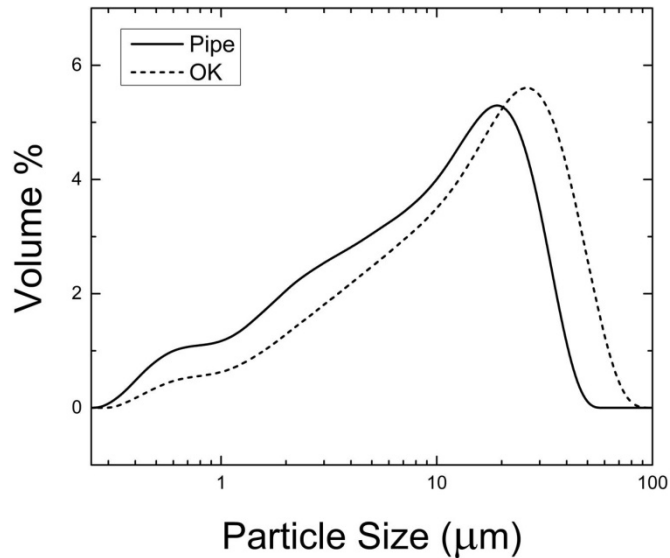
Figure 6-3: Particle size distribution for OK and Pipe ore sieved to <45 µm.

6.2.3 Leaching Tests

1 g of < 45 µm OK and Pipe ore was placed with 100 mL of leaching solution in a 250 mL Erlenmeyer flask. The leaching solutions consisted of distilled water and ligand solutions at concentrations of 0.01 M, 0.05 M and 0.1 M. The ligands tested were catechol (Acros Organics), citrate (trisodium citrate dehydrate, Alfa Aesar), EDTA (ethylenediaminetetraacetic acid, Alfa Aesar), oxalate (sodium oxalate, Alfa Aesar) and tiron (1,2-Dihydroxybenzene-3,5-disulfonic acid

147

disodium salt monohydrate, Alfa Aesar). The suspensions were agitated in a shaker at room temperature. The pH of the suspensions was adjusted to 7 or 10 over 1 hour using 37 wt.% HCl (Acros Organics) or 50 wt.% NaOH (Fisher Chemical). The total volume of HCl or NaOH added was less than 0.5 mL and had a negligible effect on the total slurry volume. After pH adjustment, the samples were agitated on the shaker at room temperature for 24 hours. Samples of 5 mL each were removed from the samples at 1, 2, 4, 6 and 24 hours using a syringe. The 5 mL samples were filtered. The supernatant collected was acidified using a drop of concentrated HCl and submitted for elemental analysis by ICP. Each test was repeated in triplicate. The ICP results, in combination with the volume of solution and mass of the solids, were used to determine the total Mg leached from the ore and the leaching rates. In some cases, the Si concentration is also used for the calculation of leaching rates (Thom et al., 2013; Daval et al., 2013). Because the feedstock in this study was not pure serpentine, and the Mg leached was the main species of interest for MCS, only the Mg concentration in solution was monitored with time. This approach has been taken previously by others (Krevor and Lackner, 2011; Prigiobbe and Mazzotti, 2011). Although CO_2 from the ambient air was not excluded from the leaching systems, it is not believed to have impacted the extent of Mg leached, and analysis of the leach residues by XRD did not indicate that magnesium carbonate or any other additional mineral phases formed during leaching.

6.2.4 Materials Characterization

X-ray fluorescence (XRF) spectroscopy (Orbis PC Micro-EDXRF Elemental Analyzer, EDAX, Mahwah, NJ, USA) and inductively coupled plasma mass spectrometry (ICP-MS) (Perkin Elmer Elan 6000, Waltham, Massachusetts, USA) were used to determine the elemental composition of the ores. ICP-MS was also used to determine the magnesium content of supernatant collected during the leaching tests. Atomic absorption spectroscopy (AAS) (Varian 220 FS, Palo Alto, California, USA) was applied to a selected number of supernatant samples to determine the silicon content. To determine the mineralogical composition of the

ores, quantitative XRD analysis was performed by PMET Inc. of New Brighton, PA using the Rietveld refinement technique. An automated Autosorb-1 gas sorption analyzer (Quantachrome Instruments, Boynton Beach, FL, USA) was used to determine the surface area of selected samples by the multi-point Brunauer-Emmett-Teller (BET) method.

6.2.4 Calculation of Leaching Rates

To determine the leaching rates, the leaching curves (magnesium concentration in solution versus time) were differentiated and then normalized by the sample BET surface area, liquid volume and solid mass using the following expression:

$$r = \frac{V_o}{3AM} \frac{d[Mg]}{dt} \tag{6-2}$$

where V_o is the volume of liquid, A is the specific surface area (m^2/g), M is the mass of mineral (g), and 3 is the mole concentration of magnesium in serpentine (Brantley and Olsen, 2014). The rate calculated is the rate of serpentine dissolution. In order to compare the rates achieved in this work with published leaching rates, it was assumed that all magnesium present in the samples originated in serpentine. It was also assumed, as per convention (Bonfils et al., 2012; Daval et al; 2013; Hänchen et al; 2006; Oelkers, 2001), that the specific surface area of the samples did not change with time. This assumption was validated by comparing the specific surface area of samples from which the most Mg was released into solution over 24 hours (4.8 m^2/g and 14.2 m^2/g for OK ore leached with 0.1 M Tiron at pH 7 and Pipe ore leached with 0.1M EDTA at pH 7, respectively) with that of fresh material (4.3 m^2/g for fresh OK ore and 13.44 m^2/g for fresh Pipe ore). The comparison revealed that the specific surface area did not change by more than 10% during leaching.

6.3 Results and Discussion

6.3.1 Solution Modeling

The distribution of magnesium species in water at 25°C is shown in Figure 6-4, while the distribution of magnesium species in water at 25°C upon the addition of a ligand are shown in Figures 6-5 to 6-9. In water alone at pH 7, Mg ions are quite soluble. With increasing pH, however, the solubility of Mg ions declines. Under the modeled conditions, only 25% of Mg in the system is soluble in water at pH 10. Upon the addition of a ligand, the solubility of Mg at alkaline pH increases. The results of solution chemistry modeling indicate that each of the ligands tested should improve the solubility of Mg at pH 10. The order of effectiveness was: EDTA > tiron > citrate > catechol > oxalate (Figure 6-10). This order of effectiveness for the improvement in Mg solubility at pH 10 by the ligands is mostly reflective of the relative magnitude of the stability constants (given in Table 6-1), except for catechol and oxalate which were modeled to solubilize less Mg at pH 10 than citrate despite having higher stability constants (for the Mg-ligand complexes). The reduced performance of catechol at pH 10 is attributed to the formation of $HCat^-$ ions, which reduce the number of MgCat complexes that form in solution (see Appendix B). For the reduced performance of oxalate, in addition to the MgOx species, oxalate also forms a $Mg(Ox)_2^{2-}$ complex at pH 10 where two oxalate ions are bound with one Mg ion (see Appendix B). The Mg solubilising efficiency of oxalate ions in the $Mg(Ox)_2^{2-}$ complex is half that of ligand ions in 1:1 complexes.
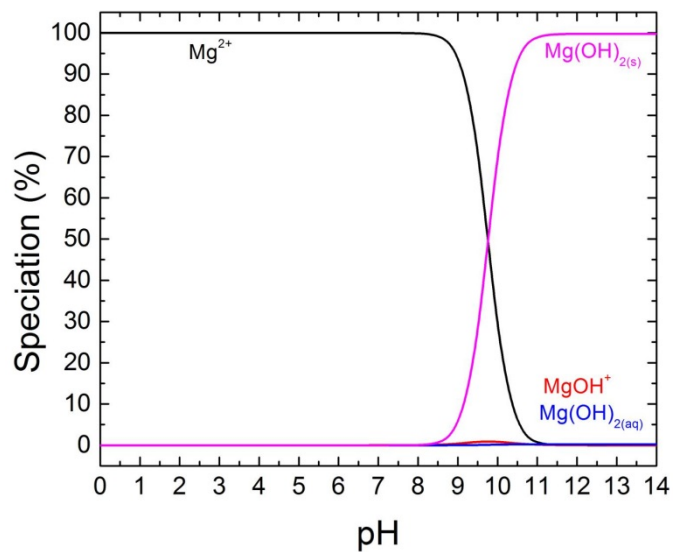
Figure 6-4: Distribution of magnesium species in water at 25ºC upon the addition of 0.1 M Mg.
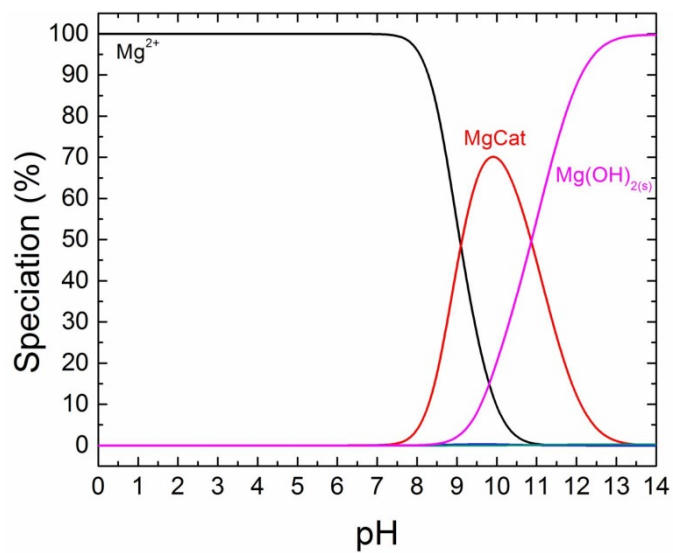
Figure 6-5: Distribution of magnesium species in water at 25ºC upon the addition of 0.1 M Mg and 0.1 M catechol.
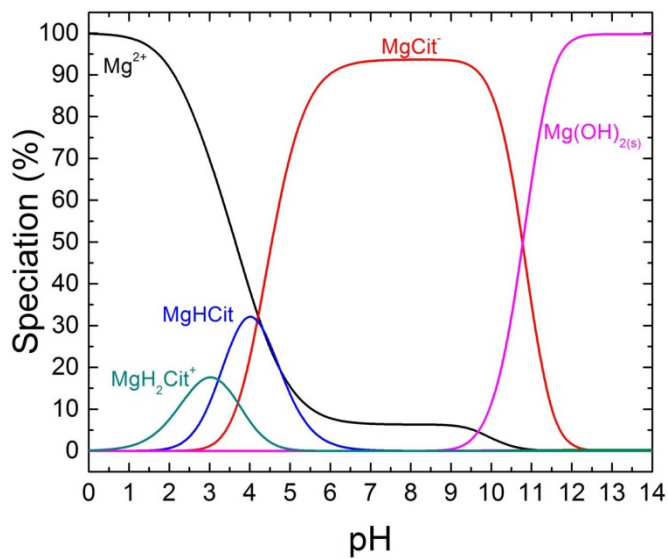
Figure 6-6: Distribution of magnesium species in water at 25ºC upon the addition of 0.1 M Mg and 0.1 M citrate.
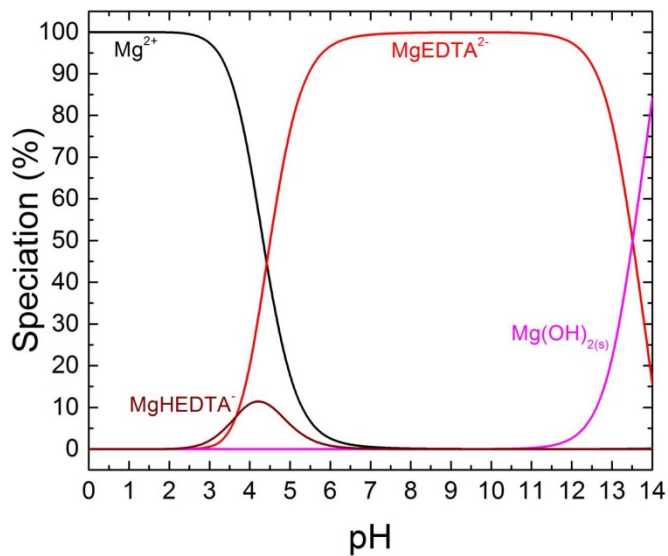
Figure 6-7: Distribution of magnesium species in water at 25ºC upon the addition of 0.1 M Mg and 0.1 M EDTA.
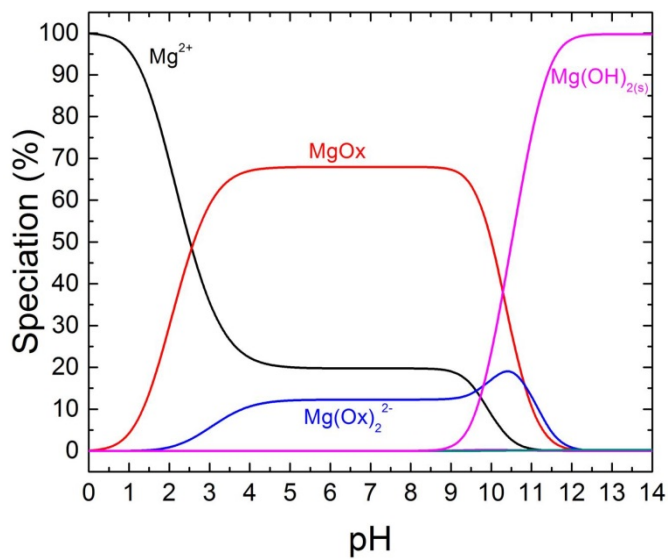
Figure 6-8: Distribution of magnesium species in water at 25ºC upon the addition of 0.1 M Mg and 0.1 M oxalate.
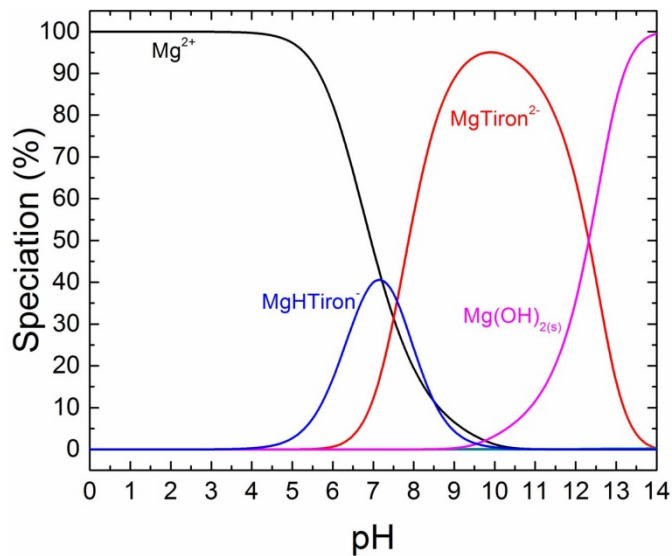
Figure 6-9: Distribution of magnesium species in water at 25ºC upon the addition of 0.1 M Mg and 0.1 M tiron.
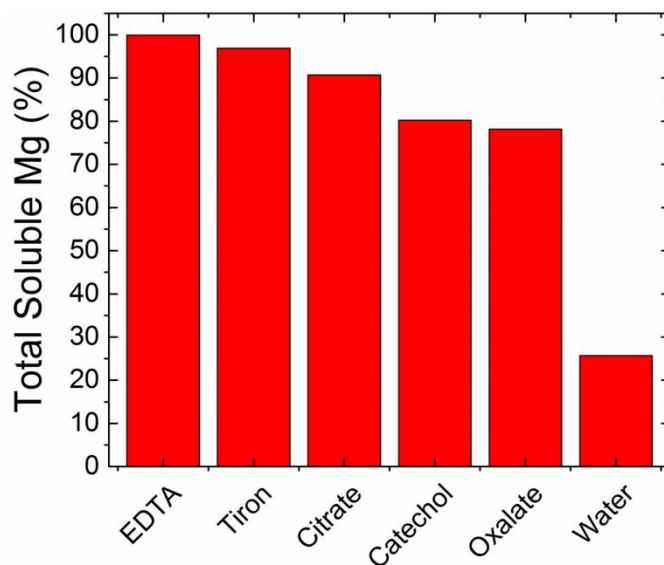
Figure 6-10: Total soluble Mg in 0.1 M Mg aqueous solutions at pH 10 and 25ºC with and without the addition of 0.1 M ligand

The effect of ligand concentration on the solubility of magnesium ions was investigated by modeling over the range of ligand to magnesium molar ratios of 0.01 to 2. At pH 7, no effect was observed as magnesium was 100% soluble at all ligand to magnesium molar ratios. At pH 10, however, the ligand concentration had a pronounced effect on the solubility of magnesium (Figure 6-11). For EDTA, tiron and citrate, the total soluble magnesium increased linearly with increasing ligand to magnesium ratios up to approximately 1.0, above which magnesium remained nearly 100% soluble. For catechol and oxalate, the linear portion of the curves ceased at lower ligand to magnesium ratios. In such systems, magnesium was not 100% soluble until ligand to magnesium molar ratios of 1.5 and 2.0 were surpassed, respectively. Catechol and oxalate were more sensitive to ligand concentration at pH 10 than the other ligands studied, most likely due to the formation of HCat⁻ in the case of catechol, and the formation of $Mg(Ox)_2^{2-}$ in the case of oxalate (see Appendix C). The solution chemistry modeling indicates that to maximize the effectiveness of the ligands, a ligand to magnesium molar ratio of 1 or higher should be used.
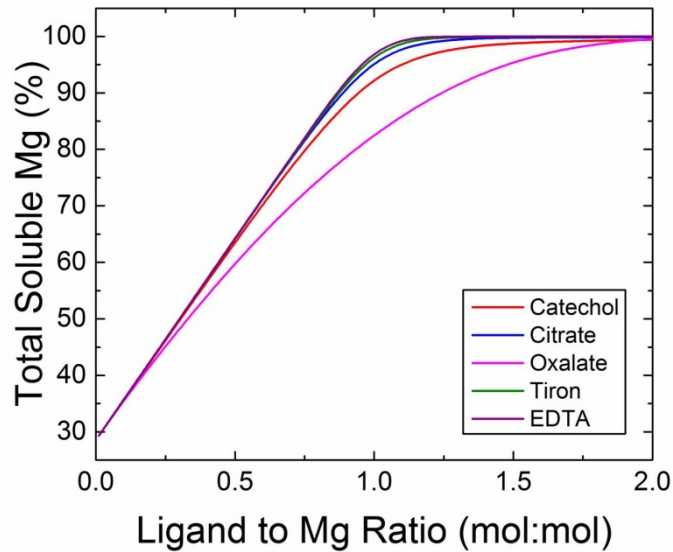
Figure 6-11: Total soluble magnesium in 1.0 M magnesium aqueous solutions at pH 10 and 25ºC as a function of ligand to magnesium molar ratio.

6.3.2 Experimental Results

6.3.2.1 Total Magnesium Leached

The total magnesium leached at pH 7 and 10 over 24 hours at room temperature as a function of ligand concentration for the Pipe and OK ores is shown in Figures 6-12 to 6-15. The ratios of Mg leached in the presence and absence of ligands (L_L/L_W) are given in Table 6-3. As expected, the total magnesium leached was higher at pH 7 than at pH 10, and increased with increasing ligand concentration. Overall, the 0.1 M ligand solutions, corresponding to a ligand to Mg molar ratio of 1, yielded the highest L_L/L_W values. Although the total Mg leached under equal conditions was always greater for the OK ore than for the Pipe ore, the L_L/L_W was generally greater for the Pipe ore than for the OK ore. For the Pipe ore, the L_L/L_W was always greater than 1, indicating that the total magnesium leached in all ligand solutions was greater than that leached in water at same pH value. While a similar trend was observed for the OK ore, the L_L/L_W values for 0.01M citrate and oxalate solutions at pH 7 were found to be close to 1. In general, while the total Mg leached was greater at pH 7 than at pH 10 for the same ligand solution, the L_L/L_W ratios for tiron, EDTA and catechol were greater at pH

155

10 than pH 7. In contrast, for oxalate and citrate, the L_L/L_W ratios at pH 10 were most often less than or equal to those at pH 7. The results suggest that at pH 10, tiron, EDTA and catechol were more effective leaching agents for Mg than oxalate and citrate. This is because maximum Mg chelation for tiron, EDTA and catechol occurs at pH 10, whereas maximum Mg chelation for oxalate and citrate occurs at pH 7.5 and pH 8 respectively (see Appendix B). Based on the total Mg leached and L_L/L_W ratios given in Table 6-3, the order of effectiveness of the ligands for leaching Mg from the Pipe ore was EDTA $\geq$ tiron > catechol > oxalate $\geq$ citrate. The order of effectiveness for the ligands at leaching Mg from the OK ore was tiron > EDTA = catechol > oxalate > citrate. The experimental leaching results indicate that EDTA, tiron and catechol may be effective leaching agents for enhancing aqueous MCS at alkaline pH with ultramafic ores as feedstock.
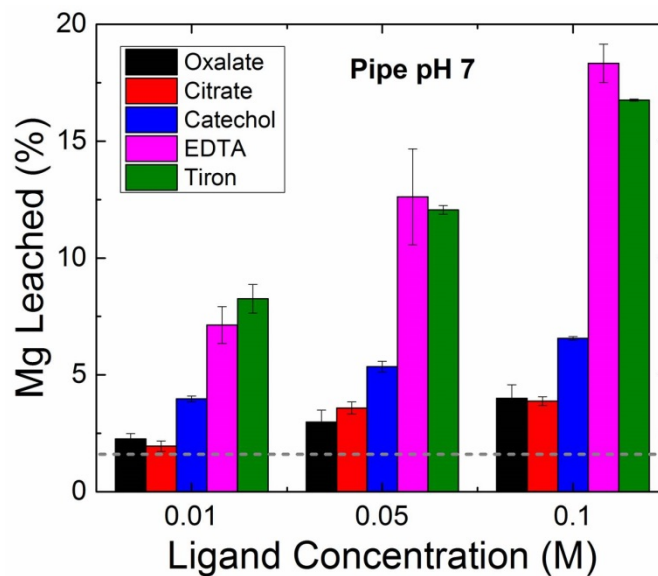
Figure 6-12: Total magnesium leached from the Pipe ore in catechol, citrate, EDTA, oxalate and tiron solutions over 24 hours as a function of ligand concentration at pH 7. The dotted grey line represents the total magnesium leached from the Pipe ore in water under the same conditions.
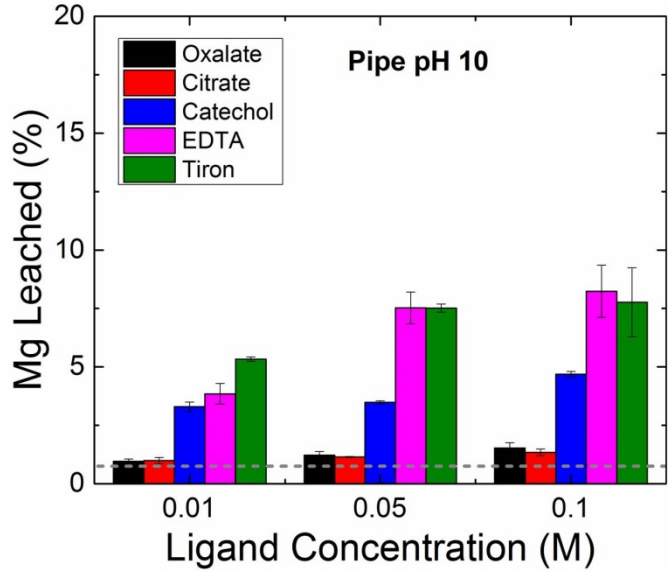
Figure 6-13: Total magnesium leached from the Pipe ore in catechol, citrate, EDTA, oxalate and tiron solutions over 24 hours as a function of ligand concentration at pH 10. The dotted grey line represents the total magnesium leached from the Pipe ore in water under the same conditions.
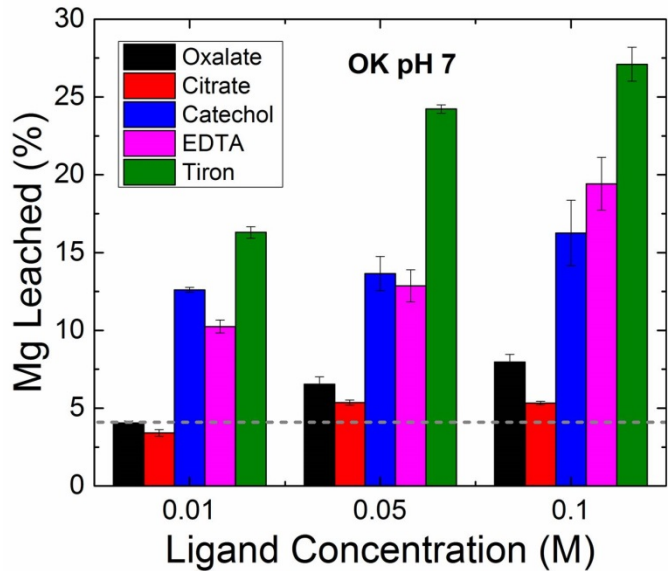
Figure 6-14: Total magnesium leached from the OK ore in catechol, citrate, EDTA, oxalate and tiron solutions over 24 hours as a function of ligand concentration at pH 7. The dotted grey line represents the total magnesium leached from the OK ore in water under the same conditions.
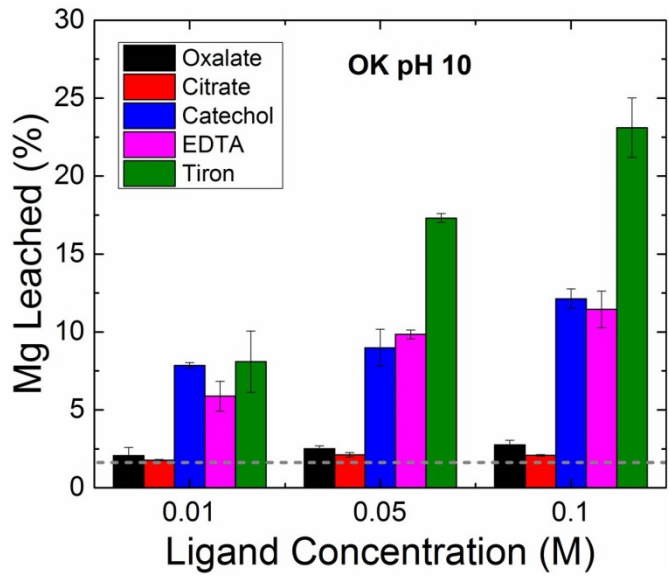
Figure 6-15: Total magnesium leached from the OK ore in catechol, citrate, EDTA, oxalate and tiron solutions over 24 hours as a function of ligand concentration at pH 10. The dotted grey line represents the total magnesium leached from the OK ore in water under the same conditions.

Table 6-3: Ratio of total magnesium leached by ligand solutions to total magnesium leached under the same conditions in water (L_L/L_w), parabolic leaching rate constants (k_{app}), initial leaching rates (R_i), final leaching rates (R_f), initial leaching rate upgrade ratios ($R_{L,i}/R_{w,i}$), and final leaching rate upgrade ratios ($R_{L,f}/R_{w,f}$) for Pipe and OK ores at 25°C. Rates given in units of $mol.m^{-2}.s^{-1}$. Rate constants in units of $M.s^{-1/2}$.

Ligand	pH	Concentration (M)	Pipe						OK					
			L_L/L_w	log k_{app}	log R_i	log R_f	$R_{L,i}/R_{w,i}$	$R_{L,f}/R_{w,f}$	L_L/L_w	log k_{app}	log R_i	log R_f	$R_{L,i}/R_{w,i}$	$R_{L,f}/R_{w,f}$
Water	7	-	-	-	-11.30	-11.30	-	-	-	-5.92	-9.66	-10.09	-	-
	10	-	-	-	-11.34	-11.34	-	-	-	-6.07	-9.81	-10.65	-	-
Catechol	7	0.01	2.5	-5.51	-9.75	-10.45	36.1	7.1	3.1	-5.06	-8.80	-9.56	7.2	3.4
		0.05	3.3	-5.33	-9.57	-10.29	54.0	10.4	3.3	-4.91	-8.66	-9.62	10.0	3.0
		0.1	4.1	-5.24	-9.48	-10.09	67.1	16.4	4.0	-4.82	-8.56	-9.39	12.5	5.0
	10	0.01	4.4	-5.48	-9.71	-10.40	42.5	8.8	4.9	-5.29	-9.03	-9.74	6.0	8.0
		0.05	4.6	-5.51	-9.75	-10.39	39.0	8.9	5.6	-5.10	-8.84	-9.71	9.2	8.6
		0.1	6.2	-5.59	-9.81	-10.15	34.5	15.5	7.5	-5.20	-8.95	-9.41	7.3	17.5
Citrate	7	0.01	1.2	-5.85	-10.09	-11.04	16.2	1.8	0.8	-5.83	-9.58	-10.36	1.2	0.5
		0.05	2.2	-5.21	-9.45	-11.24	71.5	1.2	1.3	-5.59	-9.34	-10.15	2.1	0.9
		0.1	2.4	-5.17	-9.41	-11.19	78.3	1.3	1.3	-5.18	-8.93	-11.03	5.4	0.1
	10	0.01	1.3	-6.18	-10.41	-11.06	8.5	1.9	1.1	-5.96	-9.71	-10.63	1.3	1.0
		0.05	1.5	-6.18	-10.41	-11.15	8.5	1.5	1.3	-5.73	-9.48	-10.81	2.1	0.7
		0.1	1.8	-6.05	-10.29	-11.12	11.3	1.7	1.3	-5.79	-9.54	-10.82	1.9	0.7
EDTA	7	0.01	4.4	-5.38	-9.62	-10.37	48.1	8.6	2.5	-5.45	-9.10	-10.13	3.6	0.9
		0.05	7.8	-5.13	-9.36	-10.07	86.9	17.1	3.1	-4.94	-8.68	-10.37	9.4	0.5
		0.1	11.4	-4.90	-9.13	-9.61	147.7	49.2	4.7	-4.93	-8.68	-9.32	9.6	5.9
	10	0.01	5.1	-5.55	-9.79	-11.50	35.9	0.7	3.6	-5.53	-9.27	-10.45	3.4	1.6
		0.05	10.0	-5.51	-9.75	-10.51	39.4	6.9	6.1	-5.51	-9.25	-9.88	3.6	5.9
		0.1	10.9	-5.52	-9.76	-10.49	38.1	7.1	7.1	-5.34	-9.09	-9.78	5.3	7.4
Oxalate	7	0.01	1.4	-5.90	-10.14	-11.26	14.6	1.1	1.0	-5.70	-9.44	-10.92	1.7	0.1
		0.05	1.8	-5.89	-10.13	-10.89	14.8	2.6	1.6	-5.68	-9.42	-11.18	1.7	0.1
		0.1	2.5	-5.52	-9.76	-11.10	34.8	1.6	1.9	-5.49	-9.23	-10.40	2.7	0.5
	10	0.01	1.3	-6.15	-10.39	-11.44	9.0	0.8	1.3	-6.34	-10.08	-11.03	0.5	0.4
		0.05	1.6	-6.23	-10.46	-10.98	7.6	2.3	1.5	-6.05	-9.79	-10.59	1.0	1.2
		0.1	2.0	-6.10	-10.34	-10.84	10.2	3.2	1.7	-5.66	-9.41	-10.74	2.5	0.8
Tiron	7	0.01	5.1	-5.03	-9.27	-10.40	108.1	8.0	4.0	-4.77	-8.52	-9.66	13.9	2.7
		0.05	7.5	-5.09	-9.33	-10.04	94.0	18.4	5.9	-4.67	-8.41	-9.30	17.5	6.1
		0.1	10.4	-4.95	-9.19	-9.75	129.5	35.6	6.6	-4.51	-8.26	-9.31	25.3	6.1
	10	0.01	7.1	-5.38	-9.62	-10.32	52.5	10.4	5.0	-5.16	-8.90	-9.91	8.1	5.5
		0.05	10.0	-5.26	-9.50	-10.24	70.1	12.8	10.7	-4.89	-8.63	-9.48	14.9	14.6
		0.1	10.3	-5.33	-9.57	-10.29	59.5	11.2	14.3	-4.63	-8.38	-9.39	27.1	18.1

The experimental leaching results differed in several ways from what was predicted by the solution chemistry model. The first major difference was that the experimental results showed that not all of the Mg present in the system was soluble at pH 7 and that the ligands were not equally effective in leaching Mg from the ores at this pH value. This difference was to be expected as the modeling study was done on a simplified magnesium hydroxide-in-water system whereas, in the experimental study, Mg was leached primarily from magnesium silicate minerals. The second major difference between the modeling and experimental study was in the relative order of effectiveness of the different leaching agents. Whereas the experimentally-determined order of ligand effectiveness for solubilizing Mg from the Pipe ore was in accordance with the relative strength of the stability constants (i.e., EDTA > tiron > catechol > oxalate > citrate), the model predicted this should not be the case. The agreement between the relative order of effectiveness of the ligands for the leaching of Mg from the Pipe ore and the relative strength of the stability constants suggests that the strength of the Mg-ligand complex formed is as important as the frequency with which it is formed in order to result in the release of Mg into solution. The order of effectiveness of the ligands for solubilizing Mg from the OK ore was similar to that of the Pipe ore, except for tiron which was found to be more effective than EDTA, and catechol was found to be as effective as EDTA. The ability of tiron and catechol to form complexes with silicic acid in the alkaline pH range (Bai et al., 2009; Bai et al, 2011; Bales and Morgan, 1985; Öhman et al., 1991) may have led to the improved effectiveness of these ligands for extracting Mg from the OK ore. The binding of ligands with silica groups, in addition to magnesium groups, in the leaching of serpentine would allow the mineral structure to be "attacked" and deconstructed from all sides, ultimately improving the release of Mg into solution. Since the OK ore was composed mostly of serpentine (84 wt.%), the double-action of tiron and catechol (binding with both Mg and Si groups) allowed these ligands to leach magnesium more, or as, effectively compared to EDTA, despite having lower stability constants. Similarly, catechol and tiron were more effective in leaching Mg from the OK ore

160

than from the Pipe ore since more of the magnesium present in the OK ore was from serpentine (91 wt.% versus 82 wt.% Mg in serpentine in OK and Pipe ore, respectively). Analysis of supernatant from leaching tests conducted in 0.1 M ligand solutions by atomic absorption spectroscopy confirmed that the Si upgrade ratio (Si leached in ligand solution compared to Si leached in water under same conditions) was enhanced in catechol and tiron solutions, compared to both the Si upgrade ratios for the other ligands and the analogous Mg upgrade ratios, particularly at pH 10 (Figure 6-16).
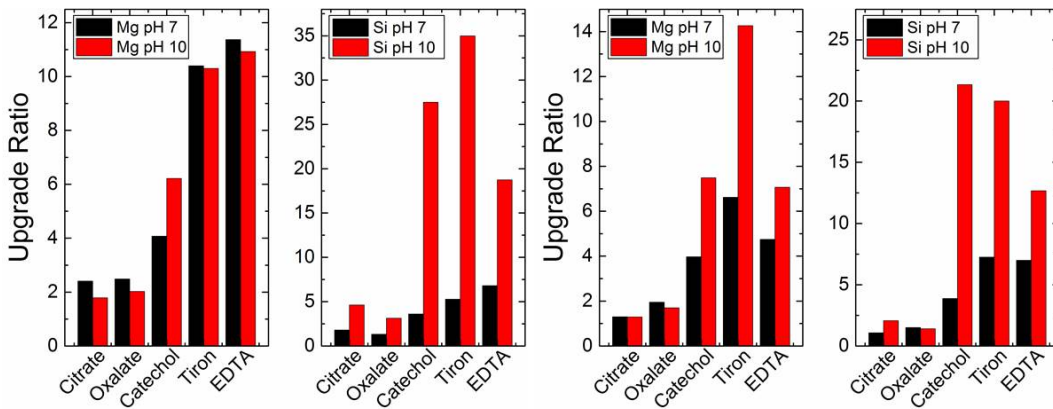
Figure 6-16: Upgrade ratios (ratio of Mg or Si leached at 25°C over 24 hours in ligand solution at pH 7 and 10 to that in water of the same pH) for Pipe (left) and OK (right) ores by 0.1 M ligand solutions.

6.3.2.2 Leaching Rates

The kinetics of leaching Mg at pH 7 and 10 from ultramafic nickel ores with ligands was studied at room temperature as a function of ligand concentration (0.01 M, 0.05 M and 0.1 M). In each case studied, the total concentration of Mg leached increased with leaching time as anticipated. For all scenarios studied, except Pipe ore in water, the release of Mg from the ores into solution initially followed a parabolic rate law (Equation 6-3), where C is the concentration of magnesium in solution (M), C_o is the y-intercept (M), k_{app} is the apparent rate constant (M.s$^{-1/2}$) and t is leaching time (s).

$$C = C_o + 2k_{app}t^{1/2} \qquad\qquad (6\text{-}3)$$

After 4-6 hours of leaching, the relationship between magnesium leached and leaching time became linear. For the Pipe ore in water, the relationship between magnesium leached and time was linear at all times. Although a number of researchers, including Krevor and Lackner (2011), Bonfils et al. (2012) and Hänchen et al. (2006), found that a shrinking particle model (as detailed in Teir et al. (2007) and Levenspiel (1999)) described the dissolution kinetics of serpentine and olivine in ligand solutions, these models did not fit the data collected in this study. In this study, the initial leaching rates were too fast to be characterized by the shrinking particle model. The parabolic-linear rate relationship that characterizes the data observed in this study, however, has been observed for the leaching of olivine and other ores by ligands (Grandstaff, 1986; Biver and Shotyk, 2012). The parabolic dissolution of silicates by ligands during the initial stages of experiments has been attributed to the preferential dissolution of fine particles and highly active sites (Holdren and Berner, 1979; Stumm and Wollast, 1990; Brantley and Olsen, 2014). Indeed, the particle size of the material used in this study was < 45 μm and was smaller and contained considerable fines (see Figure 6-3) compared to the feedstock material used in the studies which fit the shrinking particle model (74-125 μm in Krevor and Lackner (2011); < 100 μm in Bonfils et al. (2012); 90-180 μm in Hanchen et al. (2006)). An example leaching curve, showing magnesium extracted (as measured in solution) versus time for the Pipe ore leached by Tiron, is given in Figure 6-17. Leaching curves for the remaining scenarios studied can be found in Appendix D.
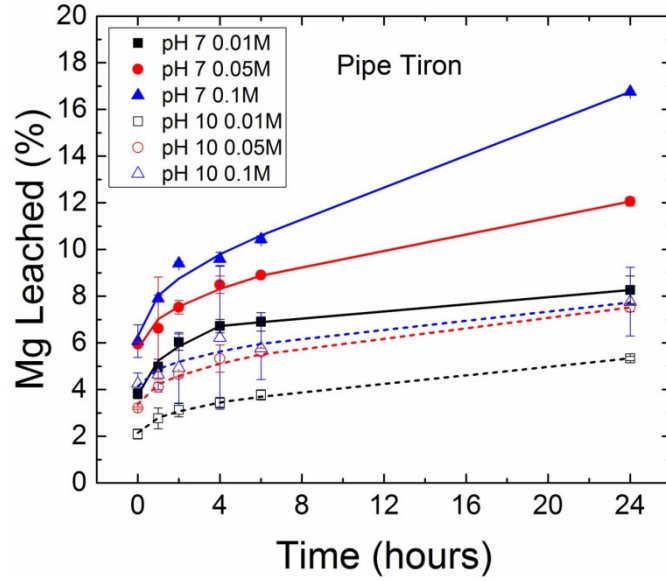
Figure 6-17: Total magnesium in solution versus time for Pipe ore leached with Tiron at concentrations of 0.01M, 0.05M and 0.1M at pH 7 and 10. Lines shown are fitted curves.

Leaching rate curves were obtained by differentiating and normalizing the leaching curves (by sample BET surface area, liquid volume and solid mass). As an example, leaching rate curves for Pipe ore in Tiron solutions are shown in Figure 6-18. The remaining leaching rate curves can be found in Appendix E.
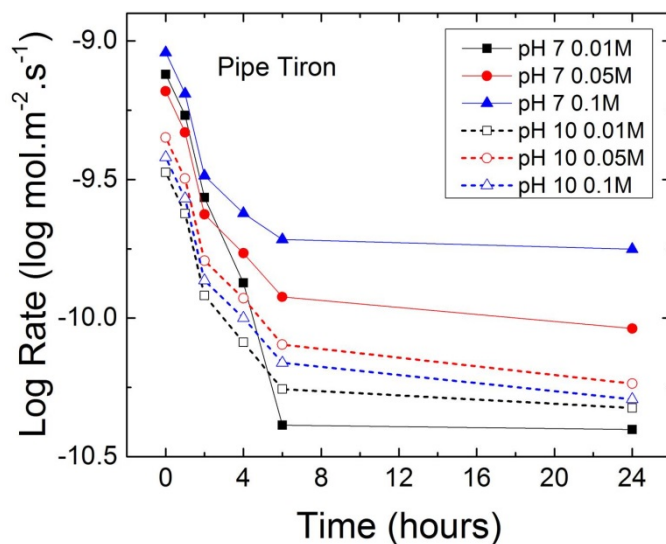
Figure 6-18: Leaching rate versus time for Pipe ore leached with Tiron at concentrations of 0.01 M, 0.05 M and 0.1 M, at pH 7 and 10.

The initial (R_i) and final (R_f) leaching rates, as well as the initial and final leaching rate upgrade ratios (ratios of initial and final leaching rates achieved by the ligand solutions ($R_{L,i}$ and $R_{L,f}$) to leaching rates achieved in water ($R_{W,i}$ and $R_{W,f}$)) for the Pipe and OK ores are given in Table 6-3. The initial leaching rates given were those calculated at 1 hour while the final leaching rates are those calculated at 24 hours. For the Pipe ore, each ligand solution increased the initial leaching rate at pH 7 and pH 10. The final leaching rates for the Pipe ore were also increased by the ligand solutions at the same pH values, except for the 0.01 M solutions of oxalate and EDTA at pH 10. For the OK ore, the initial leaching rates were improved in nearly every ligand solution (except 0.01 M and 0.05 M oxalate solutions at pH 10). The final leaching rates for the OK ore, however, were only increased in catechol and tiron solutions at all ligand concentrations at pH 7 and 10, and in some EDTA solutions. Oxalate and citrate generally did not improve the final leaching rates of the OK ore. While the leaching rates for the OK ore in ligand solutions were almost always higher than those for the Pipe ore, the OK ore upgrade ratios were usually not as high as those for the Pipe ore, indicating the ligands were more effective in improving the leaching rate of the Pipe ore compared to the OK ore.

164

More often than not, increasing the ligand concentration and reducing the pH increased leaching rates. For the Pipe ore, the initial and final leaching rate upgrade ratios tended to be higher at pH 7 than pH 10. This was generally true for the OK ore initial leaching rate upgrade ratio as well. However, the OK ore final leaching rate upgrade ratio was often higher at pH 10 than at pH 7, indicating the ligands were more effective at improving the leaching rate of the OK ore at alkaline pH than neutral pH.

The order of effectiveness of the ligands for improving the leaching rates of the Pipe and OK ores on the basis of the final leaching rate upgrade ratios ($R_{L,f}/R_{W,f}$) were the same as the orders of effectiveness of the ligands determined by the total Mg leached. On the basis of the initial leaching rate upgrade ratios ($R_{L,i}/R_{W,i}$), the order of effectiveness was nearly the same, except that citrate generally performed better than oxalate (in some cases much better). Since EDTA, tiron and catechol improved the total Mg leached, leaching rates and leaching rate upgrade ratios, these ligands appear to be the most promising for the enhancement of MCS using ultramafic nickel ores as feedstock.

6.3.2.3 Comparison of Experimental Results with Literature Values

The objective of this study was to determine if ligands can be used to improve the leaching of magnesium from serpentine in ultramafic ores at neutral to alkaline pH and room temperature, with the ultimate goal of developing an alternative MCS process. For such a process to be successful, a significant quantity of magnesium must be leached in an industrially-acceptable timeframe. Thus far it has been shown that the total Mg leached from ultramafic nickel ores, as well as the rate of leaching, is improved in ligand solutions compared to in water under the same conditions. To further evaluate the degree of success achieved, the results from this study were compared with those published in the literature. Since the examination of the ligand-promoted dissolution of serpentine in ultramafic nickel ores at neutral to alkaline pH is unique, few studies exist with which to directly compare this work. As a result, the total Mg leached and leaching rates determined in this study were compared with values determined for serpentine

and a similar mineral, olivine, at low pH, with and without ligands. Also, since steady-state leaching rates are most often given in published material, the final leaching rates (R_f) from this work were used for comparison.

Published values for total Mg leached and leaching rates are given in Table 6-4, while Figure 6-19 shows how the published values compare to the total Mg leached from ultramafic nickel ores in this study over 24 hours in tiron, EDTA and catechol solutions (data shown for ligand solutions at all three concentrations, 0.01 M, 0.05 M and 0.1 M) at 25°C. With regard to total Mg leached, most of the data published is for tests conducted at high temperature, many under a CO_2 atmosphere, and all at low pH. It can be seen in Figure 6-19 that the total Mg leached in this study was much lower (maximum 27% for OK ore in 0.1 M tiron solution at pH 7) than the total Mg leached from serpentine and olivine in strong ligand solutions at high temperature and acidic pH as reported in the literature (> 90% possible). However, the total Mg leached from the ores in a number of scenarios in this work exceeded the total Mg leached from serpentine under acidic conditions and at low temperature or in dilute ligand solutions or water. Specifically, the Mg leached from both the Pipe and OK ores at pH 7 in EDTA and tiron solutions, as well from the OK ore at pH 10 in catechol, EDTA and tiron solutions, exceeded the Mg leached from serpentine under acidic conditions as reported by Daval et al. (2013). Additionally, the total Mg leached from the Pipe ore by 0.1 M solutions of EDTA and tiron at pH 7, and from the OK ore by 0.1 M solutions of catechol and EDTA at pH 7 as well as almost all tiron solutions, exceeded the total Mg leached from olivine in dilute citrate solutions at high temperature and pH 3.5-4.5 as reported by Hänchen et al. (2006).
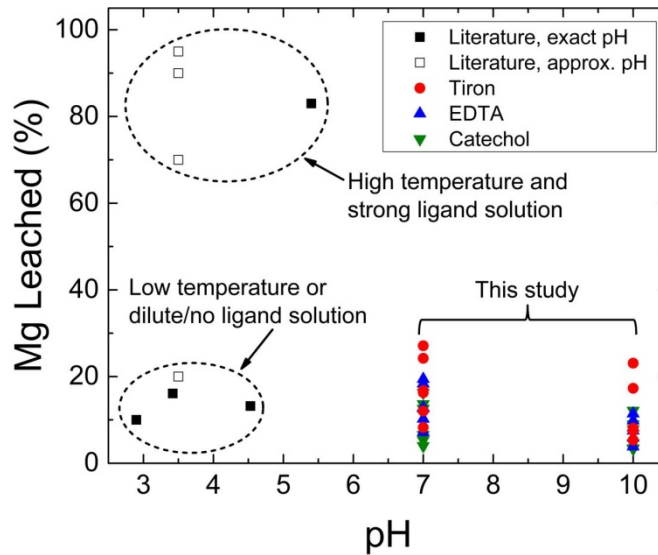
Figure 6-19: Total magnesium leached from serpentine or olivine in water or ligand solutions at various temperatures as reported in literature (detailed information given in Table 6-4) compared to that leached in this study from ultramafic nickel ores in ligand solutions (Tiron, EDTA and Catechol) at 25°C. Literature values from Bonfils et al. (2012), Daval et al. (2013), Hänchen et al. (2006), Krevor and Lackner (2011), and Park et al. (2003).

Published values for Mg leaching rates from serpentine and olivine are given in Table 6-5, while Figure 6-20 shows how the published values compare to the Mg leaching rates observed for ultramafic nickel ores in this study over 24 hours in tiron, EDTA and catechol solutions (data again shown for ligand solutions at all three concentrations, 0.01 M, 0.05 M and 0.1 M) at 25°C. Only one published data point for the leaching rate of serpentine in a ligand solution was found (Krevor and Lackner, 2011). The magnitude of the leaching rate observed by Krevor and Lackner (2011) for the leaching of serpentine in citrate solution greatly exceeds any observed value in this study, although it was collected under acidic and high temperature conditions. The final leaching rates observed in this study, however, including the leaching rates of the ores in water, exceed those reported for pure serpentine minerals at neutral to basic pH at room temperature. Since the Pipe ore contains olivine and the OK contains brucite, both having higher leaching rates than serpentine at pH 7 and 10 (see Table 6-5), this is not

167

unexpected. The final leaching rates observed in this work were also comparable to, with some exceeding, the leaching rates published for olivine at acidic to neutral pH in dilute ligand solutions or water. The leaching rates for Pipe ore in 0.1 M solutions EDTA and tiron at pH 7, and the leaching rates for the OK ore in all solutions of catechol and tiron, as well as the stronger EDTA solutions, exceeded the leaching rates for olivine in 10^{-4} M and 10^{-3} M solutions of citrate and oxalate at pH 3.5-4.5 reported by Grandstaff (1986) and Hänchen et al. (2006).
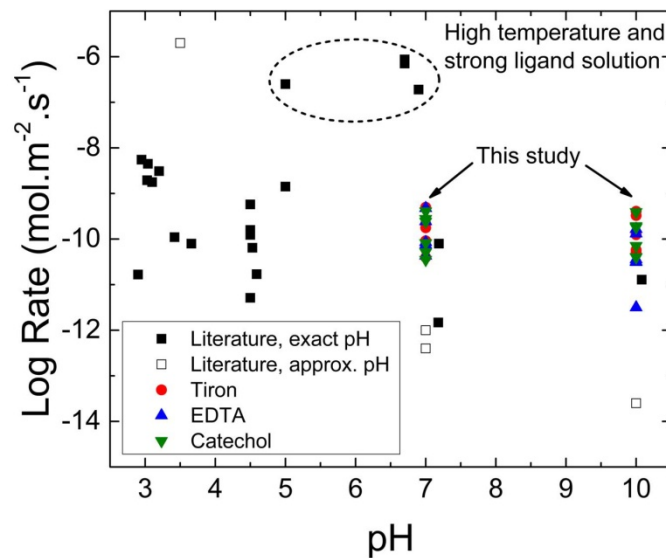
Figure 6-20: Leaching rates for serpentine or olivine in water or ligand solutions at various temperatures as reported in literature (detailed information given in Table 6-5) compared to final leaching rates observed in this study for ultramafic nickel ores in ligand solutions (Tiron, EDTA and Catechol) at 25°C. Literature values from Brantley and Olsen (2014), Daval et al. (2013), Declercq et al. (2013), Grandstaff (1986), Hänchen et al. (2006), Krevor and Lackner (2011), Pokrovsky and Schott (2000), Prigiobbe and Mazzotti (2011) and Thom et al. (2013).

The improvement in leaching rates and total Mg leached in catechol, EDTA and tiron solutions over that observed for the ores in water, as well as compared to that published for olivine in dilute ligand solutions at low pH, is promising.

While these values were lower than that achieved by others under acidic to neutral conditions at high temperature and in strong ligand solutions, the ability to enhance the rate limiting step of aqueous mineral carbonation at alkaline pH means that (1) no pH swing for carbonate precipitation is required after leaching and reagent requirements may be reduced, and (2) that the enhancement of Mg leaching and carbonate precipitation may be conducted in a single step. The total Mg leached, and Mg leaching rates, achieved in this study may be further improved by conducting leaching with strong ligand solutions (i.e. 0.1 M or higher) at high temperature under the same neutral to alkaline pH conditions.

Table 6-4: Data from literature for percent Mg extracted (I_{Mg}) from serpentine minerals (lizardite and antigorite) and olivine.

Mineral	Temperature (°C)	Time (hrs)	pH	Ligand Solution	Additional Parameters	I_{Mg} (%)	Reference
Lizardite	27	24	2.9	-	-	<10	Daval et al. (2013)[a]
Antigorite	90	15	Acid	0.1 M oxalate	20 bar CO_2	70	Krevor and Lackner (2011)[b]
Antigorite	90	24	Acid	0.1 M EDTA	20 bar CO_2	70	Krevor and Lackner (2011)[b]
Antigorite	90	24	Acid	0.1 M citrate	20 bar CO_2	70	Krevor and Lackner (2011)[b]
Antigorite	Ambient	2	Acid	1 vol.% orthophosphoric acid + 0.9 wt.% oxalic acid + 0.1 wt.% EDTA	-	20	Park et al. (2003)
Olivine	120	24	5-5.8	0.1 M oxalate	20 bar CO_2	83	Bonfils et al. (2012)
Olivine	120	24	Acid	0.1 M EDTA	20 bar CO_2	>95	Bonfils et al. (2012)[c]
Olivine	120	24	Acid	0.1 M citrate	20 bar CO_2	>90	Bonfils et al. (2012)[c]
Olivine	90	3.5	3.42	10^{-3} M citrate	-	16.1	Hanchen et al. (2006)
Olivine	90	5	4.53	10^{-4} M citrate	-	13.2	Hanchen et al. (2006)

[a] I_{Mg} extrapolated from Figure 3 in Daval et al. (2013).
[b] I_{Mg} extrapolated from Figure 11 in Bonfils et al. (2012).
[c] I_{Mg} extrapolated from Figure 4 in Krevor and Lackner (2011).

Table 6-5: Leaching rates for serpentine minerals (lizardite, antigorite and chrysotile), olivine and brucite from literature.

Mineral	Temperature (°C)	pH	Ligand	Log R	Reference
Antigorite	90	5	0.1 M citrate	-6.6	Krevor and Lackner (2011)[a]
Antigorite	90	5	-	-8.85	Krevor and Lackner (2011)[a]
Lizardite	27	2.9	-	-10.78	Daval et al. (2013)
Lizardite	25	Acid	-	-5.7	Brantley and Olsen (2014)[b]
Lizardite	25	Neutral	-	-12.4	Brantley and Olsen (2014)[b]
Chrysotile	25	Neutral	-	-12	Brantley and Olsen (2014)[b]
Chrysotile	25	Base	-	-13.6	Brantley and Olsen (2014)[b]
Chrysotile	20-22	7.18	-	-11.83	Thom et al. (2013)
Olivine	120	6.7	0.1 M oxalate	-6.06	Prigiobbe and Mazzotti (2011)
Olivine	120	6.7	0.1 M citrate	-6.15	Prigiobbe and Mazzotti (2011)
Olivine	90	6.9	0.1 M oxalate	-6.72	Prigiobbe and Mazzotti (2011)
Olivine	25	2.95	0.01 M oxalate	-8.26	Declercq et al. (2013)
Olivine	25	3.04	0.01 M citrate	-8.35	Declercq et al. (2013)
Olivine	25	3.2	0.01 M EDTA	-8.51	Declercq et al. (2013)
Olivine	25	3.03	0.1 M oxalate	-8.71	Declercq et al. (2013)
Olivine	26	3.1	-	-8.75	Declercq et al. (2013)[c]
Olivine	26	4.5	KCl + 10^{-2} M EDTA	-9.24	Grandstaff (1986)
Olivine	26	4.5	KCl + 10^{-3} M citrate	-9.8	Grandstaff (1986)
Olivine	26	4.5	KCl + 10^{-3} M oxalate	-9.91	Grandstaff (1986)
Olivine	26	4.5	KCl	-11.29	Grandstaff (1986)
Olivine	90	3.42	10^{-3} M citrate	-9.96	Hanchen et al. (2006)
Olivine	90	3.66	-	-10.10	Hanchen et al. (2006)
Olivine	90	4.53	10^{-4} M citrate	-10.19	Hanchen et al. (2006)
Olivine	90	4.59	-	-10.77	Hanchen et al. (2006)
Olivine	25	7.19	-	-10.10	Pokrovsky and Schott (2000)
Olivine	25	10.08	-	-10.89	Pokrovsky and Schott (2000)
Brucite	25	7.05	-	-7.83	Pokrovsky and Schott (2004)
Brucite	25	10.0	-	-8.53	Pokrovsky and Schott (2004)

[a] Rate values extrapolated from Figure 7 in Krevor and Lackner (2011).
[b] Rate calculated from rate constants from Table 7 in Brantley and Olsen (2014) assuming a temperature of 25°C .
[c] Average pH and rate values for experiments conducted without ligands.

6.4 Conclusions

The ligands catechol, citrate, EDTA, oxalate and tiron were investigated for their effectiveness in leaching magnesium from two ultramafic nickel ores at neutral to alkaline pH. The speciation of the ligand complexes was first modeled in a magnesium hydroxide-in-water system to determine if the ligands could increase the solubility of magnesium at the desired pH values. The modeling revealed that while magnesium is quite soluble at pH 7, the solubility decreases with increasing pH and only 25% of the magnesium present in the system is soluble under the modeled conditions at pH 10. The modeling suggested that the addition of ligands should increase magnesium solubility at pH 10 and the order of effectiveness of the ligands should be: EDTA > tiron > citrate > catechol > oxalate. The order of ligand effectiveness as determined by the modeling was mostly reflective of the relative magnitude of the stability constants, except that citrate, which had the lowest stability constant, was predicted to improve the solubility of magnesium to a greater degree than catechol or oxalate. The effect of ligand concentration on magnesium solubility was also modeled. It was determined that, in the modeled system, the ligands should have no effect on magnesium solubility at pH 7, but at pH 10, magnesium solubility should increase with increasing ligand concentration until a ligand to magnesium molar ratio of 1.0 is reached for citrate, tiron and EDTA, and until ligand to magnesium molar ratios of 1.5 and 2 are reached for catechol and oxalate, respectively.

Experimentally, it was shown that the addition of ligands to the ultramafic ore-in-water system generally improved the total solubility and leaching rates of magnesium from the ores. For both the Pipe and OK ores, the total magnesium leached was greater at pH 7 compared to pH 10 and increased with increasing ligand concentration, with the 0.1 M ligand solutions yielding the highest L_L/L_W values. In terms of leaching rates, for each scenario studied, the dissolution rates were initially parabolic and settled into a linear regime after 4-6 hours. The final leaching rates for the Pipe ore were increased in all ligand solutions tested with few exceptions. Final leaching rates for the OK ore increased only in solutions of

172

catechol and tiron, and in some EDTA solutions. Increasing ligand concentration generally resulted in higher leaching rates. While the total magnesium leached was greater for the OK ore, the L_L/L_W values were greater for the Pipe ore. Similarly, leaching rates for the OK ore were generally higher than those for the Pipe ore but the leaching upgrade ratios tended to be higher for the Pipe ore. This indicates the ligands were more effective in increasing the solubility and leaching rate of the Pipe ore compared to the OK ore. The order of ligand effectiveness based on the total magnesium leached and the final leaching rates for the Pipe ore was EDTA ≥ tiron > catechol > oxalate ≥ citrate, while the order for the OK ore was tiron > EDTA = catechol > oxalate > citrate. The order of ligand effectiveness determined experimentally for the Pipe ore was correlated with the relative strength of the stability complexes. The order of effectiveness for the OK ore was similar, except tiron and catechol proved to be more, or as, effective compared to EDTA. The enhanced performance of tiron and catechol for leaching Mg from the OK ore is believed to be due to their ability to bind with silicic acid at neutral to alkaline pH. Overall, the ligands studied in this work, particularly EDTA, tiron, and catechol, appear promising for enhancing the dissolution of serpentine in ultramafic nickel ores at neutral to alkaline pH for the purpose of mineral carbon sequestration.

6.5 References

Alexander, G., Maroto-Valer, M.M., Gafarova-Aksoy, P., 2007. Evaluation of reaction variables in the dissolution of serpentine for mineral carbonation. Fuel. 86, 273-281.

Bai, S., Okaue, Y., Yokoyama, T., 2009. Depolymerization of polysilicic acid by tiron. Polymer Degradation and Stability. 94, 1795-1799.

Bai, S., Tsuji, Y., Okaue, Y., Yokoyama, T., 2011. Complexation of silicic acid with tiron in aqueous solution under near natural condition. Journal of Solution Chemistry. 40, 348-356.

Baldyga, J., Henczka, M., Sokolnicka, K., 2010. Utilization of carbon dioxide by chemically accelerated mineral carbonation. Materials Letters. 64, 702-704.

Bales, R.C., Morgan, J.J., 1985. Dissolution kinetics of chrysotile at pH 7 to 10. Geochimica et Cosmochimica Acta. 49, 2281-2288.

Biver, M., Shotyk, W., 2012. Experimental study of the kinetics of ligand-promoted dissolution of stibnite (Sb_2S_3). Chemical Geology. 294-295, 165-172.

Bobicki, E.R., Liu, Q., Xu, Z., Zeng, H., 2012. Carbon capture and storage using alkaline industrial wastes. Progress in Energy and Combustion Science. 38, 302-320.

Bonfils, B., et al., 2012. Comprehensive analysis of direct aqueous mineral carbonation using dissolution enhancing organic additives. International Journal of Greenhouse Gas Control. 9, 334-346.

Brantley, S.L., Olsen, A.A., 2014. 7.3 − Reaction kinetics of primary rock-forming minerals under ambient conditions. Reference Module in Earth Systems and Environmental Sciences, from Treatise on Geochemistry (Second Edition), Eds: Heinrich Holland and Karl Turekian. 7, 69–113.

Daval, D., Hellmann, R., Martinez, I., Gangloff, S., Guyot, F., 2013. Lizardite serpentine dissolution kinetics as a function of pH and temperature, including effects of elevated pCO_2. Chemical Geology. 351, 245-256.

Declercq, J., Bosc, O., Oelkers, E.H., 2013. Do organic ligands affect forsterite dissolution rates? Applied Geochemistry. 39, 69-77.

Grandstaff, D.E., 1986. The dissolution rate of forsteritic olivine from Hawaiian beach sand. In: Colman SM, Dethier DP, editors. Rates of chemical weathering of rocks and minerals. Orlando: Academic Press Inc. p. 41-59.

Hänchen, M., Prigiobbe, V., Storti, G., Seward, T.M., Mazzotti, M., 2006. Dissolution kinetics of forsteritic olivine at 90-150ºC including effects of the presence of CO_2. Geochimica et Cosmochinica Acta. 70, 4403-4416.

Holdren, G.R., Berner, R.A., 1979. Mechanism of feldspar weathering – I. Experimental studies. Geochimica et Cosmochimica Acta. 43, 1161-1171.

Kakizawa, M., Yamasaki, A., Yanagisawa, Y., 2001. A new CO_2 disposal process via artifical weathering of calcium silicate accelerated by acetic acid. Energy. 26, 341-354.

Kodama, S., Nishimoto, T., Yamamoto, N., Yogo, K., Yamada, K., 2008. Development of a new pH-swing CO_2 mineralization process with a recyclable reaction solution. Energy. 33, 776-784.

Krevor, S.C.M., Lackner, K.S., 2011. Enhancing serpentine dissolution kinetics for mineral carbon dioxide sequestration. International Journal of Greenhouse Gas Control. 5, 1073-1080.

Levenspiel, O., 1999. Chapter 25: Fluid-Particle Reactions: Kinetics. In: Chemical Reaction Engineering, third ed., New York: John Wiley & Sons. p. 566-588.

Oelkers, E.H., 2001. General kinetic description of multioxide silicate mineral and glass dissolution. Geochimica et Cosmochimica Acta. 65(21), 3703-3719.

Öhman, L.-O., Nordin, A., Fattahpour, I., Sjöberg, S., 1991. Equilibrium and structural studies of silicon(IV) and aluminum(III) in aqueous solution. 28. Formation of soluble silicic acid-ligand complexes and studied by potentiometric and solubility measurements. Acta Chemica Scandinavica. 45, 335-341.

Olsen, A.A., Rimstidt, J.D., 2008. Oxalate-promoted forsterite dissolution at low pH. Gecochimica et Cosmochimica Acta. 72, 1758-1766.

Park, A.-H., Fan, L.-S., 2004. CO_2 mineral sequestration: physically activated dissolution of serpentine and pH swing process. Chemical Engineering Science. 59, 5241-5247.

Park, A.-H., Jadhav, R., Fan, L.-S., 2003. CO_2 mineral sequestration: chemically enhanced aqueous carbonation of serpentine. Canadian Journal of Chemical Engineering. 81, 885-890.

Pokrovsky, O.S., Schott, J., 2000. Kinetics and mechanism of forsterite dissolution at 25°C and pH from 1 to 12. Geochimica et Cosmochimica Acta. 64(19), 3313-3325.

Pokrovsky, O.S., Schott, J., 2004. Experimental study of brucite dissolution and precipitation in aqueous solutions: Surface speciation and chemical affinity control. Geochimica et Cosmochimica Acta. 68(1), 31-45.

Prédali, J.-J., Cases, J.-M., 1973. Zeta potential of magnesian carbonates in inorganic electrolytes. Journal of Colloid and Interface Science. 45(3), 449-458.

Prigiobbe, V., Mazzotti, M., 2011. Dissolution of olivine in the presence of oxalate, citrate, and CO_2 at 90°C and 120°C. Chemical Engineering Science. 66, 6544-6554.

Pundsack, F.L., 1967. Recovery of silica, iron oxide, and magnesium carboante from the treatment of serpentine with ammonium bisulphate. United States patent 3,338,667. 1967 Aug 29.

Smith, R.M., Martell, A.E., 1975. Critical stability constants: Volumes 1 and 3. Plenum Press, New York.

Stumm, W., 1992. Chemistry of the solid-water interface. New York: John Wiley and Sons Inc.

Stumm, W., Wollast, R., 1990. Coordination chemistry of weathering: Kinetics of the surface-controlled dissolution of oxide minerals. Reviews of Geophysics. 28(1), 53-69.

Teir, S., Revitzer, H., Eloneva, S., Fogelholm, C.-J., Zevenhoven, R., 2007. Dissolution of natural serpentine in mineral and organic acids. International Journal of Mineral Processing. 83, 36-46.

Teir, S., Eloneva, S., Fogelholm, C.-J., Zevenhoven, R., 2009. Fixation of carbon dioxide by producing hydromagnesite from serpentinite. Applied Energy. 86, 214-218.

Thom, J.G.M., Dipple, G.M., Power, I.M., Harrison, A.L., 2013. Chrysotile dissolution rates: Implications for carbon sequestration. Applied Geochemistry. 35, 244-254.

Wogelius, R.A., Walther, J.V., 1991. Olivine dissolution at 25°C: Effects of pH, CO_2 and organic acids. Geochimica et Cosmochimica Acta. 55, 943-954.

Chapter 7 Carbonation of Pre-treated Ultramafic Nickel Ores[6]

7.1 Introduction

Carbon capture and storage (CCS) is a strategy that has been identified to reduce carbon dioxide (CO_2) emissions and mitigate climate change. Mineral carbon sequestration (MCS) is the only known form of permanent CO_2 storage (Lackner et al., 1995). MCS also has the potential to capture and store CO_2 in a single step, can be used where geologic carbon storage is not feasible (Zevenhoven and Fagerlund, 2010), the products are environmentally benign, and valuable by-products, including magnesium carbonate and silica, can be produced during the process (Maroto-Valer et al., 2005). MCS is modeled on rock weathering processes where CO_2, dissolved in rain water, reacts with alkaline minerals to form solid carbonates. Although the reactions are thermodynamically favourable, in nature they occur over millennia (Huijgen and Comans, 2003). The challenge of MCS is to accelerate the carbonation of mineral feedstock with minimal energy and material losses.

MCS may be achieved by reacting alkaline minerals with CO_2 directly in either the gaseous or aqueous phase, or indirectly by first extracting Mg^{2+} (or Ca^{2+}) from minerals, separating the leached ions from the remaining solid phase, and then precipitating the ions as carbonates. Thus far, an economic MCS process has not been developed as all known MCS process schemes are energy intensive. Energy is used to prepare the feedstock, to drive carbonation at an acceptable rate, and to process the reaction products (Metz et al., 2005). In general, aqueous MCS schemes have been the most successful. The direct aqueous processes have involved fine grinding of the mineral feedstock and, in the case of serpentine, heat

---

treatment (for dehydroxylation) to render the mineral sufficiently reactive (Gerdemann et al., 2007; O'Connor et al., 2005). The combination of grinding and heat treatment by conventional means has resulted in MCS processes with net-positive CO_2 emissions (Gerdemann et al., 2007; Dlugogoreski and Balucan, 2014). Even after pre-treatment, the direct aqueous processes have required severe processing conditions to achieve high carbonate conversions (i.e. 15 MPa, 155-185°C) (Gerdemann et al., 2007; O'Connor et al., 2000). The indirect aqueous processes, while achieving high carbonate conversions under mild processing conditions even when using serpentine as feedstock, are associated with exorbitant chemical costs (Krevor and Lackner, 2011; Teir et al., 2009).

Ways to reduce the cost of MCS include identifying inexpensive and readily available mineral feedstocks, reducing the energy associated with grinding and activating mineral feedstocks, and reducing the chemical reagent requirements. The cost of MCS may be further offset by producing saleable carbonation by-products, such as precipitated magnesium carbonate and silica, and by storing CO_2 directly from flue gas streams, thereby skipping the capture step which has been estimated to cost between \$60 and \$100 per tonne of CO_2 avoided (Ho et al., 2011). The approach taken in this work to reduce the cost of MCS has been to select a waste product (serpentine waste from ultramafic nickel processing operations) as feedstock, and to use pre-treatments to increase the CO_2 reactivity of the waste material. Two different pre-treatments were investigated including microwave pre-treatment and leaching with ligands.

1.1 Microwave Pre-treatment

Microwave pre-treatment has been tested as a way to enhance both mineral processing and MCS operations. Microwave pre-treatment has been shown to successfully convert serpentine in the ores to olivine (Bobicki et al., 2014a), improve the grindability of some ores (Bobicki et al., 2013), and improve the rheology of ultramafic nickel ore slurries (Bobicki et al., 2014b). It is believed the combination of improved grindability and rheology should improve the

mineral processing of ultramafic ores. The effect of microwave pre-treatment on the carbonation of ultramafic nickel ores will be investigated in this work.

Microwave pre-treatment has been tested in a limited way by previous researchers for the enhancement of MCS. White et al. (2004) investigated the reactivity of CO_2 with serpentine at 1 bar and 375-650ºC in a gas-solid reaction in a microwave furnace, and the reaction of serpentine with bicarbonates in a microwave hydrothermal apparatus at 15 bar and 200ºC. Unfortunately, little reactivity was observed in these experiments. However, it is known both gas-solid and direct aqueous carbonation processes yield poor results at low pressures (Bobicki et al., 2012; Gerdemann et al., 2007). In this work, ultramafic nickel ores will be pre-treated with microwaves, followed by direct aqueous carbonation at pressure and temperature conditions reported to be optimal for the carbonation of conventionally heat-treated serpentine (O'Connor et al., 2005; Gerdemann et al., 2007).

1.2 Leaching with Ligands

The second pre-treatment, leaching with ligands, was tested as a way to promote the dissolution of serpentine in the ores/tailings for the enhancement of MCS without the need for a secondary pH adjustment. Five different ligands, including catechol, citrate, EDTA, oxalate and tiron, were tested for their capacity to improve the leaching of magnesium from serpentine in ultramafic nickel ores at neutral to alkaline pH. The ligands tested were all found to improve the leaching of ultramafic nickel ores in some capacity, with catechol, EDTA and tiron showing the most potential for enhancing MCS (Bobicki et al., 2014c).

While the dissolution of silicate minerals by ligands for the purpose of mineral carbon sequestration has been studied by a number of researchers (Krevor and Lackner, 2011; Bonfils et al., 2012; Hänchen et al., 2006; Park et al., 2003; Prigiobbe and Mazzotti, 2011; Declercq et al., 2013), few studies on the carbonation of ligand-leached minerals have been conducted, and none report the successful conversion of substantial Mg to carbonates. However, in studies where

the carbonation of the ligand-leached material has been attempted (Krevor and Lackner, 2011; Bonfils et al., 2012), carbonation has been conducted at relatively low temperature (90-120°C), low pH (acidic), and low CO_2 pressures (2 MPa). The approach in this work will be to carbonate ligand-leached slurries at temperature and pressure conditions reported to be optimal in direct aqueous processing schemes (O'Connor et al., 2005; Gerdemann et al., 2007), and at neutral to alkaline pH where the precipitation of $MgCO_3$ will be favored.

7.2 Materials and Methods

7.2.1 Mineral Feedstock

Two ultramafic nickel ores were used as feedstock in this study. The "OK ore" was sourced from the Okanogan nickel deposit in Washington State, USA. The "Pipe ore" was obtained from the Thompson Nickel Belt in Manitoba, Canada. The elemental composition of the ores is given in Table 3-1. The ores were crushed to < 2.5 mm using a jaw crusher (BB 200, Retsch, Burlington, ON, Canada) and milled to < 1.0 mm with a disc mill (DM 200, Retsch, Burlington, ON, Canada). The < 1.0 mm material was sieved using standard techniques to isolate the < 45 μm and 0.425-1 mm. The 0.425-1 mm size fractions of both the OK and Pipe ore were split into 100 g samples for microwave pre-treatment and grinding using a Jones riffle sample splitter. The < 45 μm material was split into 1 g samples using a spatula technique for the leaching test work.

7.2.2 Materials Characterization

X-ray fluorescence (XRF) spectroscopy (Orbis PC Micro-EDXRF Elemental Analyzer, EDAX, Mahwah, NJ, USA) and inductively coupled plasma mass spectrometry (ICP-MS) (Perkin Elmer Elan 6000, Waltham, Massachusetts, USA) were used to determine the elemental composition of the ores. ICP-MS was also used to determine the magnesium content of supernatant. Qualitative X-ray diffraction (XRD) (RU-200B Line Focus X-ray System, Rigaku Rotating Anode XRD System, Rigaku, ON, Canada) was performed to determine the mineral phases present in the ores before and after microwave pre-treatment, and before

181

and after leaching with ligands. Quantitative XRD analysis was also performed on some samples by PMET Inc. of New Brighton, PA using the Rietveld refinement technique. Total carbon for the microwave-related tests was measured using a coloumetric technique (UIC Coloumetrics Total Carbon Analyzer, Joliet, IL, USA). Total inorganic carbon for the leaching-related tests was determined by subtracting the total organic carbon (acidification technique used) from the total carbon. The carbon content of leaching-related samples was measured using a dry combustion technique (Costech Model EA 4010 Elemental Analyzer, Florence, Italy).

7.2.3 Carbonation of Microwave Pre-treated Ores

7.2.3.1 Microwave Heating

A Panasonic Flat and Wide (SF550), 1000 W, 2.45 GHz household microwave oven was used for microwave treatment of the ores. 100 g samples of 0.425-1 mm ore were placed in an insulated quartz reactor inside the microwave oven for treatment. The reactor was purged continuously with 1 L/min of nitrogen gas during treatment. The temperature achieved during treatment was ascertained by removing samples from the reactor immediately after treatment and inserting the tip of a Type K thermocouple into the centre of the sample. Samples used for temperature measurement were discarded. Samples microwave pre-treated for carbonation were allowed to cool for a minimum of two hours in the microwave reactor under a nitrogen atmosphere.

7.2.3.2 Grinding

100 g samples of 0.425-1 mm ore were ground aqueously with 250 mL distilled water in a stirred attrition mill (01-HD Laboratory Attritor with 1400 cc tank, Union Process, Akron, Ohio, USA). Grinding was conducted using 1300 g of 99.5% 3/16" alumina balls (Union Process, Akron, Ohio, USA) at 1000 rpm. Grinding times ranged from 15 to 60 minutes.

7.2.3.3 Carbonation

After microwave pre-treatment and grinding, slurry samples were diluted to 20 wt.% solids with distilled water. Some of the sample was centrifuged and filtered for pre-carbonation characterization. The filter cake was dried in the oven overnight, deagglomerated and then analyzed for total carbon content and by XRD for mineral phase identification. For carbonation, 150mL of diluted slurry was transferred to a 300 mL autoclave (4561 Mini Bench Top Reactor, Parr Instruments, Moline, IL, USA). Prior to carbonation, NaCl and $NaHCO_3$ were added to the slurries to achieve a supernatant containing 0.64 M $NaHCO_3$ and 1 M NaCl (background solution reported to achieve the highest mineral carbonate conversions (O'Connor et al., 2005)). The addition of $NaHCO_3$ to the carbonation supernatant significantly increases the concentration of carbonic ions in solution and helps drive the precipitation of $MgCO_3$ (Chen et al., 2006). The role of NaCl is not entirely agreed upon in the literature: while some claim that the Cl^- improves the solubility of magnesium silicate by forming a weak bond with MgO (Chen et al., 2006), others suggest it does not affect the carbon uptake of minerals (Gadikota et al., 2014). Initial carbonation tests were conducted with and without the $NaCl/NaHCO_3$ background for comparison. Since the tests conducted with the $NaCl/NaHCO_3$ background solution resulted in higher carbonate conversions than tests conducted with distilled water supernatant, the carbonation testwork was completed with supernatant containing 0.64 M $NaHCO_3$ and 1 M NaCl.

The slurry samples were carbonated at 155°C (optimal temperature for direct aqueous carbonation of serpentines reported by O'Connor et al. (2005)) and 12.4 MPa CO_2 (highest CO_2 pressure achievable with experimental set-up used) with a stirring speed of 1000 rpm over 1 hour. After carbonation, the slurry samples were cooled in the reactor, removed from the autoclave, and centrifuged. The centrifuge cake was dried in an oven overnight, after which it was deagglomerated for total carbon and XRD analysis. The total carbon results were used to calculate the net carbon uptake of the ore. The formula used to calculate the CO_2 uptake (C) in units of g CO_2/100 g ore is given below:

$$C = 100 \left[\frac{M_{CO_2}}{M_C} \frac{x_C}{100 - x_C} \right] \qquad (7.1)$$

where M_{CO2} is the molecular mass of CO_2, M_C is the molecular mass of carbon and x_C is the net carbon uptake of the ore measured as percent carbon. The carbonate conversion, or extent of carbonation (R_x, percent magnesium converted to magnesium carbonate), was calculated from the CO_2 uptake in the following manner:

$$R_x = 100 \left[\frac{CM_{MgO}}{x_{MgO} M_{CO_2}} \right] \qquad (7.2)$$

where M_{MgO} is the molecular mass of MgO and x_{MgO} is the percent MgO content of the ores as determined by XRF analysis.

7.2.4 Carbonation of Ligand Leached Ores

7.2.4.1 Modeling

The chemical speciation for magnesium and CO_2 in water, and magnesium, CO_2 and ligands in water was calculated iteratively across the pH range 0-14 in Microsoft Excel using the equilibrium constants tabulated in Appendix A. The ligands considered included catechol ($C_6H_4O_2^{2-}$), citrate ($C_6H_5O_7^{3-}$), EDTA (ethylenediaminetetraacetic acid, $C_{10}H_{12}O_8N_2^{4-}$), oxalate ($C_2O_4^{2-}$) and tiron ($C_6H_2O_8S_2^{4-}$). The species considered in the calculations included those found in the magnesium hydroxide-in-water system (Mg^{2+}. $MgOH^+$, $Mg(OH)_{2(aq)}$ and $Mg(OH)_{2(s)}$) and those found in the magnesite-in-water system (H_2CO_3, HCO_3^-, CO_3^{2-}, $MgHCO_3^-$, $MgCO_{3(aq)}$ and $MgCO_{3(s)}$), as well as the respective ligands, including the protonated and metal-complexed forms. The concentration of dissolved CO_2 in water at high pressure was taken from Appelo et al. (2014). A magnesium concentration of 0.1 M was selected as this is representative of the total Mg present in 1.5 g of the ores (either Pipe or OK) dissolved in 150 mL of solution (experimental conditions). All calculations were conducted at 25°C even

184

though experimental carbonation work was conducted at high temperature because the thermodynamic data required to calculate the high temperature stability constants was largely unavailable.

7.2.4.2 Leaching

1.5 g of < 45 μm OK and Pipe ore was combined with 150 mL of leaching solution and placed in a 250 mL Erlenmeyer flask. The leaching solutions consisted of distilled water and 0.1 M ligand solutions. The ligands tested were catechol (Acros Organics), citrate (trisodium citrate dehydrate, Alfa Aesar), EDTA (ethylenediaminetetraacetic acid, Alfa Aesar), oxalate (sodium oxalate, Alfa Aesar) and tiron (1,2-Dihydroxybenzene-3,5-disulfonic acid disodium salt monohydrate, Alfa Aesar). The suspensions were agitated in a shaker at room temperature and the pH was adjusted to 7 or 10 over 1 hour using 37 wt.% HCl (Acros Organics) or 50 wt.% NaOH (Fisher Chemical). The total volume of HCl or NaOH added was less than 0.5 mL. After pH adjustment, the samples continued to be agitated on the shaker at room temperature for 24 hours. Each test was completed in pairs: one sample for pre-carbonation characterization and one sample for carbonation. After 24 hours, the sample for pre-carbonation characterization was filtered and prepared for analysis.

7.2.4.3 Carbonation

The sample for carbonation was transferred to a 300 mL autoclave (4561 Mini Bench Top Reactor, Parr Instruments, Moline, IL, USA) at which point sufficient NaCl and $NaHCO_3$ was added to achieve concentrations of 1.0 M and 0.64 M, respectively (as in the microwave pre-treated carbonation tests). The leached samples were carbonated at 155°C and 12.4 MPa CO_2 with a stirring speed of 1000 rpm over 1 hour. Although the pH was controlled during pre-leaching, the pH could not be adjusted during carbonation. The final pH of every test after carbonation was approximately pH 7. After carbonation, the slurry samples were cooled in the reactor, removed from the autoclave, and filtered. The filter cake of both the uncarbonated and carbonated samples were dried in an oven overnight, after which they were deagglomerated for total inorganic carbon and XRD

185

analysis. The filtrate from both samples was submitted for elemental analysis by ICP. The total inorganic carbon results were used to calculate the net carbon uptake of the ores. The carbon uptake of the ores was calculated using Equation 7.1 while the extent of carbonation (carbonate conversion) was calculated using Equation 7.2.

7.3 Results and Discussion

7.3.1 Carbonation of Microwave Pre-treated Ore

7.3.1.1 Experimental Results

The net carbon uptake for untreated and microwave pre-treated Pipe and OK ores ground for 15 minutes is shown in Figure 7-1. The carbon uptake for both ores increased with microwave pre-treatment time after a threshold microwave heating time of 4 minutes was surpassed. Maximum net carbon uptakes (15.7 g CO_2/100 g ore for the Pipe ore and 18.3 g CO_2/100 g ore for the OK ore) were observed for ore having undergone maximum microwave pre-treatment (8 minutes for Pipe ore and 15 minutes for OK ore.). Maximum microwave pre-treatment was found to increase the carbon sequestration capacity of the Pipe and OK ores by factors of 5.2 and 3.7, respectively. The maximum carbon uptakes observed correspond to carbonate conversions (R_x, percent Mg converted to magnesium carbonate) of 36.4% for the Pipe ore and 36.6% for the OK ore. XRD analysis of the ores after carbonation showed that the carbon phase formed as a result of carbonation was magnesite ($MgCO_3$).
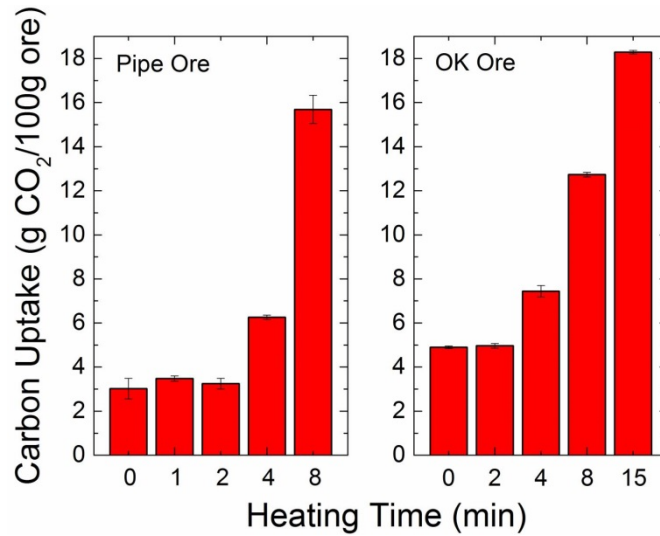
Figure 7-1: Net carbon uptake of Pipe and OK ores ground for 15 minutes versus microwave heating time.

The increased carbon sequestration capacity of the ores as a result of microwave pre-treatment could be due to several changes that occur simultaneously in the ores. The first is changes in ore mineralogy. As mentioned, the microwave pre-treatment of ultramafic nickel ores results in the conversion of the primary gangue mineral serpentine to olivine. It can be seen in Table 3-2 that 4 minutes of microwave pre-treatment resulted in a small increase in olivine content in both the OK and Pipe ores. That small increase in olivine content after 4 minutes microwave pre-treatment corresponds to the small increase in carbon uptake shown in Figure 7-1. Further microwave pre-treatment resulted in the increased conversion of serpentine to olivine, just as further microwave pre-treatment improved the carbon sequestration capacity of the ores. Figure 7-2 shows a plot of the net carbon uptake of the Pipe and OK ores versus the olivine content. It is evident from the graph that net carbon uptake increases with increasing olivine content. A linear regression of all the data (for both Pipe and OK ore) results in an R^2 value of 0.82, indicating there is a strong correlation between ore olivine content and net carbon uptake.

187
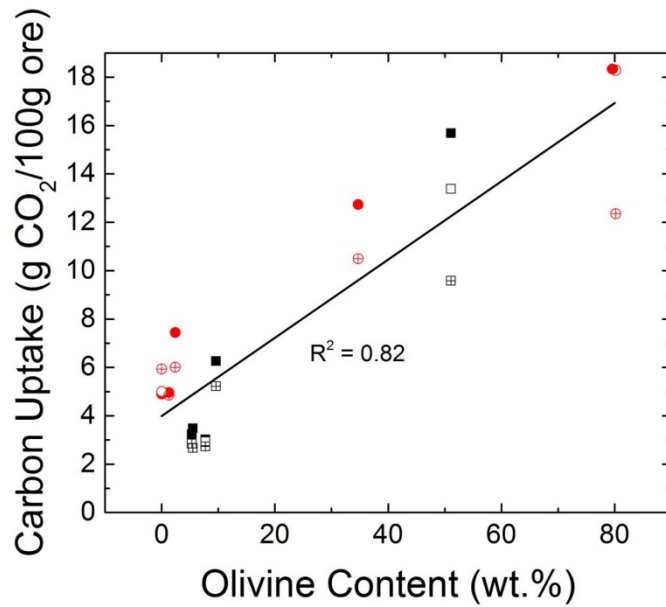
Figure 7-2: Net carbon uptake for Pipe and OK ores microwave pre-treated and ground for various lengths of time versus olivine content. Pipe ore is represented by black squares (■ = 15 min grind, □ = 30 min grind, and ⊞ = 60 min grind). OK ore is represented by red circles (● = 15 min grind, ○ = 30 min grind, and ⊕ = 60 min grind).

In addition to changes in mineralogy, the particle size distribution and specific surface area of the ores after grinding changes with different degrees of microwave pre-treatment (Bobicki et al., 2013). Decreasing particle size should theoretically improve the carbon sequestration capacity of the ores as decreased particle size generally leads to increased surface area, and increased surface area should render more Mg in the ores available for reaction with CO_2. However, since the carbon sequestration capacity of the Pipe ore improved despite increasing particle size with microwave pre-treatment (Bobicki et al., 2013), particle size is not believed to play a direct role in the carbon sequestration capacity of the ores. In this case, the specific surface area must be directly considered. As can be seen in Figure 4-9, the specific surface area of both the Pipe and OK ores increased after 8 minutes microwave pre-treatment time. To differentiate the effects of surface area and olivine content on carbon uptake, untreated and microwave pre-treated ores (8 and 15 minutes microwave pre-

treatment for Pipe and OK ores, respectively) were ground for different lengths of time and then carbonated. Figure 7-3 shows the net carbon uptake for untreated and microwave pre-treated Pipe and OK ores, ground for 15, 30 and 60 minutes. Since increased grinding time leads to increased surface area (Figure 7-4), it was hypothesized that increased grinding time for the same sample would improve the carbon sequestration capacity of the ore. However, it was found that carbon uptake decreased with increased grinding time, and that the effect was more pronounced for the microwave pre-treated ores.
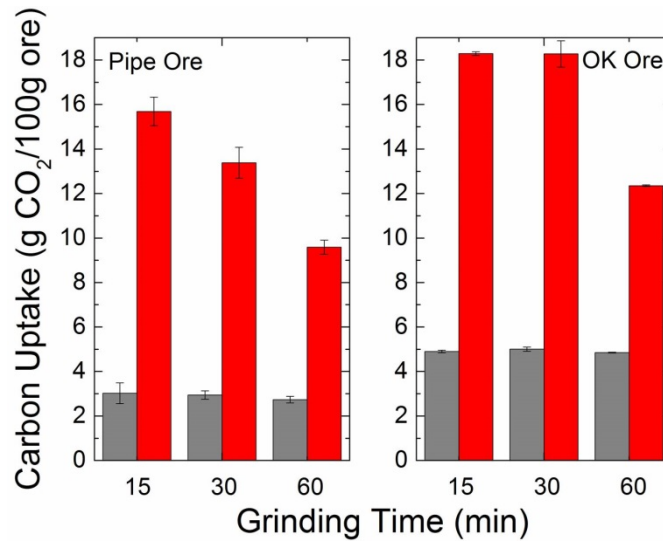
Figure 7-3: Net carbon uptake for untreated (grey) and microwave pre-treated (red) Pipe and OK ores versus grinding time. The pre-treated Pipe and OK ores were exposed to microwave radiation for 8 and 15 minutes, respectively.
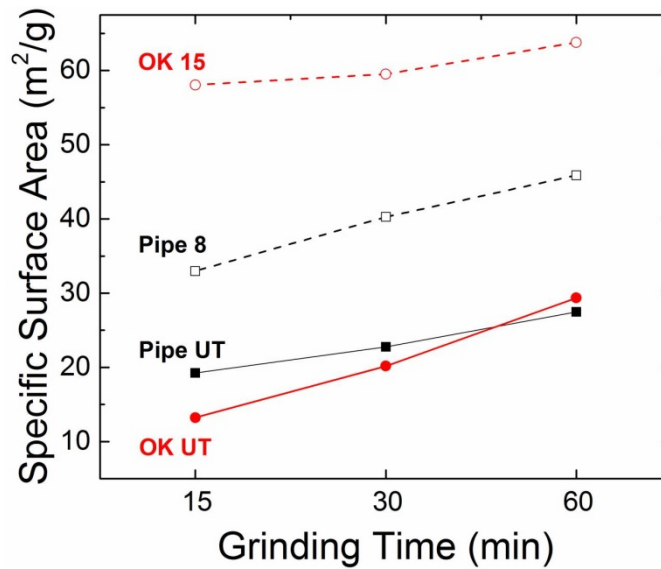
Figure 7-4: Specific surface area versus grinding time for untreated (Pipe UT and OK UT) and microwave pre-treated (OK 15 and Pipe 8) OK and Pipe ores.

To explain the reduction in carbon sequestration capacity with increased grinding time, microwave pre-treated and carbonated ores ground for different lengths of time were analyzed by XRD. The XRD patterns for Pipe ore microwave pre-treated for 8 minutes and (1) ground for 15 minutes (2) ground for 15 minutes and carbonated, and (3) ground for 60 minutes and carbonated are shown in Figure 7-5. Similar patterns were observed for the OK ore. The XRD analysis revealed that grinding the ores for longer periods of time resulted in the formation of oxidized iron products, including hematite (Fe_2O_3) and goethite (FeOOH), during carbonation. The analysis also revealed that while lizardite appeared to be the primary magnesium silicate phase in the carbonated ores, the lizardite peaks were more intense and more forsterite remained in carbonated ores ground for longer periods of time. The XRD analysis suggests that increased grinding times resulted in the leaching of iron that precipitated as iron oxide phases during carbonation. The increased leaching of iron during grinding with increased grinding time for microwave pre-treated ores was confirmed by ICP analysis (Figure 7-6). The ICP analysis also revealed that the iron concentration in the supernatant was reduced after carbonation, confirming that the leached iron

190

precipitated. The precipitated iron oxides appear to have formed a passivating layer on the ore particles that prevented the further leaching of Mg from the ores during carbonation, resulting in the hindered conversion of both lizardite and forsterite to magnesite ($MgCO_3$), and ultimately the decreased carbon uptake of samples ground for longer periods of time. The negative effects of iron passivating layers on the carbonation of magnesium silicate minerals have been acknowledged by others (Fauth et al., 2000; Alexander et al., 2007; Gadikota et al., 2014; Park et al., 2003). The effect was likely more pronounced for microwave pre-treated ores due to the increased surface area and higher exposure of iron-containing minerals to the solution.
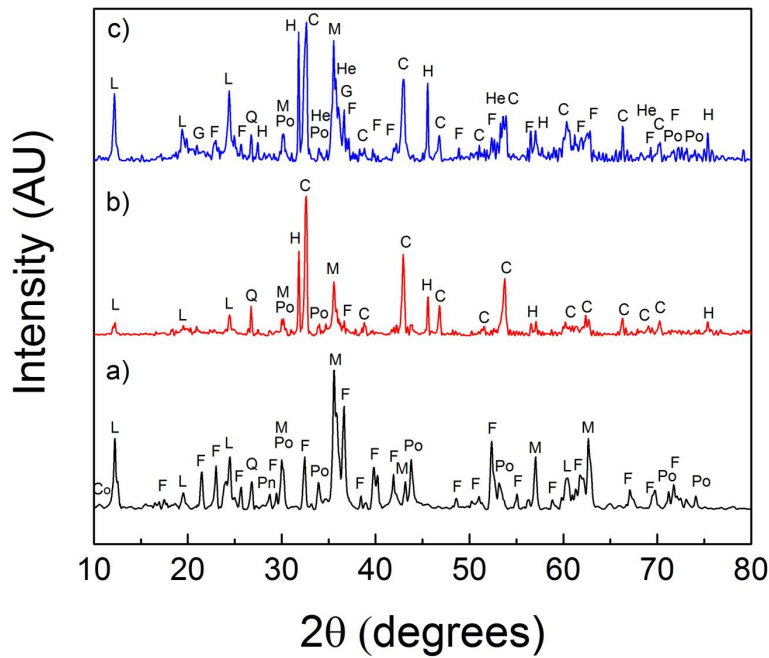
Figure 7-5: X-ray diffraction patterns for Pipe ore a) microwave pre-treated for 8 minutes and ground for 15 minutes, b) microwave pre-treated for 8 minutes, ground for 15 minutes, and carbonated, and c) microwave pre-treated for 8 minutes, ground for 60 minutes, and carbonated. Mineral phases identified include: cordierite (Co), forsterite (F), lizardite (L), goethite (G), halite (H), hematite (He), magnetite (M), magnesite (C), pentlandite (Pn), pyrrhotite (Po), and quartz (Q).
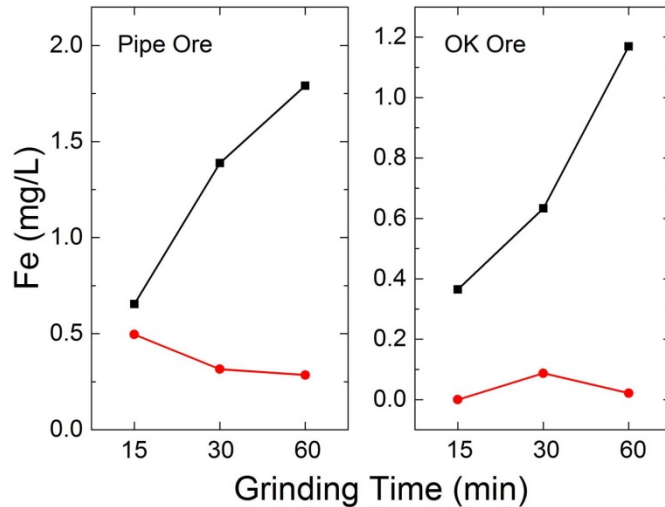
Figure 7-6: Iron concentration in slurry supernatant after grinding and before carbonation (■) and after carbonation (●) as a function of grinding time for Pipe and OK ores.

Although the increased grinding time led to reduced carbon uptake, a conclusion may still be drawn regarding the effect of surface area on the carbon sequestration capacity of ores. Figure 7-7 shows net carbon uptake for the Pipe and OK ores versus specific surface area. While the increased surface area created by longer grinding times reduced the carbon uptake, increased surface area in general was still correlated with increased carbon uptake. A linear regression of all the carbon uptake versus specific surface area data (for both Pipe and OK ores) results in an R^2 value of 0.51. Since the R^2 value for the linear regression of the carbon uptake versus olivine content is larger than the R^2 value for the linear regression of the carbon uptake versus specific surface area, the conversion of serpentine to olivine by microwave pre-treatment is believed to play a larger role in increasing the carbon sequestration capacity of ultramafic nickel ores than the increased surface area simultaneously caused by microwave pre-treatment. This conclusion is supported by the fact that the carbon sequestration capacity of the Pipe and OK ores was increased after 4 minutes microwave pre-treatment time, while the specific surface area of the ores did not increase until after 8 minutes microwave pre-treatment time.

192
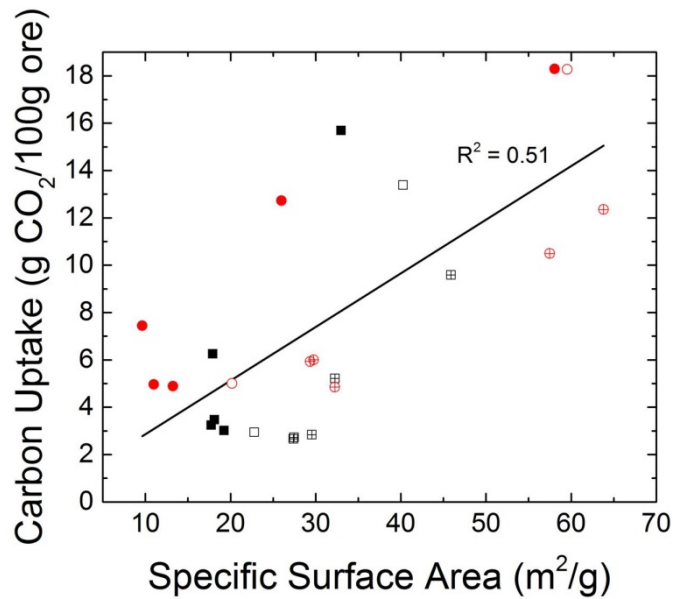
Figure 7-7: Carbon uptake versus specific surface area for Pipe and OK ores microwave pre-treated and ground for different lengths of time. Pipe ore is represented by black squares (■ = 15 min grind, □ = 30 min grind, and ⊞ =60 min grind). OK ore is represented by red circles (● = 15 min grind, ○ = 30 min grind, and ⊕ = 60 min grind).

7.3.1.2 Comparison of Results to Published Data

Values published for carbonation of serpentine containing ores by the direct aqueous process are given in Table 7-1. The extent of carbonation for untreated ores in this work (R_x = 6-7% for Pipe ore and R_x = 9-12% for OK ore depending on grinding time) was comparable to that published in the literature for untreated serpentine. The extent of carbonation for microwave pre-treated ores ground for 15 minutes after having undergone maximum pre-treatment (R_x = 36.4% for Pipe ore and R_x = 36.6% for OK ore) was comparable to that published in the literature for conventionally heat-treated lizardite carbonated under similar high temperature and pressure conditions, but lower than that published for antigorite and finely ground olivine. The fact the R_x values achieved by microwave pre-treatment are comparable to that achieved by conventional heat treatments in 1/16 to 1/8 of the time is very promising, especially considering the conversion of serpentine to olivine in the Pipe and OK ores by microwave pre-treatment was

incomplete. It is likely the reactivity of the ultramafic ores after microwave pre-treatment could be increased further by improving the design of the microwave reactor to achieve more even heating.

Table 7-1: Published results for the extent of carbonation (R_x) of serpentine and olivine minerals by direct aqueous processes.

Feedstock	Pre-treatment	Carbonation Conditions	R_x %	Reference
Antigorite	-	185°C, 11.7MPa, 6 hours, -37μm, in 1M NaCl and 0.5M NaHCO$_3$	12.1	O'Connor et al. (2005)
Lizardite	-	155°C, 15.2 MPa, 24 hours, -75μm, in 1M NaCl and 0.64M NaHCO$_3$	4.9	O'Connor et al. (2005)
Antigorite	-	185°C, 15.2 MPa, 12 hours, -75μm, in 1M NaCl and 0.64M NaHCO$_3$	12	Gerdemann et al. (2007)
Lizardite	-	185°C, 15.2 MPa, 12 hours, -75μm, in 1M NaCl and 0.64M NaHCO$_3$	9	Gerdemann et al. (2007)
Antigorite	700°C, 12 hours in air	185°C, 11.7MPa, 24 hours, -37μm, in distilled water	45.8	O'Connor et al. (2005)
Antigorite	630°C, 2 hours in CO$_2$	155°C, 15.2 MPa, 1 hour, -37μm, in 1M NaCl and 0.64M NaHCO$_3$	65.9	O'Connor et al. (2005)
Lizardite	630°C, 2 hours in air	155°C, 15.2 MPa, 1 hour, -75μm, in 1M NaCl and 0.64M NaHCO$_3$	37.8	O'Connor et al. (2005)
Antigorite	630°C, 2 hours in air	185°C, 15.2 MPa, 12 hours, -75μm, in 1M NaCl and 0.64M NaHCO$_3$	62	Gerdemann et al. (2007)
Antigorite	630°C, 2 hours in air	185°C, 15.2 MPa, 12 hours, -38μm, in 1M NaCl and 0.64M NaHCO$_3$	92	Gerdemann et al. (2007)
Lizardite	630°C, 2 hours in air	185°C, 15.2 MPa, 12 hours, -38μm, in 1M NaCl and 0.64M NaHCO$_3$	40	Gerdemann et al. (2007)
Serpentine	610°C	60°C, 0.1MPa, 5 hours, -125μm, in distilled water,	12.3	Werner et al. (2013)
Serpentine	610°C	60°C, 0.1MPa, 4 hours, , -125μm, in distilled water, with concurrent grinding	24.6	Werner et al. (2013)
Olivine	-	185°C, 15.2 MPa, 12 hours, -75μm, in 1M NaCl and 0.64M NaHCO$_3$	16	Gerdemann et al. (2007)
Olivine	-	185°C, 15.2 MPa, 12 hours, -38μm, in 1M NaCl and 0.64M NaHCO$_3$	61	Gerdemann et al. (2007)
Olivine	-	185°C, 11.7MPa, 6 hours, -37μm, in 1M NaCl and 0.5M NaHCO$_3$	72.9	O'Connor et al. (2005)

7.3.1.3 Comments on Energy Use

The energy required for the thermal dehydroxylation of lizarditic serpentine at 630°C has been calculated to be 326-359 kWh/t (Dlugogorski and Balucan, 2014; O'Connor et al., 2005). These values include the energy required to heat the mineral to 630°C as well as the energy required to drive off the hydroxyl groups. A number of researchers have recognized that, given this kind of energy input, no

mineral carbon sequestration scheme utilizing heat treated serpentine can be viable, unless combined with another process or fueled by a renewable or alternative power source (Gerdemann et al., 2007; O'Connor et al., 2005; Dlugogorski and Balucan, 2014). For example, assuming the generation of 1 kWh of electricity from a coal-fired power plant results in the production of 1kg of CO_2 (Koornneef et al., 2008), 0.33 to 0.36 tonnes of CO_2 would be produced through the generation of the power used to dehydroxylate 1 tonne of lizardite. Since the maximum carbon sequestration capacity of 1 tonne of lizardite is 0.48 tonne CO_2, 68-75% of the CO_2 that could potentially be sequestered by lizardite would be released generating the power required for heat treatment of the mineral. After grinding of the mineral feedstock and other process costs are considered, mineral carbonation schemes using conventionally heat treated serpentine result in negative CO_2 avoided, or more CO_2 generated by the process than sequestered.

In theory, the energy used in microwave pre-treatment to achieve serpentine dehydroxylation in ultramafic nickel ores should be less than that calculated for the dehydroxylation of lizardite by conventional means because (1) the ores are not entirely composed of serpentine (the entire mass does not need to be dehydroxylated and the energy required to heat the ore to the dehydroxylation temperature will be less since the heat capacity of serpentine is higher than the other minerals present in the ores (Figure 3-4)) and (2) the ores contain highly microwave responsive minerals which aid in the heating process. However, as stated in Chapter 4, the energy used in this work was exorbitant as the focus was on proof-of-concept rather than optimization. The energy used in this work by the 1 kW microwave oven for the treatment of 100 g of ore is equal to 167 kWh/t per minute of microwave pre-treatment. For the 15 and 8 minutes of microwave pre-treatment used for the OK and Pipe ores, respectively, the energy use equals 2500 kWh/t and 1333 kWh/t. These values are 4-8 times the energy calculated to be required for the thermal dehydroxylation of lizarditic serpentine at 630°C by conventional heating (Dlugogorski and Balucan, 2014; O'Connor et al., 2005) and would result in the release of 8-14 times more CO_2 (considering the assumptions

195

made above for a coal-fired power plant) than the maximum storage capacity achieved for these ores by microwave pre-treatment.

Obviously the thermal dehydroxylation of serpentine in ultramafic nickel ores by microwave pre-treatment is not viable at the lab scale. However, the energy used in microwave pre-treatment can likely be greatly reduced through scale-up, both by increasing the strength of the microwave field and increasing the sample size. As shown in equations 3.1 to 3.2, the heating rate of a dielectric material upon exposure to microwave radiation is related to the square of the electric field intensity. In a hypothetical situation where increasing the microwave power from 1 kW to 10 kW resulted in a congruent increase in electric field intensity, the heating rate would be increased by a factor of 100, thereby reducing the microwave pre-treatment time required. If the pre-treatment time required was reduced by the same factor, the energy required for pre-treatment of the OK and Pipe ores would be reduced to 250 kWh/t and 133 kWh/t respectively (assuming all other factors remained the same). If the sample size was also increased from 100 g to 1 kg, assuming the same heating rate could be maintained (which is possible since heat loss decreases as sample size increases due to the volumetric nature of microwave heating), the energy required would be reduced by yet another order of magnitude. While reducing the energy required for the microwave pre-treatment of ultramafic nickel ores by two orders of magnitude may seem extreme, great improvements in absorbed power and heating rates have been reported as a result of increasing microwave power and sample size (Pickles, 2009). If the energy required for microwave pre-treatment could be reduced to 25 kWh/t, the CO_2 released during the generation of the power used for microwave pre-treatment would represent about 15% of the total CO_2 that could be stored by the ores based on the carbon sequestration capacities achieved in this work, or about 85% CO_2 avoided.

Another way to reduce the energy intensity and CO_2 penalty of microwave pre-treatment is to use it to improve another process besides mineral carbon sequestration, such as the mineral processing of ultramafic ores (schematic of a

196

combined process is shown in Figure 7-8). As discussed in Chapters 4 and 5, microwave pre-treatment of ultramafic ores prior to grinding can improve the grindability (as observed for the OK ore) and rheology of ore slurries. If (1) a combination of microwave pre-treatment and grinding were to result in similar energy usage as grinding alone, as observed for the OK ore at a product size (P_{80}) of about 100 µm (Figure 4-12), (2) the size reduction was done for the purpose of nickel extraction, and (3) the flotation tailings were used for mineral carbon sequestration feedstock, then no extra energy would be expended for the enhanced carbon sequestration capacity of the ores. Additionally, if microwave pre-treatment reduced the viscosity of the ore slurries to a degree such that the flotation pulp density could be increased from 20 to 30 wt.% solids, the volume of the pulp could be reduced by 40 vol.%, resulting in savings in infrastructure and materials handling costs such as pumping, as well as in water usage and treatment. In a scenario where no additional energy was used in a microwave-assisted grinding circuit, where energy savings were incurred due to reductions in pulp viscosity, and the carbon sequestration capacity of the flotation tailings was increased by 4-5 times, microwave pre-treatment would likely be viable as a means to enhance both mineral processing and carbon sequestration processes.
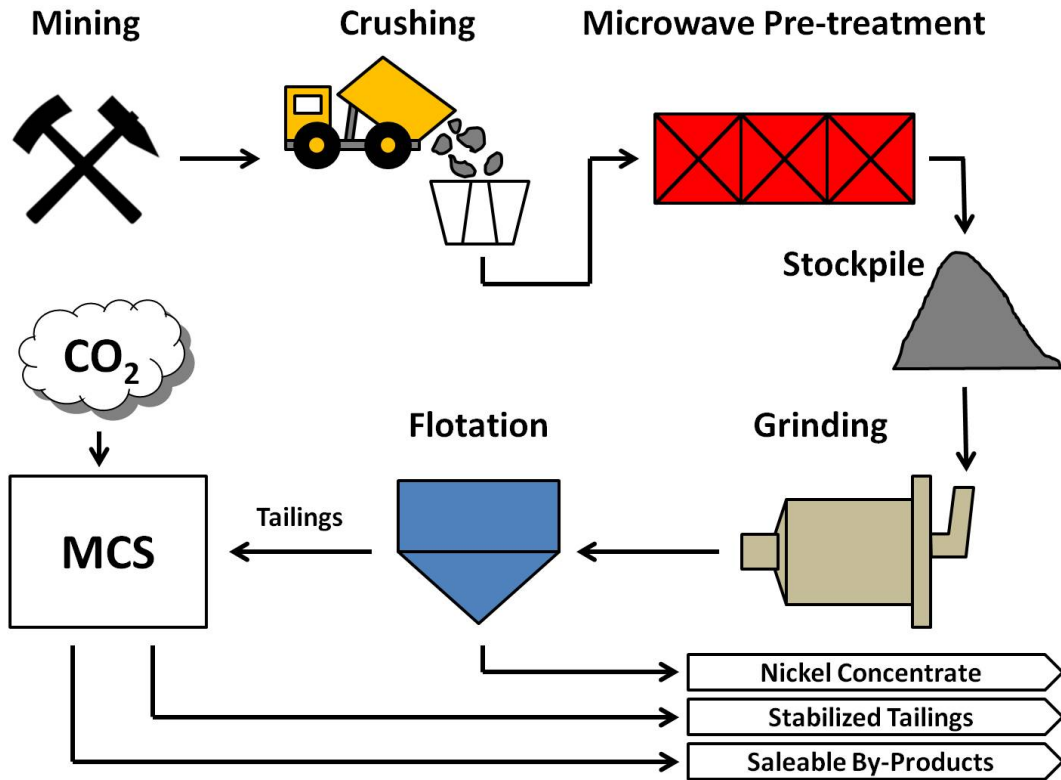
Figure 7-8: Schematic of a combined mineral processing and MCS process with microwave pre-treatment.

7.3.2 Carbonation of Ligand Leached Ore

7.3.2.1 Solution Modeling

Solution modeling was conducted to determine if $MgCO_3$ could be precipitated from Mg-ligand solutions at pH 7 and 10 under the CO_2 pressure used in experiments. The distribution of magnesium species in water upon the addition of 0.1 M magnesium at $25^{\circ}C$ under 12.4 MPa CO_2 is shown in Figure 7-9, while the distribution of magnesium species in water upon the addition of 0.1 M magnesium and 0.1 M ligand at $25^{\circ}C$ under 12.4 MPa CO_2 are shown in Figures 7-10 to 7-12. Species distributions are not shown for the Mg-Tiron-CO_2 and Mg-Catechol-CO_2 systems as these distributions are nearly identical to Figure 7-9. The total concentration of carbon species in solution at 12.4 MPa CO_2 pressure was considered to be 1.45 mol/L (Appelo et al., 2014). The solution modeling revealed that $MgCO_3$ can be precipitated from all ligand solutions considered under 12.4

198

MPa CO_2 pressure and that at pH 7 and 10 the primary species formed in each solution should be $MgCO_{3(s)}$. In each ligand solution, with the exception of EDTA, $MgCO_{3(s)}$ comprised > 99% of the magnesium species in the system at pH 7 and 10. For the EDTA system, $MgCO_{3(s)}$ comprised only 63% and 66% of the magnesium species at pH 7 and 10, respectively. The precipitation of $MgCO_3$ under the modeled conditions in the EDTA system was reduced due to the formation of substantial $MgEDTA^{2-}$ at pH 7 and 10. This result is due to the strength of the stability constant for $MgEDTA^{2-}$ (pK = -8.83) which is the strongest of all the Mg-ligand complexes studied in this work (Smith and Martell, 1975). Mg-ligand complexes were also observed to form in the citrate and oxalate systems under 12.4 MPa CO_2, but at lower pH values where the formation of $MgCO_3$ is less favoured. In the catechol and tiron systems, Mg-ligand complexes were not observed to form in any substantial quantity across the pH range under 12.4 MPa CO_2. In the presence of substantial dissolved CO_2, instead of binding with Mg ions, catechol and tiron ions bind preferentially with protons. For catechol and tiron, the stability constants of the protonated forms of the ligands are very high: in some cases the pK value of the protonated form of the ligand is double that of the Mg-ligand complex. The distribution of ligand species in water versus pH at 25°C under 12.5 MPa CO_2 with 0.1 M ligand and 0.1 M Mg can be found in Appendix F.
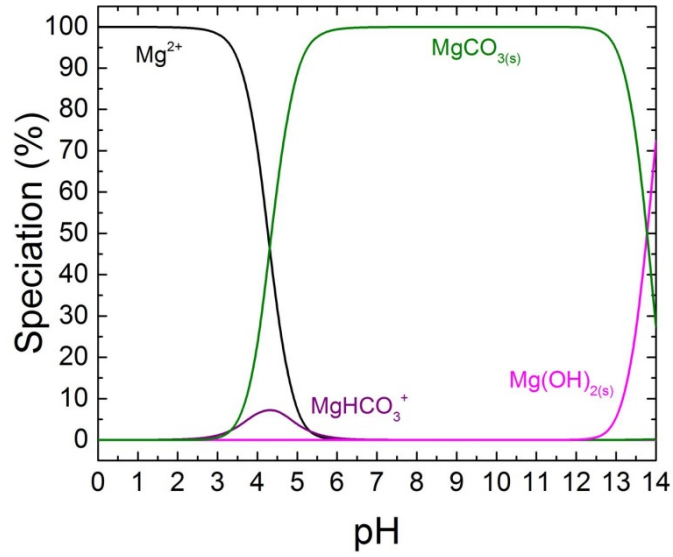
Figure 7-9: Distribution of magnesium species in water at 25ºC upon the addition of 0.1 M Mg under 12.4 MPa CO₂.
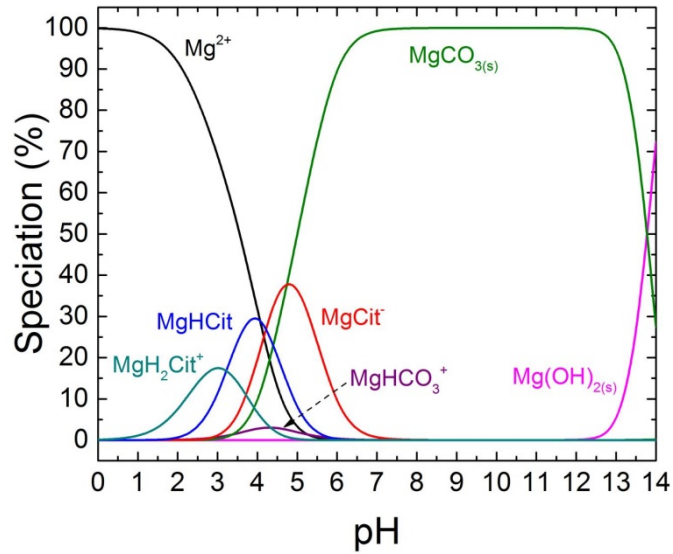
Figure 7-10: Distribution of magnesium species in water at 25ºC upon the addition of 0.1 M Mg and 0.1 M citrate under 12.4 MPa CO₂.
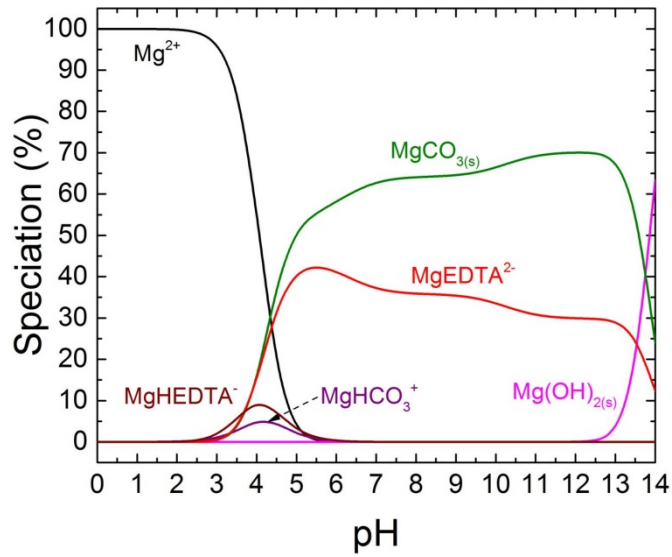
Figure 7-11: Distribution of magnesium species in water at 25ºC upon the addition of 0.1 M Mg and 0.1 M EDTA under 12.4 MPa CO₂.
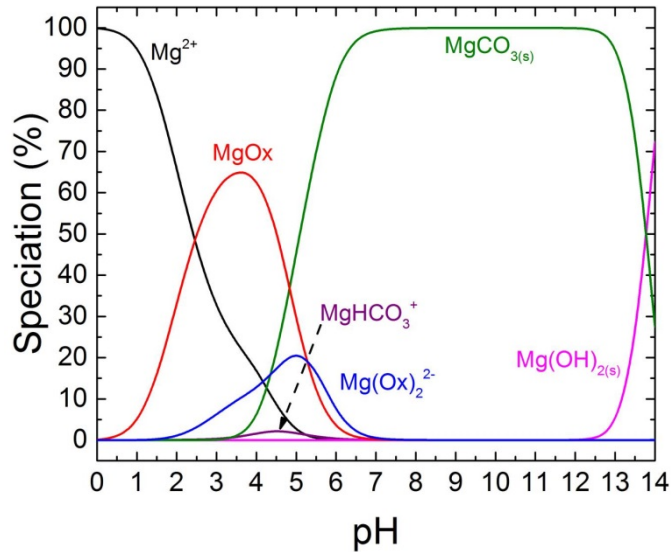
Figure 7-12: Distribution of magnesium species in water at 25ºC upon the addition of 0.1 M Mg and 0.1 M oxalate under 12.4 MPa CO₂.

The effect of CO_2 pressure on the precipitation of $MgCO_3$ in the presence of ligands at pH 7 and pH 10 was also modeled (Figures 7-13 and 7-14). At pH 7 and 10, greater than 99% of Mg can be precipitated as $MgCO_3$ at CO_2 pressures

greater than 0.4 MPa in water, as well as in catechol and tiron solutions. At this pressure, the total dissolved CO_2 in solution is equal to 0.13 M, a concentration just in excess of the modeled Mg and ligand concentrations. Because catechol and tiron readily form their respective protonated versions, a relatively small amount of dissolved CO_2 is required to precipitate nearly all Mg as $MgCO_3$. For citrate and oxalate solutions at pH 7, 99% of Mg is only precipitated after a CO_2 pressure of 4 MPa is exceeded. At 4 MPa, the total CO_2 dissolved in solution is equal to 1 M, a concentration 10 times that of the total magnesium and ligand concentration. A greater concentration of dissolved CO_2 is required to precipitate $MgCO_3$ at pH 7 in the presence of oxalate and citrate ions because $MgCit^-$, MgOx and $Mg(Ox)^{2-}$ complexes are also formed at pH 7. At pH 10, greater than 99% Mg is precipitated as $MgCO_3$ in citrate and oxalate solutions at CO_2 pressures greater than 0.4 MPa. $MgCO_3$ is precipitated more easily in citrate and oxalate solutions at pH 10 than at pH 7 because Mg does not form complexes with these ligands at pH 10. For EDTA solutions, at the highest CO_2 pressure modeled (56 MPa), only 67% and 70% of Mg can be precipitated as $MgCO_3$ at pH 7 and pH 10, respectively.
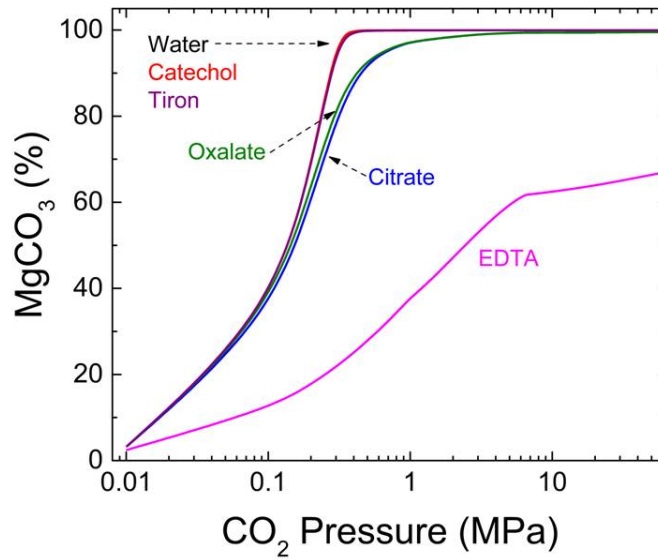
Figure 7-13: Percent of magnesium species precipitated as MgCO₃ as a function of CO₂ pressure with 0.1 M Mg and 0.1 M ligand at pH 7. Water, catechol and tiron curves are nearly indistinguishable.
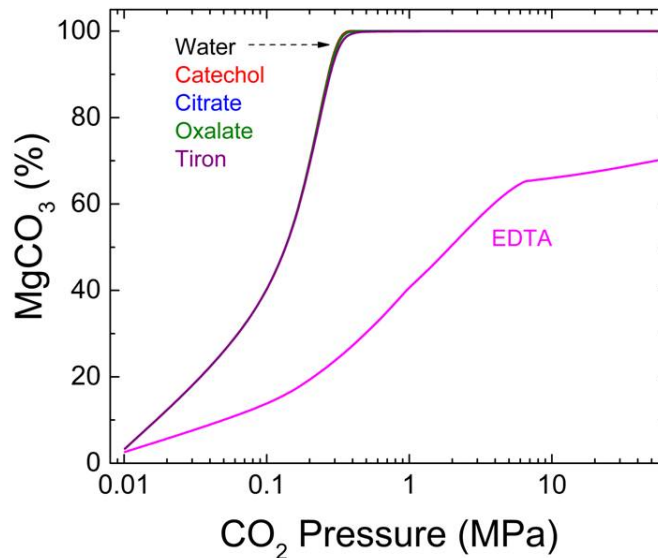
Figure 7-14: Percent of magnesium species precipitated as MgCO₃ as a function of CO₂ pressure with 0.1 M Mg and 0.1 M ligand at pH 10. Water, catechol, citrate, oxalate and tiron curves are nearly indistinguishable.

While the solution modeling until this point was completed using a magnesium concentration of 0.1 M, this value assumes that all Mg in the system is available

for reaction. ICP analysis of supernatant from samples leached for 24 hours in water and ligand solutions, however, indicated that the magnesium concentration in solution was only 10^{-4} to 10^{-2} M prior to carbonation. Thus, the effect of magnesium concentration in solution on $MgCO_3$ precipitation in the presence and absence of ligands (0.1 M solution) was modeled over the range of 0.0001 to 0.1 M under 12.4 MPa CO_2 pressure at 25°C. Across the magnesium concentration range studied, greater than 99% of the magnesium present was modeled to precipitate as $MgCO_3$ in the water, catechol, citrate, oxalate and tiron systems at both pH 7 and 10 regardless of magnesium concentration. For the EDTA system, however, the percent magnesium modeled to precipitate as $MgCO_3$ ranged from 53% to 63% at pH 7 and 58% to 66% at pH 10 across the range of magnesium concentrations studied (0.0001 to 0.1 M). Again, the reduced precipitation of $MgCO_3$ in the EDTA system was due to the formation of substantial $MgEDTA^{2-}$ in the modeled system.

While the percentage of magnesium species precipitated as $MgCO_3$ is representative of the likelihood that carbonates will form in a given system, it is not indicative of the quantity of precipitated carbonate. If only a small amount of magnesium is leached from the mineral, even if it is all precipitated as $MgCO_3$, only a small mass of CO_2 can be precipitated as $MgCO_3$ and the carbon uptake of the ores will be low. Therefore, the effect of magnesium concentration on the potential carbon uptake of ore was calculated based on the modeling results. Equation 7.3 was used to convert the modeled concentration of $MgCO_{3(s)}$ to net carbon uptake (x_c) as a percentage of ore solids, where V is the liquid volume (150 mL assumed as in experimental tests), M_c is the molecular mass of carbon, m_s is the mass of the ore sample (1.5 g assumed as in experimental tests) and $[MgCO_{3(s)}]$ is the concentration of $MgCO_{3(s)}$ calculated in molarity.

$$x_c = \frac{\left([MgCO_{3(s)}]VM_c\right)}{\left([MgCO_{3(s)}]VM_c + m_s\right)} \times 100 \tag{7.3}$$

The calculated net carbon uptake was converted to CO_2 uptake in units of g CO_2/100 g ore using Equation 7.1. Figure 7-15 shows calculated CO_2 uptake at

204

pH 10 versus magnesium concentration in 0.1 M ligand solutions and water at 25°C under 12.4 MPa of CO_2. The modeled results for the same system at pH 7 were very similar. The modeling indicated that no substantive carbon will be precipitated until a magnesium concentration of 10^{-3} M is surpassed. It also showed that carbon precipitation increases only marginally with increasing magnesium concentration between 10^{-3} M and 0.01 M, and that the carbon uptake only really becomes significant after a magnesium concentration of 0.01 M is exceeded. In addition, the results show that there is almost no difference in the dependence of carbon uptake on magnesium concentration for the water, catechol, citrate, oxalate and tiron systems. The carbon uptake for EDTA, however, increases to a lesser degree with increasing magnesium concentration compared to the other systems for the reasons discussed previously.
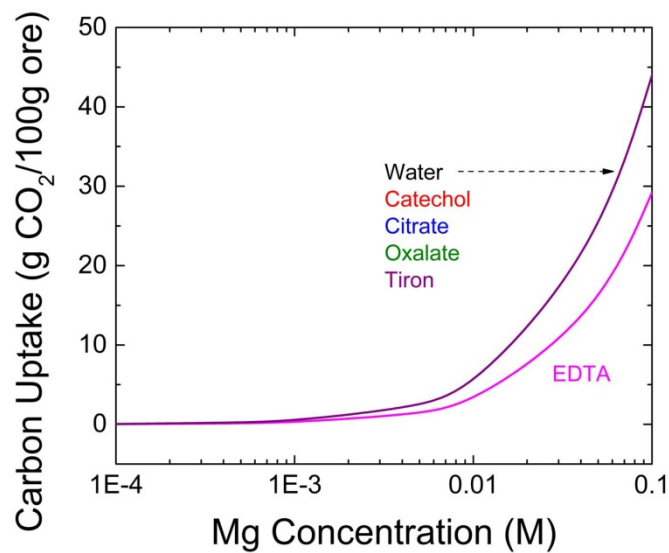
Figure 7-15: Calculated CO_2 uptake at pH 10 in water and 0.1 M catechol, citrate, EDTA, oxalate and tiron solutions at 25°C under 12.4 MPa CO_2 pressure as a function of total magnesium concentration. Lines for water, catechol, citrate, oxalate and tiron are on top of one another.

Overall, the modeled result that $MgCO_3$ can be precipitated from ligand solutions at elevated CO_2 pressure is positive since it means that $MgCO_3$ can likely be precipitated from ultramafic ore slurries that have been pre-leached with ligands.

The result that $MgCO_{3(s)}$ formation is reduced in EDTA solutions even at high CO_2 pressure suggests that EDTA may be too strong a leaching agent to substantially increase the carbon sequestration capacity of ultramafic nickel ores. Also, since a concentration close to 0.01 M magnesium was achieved after leaching (before carbonation) primarily in the catechol, EDTA and tiron systems (Figure 7-16), and since it seems EDTA may be too strong of a ligand to promote carbonation, it appears catechol and tiron may have the greatest potential to improve the carbon uptake of the ores.
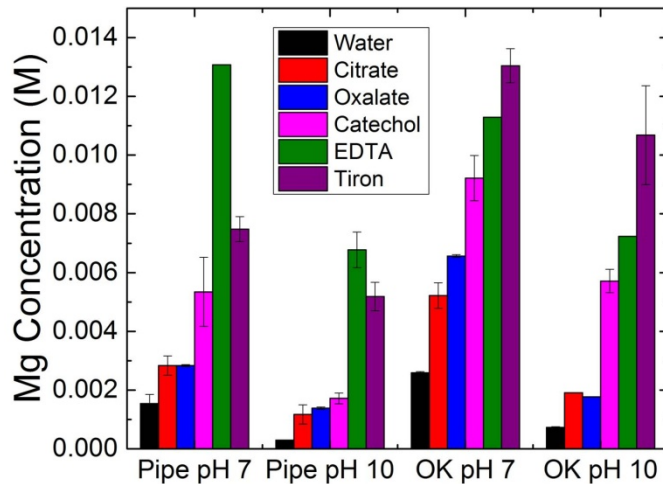
Figure 7-16: Magnesium concentration in leachate from OK and Pipe ore slurries after 24 hours. Leaching conducted in water and 0.1 M ligand solutions at 25°C, and at pH 7 and 10.

7.3.2.2 Experimental Work

XRD analysis of carbonated, ligand leached ores revealed that magnesite ($MgCO_3$) formed in ores pre-leached and carbonated in water as well as in citrate, catechol, oxalate and tiron solutions. Magnesite was not observed to form in ores pre-leached and carbonated in EDTA solutions. Just as in the microwave pre-treated and carbonated ores, magnesite was the only carbon mineral observed to form after carbonation. Figures 7-17 and 7-18 show example XRD patterns for untreated OK ore, OK ore leached in tiron and EDTA solutions, and OK ore leached in tiron and EDTA solutions and carbonated. The fact that magnesite was

not observed to form in Pipe and OK ore slurries leached and carbonated in EDTA is not surprising, given that the modeling work suggested EDTA may be too strong of a ligand to allow the successful precipitation of $MgCO_3$. Others trying to precipitate $MgCO_3$ in the presence of EDTA, albeit at lower temperatures and pressures, have met with similar failure, commenting that EDTA is too strong of ligand to promote MCS (Bonfils et al., 2012; Krevor and Lackner, 2011).
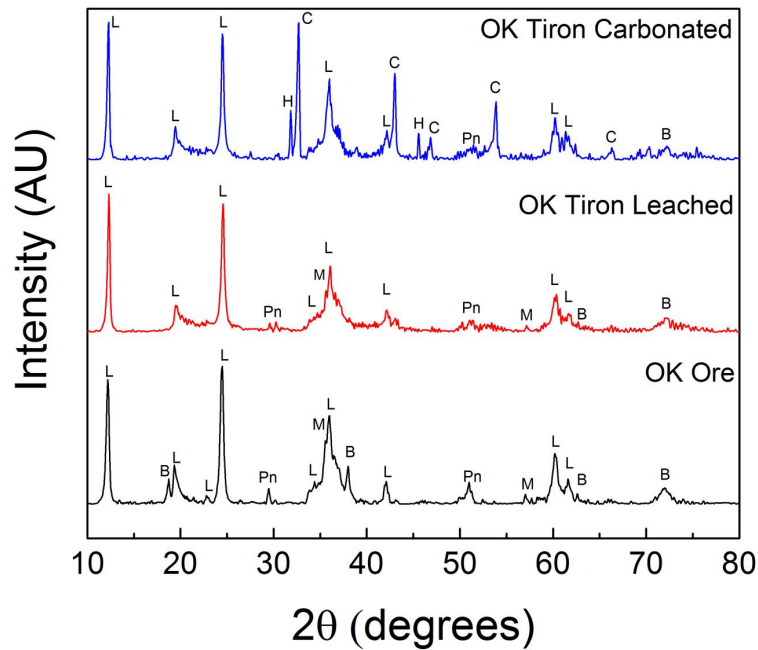
Figure 7-17: XRD patterns for OK ore, OK ore leached with 0.1 M tiron solution for 24 hours at pH 10 and 25°C, and OK ore leached with 0.1 M tiron solution for 24 hours at pH 10 and 25°C and carbonated. Mineral phases identified include brucite (B), magnesite (C), halite (H), lizardite serpentine (L), magnetite (M) and pentlandite (Pn).
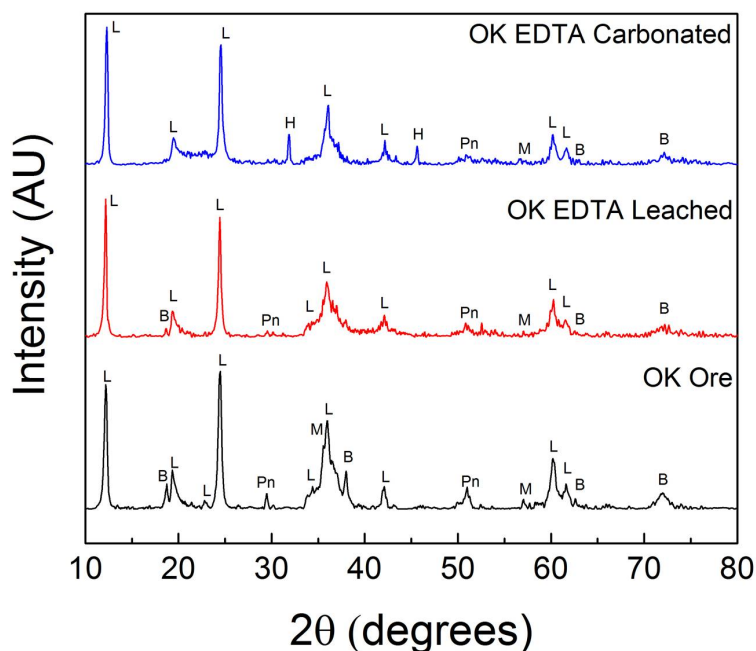
Figure 7-18: XRD patterns for OK ore, OK ore leached with 0.1 M EDTA solution for 24 hours at pH 10 and 25ºC, and OK ore leached with 0.1M EDTA solution for 24 hours at pH 10 and 25ºC and carbonated. Mineral phases identified include brucite (B), halite (H), lizardite serpentine (L), magnetite (M) and pentlandite (Pn).

The net carbon uptake for the OK and Pipe ores in water and 0.1 M catechol, citrate, oxalate and tiron solutions are shown in Figures 7-19 and 7-20. Just as for the microwave pre-treated ore, carbon uptake was higher in each case for the OK ore compared to the Pipe ore. As predicted by the solution modeling, carbon uptake was increased for Pipe and OK ores pre-leached and carbonated in catechol and tiron solutions, although carbon uptake improvements in catechol solutions for the Pipe ore were modest. The greater carbon uptake observed for the Pipe and OK ores leached and carbonated in catechol and tiron solutions is correlated with the result observed in Bobicki et al. (2014c) that both the leaching rates and total magnesium leached from the ores were higher in catechol and tiron solutions compared to oxalate and citrate solutions. Higher carbon uptakes were observed for ores leached and carbonated in catechol and tiron solutions at pH 10 compared to ores leached and carbonated in catechol and tiron solutions at pH 7.

The highest carbon uptakes (3.6 g CO_2/100 g ore for Pipe ore and 9.7 g/100 g ore for OK ore) were reported for ores pre-leached and carbonated in tiron solutions at pH 10. The carbon uptakes achieved in tiron solutions translate to carbonate conversions of 8.3% and 19.3% for the Pipe and OK ores, respectively (factored improvements of 1.7 for the Pipe ore and 2.8 for the OK ore compared to ores leached and carbonated at pH 10 in water). This is the first time that significant magnesite formation and an improvement in carbon uptake have been reported for ores leached and carbonated in the presence of ligands. In fact, in a recent paper, Bodénan et al. (2014) stated that the use of ligands for enhancing MCS was a "dead-end option which could not lead to the formation of carbonates". While the increase in carbon uptake achieved in catechol and tiron solutions was not as high as that achieved for microwave pre-treated ore, the positive results reported in this work indicate that MCS can be enhanced using ligands, and that the enhancement depends on the selection of the correct ligands. The ligands selected must be able to bind strongly with magnesium at the desired pH, but not form a complex too strong to allow the precipitation of the bound magnesium. Even more important than the finding that ligands can be used to enhance MCS is that leaching and carbonation can both be conducted at alkaline pH (highest carbon uptakes observed for solutions leached at pH 10). Thus, an aqueous MCS process where leaching and carbonation of mineral feedstock are conducted at the same pH is possible, likely resulting in reduced reagent requirements. It is probable that even greater carbon uptakes can be achieved through optimization, in terms of temperature, liquid-to-solid ratio and ligand concentration.
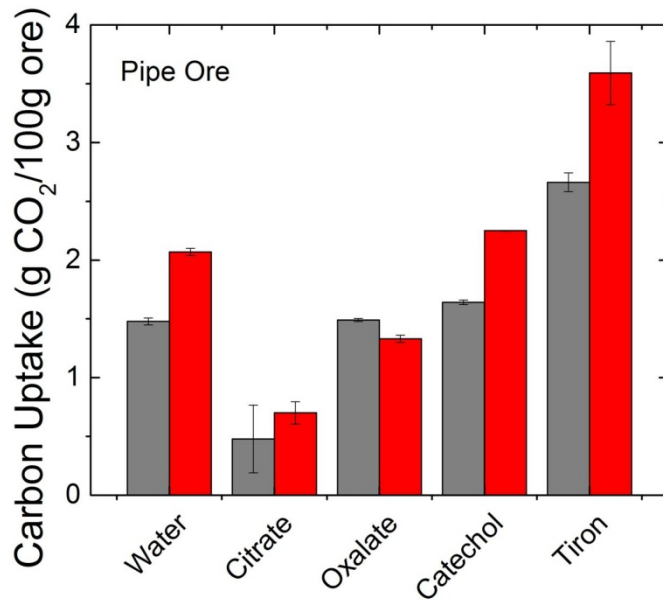
Figure 7-19: Carbon uptake for Pipe ore leached and carbonated in water and ligand solutions at pH 7 (grey) and pH 10 (red).
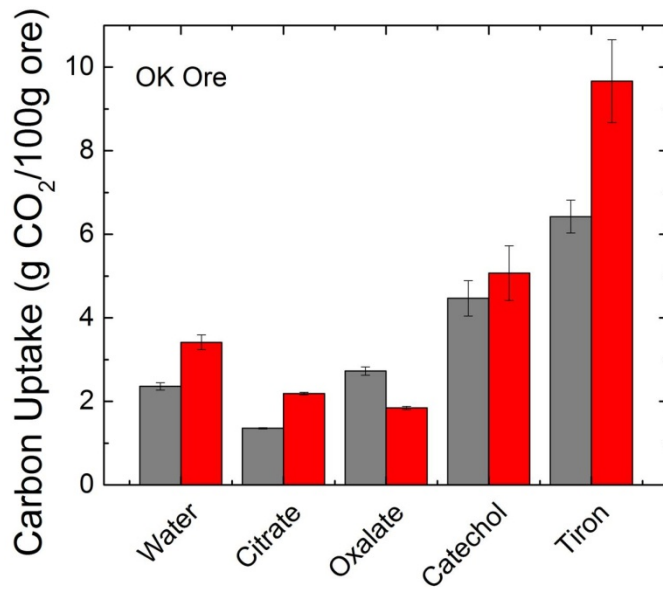
Figure 7-20: Carbon uptake for OK ore leached and carbonated in water and ligand solutions at pH 7 (grey) and pH 10 (red).

In contrast to the results achieved in catechol and tiron solutions, carbon uptake was not affected much by leaching in oxalate solutions at pH 7, and was reduced in oxalate solutions at pH 10 as well as in citrate solutions at both pH 7 and 10. It is not surprising that citrate and oxalate did not improve the carbon uptake of the OK and Pipe ores, as these ligands were not shown to markedly improve the leaching rate or total magnesium leached from the ores (Bobicki et al., 2014c). In addition, the solution modeling work presented in this study suggested that these ligands did not improve the leaching of magnesium from the ores to a degree large enough to increase the precipitation of $MgCO_3$. However, it is somewhat surprising that citrate, and oxalate at pH 10, reduced the carbon uptake. Two possibilities exist for the reduction in carbon uptake in citrate and oxalate solutions. The first possibility is that the ligands inhibited the further leaching of Mg from the ores during carbonation. Leaching curves at room temperature for Pipe and OK ores in 0.1 M citrate and oxalate solutions (Figures D-2, D-4, D-6 and D-8) indicated that during the 24 hour pre-leach, most Mg was leached in the first 4 hours. After the first 4 hours, the Mg concentration in solution did not markedly increase. Indeed, leaching rates at 25°C for the OK ore in oxalate and citrate solutions were hindered compared to leaching rates in water (Bobicki et al., 2014c). Further leaching may have been slowed by ligand molecules and Mg-ligand complexes adsorbed on the surface. The inhibition of leaching by adsorbed ligand molecules has been observed by a number of researchers (Biver and Shotyk, 2012; Stumm and Wollast, 1990; Biber et al., 1994). During carbonation, however, the temperature was increased, and the pH was reduced in the case of the pH 10 carbonations. While reports in the literature as to the effect of temperature on the dissolution of silicate minerals in the presence of ligands are mixed (Krevor and Lackner (2011) showed the dissolution of serpentine in citrate solution increased with increasing temperature while Prigiobbe and Mazzotti (2011) showed that the dissolution of olivine in oxalate did not increase with increasing temperature), it has been shown that reducing the pH enhances dissolution of ultramafic nickel ores in citrate and oxalate solutions (Bobicki et al., 2014c).

211

The second potential reason why oxalate and citrate did not improve the carbon uptake of the OK and Pipe ores is that at high temperature they formed strong Mg-complexes that reduced the precipitation of $MgCO_3$. It is reported by Prigiobbe and Mazzotti (2011) that the equilibrium constant for the formation of MgC_2O_4 increases with increasing temperature; however, this information is not particularly valuable without comparable information for the other ligands. The effect of increasing temperature on $MgCO_3$ precipitation in the presence of ligands is further complicated by the simultaneous decrease in CO_2 solubility and decrease in the $MgCO_3$ solubility product (Chen et al., 2006). The fact that the concentration of magnesium in solution increased after carbonation for Pipe and OK ores leached and carbonated in oxalate and citrate solutions (as well as in EDTA solutions) (Figure 7-21), in addition to the fact that oxalate and citrate were modeled to form complexes with Mg under 12.4 MPa CO_2 at 25^oC at near-neutral pH values, seems to support the idea that citrate and oxalate impaired the precipitation of $MgCO_3$. However, the concentration of magnesium after carbonation in citrate and oxalate solutions was not increased nearly to the degree that it was in EDTA solutions and the possibility of hindered dissolution cannot be entirely ruled out. Further investigation into the effect of temperature on both the leaching of the ores and the subsequent carbonation is needed.
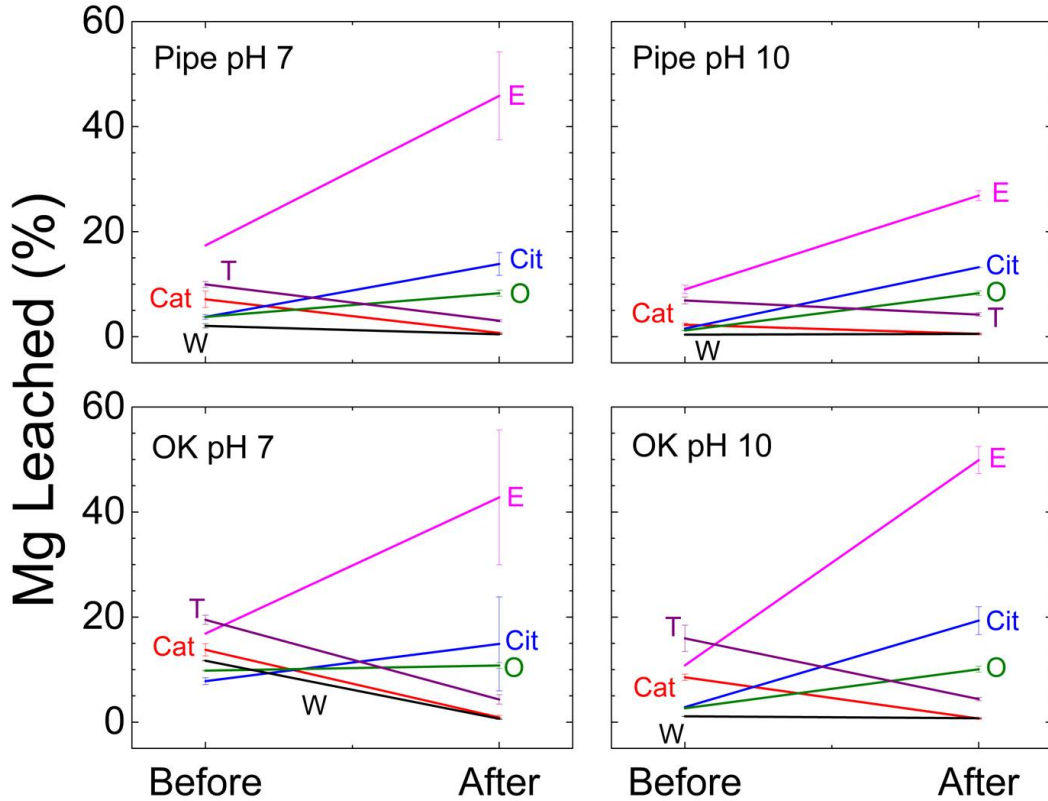
Figure 7-21: Magnesium in solution before and after carbonation for OK and Pipe ore at pH 7 and 10, leached and carbonated in water (W), catechol (Cat), citrate (Cit), EDTA (E), oxalate (O) and tiron (T) as determined by ICP analysis.

7.4 Conclusion

The carbon sequestration capacity of the Pipe and OK ores increased with microwave pre-treatment time after a threshold heating time of 4 minutes was passed. Maximum carbon uptakes of 15.7 g CO_2/100 g ore and 18.3 g CO_2/100 g ore were observed for the Pipe and OK ores, respectively. XRD analysis of microwave pre-treated and carbonated ores indicated that the product of carbonation was magnesite ($MgCO_3$). The increase in carbon uptake observed for the Pipe and OK ores was shown to be more strongly correlated with ore olivine content than surface area, both factors of which increased with microwave pre-treatment. The extent of carbonation achieved for microwave pre-treated ores was comparable to that reported for conventionally heat-treated lizardite. Although

energy use during microwave pre-treatment was very high, it can likely be reduced by increasing the sample size and microwave power. The effect of microwave pre-treatment on carbon uptake can also likely be enhanced by optimizing the design of the microwave reactor to achieve more even heating and, hence, more complete serpentine dehydroxylation. Microwave pre-treatment appears to be a promising way to enhance the carbon sequestration capacity of serpentine-containing ores since it can achieve the same improvement in carbon uptake as conventionally heat-treated ores in a fraction of the time, and can impart additional benefits for mineral processing.

Solution modeling of magnesium-ligand-water systems revealed that $MgCO_3$ can be precipitated from all ligand solutions studied under 12.4 MPa CO_2 pressure at pH 7 and 10 at 25°C. $MgCO_3$ was predicted to comprise greater than 99% of the magnesium species formed in the ligand systems studied, with the exception of the EDTA system, at pH 7 and 10. In the EDTA solution, $MgCO_3$ was modeled to comprise less than 70% of the magnesium species at pH 7 and 10, with the balance being $MgEDTA^{2-}$. The effect of CO_2 pressure and magnesium concentration on $MgCO_3$ precipitation was also modeled. Greater than 99% of magnesium was modeled to precipitate as $MgCO_3$ even at relatively low CO_2 pressures (0.4 MPa) in tiron and catechol solutions. Slightly higher CO_2 pressures (4 MPa) were modeled to be required to precipitate > 99% of magnesium as $MgCO_3$ in oxalate and citrate solutions. For EDTA, even at very high CO_2 pressures (56 MPa) only 70% of Mg could be precipitated as $MgCO_3$. In each ligand system studied, $MgCO_3$ precipitation was found to be sensitive to magnesium concentration. The modeling predicted that ore carbon uptake will only be significant if a magnesium concentration of 0.01 M in solution is surpassed. Overall, the modeling indicated that EDTA may be too strong of a ligand to result in increased carbon uptake, and that significant $MgCO_3$ may not be precipitated in oxalate and citrate solutions because sufficient Mg is not leached into solution.

214

Experimentally, it was found that magnesite was formed in ores pre-leached and carbonated in catechol, citrate, oxalate and tiron solutions. Magnesite did not form in EDTA solutions, which was not surprising since the modeling work suggested EDTA may have been too strong of a ligand to enhance MCS. While oxalate and citrate were not observed to improve the carbon uptake of either ore, the carbon sequestration capacity of OK and Pipe ores leached and carbonated in tiron and catechol solutions was observed to improve. The highest carbon uptakes observed, in tiron solutions at pH 10, were 3.6 g CO_2/100 g ore for Pipe ore and 9.7 g/100 g ore for OK ore. This is the first time ligands have been reported to improve the carbon uptake of mineral carbon sequestration feedstock. It is of note also that higher carbon uptakes were observed for ores leached and carbonated at pH 10 in catechol and tiron solutions compared to ores leached and carbonated in catechol and tiron solutions at pH 7. This suggests that leaching and carbonation can be conducted at the same pH value, eliminating the need for pH adjustment after leaching, potentially resulting in overall reagent savings. Although the carbon sequestration capacities achieved by pre-leaching the Pipe and OK ores with ligands were lower than that for microwave pre-treated ore, the fact that ligands can be used to enhance MCS is a positive step forward. In all likelihood, the carbon uptake of the ores can be enhanced through process optimization. Further work is needed to elucidate the effect of temperature on leaching and carbonation with ligands, and to determine if the ligands can be recycled.

7.5 References

Alexander, G., Maroto-Valer, M.M., Gafarova-Aksoy, P.G., 2007. Evaluation of reaction variables in the dissolution of serpentine for mineral carbonation. Fuel. 86, 273-281.

Appelo, C.A.J., Parkhurst, D.L., Post, V.E.A., 2014. Equations for calculating hydrogeochemical reactions of minerals and gases such as CO_2 at high pressures and temperatures. Geochimica et Cosmochimica Acta. 125, 49-67.

Biber, M.V., Dos Santos Afonso, M., Stumm, W., The coordination chemistry of weathering: IV. Inhibition of the dissolution of oxide minerals. Geochimica et Cosmochimica Acta. 58(9), 1999-2010.

Biver, M., Shotyk, W., 2012. Experimental study of the kinetics of ligand-promoted dissolution of stibnite (Sb_2S_3). Chemical Geology. 294-295, 165-172.

Bobicki, E.R., Liu, Q., Xu, Z., Zeng, H., 2012. Carbon capture and storage using alkaline industrial wastes. Progress in Energy and Combustion Science. 38, 302-320.

Bobicki, E.R., Liu, Q., Xu, Z., Manchak, N., Xu, M., 2013. Effect of microwave pre-treatment on grindability of ultramafic nickel ores. Proceedings of Materials Science and Technology (MS&T) 2013. 2013 October 27-31; Montreal, Quebec, Canada.

Bobicki, E.R., Liu, Q., Xu, Z., 2014a. Microwave heating of ultramafic nickel ores and mineralogical effects. Minerals Engineering. 58, 22-25.

Bobicki, E.R., Liu, Q., Xu, Z., 2014b. Effect of microwave pre-treatment on ultramafic nickel ore slurry rheology. Minerals Engineering. 61, 97-104.

Bobicki, E.R., Liu, Q., Xu, Z., 2014c. Ligand-promoted dissolution of serpentine in ultramafic nickel ores. *Accepted by Minerals Engineering.*

Bodénan, F., Bourgeois, F., Petiot, C., Augé, T., Bonfils, B., Julcour-Lebigue, C., et al., 2014. Ex situ mineral carbonation for CO_2 mitigation: Evaluation of mining waste resources, aqueous carbonation processability and life cycle assessment (Carmex project). Minerals Engineering. 59, 52-63.

Bonfils, B., et al., 2012. Comprehensive analysis of direct aqueous mineral carbonation using dissolution enhancing organic additives. International Journal of Greenhouse Gas Control. 9, 334-346.

Chen, Z.-Y., O'Connor, W.K., Gerdemann, S.J., 2006. Chemistry of aqueous mienral carbonation for carbon sequestration and explanation of experimental results. Environmental Progress. 25(2),161-166.

Declercq, J., Bosc, O., Oelkers, E.H., 2013. Do organic ligands affect forsterite dissolution rates? Applied Geochemistry. 39, 69-77.

Dlugogorski, B.Z., Balucan, R.D., 2014. Dehydroxylation of serpentine minerals: Implications for mineral carbonation. Renewable and Sustainable Energy Reviews. 31, 353-367.

Fauth, D.J., Goldberg, P.M., Knoer, J.P., Soong, Y., O'Connor, W.K., Dahlin, D.C., et al., 2000. Carbon dioxide storage as mineral carbonates. Preprints. American Chemical Society. Division of Fuel Chemistry. 45(4), 708–12.

Gadikota, G., Matter, J., Kelemen, P., Park, A.-H.A., 2014. Chemical and morphological changes during olivine carbonation for CO_2 storage in the presence of NaCl and $NaHCO_3$. Physical Chemistry Chemical Physics. 16, 4679-4693.

Gerdemann, S.J., O'Connor, W.K., Dahlin, D.C., Penner, L.R., Rush, H., 2007. Ex situ aqueous mineral carbonation. Environmental Science and Technology. 41, 2587-2593.

Hänchen, M., Prigiobbe, V., Storti, G., Seward, T.M., Mazzotti, M., 2006. Dissolution kinetics of forsteritic olivine at 90-150ºC including effects of the presence of CO_2. Geochimica et Cosmochinica Acta. 70, 4403-4416.

Ho, M.T., Allinson, G.W., Wiley, D.E., 2011. Comparison of MEA capture cost for low CO_2 emission sources in Australia. International Journal of Greenhouse Gas Control. 5, 49-60.

Huijgen, W.J.J., Comans, R.N.J., 2003. Carbon dioxide sequestration by mineral carbonation. Petten, NL: Energy Research Centre of the Netherlands.

Koornneef, J., van Keulen, T., Faaij, A., Turkenburg, W., 2008. Life cycle assessment of a pulverized coal power plant with post-combustion capture,

transport and storage of CO_2. International Journal of Greenhouse Gas Control. 2, 448-467.

Krevor, S.C.M., Lackner, K.S., 2011. Enhancing serpentine dissolution kinetics for mineral carbon dioxide sequestration. International Journal of Greenhouse Gas Control. 5, 1073-1080.

Lackner, K.S., Wendt, C.H., Butt, D.P., Joyce, E.L., Sharp, D.H., 1995. Carbon dioxide disposal in carbonate minerals. Energy. 20(11), 1153-1170.

Maroto-Valer, M.M., Kuchta, M.E., Zhang, Y., Andrésen, J.M., Fauth, D.J., 2005. Activation of magnesium rich minerals as carbonation feedstock materials for CO_2 sequestration. Fuel Processing Technology. 86, 1627-1645.

Metz, B., Davidson, O., de Coninck, H.C., Loos, M., Meyer, L.A., editors, 2005. IPCC Special Report on Carbon Dioxide Capture and Storage. Prepared by Working Group III of the Intergovernmental Panel on Climate Change. Cambridge, UK and New York, NY: Cambridge University Press. 443p.

O'Connor, W.K., Dahlin, D.C., Nilsen, D.N., Rush, G.E., Walters, R.P., Turner, P.C., 2000. CO_2 storage in solid form: A study of direct mineral carbonation. Greenhouse Gas Control Technologies: Proceedings of the 5th International Conference on Greenhouse Gas Technologies; 2000 Aug 14-18; Cairns, AU.

O'Connor, W.K., Dahlin, D.C., Rush, G.E., Gerdemann, S.J., Penner, L.R., Nilsen, D.N., 2005. Aqueous Mineral Carbonation: Final Report. Albany (NY): National Energy Laboratory, Office of Process Development. US Department of Energy. Report No.: DOE/ARC-TR-04-002.

Park, A.-H., Jadhav, R., Fan, L.-S., 2003. CO_2 mineral sequestration: chemically enhanced aqueous carbonation of serpentine. Canadian Journal of Chemical Engineering. 81, 885-90.

Pickles, C.A., 2009. Microwaves in extractive metallurgy: Part 1 – Review of Fundamentals. Minerals Engineering. 22, 1102-1111.

Prigiobbe, V., Mazzotti, M., 2011. Dissolution of olivine in the presence of oxalate, citrate, and CO_2 at 90ºC and 120ºC. Chemical Engineering Science. 66, 6544-6554.

Smith, R.M., Martell, A.E., 1975. Critical stability constants: Volumes 1 and 3. Plenum Press, New York.

Stumm, W., Wollast, R., 1990. Coordination chemistry of weathering: Kinetics of the surface-controlled dissolution of oxide minerals. Reviews of Geophysics. 28(1), 53-69.

Teir, S., Eloneva, S., Fogelholm, C.-J., Zevenhoven, R., 2009. Fixation of carbon dioxide by producing hydromagnesite from serpentinite. Applied Energy. 86, 214-218.

Werner, M., Hariharan, S.B., Bortolan, A.V., Zingaretti, D., Baciocchi, R., Mazzotti, M., 2013. Carbonation of activated serpentine for direct flue gas mineralization. Energy Procedia. 37, 5929-5937.

White, B., Silsbee, M.R., Kearns, B.J., 2004. Reaction mechanisms of magnesium silicates with carbon dioxide in microwave fields. Final Report to the U.S. Department of Energy, National Energy Laboratory. February 18, 2004. Award No. DE –FG26-02NT41545.

Zevenhoven, R., Fagerlund, J., 2010. Fixation of carbon dioxide into inorganic carbonates: the natural and artificial "weathering of silicates". In: Aresta M, editor. Carbon Dioxide as Chemical Feedstock. Weinheim, Germany: Wiley-VCH; p. 353-379.

Chapter 8 Conclusion

8.1 Concluding Remarks

Although mineral carbon sequestration (MCS) has many advantages over other carbon storage techniques, an economic MCS process has yet to be developed. Significant energy is expended in MCS in the preparation of feedstock, to drive the reaction at an acceptable rate (high temperature, high pressure, and/or high reagent requirements) and to purify or dispose of the reaction products. Two approaches were taken in this work to attempt to reduce the cost of MCS. The first approach was to use waste material, serpentine waste from ultramafic nickel ore processing, as feedstock. The second approach was to develop pre-treatments to increase the CO_2 reactivity of the waste. Two different pre-treatments were developed in this work: microwave pre-treatment and leaching with ligands at neutral to alkaline pH. In addition to having the potential to improve the CO_2 reactivity of the waste, microwave pre-treatment was also identified to have the potential to improve the mineral processing of ultramafic ores for nickel extraction.

8.1.1 Microwave Pre-treatment

Ultramafic nickel ores were found to heat well in response to microwave radiation and the temperatures achieved were sufficient to dehydroxylate serpentine. Ores that contained higher concentrations of highly microwave responsive minerals, heated better in response to microwave radiation than ores with lower concentrations of these minerals. Overall, 15 minutes microwave pre-treatment reduced the serpentine content in the OK ore from 84 wt.% to 15.8 wt.%, while 8 minutes microwave pre-treatment reduced the serpentine content in the Pipe ore from 63.7 wt% to 23.7 wt.%. Microwave pre-treatment was also found to convert pentlandite to high-temperature Fe-Ni-S phases. The transition of pentlandite to other nickel phases as a result of microwave pre-treatment may have implications for the upgrading of ultramafic nickel ores by froth flotation.

Microwave pre-treatment was found to improve the grindability of the OK ore, but to decrease the grindability of the Pipe ore. The impact of microwave pre-treatment on ore grindability was found to depend not only on the mineralogy, but also on the texture of the ore. Ores with an even texture containing well-dispersed, highly-microwave responsive minerals (such as iron oxides and sulphides) in a low-lossy gangue matrix (serpentine) respond well to microwave-assisted grinding. Ores that have an inconsistent texture, even if they contain highly-microwave responsive minerals in a low-lossy gangue, do not respond well to microwave-assisted grinding. Despite the different grindability responses, the specific surface area and pentlandite liberation in both the OK and Pipe ores were found to improve with microwave pre-treatment. Microwave pre-treatment, however, was not found to decrease the overall energy required for comminution.

Rheological characterization revealed that microwave pre-treatment reduced the slurry shear stress and viscosity (average 80% reduction at 200 s^1), as well as yield stress (peak yield stress reduced by 92-93%), of both the OK and Pipe ores. The reduction in slurry viscosity and yield stress observed as a result of microwave pre-treatment for the OK and Pipe ores was shown to be due to the destruction of serpentine minerals. The reduction in viscosity as a result of microwave pre-treatment should allow ultramafic nickel ore slurries to be process at higher slurry solids content. An increase in flotation pulp density from 20 to 30 wt.% solids would reduce the volume by 40 vol.%, likely resulting in significant savings in infrastructure and materials handling costs.

The carbon sequestration capacity of ultramafic nickel ores was found to improve with microwave pre-treatment. Maximum carbon uptakes achieved for the Pipe and OK ores were 15.7 g CO_2/100 g ore and 18.3 g CO_2/100 g ore, respectively, and the product of carbonation was determined to be magnesite ($MgCO_3$). The increase in carbon uptake was primarily attributed to the increase in olivine content that occurs as a result of microwave pre-treatment. The extent of carbonation achieved was comparable to that reported for conventionally heat-treated lizardite. This is very positive as microwave pre-treatment can be

completed in a fraction of the time of conventional heat-treatment. Although the energy used for microwave treatment of the ores in this study was high, it can likely be reduced by increasing the sample size and microwave power. Overall, microwave pre-treatment appears promising as a means to enhance the carbon sequestration capacity of ultramafic nickel ores while imparting benefits, such as improved grindability and slurry rheology, for nickel extraction operations. It is probable that a combined process where ultramafic nickel ores are treated with microwaves prior to grinding and flotation, and where the tailings are used as MCS feedstock, would result in overall energy savings, although further work is needed to verify this hypothesis.

8.1.2 Leaching with Ligands

The ligands catechol, citrate, EDTA, oxalate and tiron were investigated for their effectiveness in leaching magnesium from two ultramafic nickel ores at neutral to alkaline pH. Solution modeling suggested that each of the ligands selected should improve the solubility of magnesium in water at alkaline pH and that the order of effectiveness should be: EDTA > tiron > citrate > catechol > oxalate. The modeled order of effectiveness was mostly reflective of the relative order of the stability constants, except that catechol and oxalate, despite having higher stability constants, were modeled to be less effective than citrate. Catechol and oxalate were modeled to form other complexes that reduced their magnesium leaching efficiency at pH 10. Experimentally, it was shown that the ligands generally improved the dissolution of magnesium and the leaching rates of ultramafic nickel ores at neutral to alkaline pH. The order of ligand effectiveness based on the total magnesium leached and the final leaching rates for the Pipe ore was EDTA ≥ tiron > catechol > oxalate ≥ citrate, while the order for the OK ore was tiron > EDTA = catechol > oxalate > citrate. The order of ligand effectiveness as determined experimentally for the Pipe ore was in general accordance with the order of the relative strength of the stability constants. The order of effectiveness of the ligands for solubilizing Mg from the OK ore was similar to that of the Pipe ore, except tiron was more effective than EDTA, and

catechol was as effective as EDTA. The enhanced effectiveness of catechol and tiron was attributed to the ability of these ligands to form complexes with silicic acid in the alkaline pH range. Overall, the improvements in total magnesium leached and leaching rates achieved in catechol, EDTA and tiron solutions were more significant than those achieved in citrate and oxalate solutions. Based on the leaching work, it was concluded that the ligands catechol, EDTA and tiron had the most potential to enhance mineral carbon sequestration by improving the dissolution of serpentine in ultramafic ores at neutral to alkaline pH.

Solution modeling indicated that upon the addition of CO_2 at high pressure, $MgCO_3$ can be precipitated from all the ligand solutions studied. The modeled quantity of $MgCO_3$ precipitated, however, was reduced in EDTA solutions. The modeling also indicated substantial $MgCO_3$ may not be precipitated in solutions of citrate and oxalate because of the limited degree to which they improve the leaching of magnesium. Experimentally, it was found that magnesite ($MgCO_3$) was formed from ores pre-leached and carbonated in catechol, citrate, oxalate and tiron solutions, but not in EDTA solutions. Although EDTA can be used to improve the leaching of magnesium from ultramafic nickel ores, the $MgEDTA^{2+}$ complex that forms is too strong to allow the precipitation of the bound magnesium as a carbonate. The carbon sequestration capacity of ores leached and carbonated in catechol and tiron solutions was observed to increase, and the highest carbon uptakes were observed for ores treated at pH 10. Oxalate and citrate were not observed to improve the carbon uptake for either the Pipe or OK ore. It appears that ligands that bind strongly, but not too strongly, with magnesium at alkaline pH can be used to enhance MCS. The increase in carbon uptake of the Pipe and OK ores leached and carbonated in catechol and tiron solutions represents the first report of a ligand improving MCS. Maximum carbon uptakes for Pipe and OK ores leached and carbonated in tiron solutions at pH 10 were 3.6 g CO_2/100 g ore and 9.7 g/100 g ore, respectively. The fact that the highest carbon uptakes were observed for ores leached and carbonated at pH 10 indicates that the leaching and carbonation of MCS feedstock can be conducted at the same pH value. Cost savings could likely be achieved using an

MCS process with enhanced leaching using ligands without a secondary pH adjustment for carbonate precipitation. Although higher carbonate conversions were achieved for microwave pre-treated ore, optimization of the leaching and carbonation process would likely yield higher carbon uptake values for ores leached and carbonated in ligand solutions.

8.2 Major Contributions

1) This work represents a unique approach to mineral carbon sequestration. In the spirit of CCUS, microwave pre-treatment has been developed to enhance both mineral carbon sequestration and mineral processing. The benefits to both processes, after the optimization of microwave pre-treatment, could outweigh the costs of pre-treating mineral feedstock purely for the sake of improving MCS.

2) Ultramafic nickel ores, due to their magnetite and pyrrhotite content, were shown to heat better in response to microwave radiation compared to pure serpentine. The enhanced microwave heating response of ultramafic nickel ores means the serpentine contained in these ores can be dehydroxylated at a lower energy cost compared to pure serpentine.

3) In the conversion of serpentine to olivine by microwave pre-treatment, the serpentine brucite layer was shown to break down before the collapse of the siloxane layer. Olivine crystallizes from newly isolated silica tetrahedra surrounded by chains of dehydrated octahedral magnesium.

4) Microwave pre-treatment was shown to improve the grindability of ultramafic nickel ores only if highly-microwave responsive minerals were well dispersed throughout the ore. The grindability of ultramafic nickel ores with inconsistent texture was not shown to improve with microwave pre-treatment. In fact, without the even dispersion of highly-microwave responsive minerals, the grindability of ultramafic nickel ores was reduced due to increased ore hardness, a unique feature of these ores that occurs as a result of the conversion of serpentine to olivine upon heating.

5) Microwave pre-treatment, and the conversion of serpentine to olivine, is a totally unique and novel approach to modifying ultramafic nickel ore slurry rheology. The technique is very successful and could result in great cost savings for mineral processing operations.

6) Microwave pre-treatment is a fast and effective way to improve the carbon sequestration capacity of ores. The conversion of serpentine to olivine, as well as increased surface area, leads to the increased carbon uptake. This work represents the first time microwave pre-treatment has been reported to enhance mineral carbon sequestration.

7) Two new ligands, catechol and tiron, were tested for improving the leaching of Mg from serpentine in ultramafic nickel ores at neutral to alkaline pH. These ligands were shown to be more effective than ligands tested in the past for the leaching of serpentine. The ability of these ligands to bind with silicic acid appears to aid in their extraction of magnesium from the mineral feedstock. The approach of leaching mineral feedstock with ligands at alkaline pH for the enhancement of MCS is novel.

8) This work represents the first time ligands have been reported to improve the carbon sequestration capacity of mineral feedstock. The ligands to do so, catechol and tiron, bind strongly, but not too strongly, with magnesium at alkaline pH and allow the precipitation of $MgCO_3$ from solution.

8.3 Recommendations for Future Research

1) Optimization of microwave pre-treatment is required to realize the full benefits of the technology. The effect of increasing sample size and microwave power needs to be investigated. In addition, the microwave reactor could be better designed (such as with fluidization) to achieve more even heating and, hence, more complete serpentine dehydroxylation.

2) The effect of microwave pre-treatment on the froth flotation of ultramafic nickel ores should be studied. It is likely the increased surface area and

pentlandite liberation, as well as reduced slurry viscosity, achieved by microwave pre-treatment would greatly improve the flotation of these ores. The conversion of serpentine to olivine by microwave pre-treatment would likely also reduce the slime-coating of pentlandite, as well as the carry-over of fibrous particles to the froth, and result in increased nickel recovery and concentrate grade.

3) The surface charge of the three difference faces of serpentine minerals (brucite basal plane, siloxane basal plane and edge) should be determined to better explain their rheological behavior.

4) The effect of temperature on the leaching and carbonation of mineral carbon sequestration feedstock in the presence of ligands should be investigated.

5) Work should be done to optimize the leaching and carbonation of mineral carbon sequestration feedstock in the presence of catechol and tiron. An investigation into the recyclability of the ligands should also be conducted.

6) The capacity of ligands to extract residual nickel from ultramafic ores tailings along with Mg for MCS should be investigated.

Bibliography

Ahmaruzzaman, M., 2010. A review on the utilization of fly ash. Progress in Energy and Combustion Science. 36, 327-363.

Alexander, G., Maroto-Valer, M.M., Gafarova-Aksoy, P.G., 2007. Evaluation of reaction variables in the dissolution of serpentine for mineral carbonation. Fuel. 86, 273-281.

Alstadt, K.N., Katti, D.R., Katti, K.S., 2012. An in situ FTIR step-scan photoacoustic investigation of kerogen and minerals in oil shale. Spectrochimica Acta Part A: Molecular and Biomolecular Spectroscopy. 89, 105-113.

Alvarez-Silva, M., Uribe-Salas, A., Mirnezami, M., Finch, J.A., 2010. The point of zero charge of phyllosilicate minerals using the Mular-Roberts titration technique. Minerals Engineering. 23, 383-389.

Amankwah, R.K., Ofori-Sarpong, G., 2011. Microwave heating of gold ores for enhanced grindability and cyanide amenability. Minerals Engineering. 24, 541-544.

Anbalagan, G., Sivakumar, G., Prabakaran, A.R., Gunasekaran, S., 2010. Spectroscopic characterization of natural chrysotile. Vibrational Spectroscopy. 52, 122-127.

Appelo, C.A.J., Parkhurst, D.L., Post, V.E.A., 2014. Equations for calculating hydrogeochemical reactions of minerals and gases such as CO_2 at high pressures and temperatures. Geochimica et Cosmochimica Acta. 125, 49-67.

ASTM Standard E384-11, 2012, "Standard Test Method for Knoop and Vickers Hardness of Materials," ASTM International, West Conshohocken, PA, 2012, DOI 10.1520/E0384-11E01, www.astm.org.

Atomic Energy of Canada Limited Research Company (AECL) and Voss Associates Engineering Ltd, 1990. Microwaves and Minerals. Industrial Mineral

Background Paper #14. Ontario Ministry of Northern Development and Mines. 77p.

Baciocchi, R., Costa, G., Polettini, A., Pomi, R., 2009. Influence of particle size on the carbonation of stainless steel slag for CO_2 storage. Energy Procedia. 1, 4859-4866.

Baciocchi, R., Costa, G., Polettini, A., Pomi, R., Prigiobbe, V., 2009. Comparison of different reaction routes for carbonation of APC residues. Energy Procedia. 1, 4851-4858.

Baciocchi. R., Costa, G., Bartolomeo, E.D., Polettini, A., Pomi, R., 2009. The effects of accelerated carbonation on CO_2 uptake and metal release from incineration APC residues. Waste Management. 29, 2994-3003.

Bai, S., Okaue, Y., Yokoyama, T., 2009. Depolymerization of polysilicic acid by tiron. Polymer Degradation and Stability. 94, 1795-1799.

Bai, S., Tsuji, Y., Okaue, Y., Yokoyama, T., 2011. Complexation of silicic acid with tiron in aqueous solution under near natural condition. Journal of Solution Chemistry. 40, 348-356.

Baldyga, J., Henczka, M., Sokolnicka, K., 2010. Utilization of carbon dioxide by chemically accelerated mineral carbonation. Materials Letters. 64, 702-704.

Bales, R.C., Morgan, J.J., 1985. Dissolution kinetics of chrysotile at pH 7 to 10. Geochimica et Cosmochimica Acta. 49, 2281-2288.

Bao, W., Li, H., Zhang, Y., 2010. Selective leaching of steelmaking slag for indirect CO_2 mineral sequestration. Industrial and Engineering Chemistry Research. 49, 2055-2063.

Baranzini, A., Goldemberg, J., Speck, S., 2000. A future for carbon taxes. Ecological Economics. 32, 395-412.

Becker, M., Yorath, G., Ndlovu, B., Harris, M., Deglon, D., Franzidis, J.-P., 2013. A rheological investigation of the behaviour of two Southern African platinum ores. Minerals Engineering. 49, 92-97.

Bernstein, L., Bosch, P., Canziani, O., Chen, Z., Christ, R., Davidson, O., et al., 2007. Climate Change 2007: Synthesis Report. Contribution of Working Groups I, II and III to the Forth Assessment Report of the Intergovernmental Panel on Climate Change. Cambridge, UK and New York, NY, USA: Cambridge University Press.

Berry, A.J., Hermann, J., O'Neill, H.S.C., Foran, G.J., 2005. Fingerprinting the water site in mantle olivine. Geology. 33(11), 869-872.

Berry, T.F., Bruce, R.W., 1966. A simple method of determining the grindability or ores. Canadian Mining Journal. 7, 63-65.

Biber, M.V., Dos Santos Afonso, M., Stumm, W., The coordination chemistry of weathering: IV. Inhibition of the dissolution of oxide minerals. Geochimica et Cosmochimica Acta. 58(9), 1999-2010.

Birle, J.D., Gibbs, G.V., Moore, P.B., Smith, J.V., 1968. Crystal structures of natural olivines. American Mineralogist. 53, 807-824.

Biver, M., Shotyk, W., 2012. Experimental study of the kinetics of ligand-promoted dissolution of stibnite (Sb_2S_3). Chemical Geology. 294-295, 165-172.

Blencoe, J.G., Palmer, D.A., Anovitz, L.M., Beard, J.S., 2004. Carbonation of metal silicates for long-term CO_2 sequestration. Patent application. WO 2004/094043.

Bobicki, E.R., Liu, Q., Xu, Z., 2014. Microwave heating of ultramafic nickel ores and mineralogical effects. Minerals Engineering. 58, 22-25.

Bobicki, E.R., Liu, Q., Xu, Z., 2014. Effect of microwave pre-treatment on ultramafic nickel ore slurry rheology. Minerals Engineering. 61, 97-104.

229

Bobicki, E.R., Liu, Q., Xu, Z., 2014. Ligand-promoted dissolution of serpentine in ultramafic nickel ores. *Accepted by Minerals Engineering.*

Bobicki, E.R., Liu, Q., Xu, Z., Manchak, N., Xu, M., 2013. Effect of microwave pre-treatment on grindability of ultramafic nickel ores. Proceedings of Materials Science and Technology (MS&T) 2013. 2013 October 27-31; Montreal, Quebec, Canada.

Bobicki, E.R., Liu, Q., Xu, Z., Zeng, H., 2012. Carbon capture and storage using alkaline industrial wastes. Progress in Energy and Combustion Science. 38, 302-320.

Bodénan, F., Bourgeois, F., Petiot, C., Augé, T., Bonfils, B., Julcour-Lebigue, C., et al., 2014. Ex situ mineral carbonation for CO_2 mitigation: Evaluation of mining waste resources, aqueous carbonation processability and life cycle assessment (Carmex project). Minerals Engineering. 59, 52-63.

Bonenfant, D., Kharoune, L., Sauve, S., Hausler, R., Niquette, P., Mimeault, M., Kharoune, M., 2008. CO_2 sequestration by aqueous red mud carbonation at ambient pressure and temperature. Industrial and Engineering Chemistry Research. 47, 7617-7622.

Bonenfant, D., Kharoune, L., Sauvé, S., Hausler, R., Niquette, P., Mimeault, M., Kharoune, M., 2008. CO_2 sequestration potential of steel slags at ambient pressure and temperature. Industrial and Engineering Chemistry Research. 47, 7610-7616.

Bonfils, B., et al., 2012. Comprehensive analysis of direct aqueous mineral carbonation using dissolution enhancing organic additives. International Journal of Greenhouse Gas Control. 9, 334-346.

Bosecker, K., 1997. Bioleaching:metal solubilization by microorganisms. FEMA Microbiology Reviews. 20, 591-604.

Brantley, S.L., Olsen, A.A., 2014. 7.3 – Reaction kinetics of primary rock-forming minerals under ambient conditions. Reference Module in Earth Systems

and Environmental Sciences, from Treatise on Geochemistry (Second Edition), Eds: Heinrich Holland and Karl Turekian. 7, 69–113.

Bremmel, K.E., Fornasiero, D., Ralston, J., 2005. Pentlandite-lizardite interactions and implications for their separation by flotation. Colloids and Surfaces A: Physiochemical and Engineering Aspects. 252, 207-212.

Canadell, J.G., Le Quéré, C., Raupach, M.R., Field, C.B., Buitenhuis, E.T., Ciais, P., et al., 2007. Contributions to accelerating atmospheric CO_2 growth from economic activity, carbon intensity, and efficiency of natural sinks. PNAS. 104(47), 18866-18870.

Chen, Z.-Y., O'Connor, W.K., Gerdemann, S.J., 2006. Chemistry of aqueous mienral carbonation for carbon sequestration and explanation of experimental results. Environmental Progress. 25(2), 161-166.

Corradi, A., Siligardi, C., Veronesi, P., Marucci, G., Annibali, M., Ragazzo, G., 2003. Microwave irradiation of asbestos containing materials. Proceedings of the 3rd World Congress on Microwave and Radio Frequency Applications. 2002 September; Sydney, Australia. Westerville: American Ceramic Society.

Cruz, N., Peng, Y., Farrokhpay, S., Bradshaw, D., 2013. Interactions of clay minerals in copper-gold flotation: Part 1 – Rheological properties of clay mineral suspensions in the presence of flotation reagents. Minerals Engineering. 50-51, 30-37.

Daval, D., Hellmann, R., Martinez, I., Gangloff, S., Guyot, F., 2013. Lizardite serpentine dissolution kinetics as a function of pH and temperature, including effects of elevated pCO_2. Chemical Geology. 351, 245-256.

Declercq, J., Bosc, O., Oelkers, E.H., 2013. Do organic ligands affect forsterite dissolution rates? Applied Geochemistry. 39, 69-77.

Dilmore, R., Lu, P., Allen, D., Soong, Y., Hedges, S., Fu, J.K., et al., 2008. Sequestration of CO_2 in mixtures of bauxite residue and saline wastewater. Energy and Fuels. 22, 343-353.

Dlugogorski, B.Z., Balucan, R.D., 2014. Dehydroxylation of serpentine minerals: Implications for mineral carbonation. Renewable and Sustainable Energy Reviews. 31, 353-367.

Dooley, J.J., Davidson, C.L., Dahowski, R.T., 2009. An Assessment of the Commercial Availability of Carbon Dioxide Capture and Storage Technologies as of June 2009. Richland, WA: Pacific Northwest National Laboratory, US Department of Energy; 2009 June. Contract No.: DE-AC05-76RL01830.

Doucet, F.J., 2010. Effective CO_2-specific sequestration capacity of steel slags and variability in their leaching behaviour in view of industrial mineral carbonation. Minerals Engineering. 23, 262-269.

Dufaud, F., Martinez, I., Shilobreeva, S., 2009. Experimental study of Mg-rich silicates carbonation at 400 and 500°C and 1 kbar. Chemical Geology. 265, 79-87.

Dzuy, N.Q., Boger, D.V., 1985. Direct yield stress measurement with the vane method. Journal of Rheology. 29(3), 335-347.

Edwards, C.R., Kipkie, W.B., Agar, G.E., 1980. The effect of slime coatings of the serpentine minerals, chrysotile and lizardite, on pentlandite flotation. International Journal of Mineral Processing. 7, 33-42.

EIONET, 2009. What is waste? [Internet]. European Topic Centre on Sustainable Consumption and Production. [cited 2011 Jun 27]. Available from: http://scp.eionet.europa.eu/themes/waste/#4

Eloneva, S., Puheloinen, E.-M., Kanerva, J., Ekroos, A., Zevenhoven, R., Fogelholm, C.-J., 2010. Co-utilization of CO_2 and steelmaking slags for production of pure $CaCO_3$ - legislative issues. Journal of Cleaner Production. 18(18), 1833-1839.

Eloneva, S., Teir, S., Salminen, J., Fogelholm, C.-J., Zevenhoven, R., 2008a. Fixation of CO_2 by carbonating calcium derived from blast furnace slag. Energy. 33, 1461-1467.

Eloneva, S., Teir, S., Salminen, J., Fogelholm, C.-J., Zevenhoven, R., 2008b. Steel converter slag as a raw material for precipitation of pure calcium carbonate. Industrial and Engineering Chemistry Research. 47, 7104-7111.

Elwell, L.C., Grant, W.S., 2006. Technology options for capturing CO_2. Power Magazine. 150(8), 60.

ENCE, 2009. Declaración Ambiental 2009 [Internet]. [cited 2011 Jun 28]. Available from: http://www.ence.es/en/descargas/DA_EnceHuelva09.pdf

Etschmann, B., Pring, A., Putnis, A., Grguric, B.A., Studer, A., 2004. A kinetic study of the exsolution of pentlandite $(Ni,Fe)_9S_8$ from the monosulfide solid solution (Fe,Ni)S. American Mineralogist. 89, 39-50.

Farmer, V.C., 1974. The infrared spectra of minerals. London, England: Mineralogical Society. 539pp.

Fauth, D.J., Goldberg, P.M., Knoer, J.P., Soong, Y., O'Connor, W.K., Dahlin, D.C., et al., 2000. Carbon dioxide storage as mineral carbonates. Preprints. American Chemical Society. Division of Fuel Chemistry. 45(4), 708–12.

Feng, B., Feng, Q., Lu, Y., 2012. A novel method to limit the detrimental effect of serpentine on the flotation of pentlandite. International Journal of Mineral Processing. 114-117, 11-13.

Fernández Bertos, M., Li, X., Simons, S.J.R., Hills, C.D., Carey, P.J., 2004. Investigation of accelerated carbonation for the stabilisation of MSW incinerator ashes and the sequestration of CO_2. Green Chemistry. 6, 428-436.

Fernández Bertos, M., Simons, S.J.R., Hills, C.D., Carey, P.J., 2004. A review of accelerated carbonation technology in the treatment of cement-based materials and sequestration of CO_2. Journal of Hazardous Materials. B112, 193-205.

Fialips, C., Petit, S., Decarreau, A., Beaufort, D., 2000. Influence of synthesis pH on kaolinite "crystallinity" and surface properties. Clays and Clay Minerals. 48(2), 173-184.

Field, C.B., Raupach, M.R., editors., 2004. The global carbon cycle: Integrating humans, climate and the natural world. Washington, DC: Island Press.

Fischer, C., Werge, M., 2009. EU as a Recycling Society. ETC/SCP Working Paper 2 [Internet].   2009 [Cited 2011 Jun 27]. Available from: http://scp.eionet.europa.eu/publications/wp2009_2/wp/wp2009_2

Foresti, E., Fornero, E., Lesci, I.G., Rinaudo, C., Zuccheri, T., Roveri, N., 2009. Asbestos health hazrd: A spectroscopic study of synthetic geoinspried F-doped chrysotile. Journal of Hazardous Materials. 167, 1070-1079.

Franco, F., Pérez-Maqueda, L.A., Ramírez-Valle, V., Pérez-Rodríguez, J.L., 2006. Spectroscopic study of the dehydroxylation process of a sonicated antigorite. European Journal of Mineralogy. 18, 257-264.

Frost, R.L., Palmer, S.J., Reddy, B.J., 2007. Near-infrared and mid-IR spectroscopy of selected humite minerals. Vibrational Spectroscopy. 44, 154-161.

Fuchs, Y., Linares, J., Mellini, M., 1998. Mössbauer and infrared spectrometry of lizardite-1T from Monte Fico, Elba. Physical Chemistry of Minerals. 26, 111-115.

Fuerstenau, D.W., Pradip., 2005. Zeta potentials in the flotation of oxide and silicate minerals. Advances in Colloid and Interface Science. 114-116, 9-26.

Gadikota, G., Matter, J., Kelemen, P., Park, A.-H.A., 2014. Chemical and morphological changes during olivine carbonation for CO_2 storage in the presence of NaCl and $NaHCO_3$. Physical Chemistry Chemical Physics. 16, 4679-4693.

Gale, J., Davison, J., 2004. Transmission of CO_2 – safety and economic considerations. Energy. 29, 1319-1328.

Genc, A.M., Kilickaplan, I., Laskowski, J.S., 2012. Effect of pulp rheology on flotation of nickel sulphide ore with fibrous gangue particles. Canadian Metallurgical Quarterly. 51(4), 368-375.

Gerdemann, S.J., Dahlin, D.C., O'Connor, W.K., Penner, L.R., 2003. Carbon dioxide sequestration by aqueous mineral carbonation of magnesium silicate minerals. Albany, OR: Albany Research Center.

Gerdemann, S.J., Dahlin, D.C., O'Connor, W.K., Penner, L.R., Rush, G.E., 2004. Ex-situ and in-situ mineral carbonation as a means to sequester carbon dioxide. Proceedings of Twenty-First Annual International Pittsburgh Coal Conference; 2004 Sep 13-17; Osaka, Japan. Pittsburgh, PA: Pittsburgh Coal Conference (PCC).

Gerdemann, S.J., O'Connor, W.K., Dahlin, D.C., Penner, L.R., Rush, H., 2007. Ex situ aqueous mineral carbonation. Environmental Science and Technology. 41, 2587-2593.

Gibbins, J., Chalmers, H., 2008. Carbon capture and storage. Energy Policy. 36, 4317-4722.

Gierer, J., 1980. Chemical aspects of kraft pulping. Wood Science and Technology. 14, 241-266.

Goff, F., Lackner, K.S., 1998. Carbon dioxide sequestering using ultramafic rocks. Environmental Geosciences. 5(3), 89-101.

Goldberg, P., Chen, Z.-Y., O'Connor, W., Walters, R., Ziock, H., 2001. CO_2 mineral sequestration studies in US. Proceedings of the First National Conference on Carbon Sequestration. 2001 May 14-17; Washington, DC.

Grandstaff, D.E., 1986. The dissolution rate of forsteritic olivine from Hawaiian beach sand. In: Colman SM, Dethier DP, editors. Rates of chemical weathering of rocks and minerals. Orlando: Academic Press Inc. p. 41-59.

Grasa, G.S., Abanades, J.C., 2006. CO_2 capture capacity of CaO in long series of carbonation/calcination cycles. Industrial and Engineering Chemistry Research. 45(26), 8846-8851.

Gunning, P.J., Hills, C.D., Carey, P.J., 2010. Accelerated carbonation treatment of industrial wastes. Waste Management. 30, 1081-1090.

Gupta, H., Fan, L.-S., 2002. Carbonation-calcination cycle using high reactivity calcium oxide for carbon dioixde separation from flue gas. Industrial and Engineering Chemistry Research. 41(16), 4035-4042.

Habashi, F., 2001. Asbestos. In: Buschow KHJ, Cahn R, Flemings M, Ilschner B, Kramer E, Mahajan S, Veyssiere, editors. Encyclopedia of Materials: Science and Technology. Waltham, MA: Elsevier. pp. 1-5.

Hänchen, M., Prigiobbe, V., Storti, G., Seward, T.M., Mazzotti, M., 2006. Dissolution kinetics of forsteritic olivine at 90-150ºC including effects of the presence of CO_2. Geochimica et Cosmochinica Acta. 70, 4403-4416.

Hansson, A., Bryngelsson, M., 2009. Expert opinions on carbon dioxide capture and storage – A framing of uncertainties and possibilities. Energy Policy. 37, 2273-2282.

Haque, K.E., 1999. Microwave energy for mineral treatment processes – a review. International Journal of Mineral Processing. 57, 1-24.

Haug, T.A., Kleiv, R.A., Munz, I.A., 2010. Investigating dissolution of mechanically activated olivine for carbonation purposes. Applied Geochemistry. 25(10), 1547-1563.

Henda, R., Hermas, A., Gedye, R., Islam, M.R., 2005. Microwave enhanced recovery of nickel-copper ore: Comminution and flotatbility aspects. International Microwave Power Institute. 40(1), 7-16.

Herbst, J.A., Lo, Y.C., Flintoff, B., 2003. Size reduction and liberation. In: Principles of mineral processing, ed. M.C. Fuerstenau and K.N. Han, Englewood, CO: Society for Mining Metallurgy and Exploration, pp 61-118.

Hill, M.J., 2000. The microwave palaeointensity technique and its application to lava. Doctoral dissertation, University of Liverpool.

Hindle, S., Hitch, M., 2010. Financial feasibility of integrating mineral carbonation into proposed mining operations at the Turnagain Nickel Site, Northern BC. Proceedings of the CIM Conference and Exhibition 2010; 2010 May 10-12; Vancouver, BC.

Hitch, M., Ballantyne, S.M., Hindle, S.R., 2010. Revaluing mine waste rock for carbon capture and storage. International Journal of Mining, Reclamation and Environment. 24, 64-79.

Ho, M.T., Allinson, G.W., Wiley, D.E., 2011. Comparison of MEA capture cost for low CO_2 emission sources in Australia. International Journal of Greenhouse Gas Control. 5, 49-60.

Holdren, G.R., Berner, R.A., 1979. Mechanism of feldspar weathering − I. Experimental studies. Geochimica et Cosmochimica Acta. 43, 1161-1171.

Hotta, M., Hayashi, M., Nagata, K., 2011. High temperature measurement of complex permittivity and permeability of Fe_3O_4 powders in the frequency range of 0.2 to 13.5 GHz. ISIJ International. 51(3), 491-497.

Houghton, J.T., Ding, Y., Griggs, D.J., Noguer, M., van der Linden, P.J., Dai, X., et al., editors, 2001. Climate Change 2001: The Scientific Basis. Contribution of Working Group I to the Third Assessment Report of the Intergovernmental Panel on Climate Change. Cambridge, UK and New York, NY, USA: Cambridge University Press.

Hua, Y., Lin, C., 1996. Heating rate of minerals and compounds in microwave field. Transactions of NFsoc. 6(1), 35-40.

Huijgen, W.J.J., Comans, R.N.J., 2003. Carbon dioxide sequestration by mineral carbonation. Petten, NL: Energy Research Centre of the Netherlands.

Huijgen, W.J.J., Witkamp, G.-J., Comans, R.N.J., 2005. Mineral CO_2 sequestration by steel slag carbonation. Environmental Science and Technology. 39, 9676-9682.

Huntzinger, D.N., Gierke, J.S., Sutter, L.L., Kawatra, S.K., Eisele, T.C., 2009. Mineral carbonation for carbon sequestration in cement kiln dust from waste piles. Journal of Mazardous Materials. 168, 31-37.

Huntzinger, D.N., Eatmon, T.D., 2009. A life-cycle assessment of Portland cement manufacturing: comparing the traditional process with alternative technologies. Journal of Cleaner Production. 17, 668-675.

ICMM, 2008. Case Study: Alcoa develops carbon capture process. International Council on Mining and Metals [Internet]. 2008 [cited 2011 Mar 2]. Available from: http://www.icmm.com/page/2420/alcoa-develops-carbon-capture-process

Iizuka, A., Fujii, M., Yamasaki, A., Yanagisawa, Y., 2004. Development of a new CO_2 sequestration process utilizing the carbonation of waste cement. Industrial and Engineering Chemistry Research. 43, 7880-7887.

International Energy Agency, 2012. CO_2 Emissions from Fuel Combustion [Internet]. Paris (France): OECD/IEA; [cited 2014 Jan 29]. Available from: http://www.iea.org/co2highlights/CO2highlights.pdf

Irish Department of Finance, 2010. Finance Bill 2010: List of Items. Dublin, Ireland.

Jang, N.-H., Park, S.-K., Shim, H.-M., Kim, H.-T., 2010. Comparison of pretreatment method for the enhancement of CO_2 mineralogied sequestration using by serpentine. Journal of the Korean Industrial and Engineering Chemistry. 21, 24-28.

Johnston, M., Clark, M.W., McMahon, P., Ward, N., 2010. Alkalinity conversion of bauxite refinery residues by neutralization. Journal of Hazardous Materials. 182, 710-715.

Jones, D.A., Kingman, S.W., Whittles, D.N., Lowndes, I.S., 2005. Understanding microwave assisted breakage. Minerals Engineering. 18, 659-669.

Jürgen-Friedrich, H., Hubert, H., Olga, S., Jochen, S., 2009. CCS for Germany: Policy, R&D and demonstration activities. Energy Procedia. 1(1), 3917-3925.

Kakizawa, M., Yamasaki, A., Yanagisawa, Y., 2001. A new CO_2 disposal process via artifical weathering of calcium silicate accelerated by acetic acid. Energy. 26, 341-354.

Katsuyama, Y., Yamasaki, A., Iizuka, A., Fuhii, M., Kumagai, K., Yanagisawa, Y., 2005. Development of a process for producing high-purity calcium carbonate ($CaCO_3$) from waste cement using pressurized CO_2. Environmental Progress. 24, 162-170.

Kaya, E., 2010. Comminution behaviour of microwave heated two sulphide copper ores. Indian Journal of Chemical Technology. 17, 455-61.

Kelly, K.E., Silcox, G.D., Sarofim, A.F., Pershing, D.W., 2011. An evaluation of ex situ, industrial-scale, aqueous CO_2 mineralization. International Journal of Greenhouse Gas Control. 5, 1587-1595.

Kingman, S.W., Jackson, K., Cumbane, A., Bradshaw, S.M., Rowson, N.A., Greenwood, R., 2004. Recent developments in microwave-assisted comminution. International Journal of Mineral Processing. 74, 71-83.

Kingman, S.W., Vorster, W., Rowson, N.A., 2000. The influence of mineralogy on microwave assisted grinding. Minerals Engineering. 13(3), 313-327.

Kitakaze, A., Sugaki, A., Itoh, H., Komatsu, R., 2011. A revision of phase relations in the system Fe-Ni-S from 650ºC to 450ºC. The Canadian Mineralogist. 49, 1687-1710.

Kodama, S., Nishimoto, T., Yamamoto, N., Yogo, K., Yamada, K., 2008. Development of a new pH-swing CO_2 mineralization process with a recyclable reaction solution. Energy. 33, 776-784.

Koornneef, J., Spruijt, M., Molag, M., Ramírez, A., Turkenburg, W., Faaij, A., 2010. Quantitative risk assessment of CO_2 transport by pipelines – A review of uncertainties and their impacts. Journal of Hazardous Materials. 177, 12-27.

Koornneef, J., van Keulen, T., Faaij, A., Turkenburg, W., 2008. Life cycle assessment of a pulverized coal power plant with post-combustion capture, transport and storage of CO_2. International Journal of Greenhouse Gas Control. 2, 448-467.

Krevor, S.C., Lackner, K.S., 2009. Enhancing process kinetics for mineral carbon sequestration. Energy Procedia. 1, 4867-4871.

Krevor, S.C.M., Lackner, K.S., 2011. Enhancing serpentine dissolution kinetics for mineral carbon dioxide sequestration. International Journal of Greenhouse Gas Control. 5, 1073-1080.

Külaots, I., Goldfarb, J.L., Suuberg, E.M., 2010. Characterization of Chinese, American and Estonian oil shale semicokes and their sorptive potential. Fuel. 89, 3300-3306.

Kullerud G., 1963. Thermal stability of pentlandite. The Canadian Mineralogist. 7(3), 353-366.

Kusuma, A.M., Zeng, H., Liu, Q., 2013. Understanding mineral interaction mechanisms by zeta potential and surface force measurements. Proceedings of the 10th International Mineral Processing Conference. 2013 October 15-18; Santiago, Chile.

Lackner, K.S., 2002. Carbonate chemistry for sequestering fossil carbon. Annual Reviews of Energy and the Environment. 27, 193-232.

Lackner, K.S., 2003. Climate change: A guide to CO_2 sequestration. Science. 300, 1677-1678.

Lackner, K.S., Butt, D.P., Wendt, C.H., 1997. Progress on binding CO_2 in mineral substrates. Energy Conversion and Management. 38, S259-S264.

Lackner, K.S., Wendt, C.H., Butt, D.P., Joyce, E.L., Sharp, D.H., 1995. Carbon dioxide disposal in carbonate minerals. Energy. 20(11), 1153-1170.

Larachi, F., Daldoul, I., Beaudoin, G., 2010. Fixation of CO_2 by chrysotile in low-pressure dry and moist carbonation: Ex-situ and in-situ characterizations. Geochimica et Cosmochimica Acta. 74, 3051-3075.

Lee, S.C., Chae, H.J., Lee, S.J., Choi, B.Y., Yi, C.K., Lee, J.B., et al., 2008. Development of regenerable MgO-based sorbent promoted with K_2CO_3 for CO_2 capture at low temperature. Environmental Science and Technology. 42(8), 2736-2741.

Lekakh, S.N., Rawlins, C.H., Robertson, D.G.C., Richards, V.L., Peaslee, K.D., 2008. Kinetics of aqueous leaching and carbonization of steelmaking slag. Metallurgical and Materials Transactions B. 39B, 125-134.

Leonelli, C., Veronesi, P., Boccaccini, D.N., Rivasi, M.R., Barbieri, L., Andreola, F., Lancellotti, I., Rabitti, D., Pellacani, G.C., 2006. Microwave thermal inertisation of asbestos containing waste and its recycling in traditional ceramics. Journal of Hazardous Materials. B135, 149-155.

Levenspiel, O., 1999. Chapter 25: Fluid-Particle Reactions: Kinetics. In: Chemical Reaction Engineering, third ed., New York: John Wiley & Sons. p. 566-588.

Li, X., 2008. Recycling and reuse of waste concrete in China. Part I. Material behaviour of recycled aggregate concrete. Resources, Conservation and Recycling. 53, 36-44.

Li. X., Fernández Bertos. M., Hills, C.D., Carey, P.J., Simon, S., 2007. Accelerated carbonation of municipal solid waste incineration fly ashes. Waste Management. 27, 1200-1206.

Lim, M., Han, G.-C., Ahn, J.-W., You, K.-S., 2010. Environmental remediation and conversion of carbon dioxide (CO_2) into useful green products by accelerated carbonation technology. International Journal of Environmental Research and Public Health. 7, 203-228.

Liu, C., Xu, Y., Hua, Y., 1990. Application of microwave radiation to extractive metallurgy. Chinese Journal of Metallurgical Science and Technology. 6, 121-124.

Liu, K., Chen, Q., Hu, H., Yin, Z., 2010. Characterization of lizardite in Yuanjiang laterite ore. Applied Clay Science. 47, 311-316.

Makreski, P., Jovanovski, G., Stojančeska, S., 2005. Minerals from Macedonia XIII: Vibration spectra of some commonly appearing nesosilicate minerals. Journal of Molecular Structure. 744-547, 79-92.

Marcuson, S.W., Hooper, J., Osborne, R.C., Chow, K., Burchell, J., 2009. Sustainability in Nickel Projects: 50 Years of Experience at Vale Inco. Engineering and Mining Journal [Internet], [cited 2011 Mar 2]. Available from: http://www.e-mj.com/index.php/features/117-sustainability-in-nickel-projects-50-years-of-experience-at-vale-inco.html

Maroto-Valer, M.M., Kuchta, M.E., Zhang, Y., Andrésen, J.M., Fauth, D.J., 2005. Activation of magnesium rich minerals as carbonation feedstock materials for CO_2 sequestration. Fuel Processing Technology. 86, 1627-1645.

Maroto-Valer, M.M., Kuchta, M.E., Zhang, Y., Andrésen, J.M., Fauth, D.J., 2004. Comparison of physical and chemical activation of serpentine for enhanced CO_2 sequestration. Prepr. Pap.-Am. Chem. Soc., Div. Fuel Chem. 49(1), 373-375.

McKelvy, M.J., Chizmeshya, A.V.G., Diefenbacher, J., Béarat, H., Wolf, G., 2004. Exploration of the role of heat activation in enhancing serpentine carbon sequestration. Environmental Science and Technology. 38, 6897-6903.

Mellini, M., 1982. The crystal structure of lizardite 1T: hydrogen bonds and polytypism. American Mineralogist. 67, 587-598.

Mellini, M., Fuchs, Y., Viti, C., Lemaire, C., Linarés, J., 2002. Insights into the antigorite structure from Mössbauer and FTIR spectroscopy. European Journal of Mineralogy. 14, 97-104.

Metcalf, G.E., Weisback, D., 2009. The design of a carbon tax. Harvard Environmental Law Review. 33(2), 499-556.

Metz, B., Davidson, O., de Coninck, H.C., Loos, M., Meyer, L.A., editors, 2005. IPCC Special Report on Carbon Dioxide Capture and Storage. Prepared by Working Group III of the Intergovernmental Panel on Climate Change. Cambridge, UK and New York, NY: Cambridge University Press. 443p.

Metz, B., Davidson, O.R., Bosch, P.R., Dave, R., Meyer, L.A., editors, 2007. Climate Change 2007: Mitigation. Contribution of Working Group III to the Fourth Assessment Report of the Intergovernmental Panel on Climate Change. Cambridge, UK and New York, NY, USA: Cambridge University Press.

Montes-Hernandez, G., Pérez-López, R., Renard, F., Nieto, J.M., Charlet, L., 2009. Mineral sequestration of CO_2 by aqueous carbonation of coal combustion fly-ash. Journal of Hazardous Materials. 161, 1347-1354.

Mõtlep, R., Sild, T., Puura, E., Kirsimäe, K., 2010. Composition, diagenetic transformation and alkalinity potential of oil shale ash sediments. Journal of Hazardous Materials. 184(1-3), 567-573.

Mudd, G.M., 2010. Global trends and environmental issues in nickel mining: Sulfides versus laterites. Ore Geology Reviews. 38(1-2). 9-26.

Ndlovu, B., Farrokhpay, S., Bradshaw, D., 2013. The effect of phyllosilicate minerals on mineral processing industry, International Journal of Mineral Processing. 125(10), 149-156.

Ndlovu, B., Forbes, E., Farrokhpay, S., Becker, M., Bradshaw, D., Deglon, D., 2014. A preliminary rheological classification of phyllosilicate group minerals. Minerals Engineering. 55, 190-200.

Ndlovu, B.N., Forbes, E., Becker, M., Deglon, D.A., Franzidis, J.P., Laskowski, J.S., 2011. The effects of chrysotile mineralogical properties on the rheology of chrysotile suspensions. Minerals Engineering, 24, 1004-1009.

Nduagu, E., Romão, I., Fagerlund, J., Zevenhoven, R., 2013. Performance assessment of producing $Mg(OH)_2$ for CO_2 sequestration. Applied Energy. 106, 116-126.

New Zealand Ministry for the Environment, 2007. The Framework for a New Zealand Emissions Trading Scheme: Executive Summary. Wellington, NZ: New Zealand Ministry for the Environment and The Treasury.

Nurmesniemi, H., Pöykiö, R., Perämäki, P., Kuokkanen, T., 2008. Extractability of trace elements in precipitated calcium carbonate (PCC) waste from an integrated pulp and paper mill complex. Chemsphere. 70, 1161-1167.

O'Connor, W.K., Dahlin, D.C., Rush, G.E., Gerdemann, S.J., Penner, L.R., Nilsen, D.N., 2005. Aqueous Mineral Carbonation: Final Report. Albany (NY): National Energy Laboratory, Office of Process Development. US Department of Energy. Report No.: DOE/ARC-TR-04-002.

O'Connor, W.K., Dahlin, D.C., Nilsen, D.N., Rush, G.E., Walters, R.P., Turner, P.C., 2000. CO_2 storage in solid form: A study of direct mineral carbonation. Greenhouse Gas Control Technologies: Proceedings of the 5th International Conference on Greenhouse Gas Technologies; 2000 Aug 14-18; Cairns, AU.

O'Connor, W.K., Dahlin, D.C., Nilsen, D.N., Rush, G.E., Walters, R.P., Turner, P.C., 2000. Carbon dioxide sequestration by direct mineral carbonation with carbonic acid. Proceedings of the 25th International Technical Conf. on Coal Utilization & Fuel Systems, Coal Technology Assoc; 2000 Mar 6-9; Clear Water, FL, USA.

O'Dell, R.E., Claassen, V.P., 2009. Serpentine revegetation: A Review. Northeastern Naturalist. 16(Special Issue 5), 253-271.

Oelkers, E.H., 2001. General kinetic description of multioxide silicate mineral and glass dissolution. Geochimica et Cosmochimica Acta. 65(21), 3703-3719.

Öhman, L.-O., Nordin, A., Fattahpour, I., Sjöberg, S., 1991. Equilibrium and structural studies of silicon(IV) and aluminum(III) in aqueous solution. 28. Formation of soluble silicic acid-ligand complexes and studied by potentiometric and solubility measurements. Acta Chemica Scandinavica. 45, 335-341.

Olajire, A.A., 2010. CO_2 capture and separation technologies for end-of-pipe applications – A review. Energy. 35, 2610-2628.

Olsen, A.A., Rimstidt, J.D., 2008. Oxalate-promoted forsterite dissolution at low pH. Gecochimica et Cosmochimica Acta. 72, 1758-1766.

Park, A.-H., Fan, L.-S., 2004. CO_2 mineral sequestration: physically activated dissolution of serpentine and pH swing process. Chemical Engineering Science. 59, 5241-5247.

Park, A.-H., Jadhav, R., Fan, L.-S., 2003. CO_2 mineral sequestration: chemically enhanced aqueous carbonation of serpentine. Canadian Journal of Chemical Engineering. 81, 885-890.

Patra, P., Bhambhani, T., Nagaraj, D.R., Somasundaran, P., 2010. Effect of morphology of altered silicate minerals on metallurgical performance: Transport of Mg silicates to the froth phase. Proceedings of the 49th Conference of Metallurgists. 2010 October 3-6; Vancouver, Canada. Westmount: CIM. p. 31-42.

Patra, P., Bhambhani, T., Nagaraj, D.R., Somasundaran, P., 2012. Impact of pulp rheological behavior on selective separation of Ni minerals from fibrous serpentine ores. Colloids and Surfaces A: Physicochemical and Engineering Aspects. 411, 24-26.

Peng, Y., Seaman, D., 2011. The flotation of slime-fine fractions of Mt. Keith pentlandite ore in de-ionised and saline water. 24, 479-481.

Peng, Z., 2012. Heat transfer in microwave heating. Doctoral dissertation, Michigan Technological University, 263p.

Pérez-López, R., Castillo, J., Quispe, D., Nieto, J.M., 2010. Neutralization of acid mine drainage using the final product from CO_2 emissions capture with alkaline paper mill waste. Journal of Hazardous Materials. 177, 762-772.

Pérez-López, R., Montes-Hernandez, G., Nieto, J.M., Renard, F., Charlet., L., 2008. Carbonation of alkaline paper mill waste to reduce CO_2 greenhouse gas emissions into the atmosphere. Applied Geochemistry. 23, 2292-2300.

Pérez-López, R., Quispe, D., Castillo, J., Nieto, J.M., 2011. Acid neutralization by dissolution of alkaline paper mill wastes and implications for treatment of sulfide-mine drainage. American Mineralogist. 96, 781-791.

Pickles, C.A., 2009. Microwaves in extractive metallurgy: Part 1 − Review of Fundamentals. Minerals Engineering. 22, 1102-1111.

Pickles, C.A., 2009. Microwaves in extractive metallurgy: Part 2 − A review of applications. Minerals Engineering. 22, 1112-1118.

Pokrovsky, O.S., Schott, J., 2000. Kinetics and mechanism of forsterite dissolution at $25^{\circ}C$ and pH from 1 to 12. Geochimica et Cosmochimica Acta. 64(19), 3313-3325.

Pokrovsky, O.S., Schott, J., 2004. Experimental study of brucite dissolution and precipitation in aqueous solutions: Surface speciation and chemical affinity control. Geochimica et Cosmochimica Acta. 68(1), 31-45.

246

Potapova, E., Yang, X., Grahn, M., Holmgren, A., Forsmo, S.P.E., Fredriksson, A., Hedlund, J., 2011. The effect of calcium ions, sodium silicate and surfactant on charge and wettability of magnetite. Colloids and Surfaces A: Physicochemical and Engineering Aspects. 386, 79-86.

Power, I.M., Dipple, G.M., Southam, G., 2010. Bioleaching of ultramafic tailings by *Acidithiobacillus spp.* for CO_2 sequestration. Environmental Science and Technology. 44, 456-462.

Pöykiö, R., Nurmesniemi, H., Kuokkanen, T., Perämäki, P., 2006. The use of a sequential leaching procedure for assessing the heavy metal leachability in lime waste from the lime kiln at a cautizicing process of a pulp mill. Chemosphere. 65, 2122-2129.

Praetorius, B., Schumacher, K., 2009. Greenhouse gas mitigation in a carbon constrained world: The role of carbon capture and storage. Energy Policy. 37, 5081-5093.

Prédali, J.-J., Cases, J.-M., 1973. Zeta potential of magnesian carbonates in inorganic electrolytes. Journal of Colloid and Interface Science. 45(3), 449-458.

Prigiobbe, V., Hänchen, M., Werner, M., Baciocchi, R., Mazzotti, M., 2009. Mineral carbonation process for CO_2 sequestration. Energy Procedia. 1, 4885-4890.

Prigiobbe, V., Hänchen, M., Werner, M., Baciocchi, R., Mazzotti, M., 2009. Analysis of the effect of temperature, pH, CO_2 pressure and salinity on the olivine dissolution kinetics. Energy Procedia. 1, 4881-4884.

Prigiobbe, V., Mazzotti, M., 2011. Dissolution of olivine in the presence of oxalate, citrate, and CO_2 at 90ºC and 120ºC. Chemical Engineering Science. 66, 6544-6554.

Prigiobbe, V., Polettini, A., Baciocchi, R., 2009. Gas-solid carbonation kinetics of Air Pollution Control residues for CO_2 storage. Chemical Engineering Journal. 148, 270-278.

Pundsack, F.L., 1967. Recovery of silica, iron oxide, and magnesium carboante from the treatment of serpentine with ammonium bisulphate. United States patent 3,338,667. 1967 Aug 29.

Radziszewski, P., 2013. Energy recovery potential in comminution processes. Minerals Engineering. 46-47, 83-88.

Raghavan, V., 2004. Fe-Ni-S (Iron-Nickel-Sulfur). Journal of Phase Equilibria and Diffusion. 25(4), 373-381.

Rao, M.A., 2007. Rheology of Fluid and Semisolid Foods: Principles and Applications, second ed., Springer, New York.

Raupach, M.R., Marland, G., Ciais, P., Le Quéré, C., Canadell, J.G., Klepper, G., Field, C.B., 2007. Global and regional drivers of accelerating CO_2 emissions. PNAS. 104(24), 10288-10293.

Rayment, P., Ross-Murphy, S.B., Ellis, P.R., 1998. Rheological properties of guar galactomannan and rice starch mixtures. II. Creep measurements. Carbohydrate Polymers. 35, 55-63.

Rendek, E., Ducom, G., Germain, P., 2006. Carbon dioxide sequestration in municipal solid waste incinerator (MSWI) bottom ash. Journal of Hazardous Materials. B128, 73-79.

Robie, R.A., Hemingway, B.S., 1995. Thermodynamic properties of minerals and related substances at 298.15K and 1 bar pressure and at higher temperatures. US Geological Survey Bulletin 2131. 470p.

Rodrigues, F.A., Joekes, I., 2011. Cement industry: sustainability, challenges and perspectives. Environmental Chemistry Letters. 9:151-166.

RRUFF, 2012. Handbook of Mineralogy (PDF). http://rruff.geo.arizona.edu/doclib/hom/ *Last accessed Nov 27, 2012.*

Russell, S.D.J., Longstaffe, F.J., King, P.L., Larson, T.E., 2010. The oxygen-isotope composition of chondrules and isolated forsterite and olivine grains from the Tagish Lake carbonaceous chondrite. Geochemical et Cosmochimica Acta. 74, 2484-2499.

Sahu, R.C., Patel, R.K., Ray, B.C., 2010. Neutralization of red mud using CO_2 sequestration cycle. Journal of Hazardous Materials. 179, 28-34.

Samouhos, M., Taxiarchou, M., Hutcheon, R., Devlin, E., 2012. Microwave reduction of a nickeliferous laterite ore. Minerals Engineering. 34, 19-29.

Schneider, M., Romer, M., Tschudin, M., Bolio, H., 2011. Sustainable cement production – present and future. Cement and concrete research. 41, 642-650.

Scholtzová, E., Tunega, D., Nagy, L.T., 2003. Theoretical study of cation substitution in trioctahedral sheet of phyllosilicates. An effect on inner OH group. Journal of Molecular Structure (Theochem). 620, 1-8.

Schwartzman, D.W., Volk, T., 1989. Biotic enhancement of weathering and the habitability of the Earth. Nature. 340, 457-460.

Senior, G.D., Thomas, S.A., 2005. Development and implementation of a new flowsheet for the flotation of a low grade nickel ore. International Journal of Mineral Processing. 78, 49-61.

Shabalala, N.Z.P., Harris, M., Leal Filho, L.S., Deglon, D.A., 2011. Effect of slurry rheology on gas dispersion in a pilot-scale mechanical flotation cell. Minerals Engineering. 24, 1448-1453.

Sipilä, J., Teir, S., Zevenhoven, R. 2008. Carbon dioxide sequestration by mineral carbonation: Literature review update 2005-2007. Turku, Finland: Abo Akademi University, Faculty of Technology, Heat Engineering Laboratory.

Skjærseth, J.B., Wettestad, J., 2010. Making the EU Emissions Trading System: The European Commission as an entrepreneurial epistemic leader. Global Environmental Change. 20, 314-321.

Smith, R.M., Martell, A.E., 1975. Critical stability constants: Volumes 1 and 3. Plenum Press, New York.

Solomon, S., Qin, D., Manning, M., Chen, Z., Marquis, M., Averyt, K.B., et al., editors, 2007. Climate Change 2007: The Physical Science Basis. Contribution of Working Group 1 to the Forth Assessment Report of the Intergovernmental Panel on Climate Change. Cambridge, UK and New York, NY, USA: Cambridge University Press.

Soong, Y., Fauth, D.L., Howard, B.H., Jones, J.R., Harrison, D.K., Goodman, A.L., et al., 2006. CO_2 sequestration with brine and fly ashes. Energy Conversion and Management. 47, 1676-1685.

Stephens, J.C., 2006. Growing interest in carbon capture and storage (CCS) for climate change mitigation. Sustainability: Science, Practice and Policy. 2(2), 4-13.

Stolaroff, J.K., Lowry, G.V., Keith, D.W., 2005. Using CaO- and MgO-rich industrial waste streams for carbon sequestration. Energy Conversion and Management. 46, 687-699.

Stumm, W., 1992. Chemistry of the solid-water interface. New York: John Wiley and Sons Inc.

Stumm, W., Wollast, R., 1990. Coordination chemistry of weathering: Kinetics of the surface-controlled dissolution of oxide minerals. Reviews of Geophysics. 28(1), 53-69.

Sugaki, A., Kitakaze, A., 1998. High form pentlandite and its thermal stability. American Mineralogist. 83, 133-140.

Svensson, R., Odenberger, M., Johnsson, F., Strömberg, L., 2004. Transportation systems for CO_2 – application to carbon capture and storage. Energy Conversion and Management. 45, 2343-2353.

Tans, P., 2014. Trends in Atmospheric Carbon Dioxide [Internet]. NOAA/ESRL; 2014 [cited 2014 Jan 29]. Available from: www.esrl.noaa.gov/gmd/ccgg/trends/

Teir, S., Eloneva, S., Fogelholm, C.-J., Zevenhoven, R., 2007. Dissolution of steelmaking slags in acetic acid for precipitated calcium carbonate production. Energy. 32, 528-539.

Teir, S., Eloneva, S., Fogelholm, C.-J., Zevenhoven, R., 2009. Fixation of carbon dioxide by producing hydromagnesite from serpentinite. Applied Energy. 86, 214-218.

Teir, S., Kuusik, R., Fogelholm, C.-J., Zevenhoven, R., 2007. Production of magnesium carbonates from serpentine fro long-term storage of CO_2. International Journal of Mineral Processing. 85, 1-15.

Teir, S., Revitzer, H., Eloneva, S., Fogelholm, C.-J., Zevenhoven, R., 2007. Dissolution of natural serpentine in mineral and organic acids. International Journal of Mineral Processing. 83, 36-46.

Teramura, S., Isu, N., Inagaki, K., 2000. New building material from waste concrete by carbonation. Journal of Materials in Civil Engineering. 12, 288-293.

Thom, J.G.M., Dipple, G.M., Power, I.M., Harrison, A.L., 2013. Chrysotile dissolution rates: Implications for carbon sequestration. Applied Geochemistry. 35, 244-254.

Todd, D.B., 2004. Mixing of highly viscous fluids, polymers and pastes. In: Handbook of Industrial Mixing: Science and Practice. Eds: Paul, E.L., Atiemo-Obeng, V.A., Kresta, S.M. Hoboken: John Wiley & Sons. 987-1025.

Trittschack, R., Grobety, B., 2012. Dehydroxylation kinetics of lizardite. European Journal of Mineralogy. 24, 47-57.

Tromans, D., 2008. Mineral comminution: Energy efficiency considerations. Minerals Engineering, 21, 613-620.

Uddin, S., Rao, S.R., Mirnezami, M, Finch, J.A., 2012. Processing an ultramafic ore using fibre disintegration by acid attack. International Journal of Mineral Processing. 102-103, 38-44.

Uibu, M., Velts, O., Kuusik, R., 2010. Developments in CO_2 mineral carbonation of oil shale ash. Journal of Hazardous Materials. 174, 209-214.

Uliasz-Bocheńczyk, A., Mokrzycki, E., Piotrowski, Z., Pomykała, R., 2009. Estimation of CO_2 sequestration potential via mineral carbonation in fly ash from lignite combustion in Poland. Energy Procedia. 1, 4873-4879.

UNSD, 2010. Carbon dioxide emissions (CO_2), thousand metric tons of CO_2 (CDIAC) [Internet]. United Nations Statistics Division. [cited 2011 Mar 2]. Available from: http://mdgs.un.org/unsd/mdg/SeriesDetail.aspx?srid=749&crid=

US DOE, 2006. World Carbon Dioxide Emissions from the Consumption of Coal [Internet]. Washington, DC: Energy Information Administration, International Energy Annual, Department of Energy; [cited 2011 Jan 23]. Available from: http://www.eia.doe.gov/iea/coal.html

US EPA, 2011. Solid Waste Management and Greenhouse Gases: Documentation for Greenhouse Gas Emission and Energy Factors Used in the Waste Reduction Model (WARM). Concrete [Internet]. [cited 2011 Jun 27]. Available from: http://www.epa.gov/climatechange/wycd/waste/downloads/concrete-chapter10-28-10.pdf

van Alphen, K., Hekkert, M.P., Turkenburg, W.C., 2009. Comparing the development and deployment of carbon capture and storage technologies in Norway, the Netherlands, Australia, Canada and the United States − An innovation system perspective. Energy Procedia. 1(1), 4591-4599.

van Alphen, K., Hekkert, M.P., Turkenburg, W.C., 2010. Accelerating the deployment of carbon capture and storage technologies by strengthening the innovation system. International Journal of Greenhouse Gas Control. 4(2), 396-409.

van Alphen, K., Noothout, P.M., Hekkert, M.P., Turkenburg, W.C., 2010. Evaluating the development of carbon capture and storage technologies in the United States. Renewable and Sustainable Energy Reviews. 14, 971-986.

Van Essendelft, D.T., Schobert, H.H., 2009. Kinetics of the acid digestion of serpentine with concurrent grinding. 1. Initial investigations. Industrial and Engineering Chemistry Research. 48, 2556-2565.

van Oss, H.G., Padovani, A.C., 2003. Cement manufacture and the environment, part II: environmental challenges and opportunities. Journal of Industrial Ecology. 7(1), 93–127.

Walkiewicz, J.W., Clark, A.E., McGill, S.L., 1991. Microwave-assisted grinding. IEEE Transactions on Industry Applications. 27(2), 239-243.

Wang, H., 2006. Isothermal kinetics of the pentlandite exsolution from mss/pyrrhotite using model-free method. Tsinghua Science and Technology. 11(3), 368-373.

Wang, L., Jin, Y., Nie, Y., 2010. Investigation of accelerated and natural carbonation of MSWI fly ash with a high content of Ca. Journal of Hazardous Materials. 174, 334-343.

Werner, M., Hariharan, S.B., Bortolan, A.V., Zingaretti, D., Baciocchi, R., Mazzotti, M., 2013. Carbonation of activated serpentine for direct flue gas mineralization. Energy Procedia. 37, 5929-5937.

White, B., Silsbee, M.R., Kearns, B.J., 2004. Reaction mechanisms of magnesium silicates with carbon dioxide in microwave fields. Final Report to the U.S.

Department of Energy, National Energy Laboratory. February 18, 2004. Award No. DE –FG26-02NT41545.

Wilson, S.A., Dipple, G.M., Power, I.M., Thom, J.M., Anderson, R.G., Raudsepp, M., et al., 2009. Carbon dioxide fixation within mine wastes of ultramafic-hosted ore deposits: Examples from the Clinton Creek and Cassiar crysotile deposits, Canada. Economic Geology. 104, 95-112.

Wilson, S.A., Raudsepp, M., Dipple, G.M., 2009. Quantifying carbon fixation in trace minerals from processed kimberlite: A comparative study of quantitative methods using X-ray powder diffraction data with applications to the Diavik Diamond Mine, Northwest Territories, Canada. Applied Geochemistry. 24, 2312-2331.

Wogelius, R.A., Walther, J.V., 1991. Olivine dissolution at 25°C: Effects of pH, CO_2 and organic acids. Geochimica et Cosmochimica Acta. 55, 943-954.

Xu, M., Dai, Z., Dong, J., Ford, F., Lee, A., 2010. Fibrous minerals in ultramafic nickel sulphide ores. Proceedings of the 49th Conference of Metallurgists. 2010 October 3-6; Vancouver, Canada. Westmount: CIM; p. 223-236.

Xu, M., Scholey, K., Marcuson, S., 2011. Vale-Cytec-University Research Consortium on Processing Low Grade Ultramafic Nickel Ore. Proceedings of the 50th Conference of Metallurgists. 2011 October 2-5; Montreal, Canada. Westmount: CIM.

Yadav, V.S., Prasad, M., Khan, J., Amritphale, S.S., Singh, M., Raju, C.B., 2010. Sequestration of carbon dioxide (CO_2) using red mud. Journal of Hazardous Materials. 176, 1044-1050.

Yamasaki, A., 2003. An overview of CO_2 mitigation options for global warming – emphasizing CO_2 sequestration options. Journal of Chemical Engineering of Japan. 36(4), 361-375.

Yan, L., Masliyah, J.H., Xu, Z., 2013. Understanding suspension rheology of anisotropically-charged platy minerals from direct interaction force measurement using AFM. Current Opinion in Colloid and Interface Science. 18, 149-156.

Yang, S., Pelton, R., Abarca, C., Dai, Z., Montgomery, M., Xu, M., Bos, J.-A., 2013. Towards nanoparticle flotation collectors for pentlandite separation. International Journal of Mineral Processing. 123, 137-144.

Zevenhoven, R., Fagerlund, J., 2010. Fixation of carbon dioxide into inorganic carbonates: the natural and artificial "weathering of silicates". In: Aresta M, editor. Carbon Dioxide as Chemical Feedstock. Weinheim, Germany: Wiley-VCH; p. 353-379.

Zevenhoven, R., Kohlmann, J., Mukherjee, A.B., 2002. Direct dry mineral carbonation for CO_2 emissions reduction in Finland. Proceedings: 27th International Technical Conference on Coal Utilization & Fuel Systems; 2002 Mar 4-7. Clearwater, FL, USA.

Zhao, L., Sang, L., Chen, J., Ji, J., Teng, H.H., 2010. Aqueous carbonation of natural brucite: Relevance to CO_2 sequestration. Environmental Science and Technology. 44, 406-411.

Ziock, H.-J., Butt, D.P., Lackner, K.S., Wendt, C.H., 1998. The need and options available for permanent CO_2 disposal. 1998 Topical Conference on Pollution Prevention and Environmental Risk Reduction; 1998 Nov 15-20; Miami Beach, FL, USA.

Appendix A

Equilibrium constants used for solution modeling in Chapters 6 and 7.

Table A-1: Equilibrium constants used in speciation modeling. Temperature 25°C, ionic strength 0.1 unless otherwise noted. Note: Cat = catechol ($C_6H_4O_2^{2-}$), Cit = citrate ($C_6H_5O_7^{3-}$), EDTA = ethylenediaminetetraacetic acid ($C_{10}H_{12}N_2O_8^{4-}$), Ox = oxalate ($C_2O_4^{2-}$), tiron = $C_6H_2O_8S_2^{4-}$.

Reaction	pK	Reference
$H^+ + Cat^{2-} \leftrightarrow HCat^-$	-13.0	Smith and Martell (1975)
$H^+ + HCat^- \leftrightarrow H_2Cat$	-9.23	Smith and Martell (1975)
$Mg^{2+} + Cat^{2-} \leftrightarrow MgCat$	-5.7[a]	Smith and Martell (1975)
$H^+ + Cit^{3-} \leftrightarrow HCit^{2-}$	-5.69	Smith and Martell (1975)
$H^+ + HCit^{2-} \leftrightarrow H_2Cit^-$	-4.35	Smith and Martell (1975)
$H^+ + H_2Cit^- \leftrightarrow H_3Cit$	-2.87	Smith and Martell (1975)
$Mg^{2+} + Cit^{3-} \leftrightarrow MgCit^-$	-3.37	Smith and Martell (1975)
$Mg^{2+} + HCit^{2-} \leftrightarrow MgHCit$	-1.92	Smith and Martell (1975)
$Mg^{2+} + H_2Cit^- \leftrightarrow MgH_2Cit^+$	-0.84[b]	Smith and Martell (1975)
$H^+ + EDTA^{4-} \leftrightarrow HEDTA^{3-}$	-10.17	Smith and Martell (1975)
$H^+ + HEDTA^{3-} \leftrightarrow H_2 EDTA^{2-}$	-6.11	Smith and Martell (1975)
$H^+ + H_2EDTA^{2-} \leftrightarrow H_3EDTA^-$	-2.68	Smith and Martell (1975)
$H^+ + H_3EDTA^- \leftrightarrow H_4EDTA$	-2.0	Smith and Martell (1975)
$H^+ + H_4EDTA \leftrightarrow H_5EDTA^+$	-1.5	Smith and Martell (1975)
$H^+ + H_5EDTA^+ \leftrightarrow H_6EDTA^{2+}$	0	Smith and Martell (1975)
$Mg^{2+} + EDTA^{4-} \leftrightarrow MgEDTA^{2-}$	-8.83	Smith and Martell (1975)
$H^+ + MgEDTA^{2-} \leftrightarrow MgHEDTA^-$	-3.85	Smith and Martell (1975)
$H^+ + Ox^{2-} \leftrightarrow HOx^-$	-3.82	Smith and Martell (1975)
$H^+ + HOx^- \leftrightarrow H_2Ox$	-1.04	Smith and Martell (1975)
$Mg^{2+} + Ox^{2-} \leftrightarrow MgOx$	-2.76[c]	Smith and Martell (1975)
$Mg^{2+} + 2Ox^{2-} \leftrightarrow Mg(Ox)_2^{2-}$	-4.24	Smith and Martell (1975)
$H^+ + Tiron^{4-} \leftrightarrow HTiron^{3-}$	-12.5	Smith and Martell (1975)
$H^+ + HTiron^{3-} \leftrightarrow H_2Tiron^{2-}$	-7.61	Smith and Martell (1975)
$Mg^{2+} + Tiron^{4-} \leftrightarrow MgTiron^{2-}$	-6.86	Smith and Martell (1975)
$Mg^{2+} + HTiron^{3-} \leftrightarrow MgHTiron^-$	-1.98	Smith and Martell (1975)
$Mg^{2+} + OH^- \leftrightarrow MgOH^+$	-2.57	Prédali and Cases (1973)
$Mg^{2+} + 2OH^- \leftrightarrow Mg(OH)_{2(aq)}$	-5.81	Prédali and Cases (1973)
$Mg(OH)_{2(aq)} \leftrightarrow Mg(OH)_{2(s)}$	-2.67	Prédali and Cases (1973)
$H_2CO_{3(aq)} \leftrightarrow H^+ + HCO_3^-$	6.34	Chen et al. (2006), Pokrovsky et al. (2009)
$HCO_3^- \leftrightarrow H^+ + CO_3^{2-}$	10.33	Chen et al. (2006), Pokrovsky et al. (2009)
$Mg^{2+} + HCO_3^- \leftrightarrow MgHCO_3^+$	-1.16	Prédali and Cases (1973)
$MgHCO_3^+ \leftrightarrow H^+ + MgCO_{3(aq)}$	8.09	Prédali and Cases (1973)
$MgCO_{3(s)} \leftrightarrow MgCO_{3(aq)}$	4.51	Prédali and Cases (1973)

[a] 30°C, 0.1; [b] 25°C, 1.0; [c] 20°C, 0.1

Appendix B

Distribution of ligand species in water at 25°C upon the addition of 0.1 M Mg and ligand.
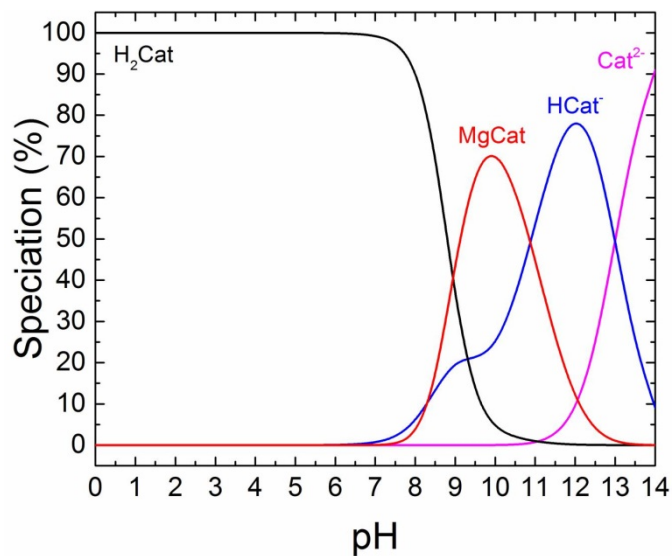
Figure B-1: Distribution of catechol species in water at 25°C upon the addition of 0.1 M Mg and 0.1 M catechol.
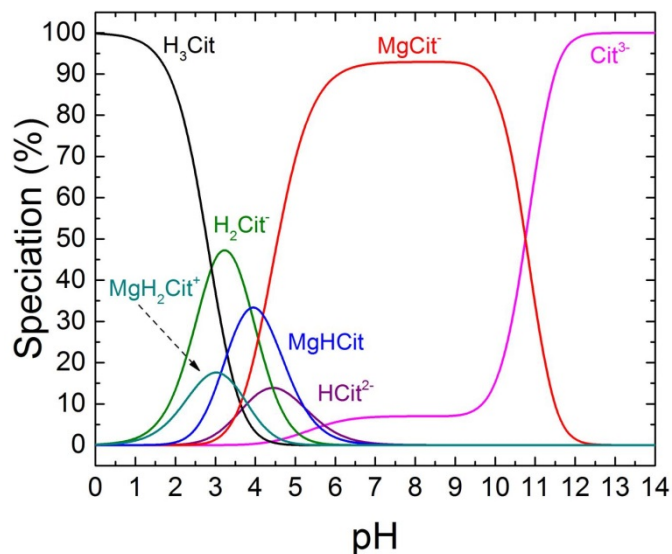
**Figure B-2: Distribution of citrate species in water at 25°C upon the addition of 0.1 M Mg and 0.1 M citrate.**

257
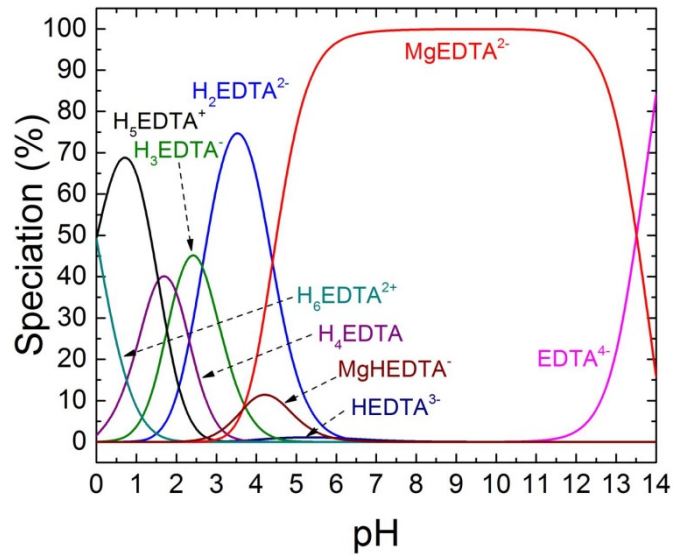
Figure B-3: Distribution of EDTA species in water at 25ºC upon the addition of 0.1 M Mg and 0.1 M EDTA.
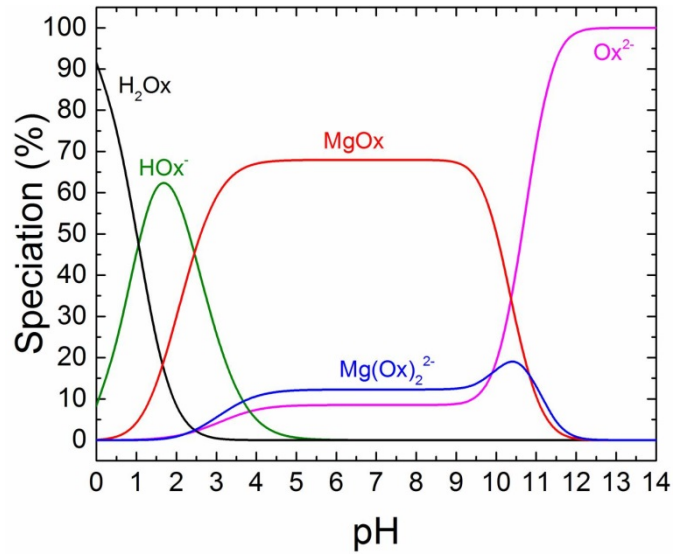
Figure B-4: Distribution of oxalate species in water at 25ºC upon the addition of 0.1 M Mg and 0.1 M oxalate.
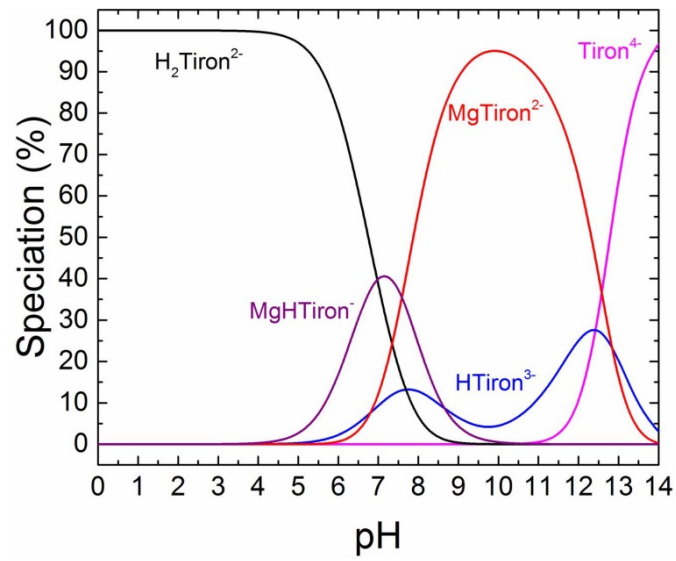
Figure B-5: Distribution of tiron species in water at 25ºC upon the addition of 0.1 M Mg and 0.1 M tiron.

Appendix C

Concentration of complexes in water at pH 10 and 25°C upon the addition of 1.0 M Mg as a function of ligand concentration.
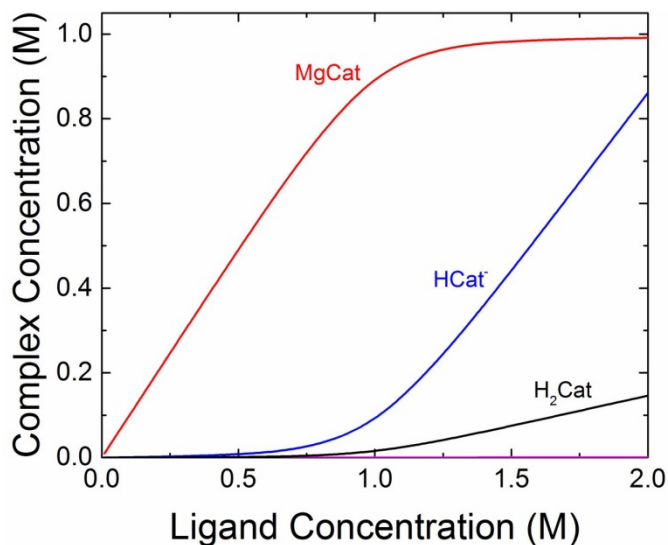
Figure C-1: Concentration of catechol complexes in water at pH 10 and 25°C as a function of ligand concentration with Mg addition of 1.0 M.
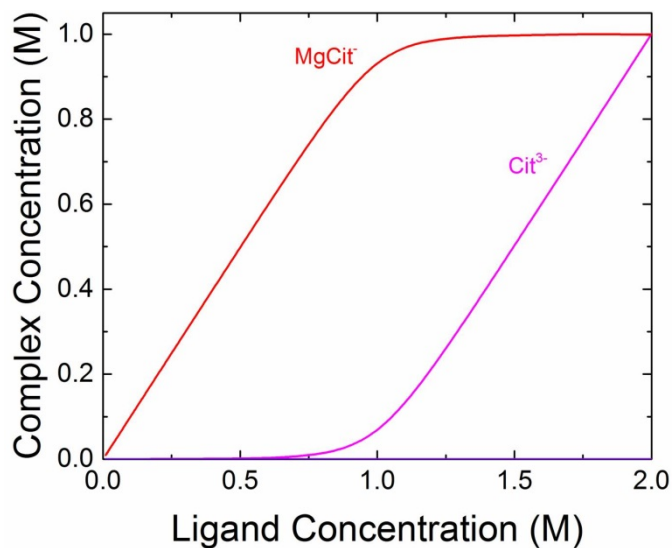
Figure C-2: Concentration of citrate complexes in water at pH 10 and 25°C as a function of ligand concentration with Mg addition of 1.0 M.
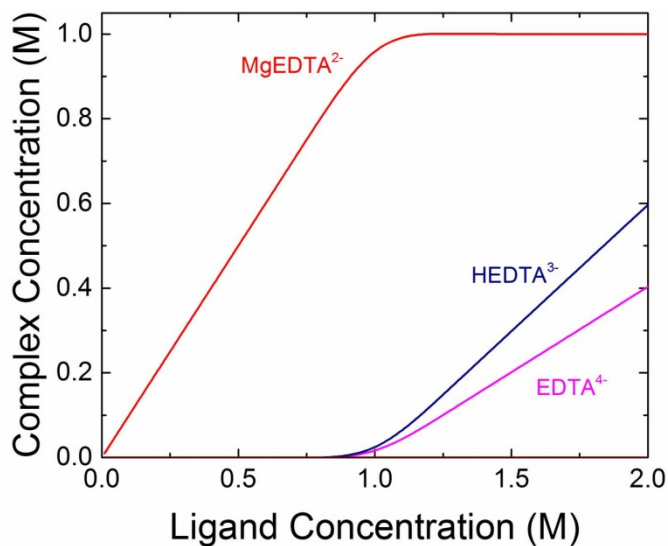
Figure C-3: Concentration of EDTA complexes in water at pH 10 and 25ºC as a function of ligand concentration with Mg addition of 1.0 M.
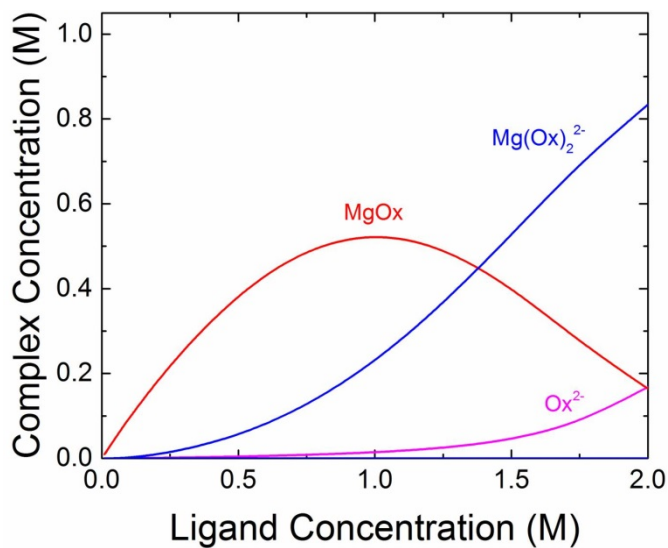
Figure C-4: Concentration of oxalate complexes in water at pH 10 and 25ºC as a function of ligand concentration with Mg addition of 1.0 M.
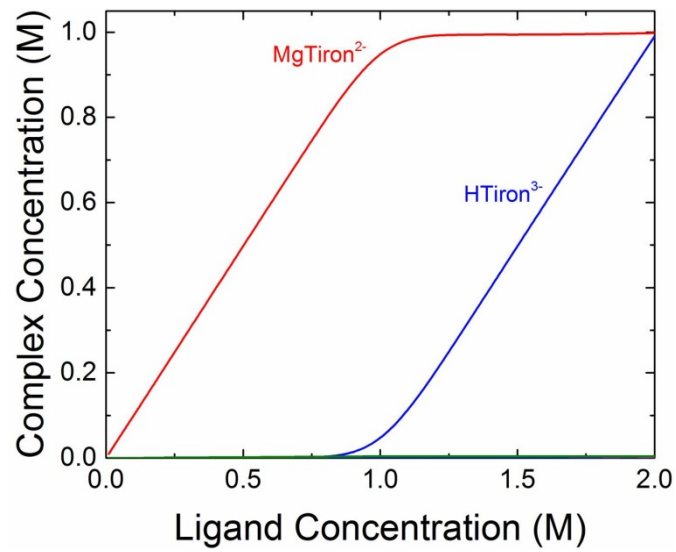
Figure C-5: Concentration of tiron complexes in water at pH 10 and 25ºC as a function of ligand concentration with Mg addition of 1.0 M.

Appendix D

Leaching curves for Pipe and OK ores leached with 0.01 M, 0.05 M and 0.1 M ligand solutions at pH 7 and 10, all at 25°C.
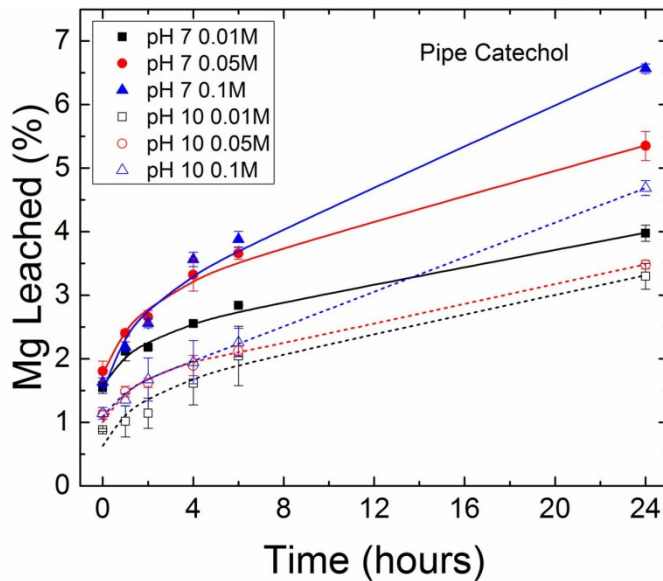
Figure D-1: Total magnesium in solution versus time for Pipe ore leached with Catechol solutions at concentrations of 0.01 M, 0.05 M and 0.1 M, at pH 7 and 10, and at 25°C. Lines shown are fitted curves.
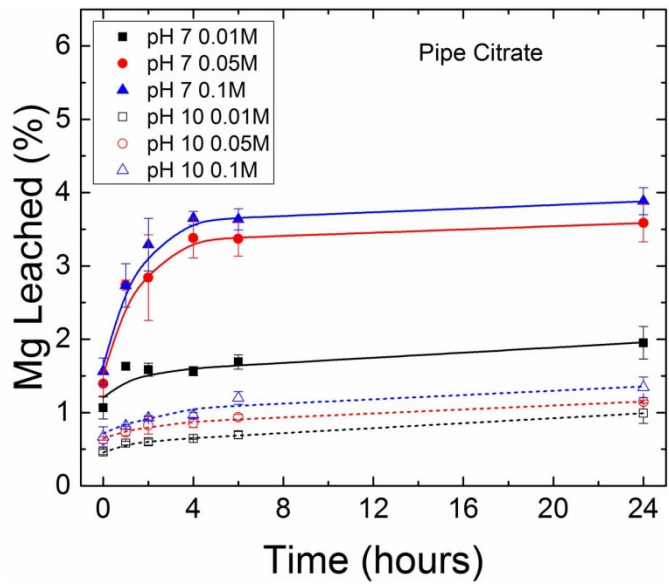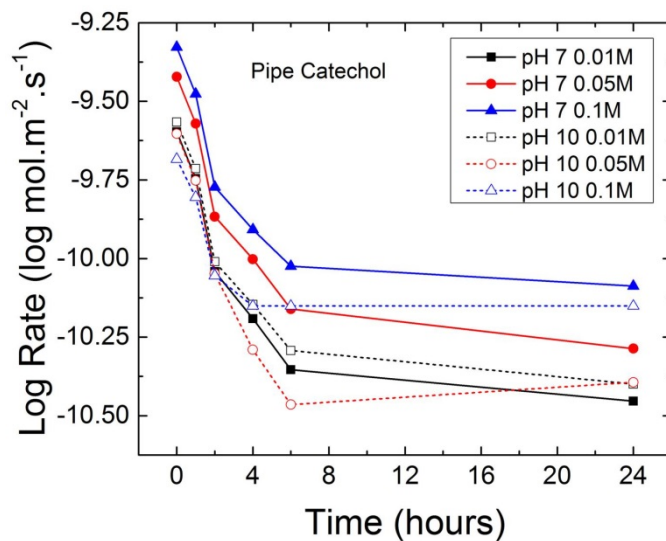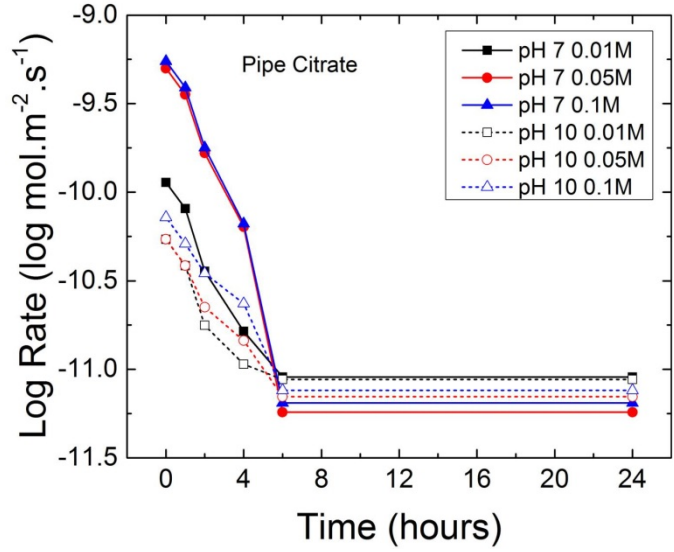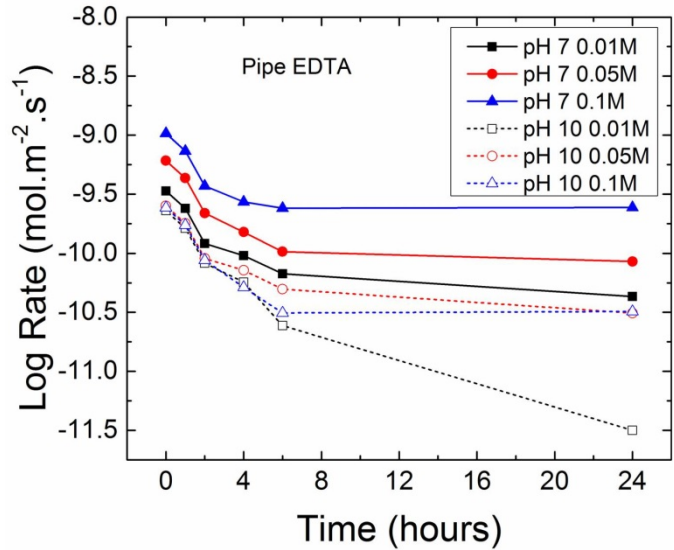
Figure D-2: Total magnesium in solution versus time for Pipe ore leached with citrate solutions at concentrations of 0.01 M, 0.05 M and 0.1 M, at pH 7 and 10, and at 25ºC. Lines shown are fitted curves.
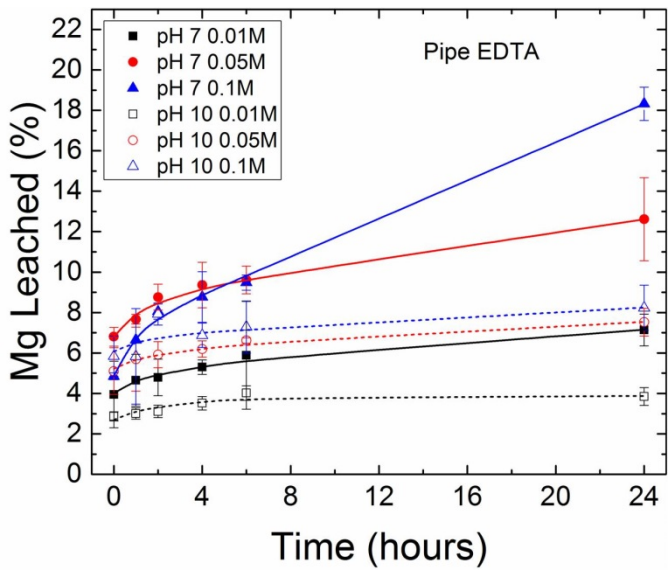
Figure D-3: Total magnesium in solution versus time for Pipe ore leached with EDTA solutions at concentrations of 0.01 M, 0.05 M and 0.1 M, at pH 7 and 10, and at 25ºC. Lines shown are fitted curves.
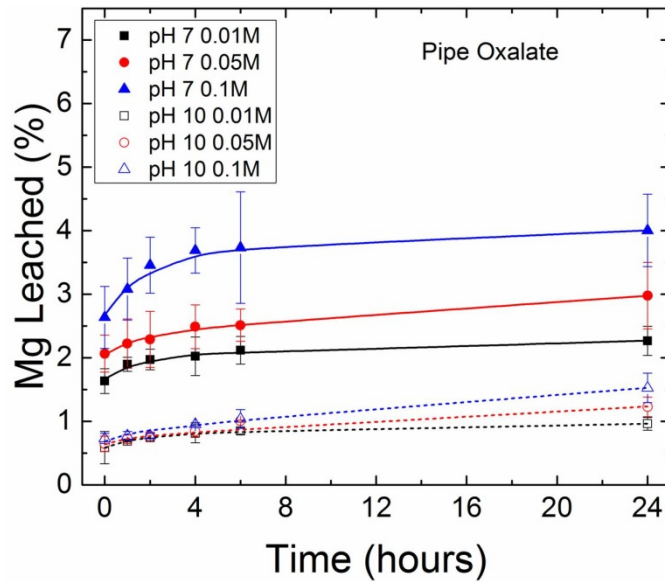
Figure D-4: Total magnesium in solution versus time for Pipe ore leached with oxalate solutions at concentrations of 0.01 M, 0.05 M and 0.1 M, at pH 7 and 10, and at 25°C. Lines shown are fitted curves.
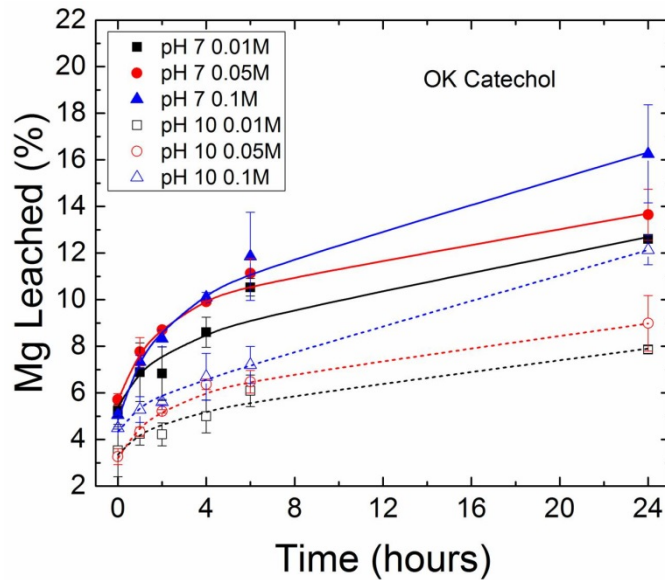

Figure D-5: Total magnesium in solution versus time for OK ore leached with catechol solutions at concentrations of 0.01 M, 0.05 and 0.1 M, at pH 7 and 10, and at 25°C. Lines shown are fitted curves.
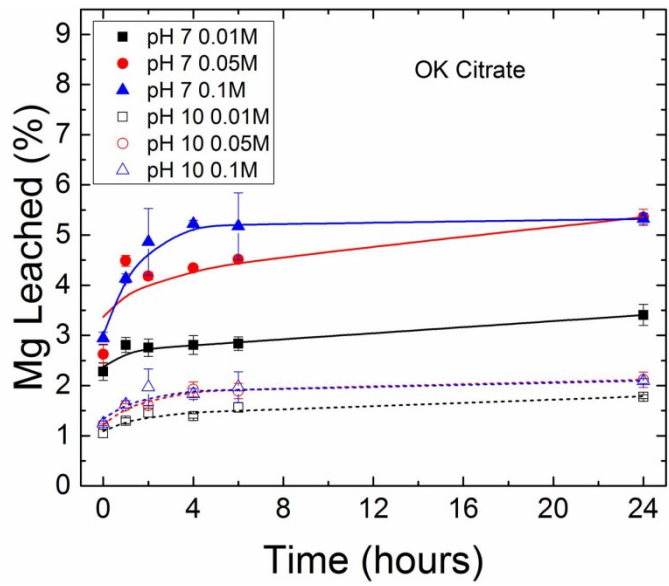
Figure D-6: Total magnesium in solution versus time for OK ore leached with citrate solutions at concentrations of 0.01 M, 0.05 M and 0.1 M, at pH 7 and 10, and at 25°C. Lines shown are fitted curves.
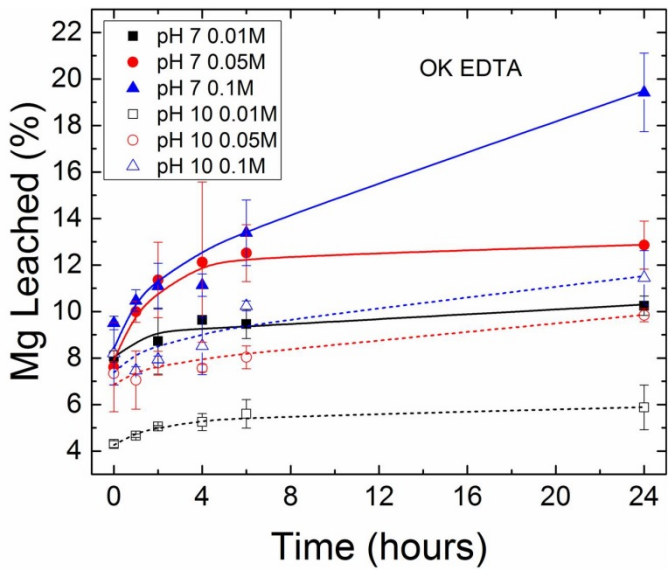
Figure D-7: Total magnesium in solution versus time for OK ore leached with EDTA solutions at concentrations of 0.01 M, 0.05 M and 0.1 M, at pH 7 and 10, and at 25°C. Lines shown are fitted curves.
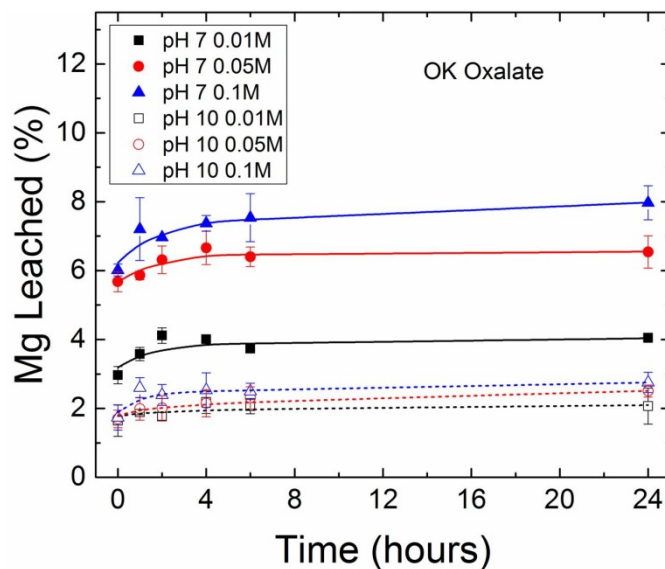
Figure D-8: Total magnesium in solution versus time for OK ore leached with oxalate solutions at concentrations of 0.01 M, 0.05 M and 0.1 M, at pH 7 and 10, and at 25°C. Lines shown are fitted curves.
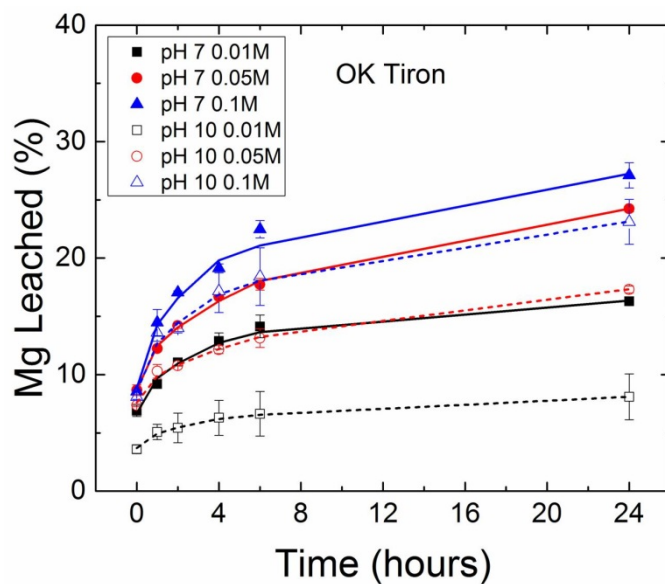
Figure D-9: Total magnesium in solution versus time for OK ore leached with Tiron solutions at concentrations of 0.01 M, 0.05 M and 0.1 M, at pH 7 and 10, and at 25°C. Lines shown are fitted curves.
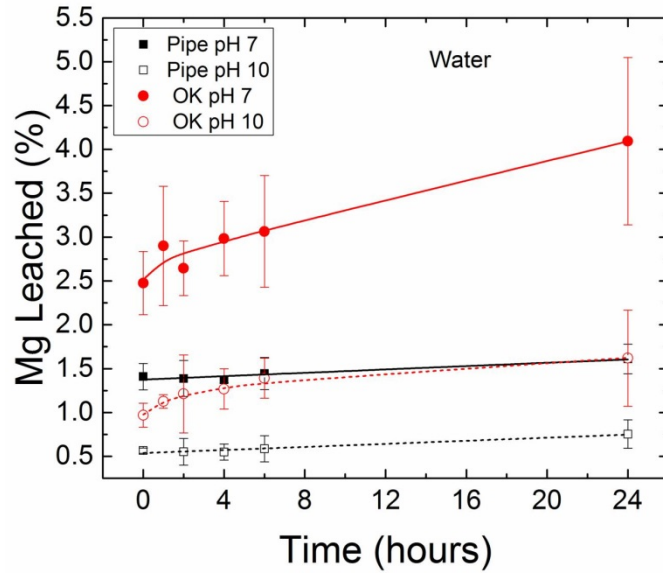
Figure D-10: Total magnesium in solution versus time for Pipe and OK ores in water at pH 7 and 10, and at 25ºC. Lines shown are fitted curves.

Appendix E

Leaching rate curves for Pipe and OK ores leached with 0.01 M, 0.05 M and 0.1 M ligand solutions at pH 7 and 10, all at 25°C.
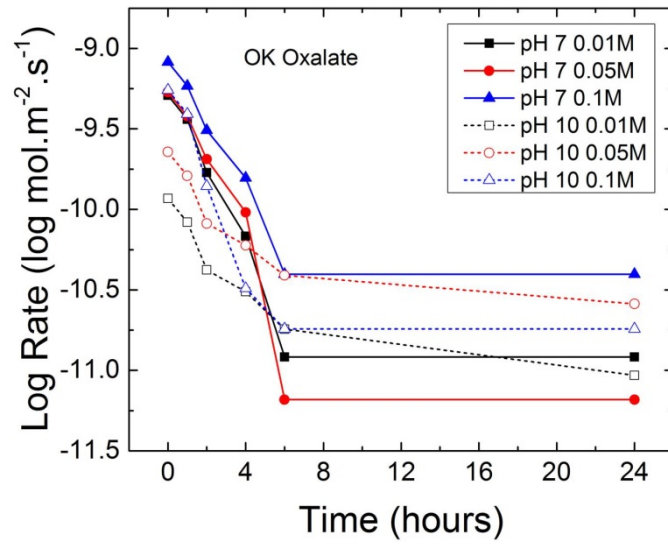

Figure E-1: Leaching rate versus time for Pipe ore leached with catechol at concentrations of 0.01 M, 0.05 M and 0.1 M, at pH 7 and 10, and at 25°C.
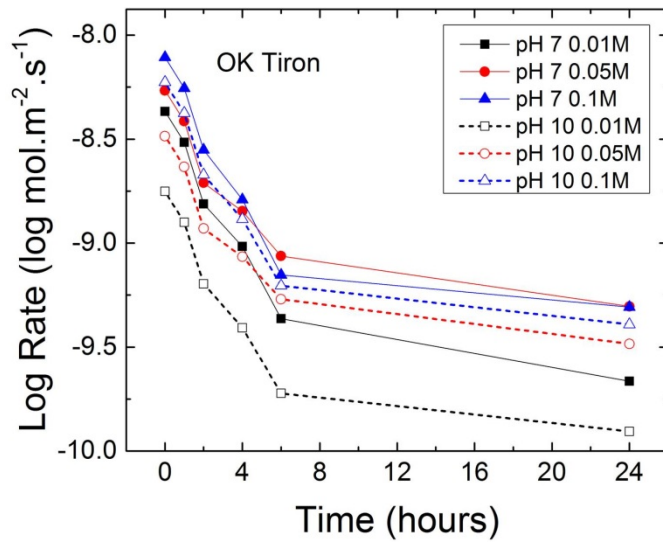
Figure E-2: Leaching rate versus time for Pipe ore leached with citrate at concentrations of 0.01 M, 0.05 M and 0.1 M, at pH 7 and 10, and at 25ºC.
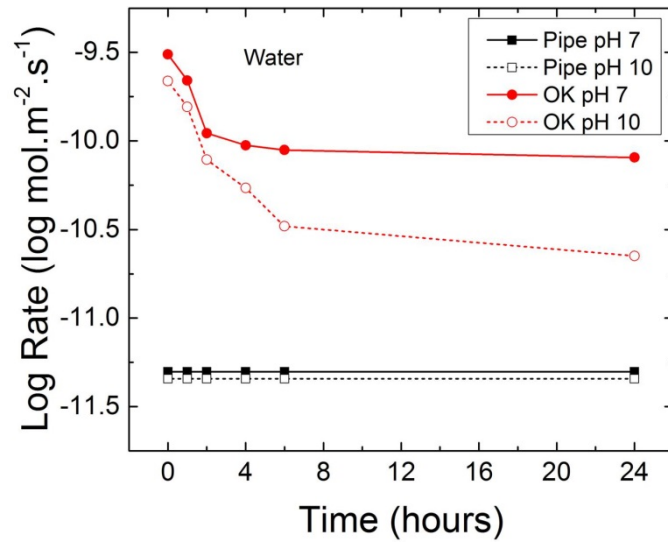

Figure E-3: Leaching rate versus time for Pipe ore leached with EDTA at concentrations of 0.01 M, 0.05 M and 0.1 M, at pH 7 and 10, and at 25ºC.
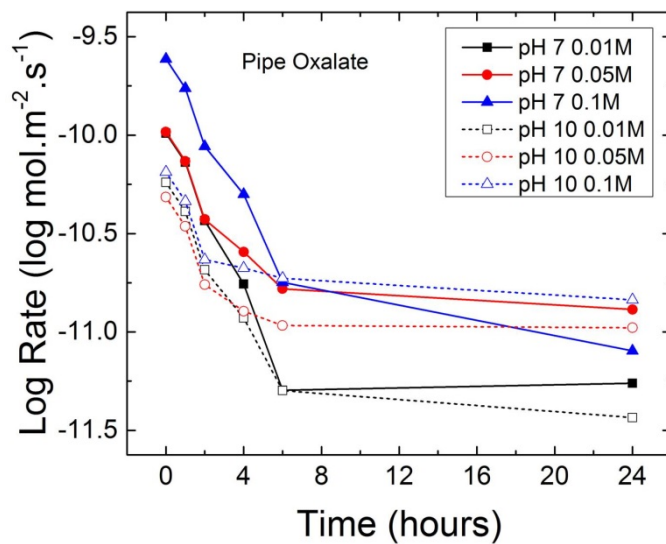
Figure E-4: Leaching rate versus time for Pipe ore leached with oxalate at concentrations of 0.01 M, 0.05 M and 0.1 M, at pH 7 and 10, and at 25ºC.
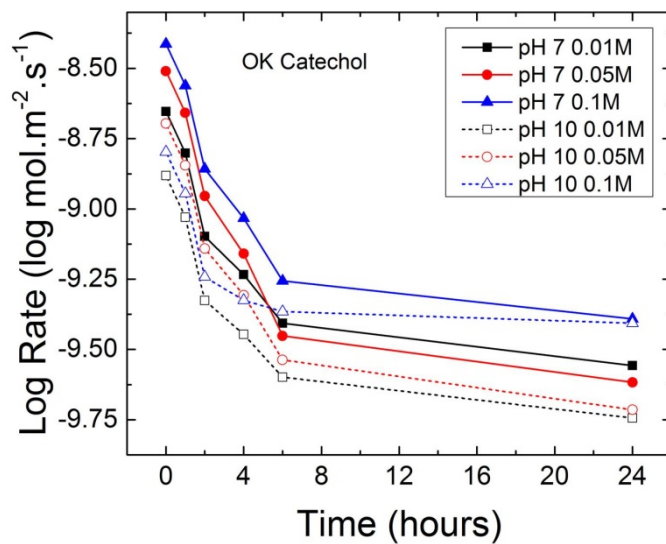

Figure E-5: Leaching rate versus time for OK ore leached with catechol at concentrations of 0.01 M, 0.05 M and 0.1 M, at pH 7 and 10, and at 25ºC.
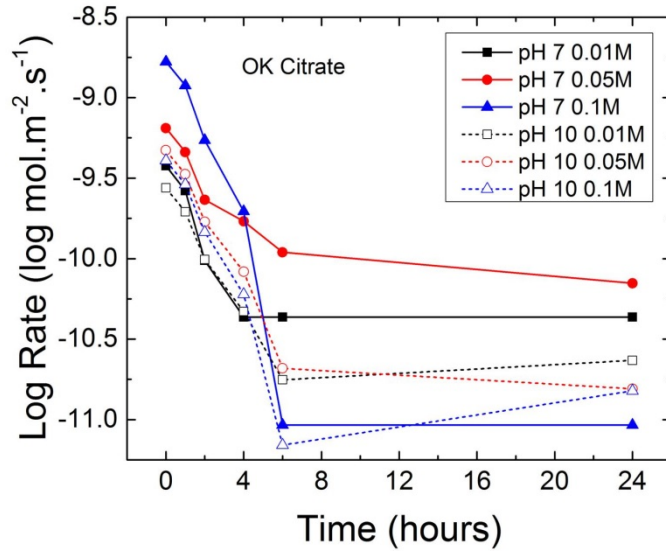
Figure E-6: Leaching rate versus time for OK ore leached with citrate at concentrations of 0.01 M, 0.05 M and 0.1 M, at pH 7 and 10, and at 25ºC.
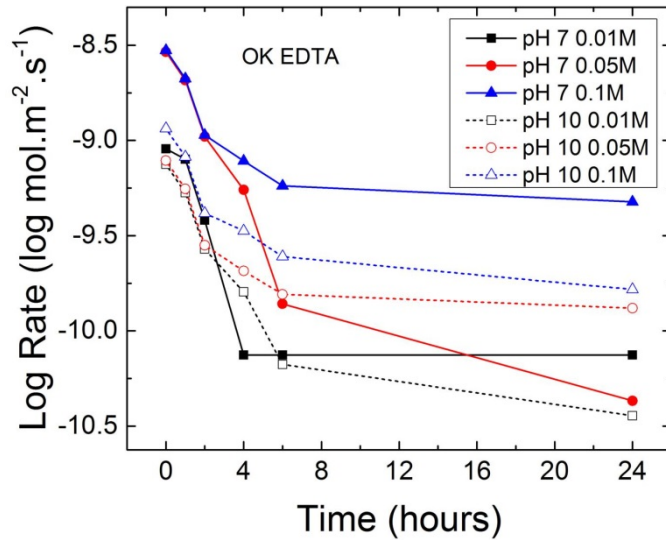
Figure E-7: Leaching rate versus time for OK ore leached with EDTA at concentrations of 0.01 M, 0.05 M and 0.1 M, at pH 7 and 10, and at 25ºC.

Figure E-8: Leaching rate versus time for OK ore leached with oxalate at concentrations of 0.01 M, 0.05 M and 0.1 M, at pH 7 and 10, and at 25ºC.

Figure E-9: Leaching rate versus time for OK ore leached with Tiron at concentrations of 0.01 M, 0.05 M and 0.1 M, at pH 7 and 10, and at 25ºC.
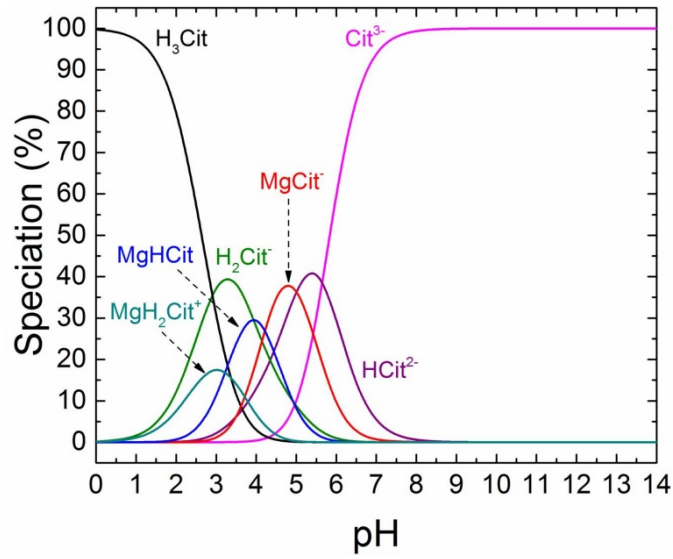
Figure E-10: Leaching rate versus time for Pipe and OK ores in water at pH 7 and 10, and at 25ºC.
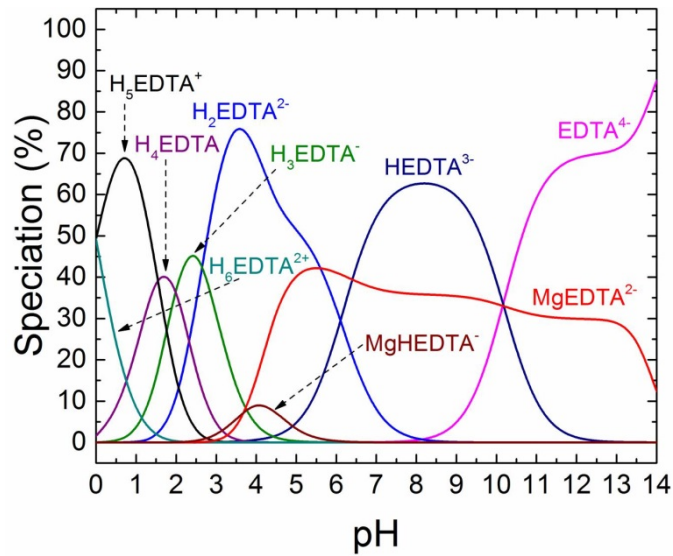
Appendix F

Distribution of ligand species in water at 25°C upon the addition of 0.1 M Mg and ligand under 12.4 MPa CO_2 pressure.
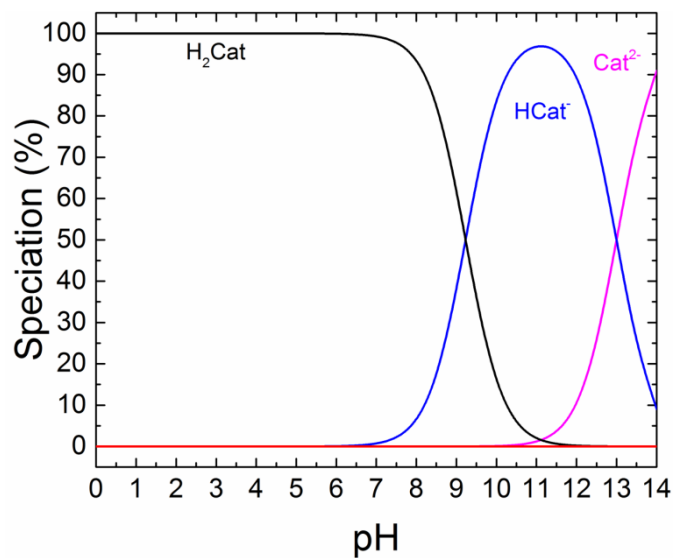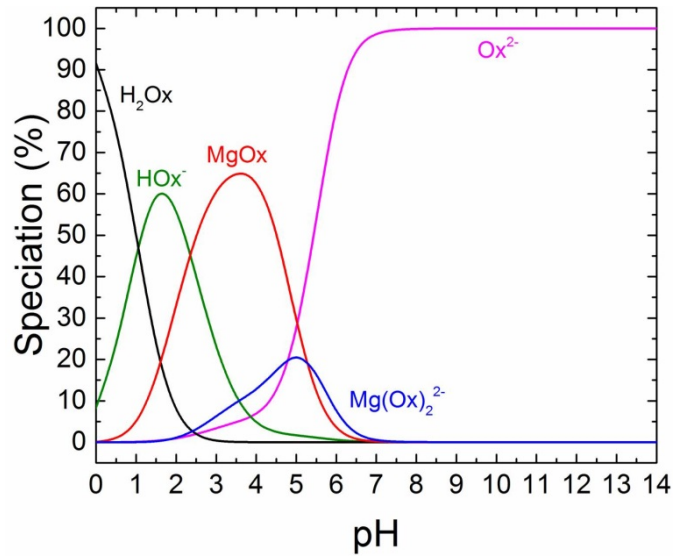

Figure F-1: Distribution of catechol species in water at 25ºC upon the addition of 0.1 M Mg and 0.1 M catechol under 12.4 MPa CO_2.
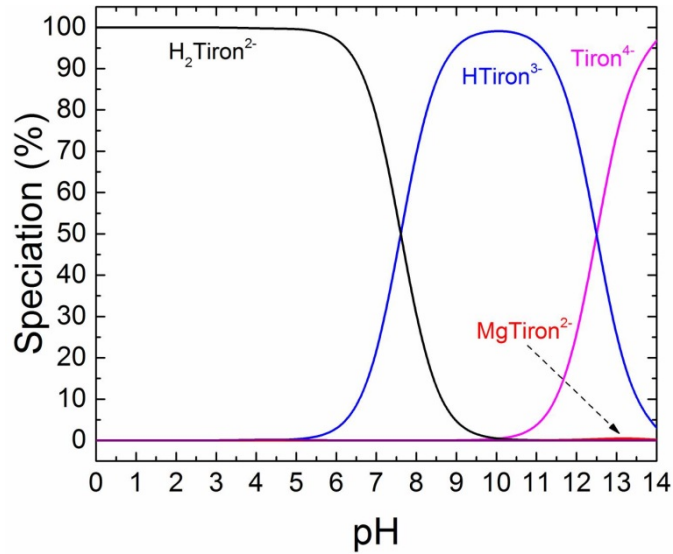
Figure F-2: Distribution of citrate species in water at 25ºC upon the addition of 0.1 M Mg and 0.1 M citrate under 12.4 MPa CO₂.

Figure F-3: Distribution of EDTA species in water at 25ºC upon the addition of 0.1 M Mg and 0.1 M EDTA under 12.4 MPa CO₂.

Figure F-4: Distribution of oxalate species in water at 25ºC upon the addition of 0.1 M Mg and 0.1 M oxalate under 12.4 MPa CO₂.

Figure F-5: Distribution of tiron species in water at 25ºC upon the addition of 0.1 M Mg and 0.1 M tiron under 12.4 MPa CO₂.